

Srpsko hemijsko društvo



Serbian Chemical Society

53. savetovanje Srpskog hemijskog društva

Kragujevac 10. i 11. jun 2016.

Ovaj kompakt disk (CD) sadrži elektronsku Knjigu radova (u pdf formatu) prezenovanih u okviru 53. savetovanja SHD

U knjizi su **plavom bojom** obeleženi aktivni linkovi ka pojedinim njenim delovima, odnosno to su prečice iz Sadržaja koje vode do naznačenih stranica.

U vrhu svake strane nalaze se prečice ka **Impresumu i Sadržaju** knjige, ka **Indexu autora**, kao i opcijama za štampanje (**Print**), zatvaranje dokumanta, odnosno izlaz iz knjige (**Exit**), i za povratak na ovu stranicu (**Intro**)

Pored toga na disku se nalazi i elektronska kopija (u pdf formatu) Programa i Kratkih izvoda radova. Možete joj pristupiti klikom **OVDE**

53rd Meeting of the Serbian Chemical Society

Kragujevac, Serbia, June 10 and 11, 2016

This CD contains Proceedings (single pdf file) from 53rd Meeting of SCS

One can navigate easily through the book contents by a single click on the appropriate links in Contents (showed in blue color)

All contents of the Proceeding can be accessed through following shortcuts existing at the top of each page: **Impresum** (Impress of the Proceedings), **Contents**, **Index** (Author Index), **Print** (Print manager), **Exit** (which closes the CD) and **Intro** (which leads to this page).

CD contains also a pdf copy of Programme and Book of Abstracts, which can be accessed by clicking **HERE**.



Srpsko hemijsko društvo
Serbian Chemical Society

**53. savetovanje
Srpskog hemijskog društva**

KNJIGA RADOVA

**53rd Meeting of
the Serbian Chemical Society**

Proceedings

Prirodno-matematički fakultet, Kragujevac 10. i 11. jun 2016.
Faculty of Science, Kragujevac, Serbia, June 10 and 11, 2016

54(082)(0.034.2)
577.1(082)(0.034.2)
66(082)(0.034.2)
66.017/.018(082)(0.034.2)
502/504(082)(0.034.2)

СРПСКО хемијско друштво. Саветовање (53 ; 2016 ; Крагујевац) Knjiga radova [Elektronski izvor] = Proceedings / 53. savetovanje Srpskog hemijskog društva, Kragujevac, 10. i 11. jun 2016. = 53rd Meeting of the Serbian Chemical Society, Kragujevac, Serbia, June 10 and 11, 2016 ; [organizator] Srpsko hemijsko društvo = [organizer] Serbian Chemical Society ; [urednici, editors Miloš Đuran, Aleksandar Dekanski]. - Beograd : Srpsko hemijsko društvo = Serbian Chemical Society, 2016 (Beograd : Razvojno-istraživački centar grafičkog inženjerstva TMF). - 1 elektronski optički disk (CD-ROM) ; 12 cm

Sistemski zahtevи: Nisu navedeni. - Nasl. sa naslovног екрана. - Radovi na srp. i engл. jeziku. - Tekst ћir. i lat. - Tiraž 150. - Bibliografija uz svaki rad. - Abstracts ; Apstrakti. - Registar. - Sadrži i: Program i kratki izvodi radova = Program & Book of Abstracts / 53. savetovanje Srpskog hemijskog društva, Kragujevac, 10-11. jun 2016.

ISBN 978-86-7132-062-7

а) Хемија - Зборници б) Биохемија - Зборници с) Технологија - Зборници д) Наука о материјалима - Зборници е) Животна средина - Зборници

COBISS.SR-ID 223815692

53. SAVETOVANJE SRPSKOG HEMIJSKOG DRUŠTVA,

PRIRODNO-MATEMATIČKI FAKULTET KRAGUJEVAC,
10. i 11. JUN 2016.

53rd Meeting of the Serbian Chemical Society,
FACULTY OF SCIENCE KRAGUJEVAC, SERBIA, JUNE 10 AND 11, 2016

Knjiga radova / Proceedings

Izdaje / Published by

Srpsko hemijsko društvo / Serbian Chemical Society, Karnegijeva 4/III, Beograd, Srbija
tel./fax: +381 11 3370 467; www.shd.org.rs, E-mail: Office@shd.org.rs

Za izdavača / For Publisher

Živoslav **TEŠIĆ**, predsednik Društva

Urednici / Editors

Miloš ĐURAN

Aleksandar DEKANSKI

Dizajn, slog i kompjuterska obrada teksta / Design, Page Making and Computer Layout

Aleksandar **DEKANSKI**

Tiraž / Circulation

150 primeraka / 150 Copy

Umnožavanje / Copying

Razvojno-istraživački centar grafičkog inženjerstva, Tehnološko-metalurški fakultet,
Karnegijeva 4, Beograd, Srbija

ISBN 978-86-7132-062-7

Svetovanje su podržali / *The meeting is supported by*

**Ministarstvo prosvete, nauke i tehnološkog razvoja
Republike Srbije**



*Ministry of Education, Science and Technological Development
of Republic of Serbia*

SUPERLAB®
INSPIRISAN KVALITETOM

Sadržaj / Contents

Plenarno predavanje / Plenary Lecture

Interactions of metal ions with old drugs.....	2
Iztok Turel	
Interakcije jona metala i jedinjenja sa poznatim farmakološkim svojstvima	5

Predavanje po pozvu / Invited Lecture

Proces recenziranja radova u časopisima iz hemije i srodnih oblasti koji se izdaju u Srbiji	7
Ivana Drvenica, Aleksandar Dekanski, Olgica Nedić	
Peer-review process in journals dealing with chemistry and related subjects published in Serbia	13

Saopštenja Contributions

Analitička hemija / Analytical Chemistry

Primena plazme indukovane TEA CO ₂ laserskim zračenjem za određivanje koncentracije magnezijuma u aluminijumskim legurama	15
Sanja M. Živković, Jelena Mutić, Jelena Savović, Miloš Momčilović	
Application of plasma induced by TEA CO ₂ laser for determining the concentration of magnesium in the aluminum alloys	18

Elektrohemija / Electrochemistry

Nanocrystalline ruthenium oxide coating on titanium, prepared by the sol–gel procedure from colloidal oxide dispersions synthesized in the microwave reactor	20
Milica Košević, Gavrilo Šekularac, Ivana Drvenica, Aleksandar Dekanski, Branislav Nikolić, Vladimir Panić	
Превлаке нанокристалног рутениум оксида на титану, добијене сол–гел поступком из колоидне оксидне дисперзије синтетисане у микроталасном ректору	24
Uticaj leucina na anodno rastvaranje halkopirita u sumpornoj kiselini.....	26
Biljana S. Maluckov, Mile Dimitrijević, Renata Kovačević, Srba Mladenović	
The effect of leucine on the anodic dissolution of chalcopyrite in sulfuric acid	29

Fizička hemija / Physical Chemistry

Efekat isoljavanja i uticaj temperature na bifazne vodene sisteme na bazi dicijanamidnih jonskih tečnosti	30
Aleksandra Dimitrijević, Nebojša Zec, Nikola Zdolšek, Sanja Dožić, Slobodan Gadžurić, Tatjana Trtić-Petrović	
The salting-out effect and impact of temperature on phase diagrams of aqueous biphasic systems based on novel synthesized dicyanamide ionic liquids	33

Hemijsko inženjerstvo / Chemical Engineering

Phosphate removal from wastewater by electrocoagulation process using aluminium electrode	34
Borislav N. Malinović, Suzana Gotovac Atlagić, Tijana Malinović, Natalija Bjelajac, Aleksandra Milovanović	
Uklanjanje fosfata iz otpadne vode procesom elektrokoagulacije primjenom aluminijumske elektrode	37

Experimental measurement of volumetric, transport, ultrasonic and refractive index properties of binary mixtures (ethyl oleate + <i>n</i> -hexadecane) at different temperatures and atmospheric pressure	39
---	----

Mohamed A. Aissa, Gorica R. Ivaniš, Ivona R. Radović, Mirjana Lj. Kijevčanin

Експериментално одређивање волуметријских, транспортних, ултразвучних својстава и индекса рефракције бинарних смеша (етил олеат + <i>n</i> -хексадекан) на различитим температурама и атмосферском притиску	42
---	----

Influence of resolution in digital characterization of sand particles size and shape	43
--	----

Zorana Arsenijević, Mihal Đuriš, Tatjana Kaluderović Radoičić

Утицај резолуције на дигиталну карактеризацију величине и облика честица песка	48
--	----

<u>Equation Chapter 0 Section 1</u> Friction factor for water flow through packed beds of spherical particles	49
---	----

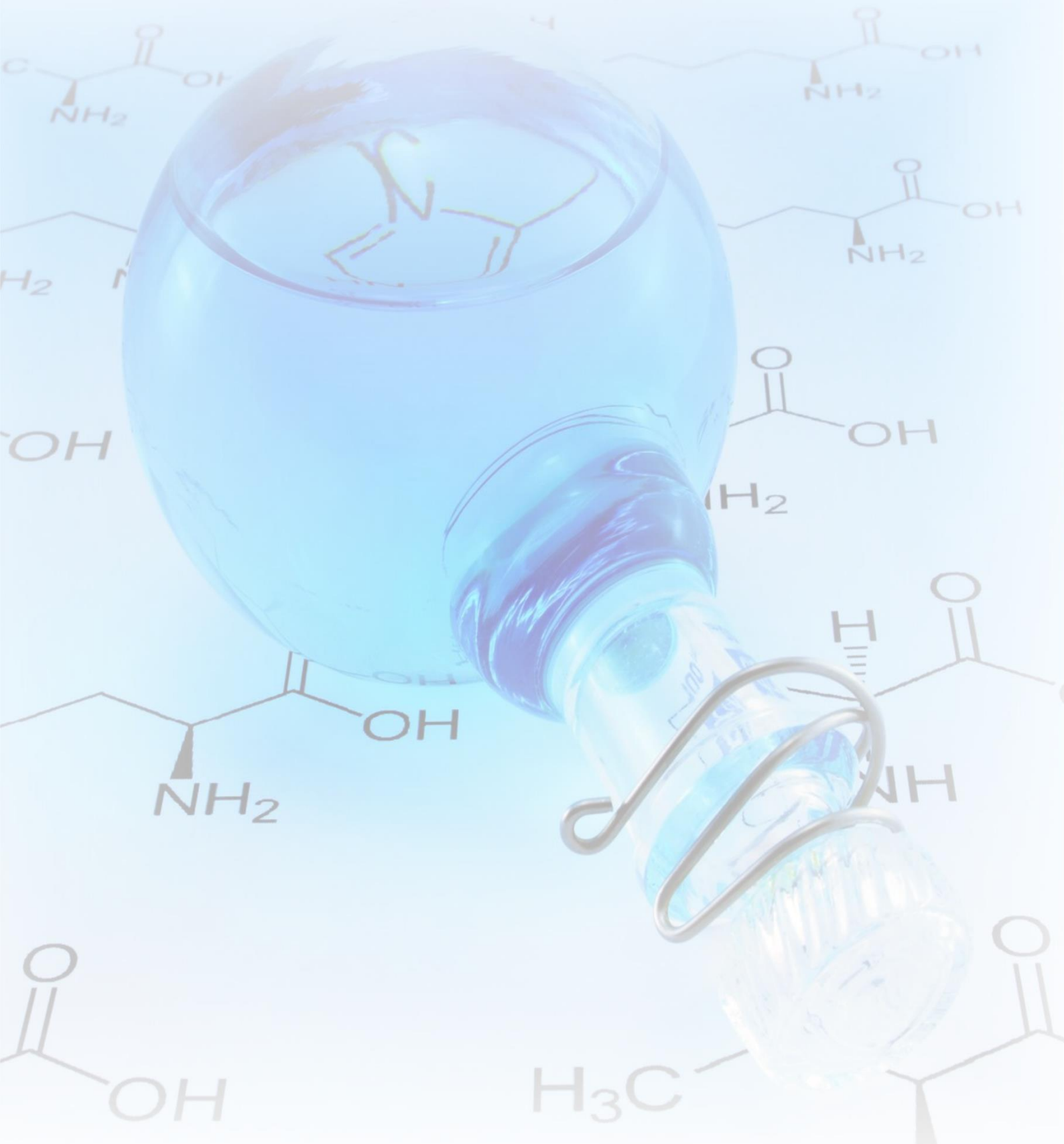
Mihal Đuriš, Zorana Arsenijević, Nevenka Bošković-Vragolović*, Radmila Garić-Grulović, Tatjana Kaluderović Radoičić

Koefficijent trenja pri strujanju vode kroz pakovani sloj sferičnih čestica.....	53
--	----

Pressure drop in packed beds of spherical particles at ambient and elevated air temperatures	54
<i>Tatjana Kaluđerović Radojičić, Radojica Pešić, Nevenka Bošković-Vragolović, Zorana Arsenijević, Mihal Đuriš</i>	
Pad pritiska u pakovanom sloju sferičnih čestica na sobnoj i povišenim temperaturama	57
Densities, viscosities and refractive indices of binary system N,N-dimethylaniline + 1-butyl-3-methylimidazolium triflate at 288.15 to 333.15 K and at atmospheric pressure	58
<i>Danijela Soldatović, Nikola Grozdanić, Jelena Vuksanović, Ivona Radović, Mirjana Kijevčanin</i>	
Gustina, viskoznost i indeks refrakcije binarnog sistema N,N-dimetilanilin+ 1-butil-imidazolium triflatna temperaturama od 288.15 do 333.15 K i na atmosferskom pritisku	62
Molecular interactions in the binary system diethyl succinate + 1-hexanol according to mixing deviation properties and FT-IR analysis	63
<i>Divna M. Majstorović, Emila M. Živković, Jovan D. Jovanović, Slobodan P. Šerbanović, Mirjana Lj. Kijevčanin</i>	
Molekulske interakcije prisutne u binarnom sistemu dietil sukcinat + 1-heksanol prema izvedenim veličinama mešanja i FT-IR analizi	67
Meat processing industry wastewater – screening analysis	68
<i>Maja M. Sremački, Jovana Lj. Simić, Jelena R. Radonić, Maja M. Turk Sekulić, Mirjana B. Vojinović Miloradov</i>	
Otpadna voda mesne industrije – skrining analiza	71
Study of pertechnetate adsorption from aqueous solution by surfactant-modified clinoptilolite	73
<i>Dorđe Petrović, Sonja Miličević, Ljiljana Matović, Andelka Đukić, Vladan Milošević, Divna Đokić, Ksenija Kumrić</i>	
Proučavanje adsorpcije pertehnetata iz vodenog rastvora primenom površinski modifikovanog klinoptilolita	76
Hemija i tehnologija hrane / Chemistry and Technology of Food	
Određivanje sastava masnih kiselina tokom fermentacije mleka kombuhom i konvencionalnim starter kulturama	78
<i>Snežana Kravić, Spasenija Milanović, Dajana Hrnjez, Zvonimir Suturović, Ana Đurović, Tanja Brezo, Zorica S. Stojanović</i>	
Determination of fatty acids during the fermentation of milk by kombucha and conventional starter cultures	81
Sadržaj sekundarnih metabolita i njihov uticaj na antioksidativnu aktivnost u različitim sortama jagoda	83
<i>Zoran Kukrić, Iva Martić, Ladislav Vasilišin, Goran Vučić</i>	
The content of secondary metabolites and their impact on the antioxidant activity in different varieties of strawberries	86
Hemija i tehnologija makromolekula / Chemistry and Technology of Macromolecules	
Comparative analysis of hydrolytic, enzymatic and degradation in compost of PCL/PEO diblock copolymers	87
<i>Marijana M. Ponjavić, Marija S. Nikolić, Jasmina Nikodinović-Runić, Sanja Jeremić, Sanja Stevanović, Jasna Djonlagić</i>	
Poređenje hidrolitičke, enzimske i degradacije u kompostu PCL/PEO diblok kopolimera	91
Neorganska hemija / Inorganic Chemistry	
Dinuklearni Pt(II) kompleksi kao efikasni katalitički reagensi za selektivnu hidrolizu peptida	92
<i>Snežana Rajković</i>	
Dinuclear Pt(II) complexes as effective catalytic reagents for the selective hydrolysis of peptides	96
Adsorpcija bakarnih jona na modifikovanom i nemodifikovanom zeolitu 5A	97
<i>Zora M. Levi, Jelena V. Penavin-Škundrić, Rada R. Petrović, Darko R. Bodroža</i>	
Adsorption of copper ions on modified and unmodified 5A zeolite	101
Organска hemija / Organic Chemistry	
Biološki aktivno vlakno sa ceftriaksonom	102
<i>Pero S. Sailović, Branka B. Rodić Grabovac, Ljiljana N. Topalić-Trivunović</i>	
Biologically active fiber containing ceftriaxone	105
Index Autora / Author Index	107

Plenarno predavanje

Plenary Lecture



Interactions of metal ions with old drugs

Iztok Turel

Department of Chemistry and Biochemistry, Faculty of Chemistry and Chemical Technology, University of Ljubljana,
Večna pot 113, SI-1000 Ljubljana, Slovenia

Introduction

One of important fields that bioinorganic chemistry deals with are interactions of metal ions with biologically important compounds. Without any doubt it was Rosenberg's discovery of cisplatin's cytotoxic properties¹ that was the most important cause for great interest and development in this field of chemistry.

Nowadays, it is well established that many drugs used in clinical practice require the presence of metal ions for their activity. On the other hand, metal ions can also react with drugs and decrease their activity (e.g. due to formation of sparingly soluble compounds). Moreover, it became evident that metal complexes of clinical drugs (that frequently contain electron donor atoms or groups) might exert increased or changed biological activity. With other words – a so called synergistic activity can occur.²

The design of a novel drug is a long-lasting and extremely expensive process.³ Therefore the repurposing of old drugs is very attractive topic nowadays. The quote of Sir James Whyte Black (winner of the 1988 Nobel Prize in medicine) that 'The most fruitful basis for the discovery of a new drug is to start with an old drug', is thus very stimulating.⁴

In the last two decades my lab was and still is involved in studies of metal ions interactions with drugs used in clinical practice (see Figure 1). In this review I will shortly present our efforts in the most representative systems. Quinolone antibacterial agents act most commonly as O,O- ligands. Bidentate bonding of oxygen atoms to the metal center is also typical for some ligands from non-steroidal anti-inflammatory drugs (NSAID) family and also pyrithione analogues (in some of these also O,S-coordination is possible). We have also studied interactions with molecules that contain nitrogen atoms which coordinate to the metal. Among these I will present the cases of antiviral drug acyclovir (N or N,O- binding) which is a representative of nucleobase molecules, antibacterial agent clioquinol and its derivatives (N,O- binding) and antifungal azoles (N- binding).

Results and discussion

Quinolones (also quinolonecarboxylic acids or 4-quinolones) are a group of synthetic antibacterial agents containing a 4-oxo-1,4-dihydroquinoline skeleton. More than 10000 analogues are known and more than thirty are or were used for the treatment of bacterial infections of humans and animals. Long ago Höffken *et al.*⁵ reported that concurrent administration of magnesium-aluminium containing antacid and quinolone family member ciprofloxacin (cfH) resulted in a nearly complete loss of activity of the drug in serum.

They have proposed that quinolones interact with metal cations through chelation between the metal and the 4-oxo and adjacent carboxyl groups. Several crystal structures with many metals reported later in the literature clearly confirm this hypothesis.⁶ These functional groups are also required for antibacterial activity, but it is well-known that magnesium ions which coordinate to this part of quinolone molecule are crucial for their activity. So on the one hand metal ions are required for their activity but on the other hand they can completely annul their biological effect. We have been working on the interactions of metal ions with quinolone molecules for many years and most of our results were obtained with this family of drugs. A variety of ligands from this group have been involved in these studies as well as many elements of the periodic table (B, Mg, V, Mn, Co, Ni, Cu, Zn, Ru, Eu and Bi). Apart from complete physico-chemical characterization, these complexes were evaluated in regard to the properties of the free ligand and the intrinsic biological properties of the metallic species (antibacterial tests, cytotoxicity, enzyme inhibition, interaction of complexes with DNA and serum proteins, etc). The most systematic work was performed on Mg, Cu and Ru complexes. We have been able to isolate a range of magnesium quinolone complexes and determined their crystal structures. Different metal:quinolone ratio and coordination mode of ligand was observed in these complexes. Importantly, these structures were used in studies dealing with details of quinolone mode of action.⁷ From the point of coordination chemistry, copper complexes of quinolones are very interesting and

versatile. We were able to isolate mixed-valence ($\text{Cu(II)}/\text{Cu(I)}$), mixed ligand (quinolone and N,N-ligand) and ionic type compounds (with protonated quinolones). In these complexes different coordination numbers and geometries were observed.⁸ In isolated ruthenium(II) complexes the quinolones are always bidentately coordinated to the metal through the ring carbonyl and one of the carboxylic oxygen atoms. It was revealed by various spectroscopic methods that these complexes interact with DNA and it was also shown that they can provoke DNA shrinkage. Although hydrolytic behaviour of these compounds is different there are no big differences in their interactions with human serum albumin. Most of compounds are not cytotoxic but moderate inhibitory potency against two enzymes of the cathepsin family was observed.⁹

Non-steroidal anti-inflammatory drugs (NSAIDs) are the most frequently used drugs used as analgesic, anti-inflammatory and antipyretic agents.¹⁰ There are several chemical classes of NSAIDs including salicylate derivatives, phenylalkanoic acids, oxicams, anthranilic acids, sulfonamides and furanones.¹¹ It was found that metal ions react with these drugs and metal complexes of NSAIDs have also exhibited synergistic activity. In the fruitful cooperation with Prof. G. Psomas from Aristotle University of Thessaloniki, a series of mixed-ligand complexes with various nitrogen donor heterocyclic ligands and NSAID ligands were prepared with several metals (Cu, Co, Mn, and Zn). For all these metal complexes interactions with DNA and serum proteins were tested. For some compounds their antioxidant and free radical scavenging activity as well as their *in vitro* inhibitory activity against soybean lipoxygenase was also studied.¹²

Transition metal ionophores are an emerging class of ligands used in the design of anticancer drugs and bioactive metal-based compounds.¹³ Pyrithione is the conjugate base obtained from 2-mercaptopypyridine-N-oxide which is a derivative of pyridine-N-oxide. Zinc pyrithione complex is used as a bacteriostatic and fungistatic agent in dandruff shampoos and baby zinc powder. This compound blocks the proton pumps¹⁴ and thus disrupts the membrane transport. We have studied the biological activity of two types of ruthenium complexes of zinc ionophores pyrithione and its oxygen-containing analogue 2-hydroxypyridine N-oxide. Apart from physico-chemical characterization, we have also examined the inhibition of AKR1C enzymes known to be implicated in pathophysiology of variety of cancers, including breast cancer, and their potential cytotoxic effects on the model cell line of hormone-dependent breast cancer MCF-7.¹⁵

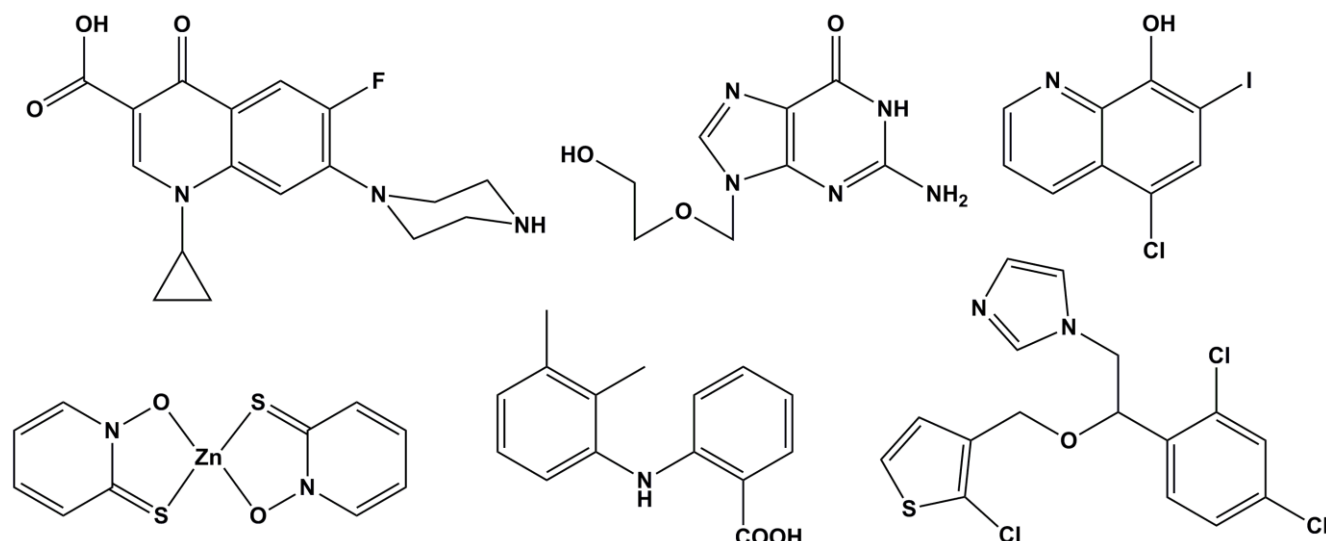


Figure 1. Clinically used drugs. Top – quinolone antibacterial agent ciprofloxacin (left), purine antiviral drug acyclovir (middle), and 8-hydroxyquinoline clioquinol (right); bottom – antifungal agent zinc pyrithione (left), NSAID mefenamic acid (middle) and azole antifungal tioconazole (right).

Antimetabolites prevent or inhibit the biosynthesis of normal cellular metabolites. Such compounds have usually a similar chemical structure to the metabolite that they interfere with¹⁶ and are for example used widely in chemotherapy. In anticancer therapy pyrimidine antimetabolites are frequently used and example of such drug is 5-fluorouracil (5-FU). Such compounds can interfere with nucleic acid replication not only in cancer cells but also viruses. Acyclovir (acv) is a well-known antiviral agent and has a strong activity against several DNA viruses (especially from the *herpes simplex* family). This

drug is a synthetic analogue of deoxyguanosine and has a well-established mode of action.¹⁷ The main feature of this mode is that acyclovir triphosphate is incorporated into the viral DNA and with this incorporation the viral DNA elongation is terminated. Not too many crystal structures of the metal complexes with the nucleobase or nucleoside analogues that are used as anticancer and antiviral agents were published. We have prepared copper, zinc and ruthenium complexes of acv and its analogues and studied their biological properties.¹⁸

8-Hydroxyquinoline (8-hqH) and its derivatives are excellent ligands and have been studied for a long time for various applications. For example, aluminium complexes exert luminescence properties and are component of organic light-emitting diodes (OLEDs). Their potential medical applications are extensively studied since these compounds have demonstrated activity as antimicrobial and anticancer agents and are also tested in the treatment of neurodegenerative diseases. Members of this family are well-known bidentate chelating agents that readily form metal complexes in the biological systems. Such complexes may exert various biological effects and can affect for example metal homeostasis, act as ionophores, inhibit enzymes and influence protein aggregation. Medicinal applications of 8-hydroxyquinolines and their metal chelating properties were reviewed recently.¹⁹ Interestingly, parent compound 8-hqH is also known to possess an antimalarial effect and it was reported that the inhibition of the malaria-causing *Plasmodium falciparum* and the chelating ability of the ligands were directly correlated.²⁰ Clioquinol (CqH) is also a member of a 8-hydroxyquinolone family and shows a wide range of biological activities. For many years it has been used as an antimicrobial agent, additionally, very encouraging data have been reported for clioquinol use in the treatment of Alzheimer's and Parkinson's diseases.²¹ We have synthesized and fully characterized the clioquinol–ruthenium complex and determined its crystal structure. The cytotoxicity studies show that it has antiproliferative activity in leukaemia cell lines that is mediated through caspase activation and is copper independent. The mechanism-of-action studies show that ruthenium complex of clioquinol does not intercalate between DNA base pairs and shows proteasome-independent inhibition of the NF κ B signalling pathway. Our findings provide an important step towards the elucidation of the precise mode of action of this metal complex and further studies are in progress.²²

Azole-type molecules are known sterol biosynthesis inhibitors. They prevent the growth of certain fungi and parasites by inhibiting the cytochrome P-450-dependent C-14- α demethylation of lanosterol to ergosterol and cholesterol, respectively. The latter two compounds are essential components of cell membranes.²³ Many of azole analogues were and some still are in clinical use, mostly as antifungal agents. We have prepared a set of ruthenium complexes with azole ligands. We wanted to test the antifungal potential of these novel ruthenium compounds and we were especially interested to see if blocking the N3 atom of azole drug results in the loss of the antifungal activity. We have selected a model fungal organism *Curvularia lunata* which is a known plant and human pathogen. On the other hand, due to the promising results of the ruthenium compounds against parasites causing tropical diseases reported in the literature we have also decided to perform the tests against the human parasite *Schistosoma mansoni* that causes schistosomiasis. Nine organoruthenium complexes of three azole antifungal agents (clotrimazole, miconazole and tioconazole) were synthesized and evaluated as potential antifungal and antiparasitic agents. It was found that ruthenium complexes statistically significantly reduced fungal growth rate at 0.5 mM concentration. Since in these novel ruthenium complexes N3 atoms of azole ligands cannot bind to the heme iron within the active site of lanosterol 14 α -demethylase, a different mechanism of inhibition is probable. The miconazole complexes have showed moderately good antischistosomal activity and we have observed the gender selectivity for one compound.²⁴

Conclusion

In bioinorganic chemistry the search for synergism by combining a metal ion to a bioactive ligand (e.g. drug) is a well-established concept. It is assumed that binding of the metal ion, even when the active site of the ligand seems thus blocked, can result in changed biological activity. In worst case the original activity can just be lost but positive effects can also be obtained (different type of activity, increased absorption, higher solubility, etc.). Our results from old drug-metal systems have clearly shown that such systems in ideal conditions might also be interesting for a design of novel drugs.

Acknowledgement: I am grateful for the financial support from the program grant P1-0175, funded by the Slovenian Research Agency (ARRS) and EN →FIST Centre of Excellence, Dunajska 156, SI-1000 Ljubljana for the use of the SuperNova diffractometer. Many thanks also to all collaborators involved in these studies.

Interakcije jona metala i jedinjenja sa poznatim farmakološkim svojstvima

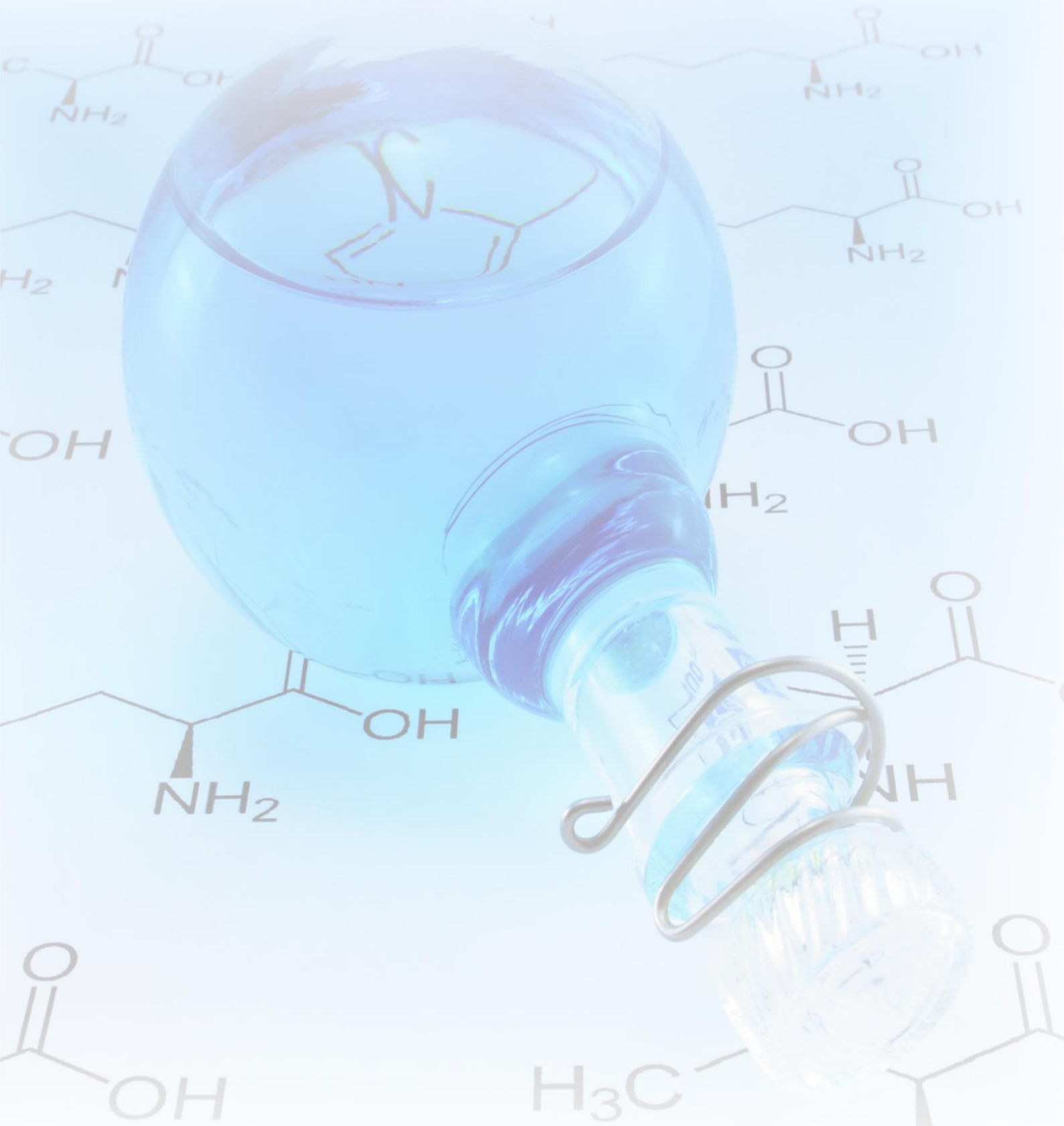
Vec duži niz godina veliki značaj u razvoju bioneorganske hemije ima ispitivanje sinergije interakcije jona metala sa biološki aktivnim ligandima. Pretpostavka je da koordinacija jona metala, iako blokira aktivno mesto liganda, može dovesti do promene njegove biološke aktivnosti pri čemu ligand može u potpunosti izgubiti aktivnost. Međutim, u pojedinim slučajevima ova aktivnost može biti povećana (različita aktivnost, veća absorpcija, veća rastvorljivost). Naši rezultati, dobijeni ispitivanjem reakcija jona metala i liganada sa već poznatim farmakološkim svojstvima, pokazuju da takvi sistemi u idealnim uslovima mogu biti od značaja za sintezu novih jedinjenja sa većom biološkom aktivnošću.

References

1. B. Rosenberg, L. Vancamp, J. E. Trosko, V. H. Mansour, *Nature*, **222** (1969), 385-386.
2. I. Turel, J. Kljun, *Curr. Top. Med. Chem.*, **11** (2011), 2661-2687 and the references therein.
3. D. J. Payne, M. N. Gwynn, D. J. Holmes, D. L. Pompiano, *Nat. Rev. Drug Disc.*, **6** (2007), 29-40.
4. T. N. K. Raju, *Lancet*, **355** (2000), 1022.
5. G. Hoffken, K. Borner, P. D. Glatzel, P. Koeppe, H. Lode, *Eur. J. Clin. Microbiol. Infect. Dis.*, **4** (1985), 345-345 and the references therein.
6. I. Turel, *Coord. Chem. Rev.*, **232** (2002), 27-47 and the references therein.
7. A. Wohlkonig, P. F. Chan, A. P. Fosberry, P. Homes, J. Z. Huang, M. Kranz, V. R. Leydon, T. J. Miles, N. D. Pearson, R. L. Perera, A. J. Shillings, M. N. Gwynn, B. D. Bax, *Nat. Struct. Mol. Biol.*, **17** (2010), 1152-1153.
8. J. Kljun, A. K. Bytzek, W. Kandioller, C. Bartel, M. A. Jakupc, C. G. Hartinger, B. K. Keppler, I. Turel, *Organometallics*, **30** (2011), 2506-2512; P. Drevensek, N. P. Ulrich, A. Majerle, I. Turel, *J. Inorg. Biochem.*, **100** (2006), 1705-1713; P. Drevenšek, J. Košmrlj, G. Giester, T. Skauge, E. Sletten, K. Sepčić, I. Turel, *J. Inorg. Biochem.*, **100** (2006), 1755-1763; P. Drevenšek, T. Zupančič, B. Pihlar, R. Jerala, U. Kolitsch, A. Plaper, I. Turel, *J. Inorg. Biochem.*, **99** (2005), 432-442 and the references therein.
9. J. Kljun, I. Bratsos, E. Alessio, G. Psomas, U. Repnik, M. Butinar, B. Turk, I. Turel, *Inorg. Chem.*, **52** (2013), 9039-9052 and the references therein.
10. C. P. Duffy, C. J. Elliott, R. A. O'Connor, M. M. Heenan, S. Coyle, I. C. Cleary, K. Kavanagh, S. Verhaegen, C. M. O'Loughlin, R. NicAmhlaoibh, M. Clynes, *Eur. J. Cancer*, **34** (1998), 1250-1259.
11. J. E. Weder, C. T. Dillon, T. W. Hambley, B. J. Kennedy, P. A. Lay, J. R. Biffin, H. L. Regtop, N. M. Davies, *Coord. Chem. Rev.*, **232** (2002), 95-126.
12. A. Tarushi, Z. Karaflou, J. Kljun, I. Turel, G. Psomas, A. N. Papadopoulos, D. P. Kessissoglou, *J. Inorg. Biochem.*, **128** (2013), 85-96 and the references therein.
13. W. Q. Ding, S. E. Ling, *IUBMB Life*, **61** (2009), 1013-1018.
14. C. J. Chandler, I. H. Segel, *Antimicrob. Agents Chemother.*, **14** (1978), 60-68.
15. J. Kljun, M. Anko, K. Traven, M. Sinreich, Ž. Ude, E. E. Codina, J. Stojan, T. Lanišnik Rižner, I. Turel, *Dalton Trans.*, manuscript under revision.
16. D. A. Williams, T. L. Lemke, *Foye's principles of medicinal chemistry*. 5th ed.; Lippincott Williams & Wilkins: 2002.
17. G. B. Elion, P. A. Furman, J. A. Fyfe, P. Demiranda, L. Beauchamp, H. J. Schaeffer, *Proc. Nat. Acad. Sci. U.S.A.*, **74** (1977), 5716-5720.
18. I. Turel, M. Pečanac, A. Golobič, E. Alessio, B. Serli, A. Bergamo, G. Sava, *J. Inorg. Biochem.*, **98** (2004), 393-401 and the references therein.
19. V. Prachayasittikul, S. Prachayasittikul, S. Ruchirawat, V. Prachayasittikul, *Drug Des. Devel. Ther.*, **7** (2013), 1157-1178.
20. L. W. Scheibel, A. Adler, *Mol. Pharmacol.*, **22** (1982), 140-144.
21. P. A. Adlard, R. A. Cherny, D. I. Finkelstein, E. Gautier, E. Robb, M. Cortes, I. Volitakis, X. Liu, J. P. Smith, K. Perez, K. Laughton, Q. X. Li, S. A. Charman, J. A. Nicolazzo, S. Wilkins, K. Deleva, T. Lynch, G. Kok, C. W. Ritchie, R. E. Tanzi, R. Cappai, C. L. Masters, K. J. Barnham, A. I. Bush, *Neuron*, **59** (2008), 43-55.
22. M. Gobec, J. Kljun, I. Sosič, I. Mlinarič-Raščan, M Uršič, S. Gobec, I. Turel, *Dalton Trans.*, **43** (2014), 9045-9051.
23. D. J. Sheehan, C. A. Hitchcock, C. M. Sibley, *Clin. Microbiol. Rev.*, **12** (1999), 40-79.
24. J. Kljun, A. J. Scott, T. Lanišnik Rižner, J. Keiser, I. Turel, *Organometallics*, **33** (2014), 1594-1601.

Predavanje po pozvu

Invited Lecture



Proces recenziranja radova u časopisima iz hemije i srodnih oblasti koji se izdaju u Srbiji

Ivana Drvenica, Aleksandar Dekanski*, Olgica Nedic**

Inovacioni centar Tehnološko-metalurškog fakulteta, Univerzitet u Beogradu, Srbija (ikostic@tmf.bg.ac.rs)

**Institut za hemiju, tehnologiju i metalurgiju, Centar za elektrohemiju, Univerzitet u Beogradu, Srbija*

***Institut za primenu nuklearne energije (INEP), Univerzitet u Beogradu, Srbija*

Uvod

Kvalitet naučnog časopisa u kojem su štampani radovi je kategorija na osnovu koje se vrednuje učinak pojedinačnog istraživača i naučnih timova, čime se utiče na napredovanje u naučnim zvanjima, dobijanje projekata (pa i zaposlenja), definiše se prepoznatljivost u oblasti, institucije se rangiraju na nacionalnom i međunarodnom nivou. Vrednovanje časopisa je zato često predmet interesovanja naučne javnosti. Postoje nekoliko metoda vrednovanja časopisa, pre svega kvantitativnih, a u cilju njihovog rangiranja [1–3]. Najpoznatije je vrednovanje uticajnosti časopisa putem Impakt faktora - IF (Science Citation Index Expanded™, dostupan preko Web of Science™)[4]. Vodi se intenzivna debata o pozitivnim i negativnim aspektima evaluacije časopisa preko IF, a posebno pojedinačnih radova i autora. Vrednost jednog rada se svakako ne može meriti samo posredstvom IF časopisa u kojem je objavljen. Praksa je pokazala da su neki izuzetno kvalitetni radovi (koji su kasnije bili među najcitanijim u svetskim razmerama) prvo odbijeni u časopisima sa velikim IF, a zatim štampani u časopisima sa manjim IF [5]. Za procenu kvaliteta autora, Jorge E. Hirsch je pre desetak godina ustanovio parametar koji je po njemu dobio ime Hirsch index, ili skraćeno h-index [6], a koji meri uticajnost autora preko broja citata svih njegovih radova. Naravno, i ovaj način vrednovanja ima svoje mane, jer će autori koji duže objavljaju radove, logično, imati veći h-index.

Bez obzira kako se vrši vrednovanje kvaliteta časopisa, preduslov je da radovi objavljeni u njemu budu kvalitetni (donose nove, značajne i korisne rezultate) i da budu citirani. Jedan od ključnih činilaca u tom nastojanju je kvalitetna i kompetentna recenzija. Zato je na recenzentima velika odgovornost, kao i na urednicima i uređivačkim odborima koji traže recenzente. Časopisi primenjuju različite uređivačke politike i postupke recenziranja u cilju dobijanja kvalitetnih recenzija, od kojih su do danas poznata četiri osnovna [7]:

- jednostruko slepo (single blind - recenzent zna identitet autora),
- dvostruko slepo (double blind, identiteti autora i recenzenta su međusobno nepoznati),
- otvoreno recenziranje (open peer review, svi identiteti su poznati) i
- recenziranje nakon publikovanja (post publication review, neograničeni komentari).

U izdavaštvu naučnih publikacija bitno je insistirati na nekim opštim preporukama:

- a. jasno definisan delokrug rada časopisa (da bi recenzenti prepoznali oblasti kojim se bave),
- b. transparentnost i postojanje sajta časopisa sa definisanim pravilima publikovanja u časopisu,
- c. pozivanje svetskih eksperata da budu recenzenti ili deo uređivačkog odbora,
- d. davanje dovoljno vremena recenzentima da urade recenzije,
- e. davanje jasnih instrukcija recenzentima o tehničkim i suštinskim zahtevima pri recenziranju,
- f. izbegavanje konflikta interesa,
- g. primena On-Line sistema za podnošenje i obradu radova i recenzija i slično.

Dosadašnja iskustva su pokazala da su autori često nezadovoljni brzinom i kvalitetom recenzije. Smatraju da proces predugo traje, a da su recenzije koje dobiju nekad nekompetentne, pristrasne i neprofesionalno napisane. Mora se priznati da je to, nekada, tačno. Osim subjektivnog utiska, međutim, autori obično nisu upoznati sa teškoćama na koje nailazi uredništvo časopisa, da bi proces recenziranja bio brz i kvalitetan.

U cilju unapređenja procesa recenziranja naučnih radova u oblasti hemije, hemijske tehnologije i srodnih naučnih disciplina koji se publikuju u Srbiji (ali i procesa recenziranja uopšeno), napravljeno je istraživanje kroz anketu namenjenu urednicima časopisa iz navedenih oblasti. Cilj ankete je bio da se sagledaju problemi sa kojima se uredništva časopisa sreću u procesu recenziranja radova, od pronalaženja kompetentnih reczenzata, kvaliteta recenzija, do odgovornosti i ažurnosti reczenzata. Pored toga, kroz anketu smo želeli da saznamo stavove i mišljenja urednika o najvećim problemima u procesu recenziranja i rešenjima koja oni vide za unapređenje tog procesa i podizanje kvaliteta

recenzija. Istraživanje je realizovano kao deo aktivnosti autora rada u okviru COST akcije TD1306, pod imenom: New frontiers of peer review (PEERE) [8].

Eksperimentalni deo

Kriterijum za izbor časopisa koji će biti uključen u anketu bio je da objavljuje radove iz oblasti hemije, hemijske tehnologije i srodnih disciplina, da redovno izlazi i da je kategorisan u skladu sa odlukom o kategorizaciji časopisa koji izlaze u Srbiji, a koju donosi Ministarstvo nadležno za naučnoistraživačku delatnost. Pregledom raspoloživih podataka našli smo 27 takvih časopisa.

Anketa se sastojala iz pitanja podeljenih u dva dela. Prvi deo se odnosio na opšte podatke o časopisima i na njih su odgovarali samo glavni i odgovorni urednici, dok je drugi deo ankete bio namenjen svim urednicima časopisa (područni, sekcijski) i odnosio se na proces recenziranja.

Poziv za popunjavanje ankete poslat je sredinom oktobra 2015. godine na adresu 70 urednika iz 27 časopisa, a zaključen je sredinom decembra 2015., nakon što je u dva navrata poslat podsetnik i ponovljena molba za popunjavanje. Odgovor je primljen od 50 urednika (71,4 % od broja pozvanih) iz 22 časopisa (81,5 %).

Rezultati i diskusija

Opšti podaci o časopisima

U Tabeli 1 prikazani su osnovni podaci za časopise, dobijeni od glavnih i odgovornih urednika. Za pet časopisa nismo primili odgovore, te su podaci za tabelu prikupljeni indirektno, najčešće sa internet sajtova samih časopisa. Za neke od navedenih podataka nismo sigurni (indirektno smo zaključivali na osnovu raspoloživih podataka), a neke podatke nismo uspeli da pronađemo. Sve ove nesigurnosti su označene u Tabeli 1 znakom upitnika (?). Od 27 časopisa obuhvaćenih anketom, 18 (66,7 %) ima samo glavnog i odgovornog urednika. Većina (22 ili 81,5 %) je u režimu slobodnog pristupa sadržaju časopisa (Open Access). Samo 4 časopisa (15,0%) imaju On-Line sistem prijema i obrade radova i isto toliki broj deo procesa (najčešće prijem radova) sprovodi On-Line, a ostatak putem elektronske pošte. Najveći broj časopisa (23 ili 85,2 %) se delimično (17 ili 63,0 %) ili potpuno (6 ili 22,2 %) finansira uz pomoć nadležnog Ministarstva, dva časopisa (7,4 %) se samostalno finansiraju, a jedan (3,7 %) finansiraju sponzori. Za jedan časopis nije bilo moguće ustanoviti način finansiranja. Na osnovu dobijenih odgovora i dostupnih podataka ustanovljeno je da dve trećine časopisa (18) ima definisano uputstvo za recenzente.

Proces recenziranja radova

Postavljanjem nekoliko konkretnih pitanja, prikupljeni su osnovni podaci o procesu recenziranja u navedenim časopisima. U nekim časopisima više urednika (glavni, sekcijski, područni) nezavisno sprovode postupak recenziranja, pa je i obrada dobijenih odgovora sprovedena tretirajući svaki odgovor nezavisno. Drugim rečima, odgovori nisu stavljeni u korelaciju sa časopisom u kojem je učesnik ankete urednik. U daljem tekstu biće prikazana kratka analiza odgovora na svako od pitanja.

Na koji način najčešće tražite recenzente? Pored nekoliko ponuđenih odgovora, urednik je mogao nавести i dodatni način („drugo“). Bilo je moguće izabrati više odgovora, te je 50 urednika dalo ukupno 120 odgovora. Na Slici 1 prikazana je raspodela odgovora, po broju i procentnom udelu u ukupnom broju. Napomenimo da se pod „drugo“ pored opisanih navode i sledeći odgovori: Recenzente predlaže Uređivački odbor na osnovu oblasti istraživanja/tematike; Pitam priznate stručnjake iz (navedene dve skraćenice); Pitam kolege iz tražene oblasti da predlože inostrane autore kao recenzente.

Kolikom broju reczenata se obraćate u prvom krugu? Tražite li potvrdu recenzenta da će uraditi recenziju? Da li podsećate recenzenta koji je prihvatio da recenzira rad, ukoliko kasni sa odgovorom? Većina urednika (54,0 %) se u prvom krugu obraća samo jednom ili dvoje reczenata, njih 28,0 % pozive šalje na tri adrese, jedan (4,0 %) na četiri, a 16,0 % na više od četiri adrese. Očigledno je da je praksa traženja reczenata vrlo raznolika. Takođe je očigledno da se određeni broj urednika, od početka, zadovoljava idejom da ima samo jednu recenziju za rad, što nije preporučljivo. Većina urednika (86,0 %) traži potvrdu recenzenta da prihvata recenziranje rada i podseća ga (94,0 %) ukoliko recenzija nije poslata u zahtevanom roku.

Tabela 1. Osnovni podaci o časopisima

Časopis	Odgovorno lice ¹	Broj urednika	Broj članova uredništva	Finansiranje ²	Open Access	Prijem i obrada radova ³	Uputstvo za recenzente	Participacija autora	Jezik publikovanja	Referisan u WoS	IF 2014	Kategorija	Svezaka godišnje	Radova godišnje
Acta Period. Technol.	Glavni		13	MPNTR	■	E-mail			Eng		M24	1	25	
Arhiv za farmaciju	Glavni		21	Samostalno	■	E-mail	■		Srp-Eng		M52	6	25	
CI&CEQ	Glavni		30	MPNTR +	■	E-mail/OL		■	Eng	■	0,892	M23	4	60
FU Phys. Chem. Tech.	Glavni + 1	1	15	MPNTR +	■	On-Line	■		Eng		M52	2	6	
Hem Ind.	Glavni + 7	7	17	MPNTR +	■	E-mail/OL	■	■	Srp-Eng	■	0,364	M23	6	75
Hemski pregled	Glavni +		8	MPNTR +	■	E-mail			Srp		M53	6	20	
Int. J. Electrochem. Sci.	Glavni		39	Samostalno	■	E-mail	■	■	Eng	■	1,500	M23	12	750
J. Med. Biochem.	Glavni		36	MPNTR +	■	E-mail	■		Eng	■	1,045	M23	4	45
J. Min. Met. B	Glavni	2	37	MPNTR	■	On-Line	■		Eng	■	0,832	M22	2	15
J. Serb.Chem. Soc.	Glavni + 15	15	58	MPNTR +	■	On-Line	■		Eng	■	0,871	M23	12	130
Kragujevac J. Sci.	Glavni		15	MPNTR		E-mail	■		Eng	■	0,000	M23	1	25
MATCH	Glavni		25	MPNTR +		E-mail	■		Eng	■	1,466	M21	6	100
Matica srpska J. Nat. Sci.	Glavni		18	MPNTR	■	E-mail			Eng			M51	2	22
Nucl. Technol. Rad. Prot.	Glavni		8	MPNTR +	■	E-mail	■		Eng	■	0,560	M23	4	55
Proc. Appl. Ceramics	Glavni		20	MPNTR +	■	E-mail/OL	■		Eng			M24	4	30
Reciklaža i održivi razvoj	Glavni +		12	Sponzor	■	E-mail	■		Srp-Eng			M52	1	5
Adv. Techn.	Glavni		22	MPNTR	■	E-mail	■		Eng			M52	2	25
Tehnika	Glavni +		10	MPNTR +		E-mail	■		Srp-Eng			M52	6	14
Therm. Sci.	Glavni		13	MPNTR +	■	E-mail	■	■	Eng	■	1,222	M21	6	210
Voda i sanitarna tehnika	Glavni		6	MPNTR +		E-mail/OL	■		Srp-Eng			M51	6	30
Vojnotehnički glasnik	Glavni	4	32	MPNTR	■	On-Line	■		Srp-Eng			M51	4	40
Zaštita materijala	Glavni		27	MPNTR +	■	E-mail	■		Srp-Eng			M24	4	65
Sci. Sint.	Glavni + 28 (?)	28 (?)	31	MPNTR + ?	■	E-mail	?		Eng	■	0,575	M23	3	36
Bakar	Glavni		19	MPNTR + ?	■	E-mail	?		Srp ?			M52	2	20
Metallur. Mat. Eng.	Glavni	11	17	MPNTR +	■	E-mail			Eng			M51	4	28
Sci. Tech. Rev.	Glavni +		20	MPNTR + ?	■	Poštom ?	?		Eng			M52	4	30
Svet polimera	Glavni ?		12	Pretplata ?		E-mail ?	?		Srp			M52	4	30

¹ Glavni – časopis ima samo jednog, glavnog i odgovornog urednika, Glavni + - časopis sem glavnog uređuju i područni, sekcijski.... urednici

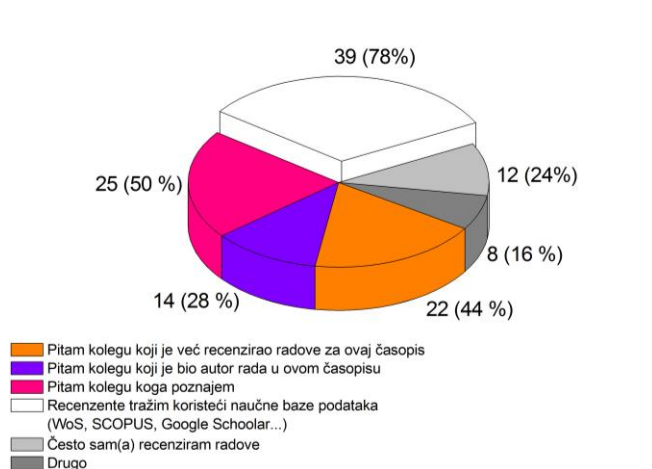
² Način finansiranja časopisa: MPNTR – potpuno od strane Ministarstva za prosvetu, nauku i tehnološki razvoj; MPNTR + delom od strane Ministarstva

³ Način podnošenja rukopisa i postupak recenziranja: E-mail – isključivo elektronskom poštom; E-mail/OL – delom elektronskom poštom, delom On-Line; On-Line – isključivo On-Line

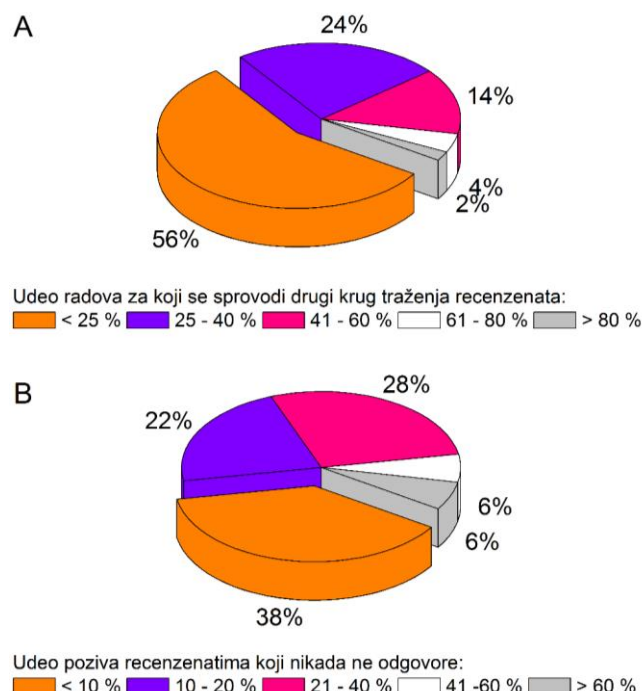
Na anketu nisu odgovorili glavni urednici poslednjih 5 časopisa, te su podaci u Tabeli navedeni na osnovu informacija pronađenih na internet stranicama časopisa. Uz nepouzdane i/ili nepostojeće podatke je upisivan upitnik (?).

Za koliko radova (u % na godišnjem nivou) morate sprovesti drugi krug traženja reczenzata? Po Vašoj proceni, koliki je udeo (%) poziva recenzentima na koje nikad ne dobijete odgovor?

Grafički prikaz raspodele odgovora na ova dva pitanja dat je na Slici 2. Dok je broj urednika koji češće moraju da traže recenzente u drugom krugu (za više od 40,0 % od ukupnog broja radova) 10 (20,0 %) – Slika 2A, broj urednika koji za više od 40,0 % poslatih poziva nikada ne dobiju odgovore je 6 (12,0 %) – Slika 2B.



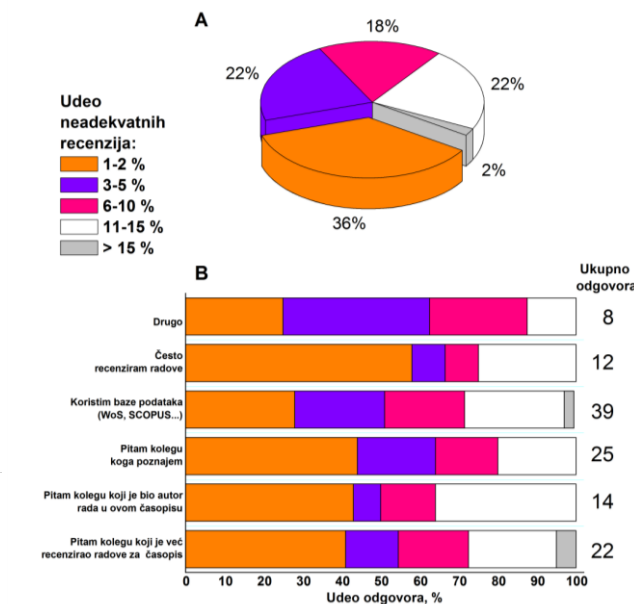
Slika 1. Način na koji urednici traže recenzente.



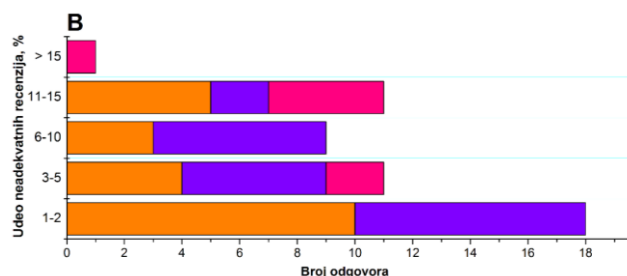
Slika 2. Raspodela odgovora na pitanja:

- A - Za koliko radova (u % na godišnjem nivou) morate sprovesti drugi krug traženja reczenzata? i
B - Po Vašoj proceni, koliki je udeo (%) poziva recenzentima na koje nikad ne dobijete odgovor?

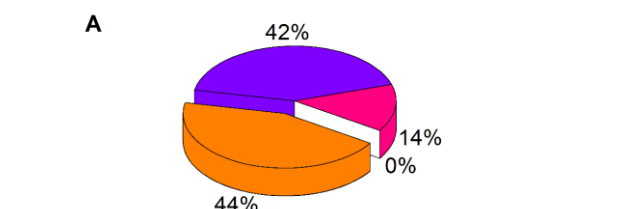
Po Vašoj proceni, koliki je udeo (%) neadekvatnih recenzija (nestručne ili sadrže nekorektne komentare)? Broj neadekvatnih recenzija, koje podrazumevaju i neetičke komentare, nije veliki. Samo jedan urednik (2,0 %) je naveo da prima više od 15,0 %, a njih 11 (22,0 %) 11-15,0 % neadekvatnih recenzija. Istovremeno, više od polovine reczenzata (58,0 %) prima do 5,0 %, a nešto više od trećine (36,0 %) do 2,0 % nestručnih ili nekorektnih recenzija (Slika 3A). Kada se broj ovih recenzija analizira u odnosu na način na koji urednici traže recenzente (Slika 3B), uočljivo najmanji broj neadekvatnih recenzija dobijaju urednici koji često sami recenziraju radove. Naime, blizu 70,0 % njih dobija do 5,0 %



Slika 3. A – Raspodela odgovora na pitanje: Po Vašoj proceni, koliki je udeo (%) neadekvatnih recenzija (nestručne ili sadrže nekorektne komentare)? i B – Raspodela odgovora na isto pitanje u zavisnosti od načina traženja reczenzata.



A



B

Legend: dobre (orange), pretežno dobre (purple), podjednaki broj dobrih i loših (pink), loše (white).

Slika 4. A – Raspodela ocena kvaliteta recenzija; B – Udeo neadekvatnih recenzija

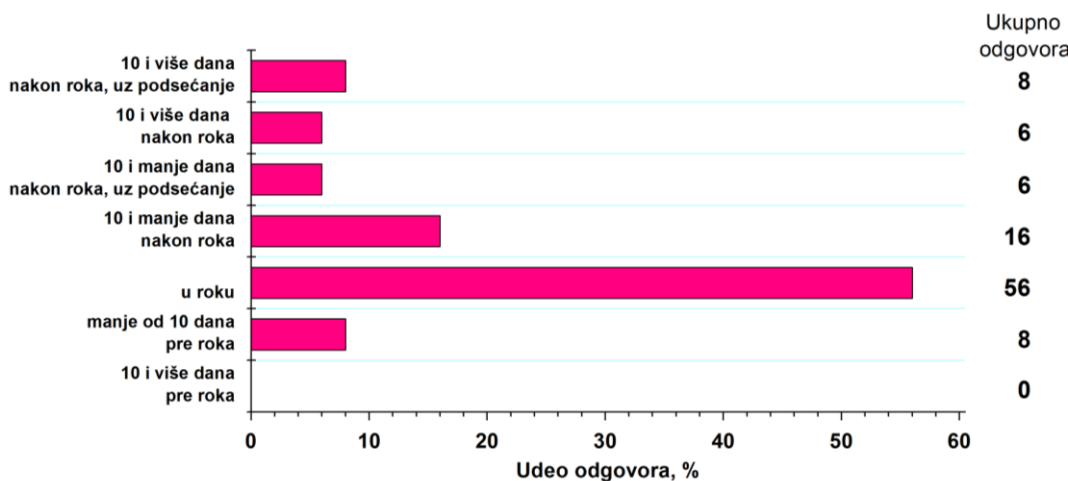
takvih recenzija, a više od 50,0 % do 2,0 %. S druge strane, 50,0 % urednika koji se pri traženju recenzentata oslanjaju na naučne baze, kao i oni koji za recenzente pozivaju kolege koje su prethodno bili autori u istom časopisu, dobija više od 5,0 % neadekvatnih recenzija. Čak 35,0 % urednika koji pozivaju kolege koje su objavljivale u časopisu dobija više od 10,0 % neadekvatnih recenzija.

Kako ocenjujete kvalitet recenzija (stručnost, jasnoća, dobromernost u cilju poboljšanja kvaliteta rada)?

Slika 4A jasno pokazuje da ni jedan urednik ne dobija pretežno loše recenzije. Samo 7 njih (14,0 %) smatra da dobija podjednak broj dobrih i loših recenzija, dok 22 ili 44,0 % dobijaju uglavnom dobre, a 21 ili 42,0 % pretežno dobre recenzije, ukupno 86,0 %. Ako se isti podaci prikažu u korelaciji sa brojem neadekvatnih recenzija (Slika 4B), dobija se sledeći rezultat – urednici koji smatraju da primaju više neadekvatnih navode da primaju i više loših recenzija. I obrnuto. Dobijeni podaci upućuju na pretpostavku da se urednici mogu grupisati prema ličnom kriterijumu. Neki su, uglavnom, zadovoljni kvalitetom recenzija i ne primećuju neadekvatne tonove u izveštajima. Drugi su znatno kritičniji i u pogledu kvaliteta recenzije i etičkih principa.

U proseku, u kom roku dobijate recenzije?

Nepoštovanje roka za slanje recenzija je često veliki problem urednika, a i autora koji iščekuju evaluaciju svojih radova. Ipak, većina anketiranih urednika u ovoj studiji (64,0 %) je izjavila da recenzije uglavnom dobija u roku (56,0 %) ili čak pre roka (8,0 %) (Slika 5). Ako se ovom broju dodaju i urednici koji najčešće dobijaju recenzije do 10 dana nakon roka, bez (16,0 %) ili nakon podsećanja recenzentata (6,0 %), moglo bi se zaključiti da je najveći broj recenzentata odgovoran i svestan važnosti slanja izveštaja na vreme. Samo 14,0 % urednika izveštaje recenzentata uglavnom dobija sa više od 10 dana zakašnjenja.



Slika 5. Raspodela odgovora na pitanje: U proseku, u kom roku dobijate recenzije?

Na šta biste dodatno skrenuli pažnju u postupku recenziranja? Šta biste predložili u cilju poboljšanja postupka recenziranja i povećanja kvaliteta recenzija?

Anketirani urednici su, na kraju upitnika, imali mogućnost da u slobodnoj formi ukažu na probleme sa kojim se sreću u procesu recenziranja (PRIMEDBE) i da predlože mere poboljšanja (SUGESTIJE). Pristigle primedbe i sugestije smo sistematizovali po tematskim grupama (Tabela 2).

Četiri urednika su navela da nailaze na predrasude recenzentata i tom pitanju je potrebno posvetiti dodatnu pažnju. Poznanstvo autora i recenzenta može biti uzrok neopravdano pozitivne ili negativne recenzije. Takođe, neke studije su pokazale da radovi autora iz zemalja u razvoju ili neuticajnih institucija češće (neopravdano) dobijaju loše recenzije, dok se radovi iz prestižnih institucija, iza kojih stoje poznata imena u naučnoj sredini, ponekad (neopravdano) „propuste“ u postojećoj formi [9]. Ukoliko su u pitanju „etičke predrasude“, tj. kada je recenzija smisljeno i zlonamerno negativna, bez obzira na kvalitet rada, autore tih recenzija bi trebalo staviti na „crnu listu“, a možda preuzeti i sankcije prema njima (na primer, javno ih imenovati ili im onemogućiti publikovanje u časopisu na određeni period). Načelno, kvalitetni radovi i profesionalni odnos uredništva su preduslovi za dobru reputaciju časopisa i pozitivan odnos recenzentata.

Tabela 2. Primedbe i sugestije urednika za proces recenziranja

Primedbe	Učestalost	Sugestije	Učestalost
Loš odziv reczenata	13/32	Prepoznavanje rada reczenata (zahvalnica, bodovanje aktivnosti, licenca, širenje svesti o važnosti recenziranja)	11/26
Loš kvalitet recenzija	10/32	Detaljno uputstvo za recenzente, On-Line upitnik, nabavka programa za proveru plagijata	9/26
Predrasude reczenata	4/32	Izbegavanje sugestije autora za recenzente (ili ograničenje samo na jednog, uz obaveznu proveru zadovoljenja etičkih principa)	4/26
Tehničke prirode (podaci o samom časopisu)	3/32	Stvaranje odbora stalnih reczenata iz tematike časopisa (doprinosi kvalitetu i brzini recenziranja, možda uz plaćanje)	4/26
Nesnalaženje reczenata sa pravilima recenziranja i/ili On-Line sistemom	3/32	Zadovoljstvo postojećim stanjem, bez potrebe za promenom	4/26
Urednik kratko na dužnosti da bi imao primedbe	2/31	Veće angažovanje urednika u proveri kvaliteta radova pre slanja na recenziju	3/26
Plagijati radova	1/32	Recenzente tražiti među autorima	2/26
Zadovoljstvo postojećim stanjem	1/32	Dvostruko slepa recenzija	2/26
		Ograničenje vremena izrade recenzije na 30 dana	1/26
		Ograničenje broja recenzija po recenzentu za isti časopis	1/26
		Autorima dati mogućnost ocene kvaliteta recenzija	1/26
		Organizovanje edukativnih seminara o potrebi recenziranja, veću pažnju posvetiti mladim stručnjacima (više su motivisani)	1/26
		Isticanje pojedinačnog doprinosa autora	1/26

Deo predloženih sugestija za poboljšanje procesa recenziranja odnosi se na tehničku stranu procesa, odnosno postupke koji bi doprineli lakšem i bržem recenziranju (Tabela 2). Iako većina urednika navodi da časopis poseduje uputstvo za recenzente, nisu svi zadovoljni njegovim kvalitetom. Uvođenje On-Line sistema bi, prema mišljenju nekih urednika, pomoglo bržem i kvalitetnijem procesu recenziranja, ali, prema iskustvima drugih urednika, koji ga već koriste, postoji problem nesnalaženja izvesnog broja recenzenta u njemu.

Najveći broj urednika je sugerisao da se nešto učini u cilju prepoznavanja važnost recenziranja i njegovog vrednovanja (Tabela 4). I ovo pitanje dobija na aktuelnosti u svetskim razmerama, a veliki izdavači kreiraju svoje baze podataka reczenata kojima šalju sertifikate [10]. Pre nekoliko meseci je kreiran program i baza podataka, iza kojih stoji kompanija Publons, a omogućava sakupljanje i grupisanje svih recenzija koje je istraživač/recenzent uradio tokom svog radnog veka [9]. Kreatori Publons-a verifikuju materijal koji dobijaju od reczenata direktno kod izdavača. Jedan od načina da se prikupe podaci o procesu recenziranja je da se anketiraju autori i, eventualno, ocenjuju recenzenti [11]. Svest recenzenta da ga autor procenjuje i da će to mišljenje videti urednik, će svakako uticati na njegovu odgovornost i kvalitet recenzije. U okviru COST akcije TD1306: New frontiers of peer review [8], u toku je priprema jednog takvog istraživanja na međunarodnom nivou.

Zaključak

Najveći problemi sa kojima se urednici sreću u procesu recenziranja su slab odziv reczenata, recenzije lošeg kvaliteta, nekad uz predrasude reczenata i nesnalaženje i/ili nerazumevanje procesa recenziranja. Način traženja i pozivanja reczenata nema suštinskog uticaja na kvalitet recenzija. Značajan broj urednika često sam recenzira radove. Pozivanje reczenata na predlog autora, barem u anketiranim časopisima, relativno često je uzrok neadekvatnih recenzija.

Uvođenje On-Line procesa i kreiranje dobrih uputstava za recenzente, edukacija potencijalnih reczenata, kao i društveno, javno i profesionalno prepoznavanje i vrednovanje rada reczenata, urednici vide kao najbitnije faktore koji mogu unaprediti kvalitet celog procesa, pa time i kvalitet publikovanih radova i časopisa.

Podaci koje smo sakupili ostavljaju prostora za dodatnu analizu i korelaciju dobijenih odgovora sa brojem publikovanih radova, uticajnošću časopisa i drugim parametrima, ali u ovom radu smo izneli najosnovnije zaključke, sagledavajući sve časopise kao celinu.

Zahvalnica: Autori se zahvaljuju svim urednicima časopisa koji su uzeli učešća u anketi.

Peer-review process in journals dealing with chemistry and related subjects published in Serbia

A survey was conducted among editors of journals publishing in the field of chemistry, chemical technology and related topics in Serbia, aiming to collect information on their experiences, problems and difficulties during peer-review process. Editors from 22 journals out of 27 which regularly published during 2015 replied. Principle data on journals were collected from responses obtained from editors-in-chief, whereas all editors (including sub-editors and section editors) participated in a questionnaire concerning peer-review procedure. Additionally, they were asked to evaluate quality of reports and attitude of reviewers, discuss present situation and suggest measures to improve peer-review process.

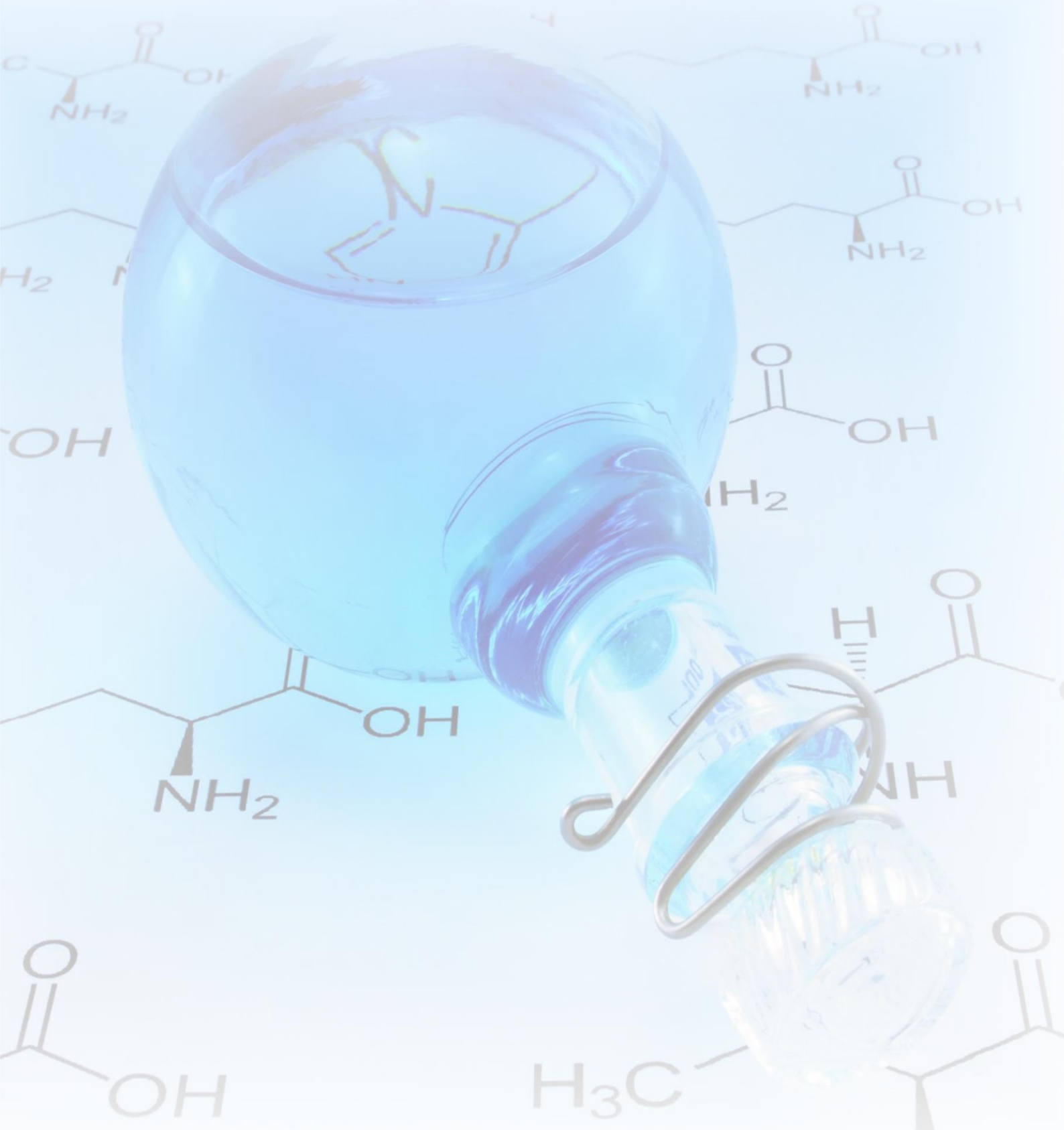
The greatest problems encountered by editors in peer-review proces can be summarized as follows: low rate of acceptance to review, low quality of reports, sometimes due to reviewer's bias or his/her inability to properly understand review process. A method used to search for reviewers does not substantially influence quality of reports. Significant number of editors often perform peer-review by him/herself. Invitation of reviewers suggested by authors, at least in the surveyed journals, also relatively often results in inadequate reports. Editors agree that introduction of On-Line process and creation of precise instructions for reviewers, education of potential reviewers, as well as social, public and professional recognition and appreciation of reviewers' work, are the most important measures to improve quality of peer-review process and, consequetively, quality of published articles and journals.

Literatura

1. J. Garner, A. L. Porter, and N. C. Newman, *Scientometrics* **100**(3) (2014) 687–703.
2. K. Iyengar, and V. Balijepally, *Scientometrics* **102**(1) (2014) 5–23.
3. G. Palla, G. Tibély, E. Mónes, P. Pollner, and T. Vicsek, *Palgrave Commun.* **1** (2015) 15016.
4. Web of Science - IP & Science - Thomson Reuters, <http://wokinfo.com/> (30. 01. 2016).
5. K. Siler, K. Lee, and L. Bero, *Proc. Natl. Acad. Sci.* **112**(2) (2014) 201418218.
6. J. E. Hirsch, *Proc. Natl. Acad. Sci. USA* **102**(46) (2005) 16569–72.
7. J. Patel, *BMC Med.* **12** (2014) 128.
8. New Frontiers of Peer Review (PEERE), <http://www.peere.org/peeer-in-a-nutshell/> (11. 01. 2016).
9. Get credit for peer review | Publons, <https://publons.com/> (16. 01. 2016).
10. Certificate of Excellence in Reviewing, <https://www.elsevier.com/reviewers-update/story/peer-review/certificate-of-peer-reviewing-excellence> (16. 01. 2016).
11. Economics Job Market Rumors, <http://www.econjobrumors.com/journals.php> (11. 01. 2016).

Saopštenja

Contributions



Analitička hemija / Analytical Chemistry

Primena plazme indukovane TEA CO₂ laserskim zračenjem za određivanje koncentracije magnezijuma u aluminijumskim legurama

Sanja M. Živković, Jelena Mutić*, Jelena Savović, Miloš Momčilović

Institut za nuklearne nauke "Vinča", Laboratorija za fizičku hemiju, PF 522, 11001 Beograd

**Univerzitet u Beogradu, Hemski fakultet, Studentski trg 12-16, pr. 158, 11000 Beograd*

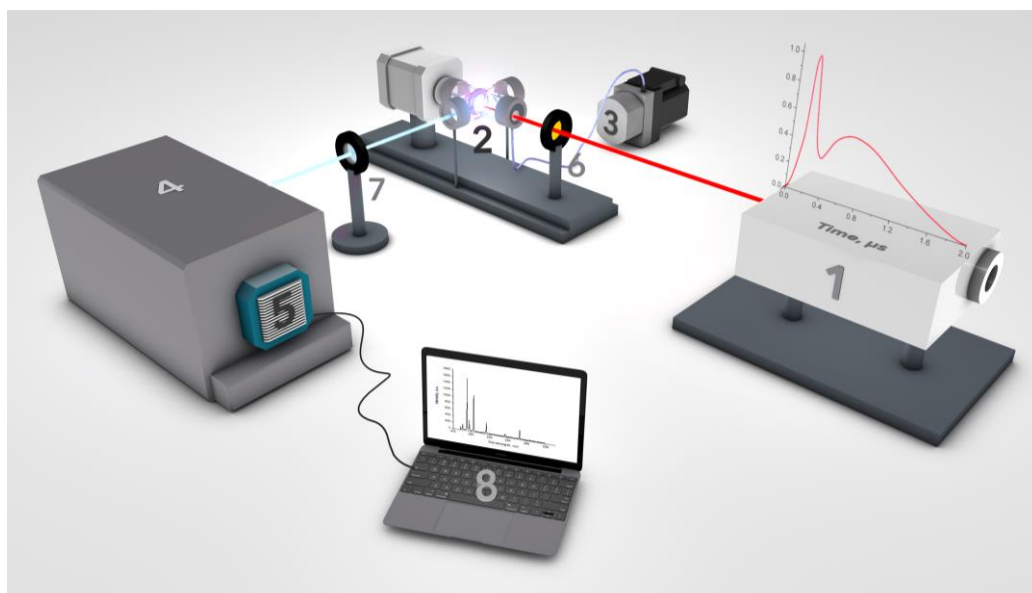
Uvod

Laserski indukovana plazma predstavlja široko korišćeni emisioni izvor za spektroskopiju. Ova analitička tehnika poznata je pod nazivom spektroskopija laserski indukovanih proba – LIBS (Laser Induced Breakdown Spectroscopy). LIBS se može koristiti za analizu bilo koje vrste uzorka (čvrstih, tečnih, gasovitih), najčešće bez prethodne pripreme a masa potrebna za analizu je vrlo mala¹. Zbog svoje univerzalnosti i jednostavnosti, LIBS je našla veliku primenu kao metoda spektrohemijske analize u različitim oblastima: geologiji, biohemiji, arheologiji, monitoringu životne sredine, praćenju industrijskih procesa, svemirskim istraživanjima i mnogim drugim¹⁻⁵. Brza i pouzdana analiza elemenata prisutnih u legurama veoma je važna za kontrolu kvaliteta proizvoda. Legure aluminijuma imaju veliku primenu u savremenoj industriji a jedan od glavnih legirajućih elemenata je magnezijum koji pojačava tvrdoću aluminijuma i otpornost na koroziju, ali istovremeno smanjuje formabilnost i provodljivost. Kvantitativna analiza legura aluminijuma LIBS-om često je bila predmet proučavanja⁶⁻⁸. Za ovu svrhu uobičajeno se koristi LIBS sistem koji se sastoji iz Nd:YAG lasera, spektrometra i detektora sa vremenskom rezolucijom. Primena TEA CO₂ laserskog zračenja ($\lambda=10,6\mu\text{m}$) za analizu metala i metalnih legura mnogo je ređa zbog manje energije fotona u odnosu na Nd:YAG laser, kao i visoke reflektivnosti metala u infracrvenom delu spektra. Sa druge strane, TEA CO₂ laser ima i prednosti zbog talasne dužine zračenja i vremenskog profila laserskog impulsa. Interakcija nanosekundnog laserskog impulsa sa metalnom metom dovodi do ablacije, isparavanja i ionizacije materijala, a pri dovoljno velikoj gustini snage i do stvaranja plazme iznad površine mete⁹. Indukovana plazma apsorbuje preostali deo TEA CO₂ laserskog impulsa kroz proces inverznog zakočnog zračenja, što dovodi dodatnog zagrevanja i povećanja ekscitacije. Apsorpcioni koeficijent plazme proporcionalan je kvadratu talasne dužine laserskog zračenja zbog čega je ovaj proces mnogo efikasniji za TEA CO₂ nego za Nd:YAG lasersko zračenje. Laboratorijski LIBS spektrometar na bazi TEA CO₂ lasera uspešno je primenjen za analizu bakra i njegovih legura i postignute su zadovoljavajuća osetljivost i niske granice detekcije^{3,4}. Cilj ovog rada je ispitivanje mogućnosti primene plazme indukovane TEA CO₂ laserom za određivanje Mg u legurama aluminijuma.

Eksperimentalni deo

Na slici 1. prikazan je šematski dijagram eksperimentalne postavke korišćene za LIBS analizu aluminijumskih meta. Za ovaj eksperiment korišćen je transverzalno ekscitovani atmosferski ugljendioksidni (TEA CO₂) laser koji je razvijen u Institutu Vinča¹⁰. Ovaj kompaktni, impulsni, nanosekundni laser radi u visoko multimodnom režimu i emituje zračenje u infracrvenom delu spektra na 10,6 μm. Karakteristike laserskog impulsa su sledeće: širina na polovini maksimuma visine početnog „pika“ iznosi oko 100 ns dok je dužina „repa“ impulsa oko 2μs. Uzorci su smešteni unutar staklene vakuumske komore čija je zapremina oko 500 cm³ i na čijim krajevima se nalaze prozori od NaCl i CaF₂. Komora je povezana sa vakuum pumpom, a pritisak vazduha tokom eksperimenta iznosio je 0,5 mbar. Površina uzorka ozračivana je laserskim snopom fokusiranim uz pomoć ZnSe sočiva koje je propusno za infracrveno zračenje i čija žižna duljina je 13,0 cm. Sočivo je smešteno u poseban metalni držać koji omogućava njegovo pomeranje do ± 2,0 cm u odnosu na položaj žiže. Upadni ugao laserskog zračenja u odnosu na površinu mete bio je 90° sve vreme ozračivanja. Za konstruisanje kalibracionih krivih korišćeni su sertifikovani uzorci (standardi) aluminijumskih legura, a koncentracije magnezijuma prikazane su u tabeli 1. Standardi legura aluminijuma AL-6016, AL-6063, AL-3105, AL-5005a i AL-6061 i kontrolni uzorak aluminijumske legure sa nepozatom koncentracijom magnezijuma AL-XX su bili u obliku diska prečnika 35 mm i debljine 5 mm. Pre ozračivanja, svi uzorci su tretirani standardnim metalografskim postupkom koji podrazumeva brušenje silicijum karbidnim brusnim papirom

granulacije 800, zatim ultrazvučno čišćenje alkoholom i sušenje u struji toploga vazduha. Za nastajanje stabilne i reproducibilne plazme neophodna je sveža površina uzorka između dva laserska impulsa što je postignuto rotacijom uzorka korišćenjem kontinualnog servo motora čija je brzina iznosila 0,5 o/min. Za spektralnu analizu plazme i merenja spektralnih linija magnezijuma korišćena je vremenski-intergraljena prostorno-razložena emisiona spektroskopija laserski indukovane plazme (TISR-LIPS). Ova metoda se zasniva na činjenici da se intenzivna emisija kontinuuma uglavnom emituje iz zone plazme koja je u neposrednoj blizini površine mete, dok sa udaljavanjem od mete intenzitet kontinualnog zračenja brzo opada. Zbog toga je moguće dobiti dobar odnos signala i pozadine snimanjem spektralne emisije iz prostorno razdvojenog dela plazme, bez vremenskog razdvajanja signala. Prednost ove metode, u odnosu na vremenski razloženu spektroskopiju laserski indukovane plazme, je smanjena kompleksnost i cena detekcionog sistema.



Slika 1. Šematski dijagram LIBS sistema. 1-TEA CO_2 laser i vremenski profil laserskog impulsa, 2-staklena vakuumska komora sa držačem uzora, 3-vakuum pumpa 4- monohromator, 5-CCD kamera, 6 i 7 sočiva, 8-računar

Optička emisija iz laserski indukovane plazme posmatrana je u pravcu paralelnom površini mete, na rastojanju 3 mm od površine mete. Izabrani deo plazme projektovan je pomoću ahromatskog sočiva na ulazni razrez Carl-Zeiss PGS2 monohromatora sa CCD kamerom ALTA F1007 kao detekcionim sistemom. U primjenjenim uslovima, laser je radio na frekvenciji 1,3 Hz dok je vreme ekspozicije kamere bilo 60 s za sve snimljene spekture. Dobijeni spektri odgovaraju akumulaciji ~ 80 uzastopnih spektara. Intenzitet laserskog zračenja kojim su ozračivane sve mete iznosio je 30 MW cm^{-2} .

Tabela 1. Koncentracije magnezijuma u standardima aluminijumskih legura

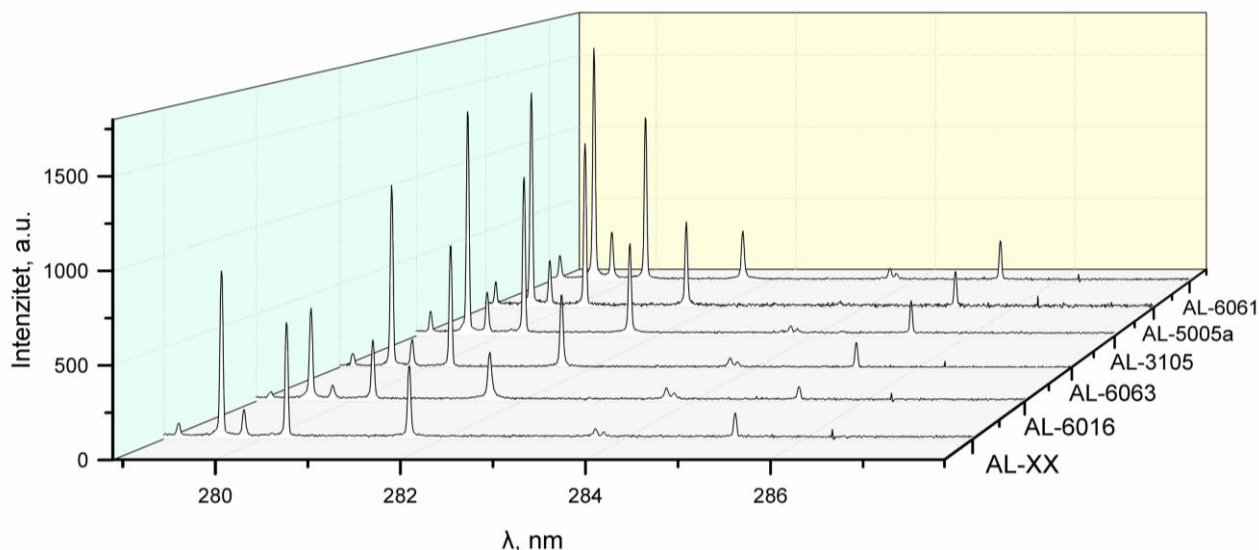
Oznaka	AL-6016	AL-6063	AL-3105	AL-5005a	AL-6061
$c_{\text{Mg}} / \% (\text{m/m})$	$0,26 \pm 0,01$	$0,49 \pm 0,01$	$0,70 \pm 0,02$	$0,78 \pm 0,01$	$1,10 \pm 0,01$

Referentna metoda – ICP-OES

Radi provere tačnosti dobijene koncentracije Mg u kontrolnom uzorku aluminijumske legure primenom LIBS tehnike, napravljen je špon mase 250 mg koji je tretiran sa 10 ml 36,46% HCl (Fisher Chemicals) i 2 ml 65% HNO_3 (Macron Fine Chemicals). Dobijeni rastvor razblažen je do 100 ml bidestilovanom vodom i analiziran na Spectroflame ICP spektrometru koji je prethodno kalibriran serijom kalibracionih rastvora dobijenih razblaživanjem standardnog rastvora magnezijuma koncentracije 1000 ppm (J.T. Baker).

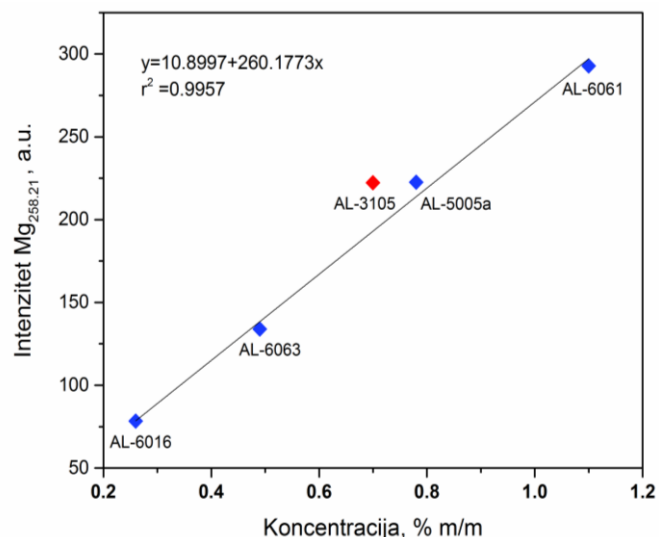
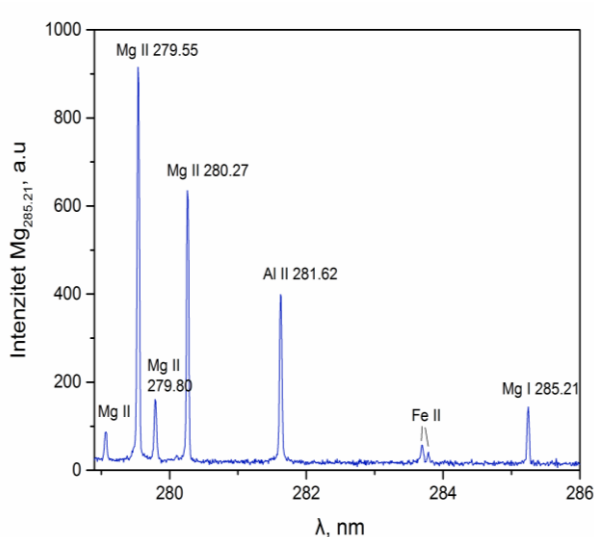
Rezultati i diskusija

Plazma je generisana ozračivanjem uzorka TEA CO₂ laserskim zračenjem u atmosferi vazduha na pristisku 0,5 mbar. Prostirala se oko 8 mm od površine mete i uočavala su se dva različita i jasno odvojena dela: a) primarna plazma veličine oko 1 mm izrazito bele boje i b) sekundarna plazma veličine oko 7 mm svetlo ljubičaste boje. Optička emisija plazme posmatrana je na 3 mm od površine mete i svaki spektar snimljen je tri puta. Vremenski-integraljeni spektri za Mg prikazani su na slikama 2 i 3. Spektri se sastoje od dobro razdvojenih, oštrih emisionih linija sa niskim intenzitetom emisije pozadine. Za konstruisanje kalibracione krive korišćeni su intenziteti koji su dobijeni *Lorencovim* fitovanjem atomske linije Mg (285,21 nm). Ova linija je izabrana zato što je simetrična, dovoljno osetljiva u ispitivanom opsegu koncentracije Mg i pored nje ne postoje linije koje se delimično preklapaju sa njom kao što je to slučaj kod jonskih linija Mg koje su intenzivnije.



Slika 2. 3D dijagram dobijenih spektara za sve uzorke u spektralnoj oblasti od 279-288 nm

Kalibraciona kriva Mg prikazana je na slici 4. Korelacija između LIBS signala (intenziteta emisionog pika) i koncentracije analita u standardima aluminijumskih legura bila je linearna u opsegu koncentracija 0,26 - 1,10 % m/m. Dobijeni rezultati određivanja nepoznate koncentracije magnezijuma u kontrolnom uzorku legure aluminijuma predstavljeni su kao srednja vrednost tri merenja \pm relativna greška ocitavanja i upoređeni sa rezultatima dobijenim ICP-OES metodom, tabela 2. Primenom *F*-testa upoređene su varijanse dobijenih rezultata radi poređenja preciznosti a primenom *t*-testa upoređene su eksperimentalno određene srednje vrednosti radi poređenja tačnosti. U tabeli 2. prikazane su izračunate i kritične vrednosti za parametre *F* i *t* (nivo poverenja 95%). Iz priloženog možemo videti je $F_{izr} < F_{krit}$, i $t_{izr} < t_{krit}$ odnosno da ne postoje statistički značajne razlike u preciznosti i tačnosti između ove dve metode.



Slika 3. Deo vremenski-integraljenog spektra plazme indukovane na meti AL-XX**Slika 4.** Kalibraciona kriva Mg za legure aluminijuma

Standardna devijacija pozadine σ , izmerena u okolini izabrane emisione linije, i nagib kalibracione krive s, iskorišćeni su za računanje limita detekcije ovog elementa pomoću formule LOD = $3\sigma/s^1$.

Tabela 2. Koncentracija Mg u kontrolnom uzorku AL-XX i vrednosti dobijene primenom F i t testa

LIBS	ICP-OES	F_{izr}/F_{krit}	t_{izr}/t_{krit}	LOD	
$c_{Mg} / \% (m/m)$	$0,50 \pm 0,04^*$	$0,496 \pm 0,009$	3,67/19,00	3,02/3,18	0,008 (0,01)

* procenjena greska za nivo poverenja 95 %

Zaključak

Plazma je generisana ozračivanjem uzoraka aluminijumskih legura sa TEA CO₂ laserskim zračenjem intenziteta 30 MWcm⁻² u atmosferi vazduha na pritisku 0,5 mbar. Vremenski integrисани emisioni spektri magnezijuma prisutnog u uzorcima aluminijumskih legura upotrebljeni su za konstruisanje kalibracione krive zavisnosti LIBS signala od koncentracije analita. Dobijena je linearна korelација ($r^2=0,9957$) u opsegu koncentracija od 0,26-1,10 % m/m, a potom je izvršeno određivanje koncentracije magnezijuma u uzorku legure aluminijuma. Upotreбom statistичких testova upoređeni su rezultati i utvrđeno je da nema statistички značajne razlike u preciznosti i tačnosti između određenih koncentracija Mg u uzorku primenom LIBS i ICP-OES metode. Na osnovu dobijenih rezultata može se zaključiti da se laboratorijski LIBS spektromетар baziran na impulsном TEA CO₂ laseru može uspešno primeniti za kvantitativnu analizu magnezijuma u legurama aluminijuma.

Zahvalnica: Ova istraživanja su podržana od strane Ministarstva prosvete, nauke i tehnološkog razvoja Republike Srbije (projekat br. 172019).

Application of plasma induced by TEA CO₂ laser for determining the concentration of magnesium in the aluminum alloys

The analytical capability of plasma induced by nanosecond infrared TEA CO₂ laser radiation under reduced air pressure for determination of Mg in aluminum alloys was investigated. Sharp and well resolved spectral lines of Mg, with negligibly low background emission, were obtained from a plasma region 3 mm above the target surface. A calibration curve for Mg was constructed using certified aluminium alloy samples. A linear relationship between LIBS signal and analyte concentration was obtained ($r^2 = 0.9957$) in the range from 0,26 -1,10 % w/w, and used for determination of Mg in a control sample. As a reference method for quantification of Mg in the control sample inductively coupled plasma - optical emission spectroscopy (ICP-OES) was used. Good agreement between LIBS and ICP-OES results was obtained. The results confirm that TEA CO₂ LIBS is an effective technique for quantitative analysis of Mg in aluminum alloy samples.

Reference

1. D.W. Hahn, N. Omenetto *Appl Spectrosc.* 66 (2012) 347-419.
2. J. Savovic, M. Stoiljkovic, M. Kuzmanovic, M. Momcilovic, J. Ciganovic, D. Rankovic, S. Zivkovic, M. Trtica, *Spectrochim. Acta B* 118 (2016) 127-136.
3. M. Momcilovic, M. Kuzmanovic, D. Rankovic, J. Ciganovic, M. Stoiljkovic, J. Savovic, M. Trtica, *Appl. Spectrosc.* 69 (2015) 419-429.
4. M. Momčilović, J. Čiganić, D. Ranković, U. Jovanović, M. Stoiljković, J. Savović, M. Trtica, *J. Serb. Chem. Soc.* 80 (2015) 1505-1513.
5. M.S. Trtica, J. Savovic, M. Stoiljkovic, M. Kuzmanovic, M. Momcilovic, J. Ciganovic, S. Zivkovic, *Proc. SPIE* 9810 (2015) 981010.
6. G. Cristoforetti, S. Legnaioli, V. Palleschi, A. Salvetti, E. Tognoni, P. A. Benedetti, F. Brioschib, F. Ferrario, *J. Anal. At. Spectrom.* 21 (2006) 697-702.
7. M. Sabsabi, P. Cielo, *Appl. Spectrosc.* 49, (1995) 499-507
8. L. Hong-kun, L. Ming, C.Zhi-jiang, L. Run-hua, *Trans. Nonferrous Met. Soc. China* 18 (2008) 222.

9. J. Herman, C. Boulmer-Leborgne, I.N. Mihailescu, B. Dubreuil, J. Appl. Phys. 73 (1993) 1091-1000.
10. Milan S. Trtica, *Proc. SPIE* 1276 (1990) 106.

Elektrohemija / Electrochemistry

Nanocrystalline ruthenium oxide coating on titanium, prepared by the sol–gel procedure from colloidal oxide dispersions synthesized in the microwave reactor

Milica Košević, Gavrilo Šekularac, Ivana Drvenica*, Aleksandar Dekanski,
Branislav Nikolić**, Vladimir Panić

*Institute of Chemistry, Technology and Metallurgy, Department of Electrochemistry,
University of Belgrade, Belgrade, Serbia*

**Innovation Center of the Faculty of Technology and Metallurgy, Belgrade, Serbia*

***Faculty of Technology and Metallurgy, University of Belgrade, Belgrade, Serbia*

Abstract

Ruthenium oxide coating on titanium was prepared by the sol–gel procedure from well-defined colloidal oxide dispersions synthesized by the microwave (MW)-assisted hydrothermal route under defined temperature and pressure heating conditions. The dispersions were characterized by dynamic light scattering (DLS) measurements and scanning electron microscopy (SEM). The electrochemical properties were analyzed as capacitive performances gained by cyclic voltammetry and electrochemical impedance spectroscopy, and as the electrocatalytic activity for oxygen evolution from acid solution. The obtained dispersions were polydisperse and contained single particles and agglomerates of increasing surface energy and decreasing particle size as the MW-assisted heating conditions were intensified. Owing to these features of the precursor dispersions, the obtained coatings had considerably improved capacitive performances and good electrocatalytic activity for oxygen evolution at high overpotentials.

Introduction

Dimensionally stable anodes (DSA), or activated titanium anodes, are well-known electrocatalytic material with industrial applications in chlorine (CER) and oxygen evolution reactions (OER). Their activity originates from conductive noble metal oxides, especially RuO₂ and IrO₂, applied as a coating on a titanium substrate^{1–4}. The oxide coating on a DSA is usually prepared *in-situ* from HCl or alcoholic solutions of the metal chlorides^{1,5} by pyrolysis⁶, chemical vapor⁷, laser⁸ or induction heating⁹ deposition techniques. The oxides can also be synthesized *ex-situ* as hydrothermal colloidal dispersions and then subjected to the mentioned deposition techniques within sol–gel procedure for coating preparation^{10,11}.

MW-assisted methods were successfully applied for the synthesis of noble metal oxides, including RuO₂, of characteristic textures and with considerably enhanced supercapacitance performances^{12,13}.

Present paper reports an attempt to obtain a RuO₂ coating on Ti in a traditional DSA form starting from a colloidal oxide dispersion of well-defined physicochemical properties synthesized under controlled heating conditions of the MW-assisted hydrothermal route.

Experimental

Synthesis of RuO₂ dispersions. The precursor for the preparation of RuO₂ coatings on Ti, the RuO₂ colloidal dispersion, was synthesized by simple one-step temperature- or power/pressure-controlled microwave (MW) irradiation in an autoclave. The pH value of the starting water solution of 1.54 mg cm⁻³ of RuCl₃·nH₂O was adjusted to around 2.5 by the addition of HCl. The solution was continuously stirred at 600 rpm and irradiated isothermally to 200 and 220 °C in a MW oven. The temperature was maintained constant for 5 min. The reaction mixture was then left to cool down spontaneously to 60 °C. The dispersions obtained at mentioned temperatures and corresponding electrodes formed later on are denoted as MWR_{i200} and MWR_{i220}. In case of pressure-controlled synthesis, the MW heating power was allowed to reach the oven limit of 850 W and the heating was interrupted when the pressure in the autoclave reached 30 bar (this procedure required 64 s to reach the temperature of 232 °C). This sample was abbreviated as MWR_{p30}. After moderate drying of the suspensions (110 °C, air) the concentration of RuO₂ solid phase was found to be 0.71 mg cm⁻³ in all samples. The synthesis resulted in the formation of black RuO₂ suspensions, the solid phase of which almost completely precipitated within a few minutes. This indicates that obtained particles tend to form agglomerates. However, the solid phase can

easily be re-suspended upon ultrasonication, and repeated sonication steps produce more and more stable suspensions. Phase separation was not visible for days already after application of only few 5-min sonication steps.

Material characterization. The solid phase consisting of MW-generated RuO₂ particles in the suspension was characterized by dynamic light scattering (DLS). Surface morphology was characterized by scanning electron microscopy (SEM).

Coating preparation. Obtained RuO₂ suspensions were used for the formation of a coating on Ti. Sand-blasted titanium rods, 3 mm in diameter, were thoroughly etched in hot HCl solution (1:1 volume ratio of water and conc. HCl) for 20 min, rinsed by water and dried at 100 °C. Just before deposition of a suspension onto Ti rods, it has been ultrasonicated for 15 min. After deposition, the rod was dried at 120 °C for 30 min. These two steps were repeated and finally the coating was formed during the thermal treatment at 300 °C for 2 h. In order to avoid possible detachment, the coating was deposited as rather thin layer in amount of 0.11 mg cm⁻² (the coating amount in usual experimental DSA preparation procedures is 10 to 20 times larger). Thus prepared RuO₂/Ti served as working electrodes in electrochemical testing.

Electrochemical measurements. The electrochemical experiments were carried out using a three-electrode cell, with Pt gauze electrode and saturated calomel electrode (SCE; all potentials are expressed vs. SCE) as counter and reference electrodes, respectively. Cyclic voltammetry (CV) and electrochemical impedance spectroscopy (EIS) measurements were performed with a SP-200 potentiostat/galvanostat (Bio-Logic SAS, Claix, France) at room temperature. EIS data were recorded with ac potential amplitude of 10 mV (rms) in a multi-sine mode.

Results and discussion

Particle size distribution (PSD) data for the prepared and freshly sonicated RuO₂ suspensions, as obtained by dynamic light scattering (DLS) measurements, are shown in Fig. 1. The PSD by volume (V_p) for the isothermally prepared samples indicated the presence of particles well resolved through the diameter spectrum immediately upon sonication, with the polydispersity index (PDI), Fig. 1C, below 0.3. MWR_{p30} was the most polydisperse in character (PDI 0.37), with a continuous distribution of the diameters of the particles (and/or agglomerates) in the quite wide range of 20 nm–1 µm. Bearing in mind that the two peaks in the PSD by V_p spectrum for MWR_{t200} (Fig. 1A) are positioned close to one another, the aggregation of the smaller particles into larger ones is hardly the possible cause of the formation of the *ca.* 250 nm-sized particles. It appears to be that particles of the two different diameters were formed separately from the nuclei generated in the different irradiation times. The initial ones grew to *ca.* 250 nm-sized particles, whereas the continuously born “younger” nuclei had enough time to grow into particles with diameters in the range 60–110 nm during the 5 min of MW irradiation. The increase in the synthesis temperature to 220 °C generated two additional features in the PSD. There was another well resolved fraction of particles with diameters in the range 30–40 nm due to the more rigorous initial heating conditions, and a fraction of huge agglomerates of around 5 µm (Fig. 1A). Due to this more pronounced polydisperse character, the PDI of MWR_{t220} was a little higher with respect to MWR_{t200}, while the slight increase during the DLS runs was preserved. Finally, the most rigorous initial heating conditions (MWR_{p30}) returned the similar PSD features, with a fraction of the smallest particles of 20–30 nm and an increase in the size of the fraction of the largest particles to diameters of *ca.* 500 nm. The PSD of the latter fraction in MWR_{p30} was much wider than in the cases of MWR_{t200} and MWR_{t220}, and extends up to 1 µm. Since the synthesis time was considerably shorter in comparison to the isothermal conditions, this is an indication that the smaller particles are of high energy and tend to relax by joining into large agglomerates. This is fairly well demonstrated if the PSD in DLS run 1 was compared to that in run 10 (Fig. 1B).

The largest fraction was not detectable for MWR_{t220} in run 10, although it was present in the 1st run. This means that this fraction is unstable and cannot form a stable dispersion, which is not the case for largest agglomerates present in the MWR_{p30} sample, due to the higher tendency of its smallest particles to be relaxed into agglomerates, and consequently high surface energy of agglomerates.

Despite these differences in the PSD among the prepared samples, the general observation was that the applied synthesis procedure by MW irradiation generates at least two stable particle fractions: one around 70 nm and the other in a wide range between 0.1 and 2 µm, with the dominant presence of grains of *ca.* 300 and 500 nm. In order to resolve the quite complex pathways of nucleation, particle

growth and aggregation, the generated solid phase was investigated by SEM. To provoke fast physical aggregation, the MWR_{t200} sample as the most stable one according to the DLS analysis, was diluted with ethanol (1:100, V/V) and dried onto a glassy carbon substrate. The typical appearance is illustrated in Fig. 2.

Two distinct formations are seen at the micro-level, Figs. 2A and 2B: huge monolithic regularly rectangle-shaped clusters with dimensions of several μm . These clusters can be interconnected or can appear as separate blocks as illustrated by the two micrographs on Figs 2A and 2B. The clusters are decorated by sub- μm -sized grains, which consist of spherical particles of the size close to 100 nm (sub-micrograph, Fig. 2C). Finally, the sub-micrograph reveals the presence of spherical particles few tens of nm in size (three typical examples are in white circle), which appears to be the building elements of the huge clusters.

Electrochemical behavior of the prepared RuO_2 was checked through voltammetric response, O_2 evolution activity and electrochemical impedance spectroscopy of the RuO_2 coating on Ti in H_2SO_4 solution. The cyclic voltammetry (CV) curves (as specific currents per mass of the coating) for the electrodes prepared from MWR_{t200} , MWR_{t220} and MWR_{p30} suspensions are shown in Fig. 3. The shape of CVs is usual for DSA-type electrodes synthesized by traditional thermal decomposition of metal chlorides or by the sol-gel procedure^{1,14}.

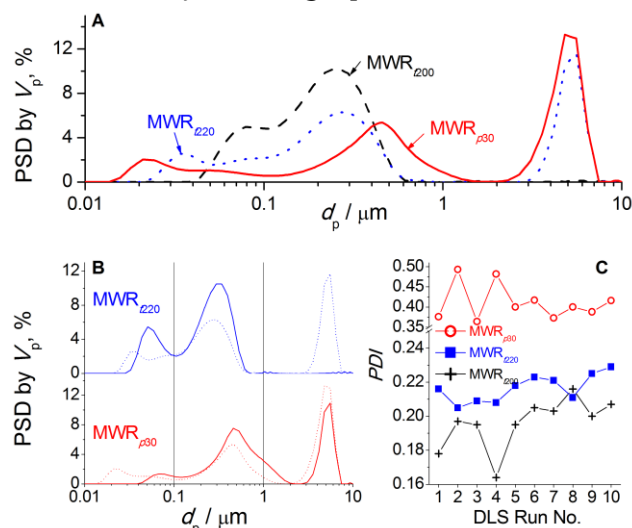


Fig. 1. Dynamic light scattering (DLS) data presented as particle size distribution (PSD) by volume (V_p) for the microwave-synthesized RuO_2 suspensions obtained after the first (A) and the tenth in comparison to the first DLS run (B, dashed and full line, respectively); C) the changes in polydispersity index (PDI) during the ten DLS runs.

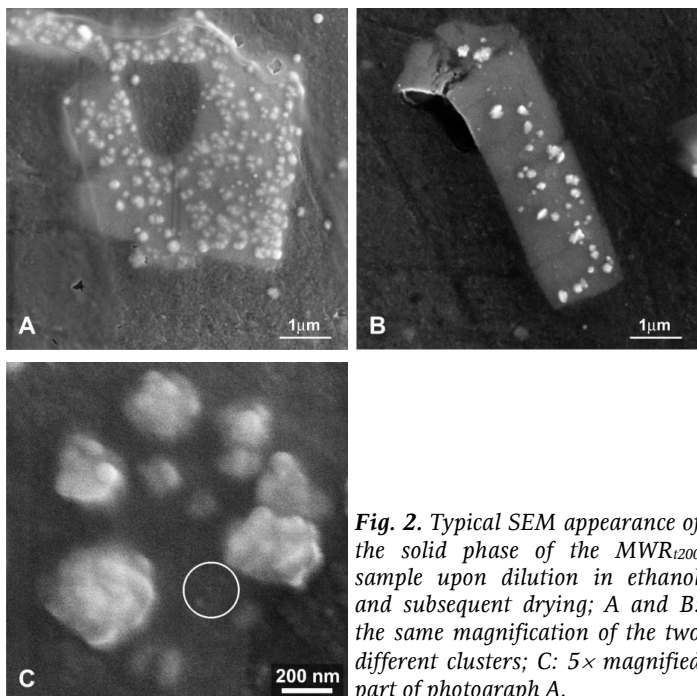


Fig. 2. Typical SEM appearance of the solid phase of the MWR_{t200} sample upon dilution in ethanol and subsequent drying; A and B: the same magnification of the two different clusters; C: 5× magnified part of photograph A.

The broad pseudocapacitive redox transition peaks^{15–17} appear better resolved for the samples prepared under the more rigorous heating conditions (MWR_{t220} and MWR_{p30}), the CVs of which resemble greatly those for RuO_2 or $\text{RuO}_2\text{-TiO}_2$ electrodes of high RuO_2 content^{14,15,18}. On the other hand, the CV of MWR_{t200} sample is more featureless and of lower currents, which indicates higher amounts of TiO_2 in the coating¹⁴ and/or its lower real surface area¹⁹ in comparison to the MWR_{t220} and MWR_{p30} samples. The later cause could be due to the particles in the fraction of smallest particles being larger for MWR_{t200} (Fig. 1; peak positions at ca. 70, 32 and 21 nm for MWR_{t200} , MWR_{t220} and MWR_{p30} , respectively), which could also affect the TiO_2 content since the origin of TiO_2 is the oxidation of the Ti substrate during the thermal treatment of the coating. It could diffuse through the RuO_2 layer and form mixed $\text{RuO}_2\text{-TiO}_2$ oxide throughout the coating. It is to be expected that a more porous RuO_2 layer (consisting of larger particles) is able to form mixed oxides more easily and with higher TiO_2 contents. Since the smallest particles were found in the MWR_{p30} sample, it showed the largest specific CV currents, although the values were similar to the CV currents of MWR_{t220} . The difference appeared in the anodic branch between –0.2 and 0.7 V.

The registered CV currents appeared rather high in comparison to the currents usually registered for DSA electrodes^{14,15}. A similar finding could also be found in the literature reporting a fast laser-induced synthesis procedure for DSA²⁰ or for C/ RuO_2 sandwiched hierarchical structures prepared at low

temperatures²¹. Fig. 3 indicates that a specific capacitance as high as 250 F g^{-1} was reached, which is quite unusually high value for DSA electrodes of any composition. This suggests that MW irradiation, by causing rigorous heating conditions, is able to produce characteristic structures and high energy-governed hierarchy²¹ of the synthesized materials, which are unreachable by traditional preparation procedures, such as thermal treatment or ordinary sol–gel processes. The appearance of the synthesized oxide as illustrated by Fig. 2, along with the data reported in Fig. 3, strongly suggests that the fractions found by PSD (Fig. 2), beside the particle size as a physical criterion, could also differ in chemical composition. In order to check this possibility, the prepared electrodes were tested for their activity in oxygen evolution.

In order to check the state and properties of thermally-formed TiO_2 , the samples with the most pronounced difference in electrochemical properties, MWR_{t200} and MWR_{p30} , were subjected to impedance (EIS) measurements. The recorded data are shown in Fig. 4A-C (symbols: measured data at open circuit potential (OCP), 470 and 870 mV - the last two datasets only for MWR_{t200} ; lines: equivalent electrical circuit (EEC) data). The structures of EECs applied to fit the experimental data are also shown in Fig. 4D.

The registered EIS response and the EEC structures are typical for DSAs with a well-developed inert oxide-rich (TiO_2) layer^{12,22,23}. Its EIS characteristics are seen as a semicircle-like dependence in a impedance complex plane plot (Fig. 4B) and finds equivalence in CPE1 and R3 in parallel (Fig. 4D). Since the responses were registered at the open circuit potential (OCP), they transfer to typical capacitive response for the DSA as the frequency decreases (well-resolved capacitive loops can be seen in the capacitive complex plane plots, Fig. 4A), which could be fitted reliably to a transmission line form of EEC (TLEEC)²⁴.

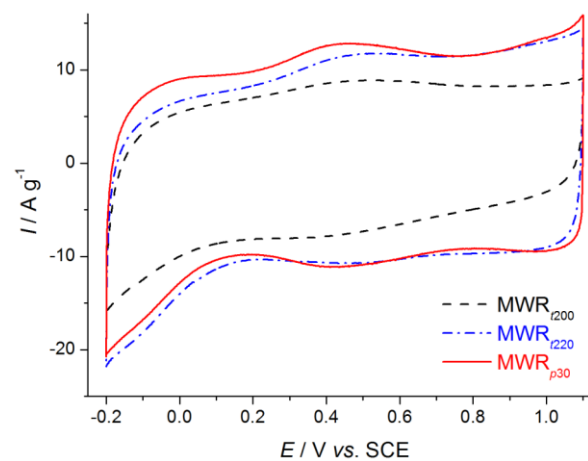


Fig. 3. CV curves for the RuO_2/Ti electrodes prepared from MWR_{t200} , MWR_{t220} and MWR_{p30} suspensions; electrolyte: $1.0 \text{ M H}_2\text{SO}_4$, room temperature; sweep rate: 50 mV/s

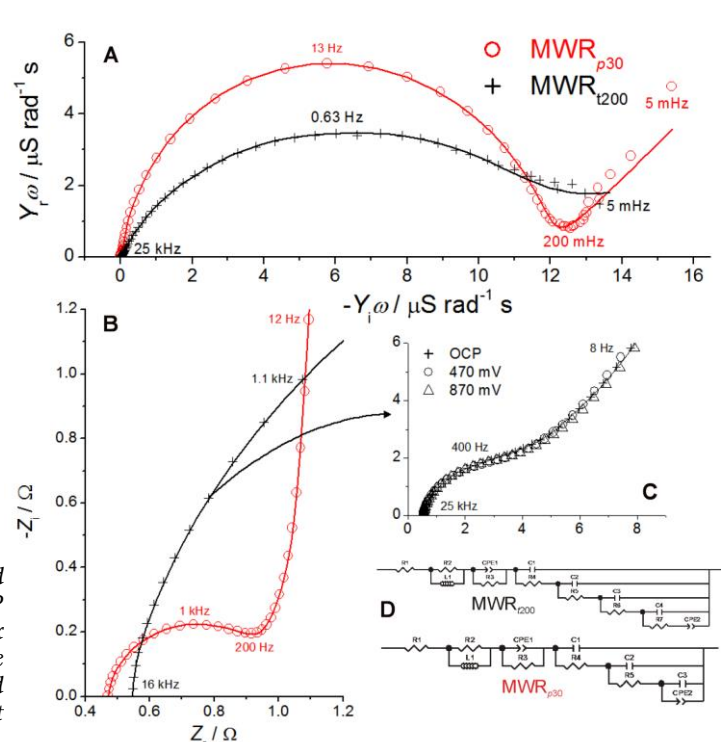


Fig. 4 The EIS response of the RuO_2/Ti electrodes prepared with MWR_{p30} and MWR_{t200} suspensions at OCP (A - capacitive complex plane plots; B- impedance complex plane plot); C - high frequency domain of the impedance complex plane plots for MWR_{t200} sample at OCP, 470 and 870 mV; symbols: measurements, lines: data of equivalent electrical circuits (D).

The EECs also contained an inductive element to fit the high frequency data (not shown), which did not depend on the sample type and applied potential. Apparently, the origin of inductive behavior lies in the measuring system itself, and will not be commented here. However, it was just taken into account for the fitting in order to ensure the accuracy of the values of the other circuit parameters.

To confirm fully the assignment of the EIS behavior in the high-frequency domain to the presence of a TiO_2 -rich layer in the coating/Ti substrate interface, the EIS response was recorded at two additional potentials out of OCP (470 and 870 mV), Fig. 4C. No differences in responses were registered due to the pure electrical response of the layer¹², which confirms its TiO_2 -rich feature. The considerable difference in EIS data of MWR_{t200} and MWR_{p30} in the frequency domains for both the TiO_2 -rich layer and the

capacitive response is seen. The high frequency semicircle was better developed and of considerable lower diameter for MWR_{p30} than for MWR_{t200} – Fig. 4B (the corresponding resistances obtained by fitting to the EEC are 0.52 and $3.2\ \Omega$, respectively). This indicates that the layer was much thinner in MWR_{p30} and more definitely separated from the applied coating. On the other hand, a TLEEC of higher order was required to fit the capacitive EIS response of the MWR_{t200} coating, whereas the TLEEC for MWR_{p30} contained a CPE2 in the last branch with pronounced diffusion characteristics ($n = 0.5$ and corresponding admittance of the order of $10^{-4}\ S$, seen as “the tail” in low frequency domain of the capacitance complex plane plot, Fig. 4A). These findings strongly indicate that the MWR_{p30} coating was more compact. The generation of TiO_2 was suppressed during the thermal treatment since the solid phase of the MWR_{p30} dispersion covers more uniformly the Ti substrate than in case of the MWR_{t200} suspension. The more compact characteristics of the MWR_{p30} coating could originate from the presence of considerably smaller particles in the lowest fraction, as found in the DLS analysis (Fig. 1), which had greater ability to pack tightly and more uniformly than the more relaxed larger particles of MWR_{t200} .

Another finding underpinning the consideration about the differences in the morphologies of the MWR_{t200} and MWR_{p30} coatings concerns the distribution of the capacitance and pore resistance throughout the coating, as obtained from the TL branches of the EEC (Fig. 4D). A considerable amount of the overall capacitance of the compact MWR_{p30} coating (8.1 mF) was readily available behind the internal coating resistance of only $0.5\ \Omega$ (R3), whereas almost the complete coating capacitance of 11.2 mF was available through an additional pore resistance of only $1.3\ \Omega$ (R4). The remaining 0.7 mF (C3) was available behind $43\ \Omega$ (R5) of pore resistance. On the other hand, only half of the available capacitance of the MWR_{t200} coating (10.7 mF, C1+C2+C3) was accessible through $15.6\ \Omega$ (R3+R4+R5) of the coating resistance. Overall, $170\ \Omega$ of the total MWR_{t200} coating resistance had to be overcome to gain full capacitive performances. It follows that the compact MWR_{p30} coating could express its full electrochemical performances with negligible contribution of the parts accessible through the cracks appearing only locally. The MWR_{t200} coating was more porous and of diverse texture, and hence contained larger amounts of pore-hidden electrocatalytic material in the regions of loose grain boundaries.

Conclusions

Highly active RuO_2 coatings on Ti could be prepared from the colloidal dispersions of the oxide synthesized under rigorous heating conditions induced by microwave irradiation. Although being of multifractional particle size distribution, the polydispersity of the dispersions was fairly defined and preserved. Intensification of the heating conditions through increased reaction temperature and pressure produced smaller particles and increased their surface energy. The most rapid heating conditions generated the smallest high-energy oxide particles of *ca.* 20 nm, which were able to form compact RuO_2 coatings of high electrochemical activity due to pronounced tendency of the particles towards aggregation. The coating capacitive performances and the activity for oxygen evolution seemed considerably improved with respect to those of the coating prepared by traditional thermal decomposition of chloride or usual hydrothermal processing routes. The improvement was not obviously related to the increase in the real surface area of the coating, but more to the generation of high-energy oxide surface states exclusively related to the microwave-assisted synthesis under rigorous heating conditions. The improvement in the electrocatalytic activity for oxygen evolution was considerable in the regions of high overpotentials, where water splitting over two surface O-terminals is believed to occur.

Acknowledgement: The financial support from the Ministry of Education, Science and Technological Development (project No. 172060) is acknowledged.

Превлаке нанокристалног рутениум оксида на титану, добијене сол–гел поступком из колоидне оксидне дисперзије синтетисане у микроталасном ректору

На титанској основи формирана је превлака нанокристалног рутенијум оксида сол–гел поступком, и олазећи од дефинисане колоидне дисперзије оксида синтетисаног хидротермалном реакцијом у микроталасном реактору у условима кониролисаног приплика и температуре током зајревања. Дистрибуција величине честица у сусиснији одређена је методом динамиког расијања светлосни

(Dynamic Light Scattering - DLS), а површинска морфологија скенирајућом електронском микроскопијом. Електрохемијска карактеризација превлаке је укључивала одређивање катализитивних особина путем цикличне волтаметрије и спектроскопије електрохемијске импеданције и одређивање електрокаталитичке активности за реакцију издавања кисеоника у киселом раствору. Добијене честине су полидисперзне и садрже како појединачне честице шако и аломерате. Са интензивирањем услова микроталасног затревања површинска енергија честица расте, а њихова величина се смањује. Захваљујући оваквим особинама прекурсора (дисперзије), добијене превлаке имају побољшане катализитивне особине и добру електрокаталитичку активност за реакцију издавања кисеоника при високим пренапоностима.

References:

1. S. Trasatti, in *Interfacial Electrochemistry—Theory, Experiment and Applications*, A. Wieckowski Ed., Marcel Dekker Inc., New York, USA, 1999, p. 769
2. M. H. P. Santana, L. A. De Faria, J. F. C. Boodts, *Electrochim. Acta* **49** (2004) 1925
3. M. Yagi, E. Tomita, T. Kuwabara, *J. Electroanal. Chem.* **579** (2005) 83
4. P. S. Patil, R. W. Kawar, S. B. Sadale, *Electrochim. Acta* **50** (2005) 2527
5. V. Jovanović, A. Dekanski, P. Despotov, B. Nikolić, R. Atanasoski, *J. Electroanal. Chem.* **339** (1992) 147
6. A. Marshall, B. Borresen, G. Hagen, M. Tsypkin, R. Tunold, *Mater. Chem. Phys.* **94** (2005) 226
7. R. S. Chen, A. Korotcov, Y. S. Huang, D. S. Tsai, *Nanotechnology* **17** (2006) R67
8. M. X. Xia, C. B. Wang, Y. S. Gong, Q. Shen, L. M. Zhang, *Rare Metal Mater. Eng.* **35** (2006) 820
9. C. Mousty, G. Fóty, Ch. Comminellis, V. Reid, *Electrochim. Acta* **45** (1999) 451
10. V. V. Panić, B. Ž. Nikolić, *J. Serb. Chem. Soc.* **73** (2008) 1083
11. L. Xu, Y. Xin, J. Wang, *Electrochim. Acta* **54** (2009) 1820
12. S. Faraji, F. Nasir Ani, *J. Power Sources* **263** (2014) 338
13. J-Y. Kim, K-H. Kim, H-K. Kim, S-H. Park, K. Y. Chung, K-B. Kim, *RSC Adv.* **4** (2014) 16115
14. L. D. Burke, O. J. Murphy, *J. Electroanal. Chem. Interf. Electrochem.* **112** (1980) 39-50
15. S. Ardizzone, S. Trasatti, *Adv. Colloid Interface Sci.* **64** (1996) 173.
16. T. Liu, W. G. Pell, B. E. Conway, *Electrochim. Acta* **42** (1997) 3541
17. B. Conway, *Electrochemical Supercapacitors—Scientific Fundamentals and Technological Applications*, Plenum Publishers, New York, USA, 1999, pp. 277-286
18. V. Panić, A. Dekanski, S. Milonjić, R. Atanasoski, B. Nikolić, *Mater. Sci. Forum* **352** (2000) 117
19. S. Trasatti, O. A. Petrii, *J. Electroanal. Chem.* **327** (1992) 353
20. R. R. L. Pelegrino, L. C. Vicentin, A. R. De Andrade, R. Bertazzoli, *Electrochim. Commun.* **4** (2002) 139
21. Y. Wang, C. Y. Foo, T. K. Hoo, M. Ng, J. Lin, *Chem. Eur. J.* **16** (2010) 3598
22. V. A. Alves, L. A. Silva, J. F. C. Boodts, *J. Appl. Electrochem.* **28** (1998) 899
23. T. A. F. Lassali, J. F. C. Boodts, L. O. S. Bulhões, *J. Appl. Electrochem.* **30** (2000) 625
24. V. Panić, T. Vidaković, A. Dekanski, V. Mišković-Stanković, B. Nikolić, *J. Electroanal. Chem.* **609** (2007) 120

Uticaj leucina na anodno rastvaranje halkopirita u sumpornoj kiselini

Biljana S. Maluckov, Mile Dimitrijević, Renata Kovačević*, Srba Mladenović

Tehnički fakultet u Boru, Univerzitet u Beogradu, Vojske Jugoslavije 12, 19210 Bor, Srbija

*Institut za rudarstvo i metalurgiju, Zeleni bulevar 35, 19210 Bor, Srbija

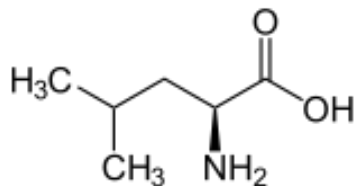
Apstrakt

U radu je ispitivano anodno rastvaranje halkopirita u sumpornoj kiselini u prisustvu leucina. Snimani su ciklični voltamogrami u rastvorima 10^{-2} mol L⁻¹ H₂SO₄ i 10^{-2} mol L⁻¹ Leu pri brzinama od 1 mVs⁻¹, 5 mVs⁻¹, 10 mVs⁻¹ i 20 mVs⁻¹, a nakon toga je izvršena analiza rastvora. Rezultati su pokazali da pri svim brzinama prisustvo leucina pospešuje rastvaranje bakra, a smanjuje rastvaranje gvožđa iz halkopirita u odnosu na sumpornu kiselinu bez leucina. Najveće količine bakra i gvožđa se u oba rastvora oslobađaju pri brzini od 1 mVs⁻¹.

Uvod

Halkopirit je sulfidni mineral bakra i gvožđa (CuFeS₂). Iz njega se pomoću mikroorganizama - bioluženjem dobija bakar¹⁻³.

Jedan od najčešće korišćenih mikroorganizama u procesima bioluženja je bakterija *A. ferooxidans*⁴. Njena uloga u procesima bioluženja je da oksiduje Fe (II) u Fe (III)⁵. *A. ferooxidans* sintetiše protein rusticianin koji učestvuje u procesima oksidacije Fe (II)⁶⁻¹⁰. U ovom proteinu amino kiselinska sekvenca koja je odgovorna za vezivanje bakra se sastoji iz cisteina, histidina i metionina⁶. Umesto metionina se kod nekih mutacija rusticianina javlja leucin¹¹. Elektrohemijska ispitivanja uticaja amino kiselina na metale i legure su pokazala da leucin u kiseloj sredini pospešuje rastvaranje bakra¹², a inhibira rastvaranje čelika¹³⁻¹⁵. Takođe se pokazalo da leucin slabije inhibira koroziju gvožđa od metionina^{16,17}. Leucin je nepolarna hidrofobna amino kiselina koja je u kiseloj sredini u protonovanom obliku^{12,13}. Strukturalna formula leucina je prikazana na slici 1.



Slika 1. Strukturalna formula leucina

U radu je ispitivan uticaj dodavanja leucina na anodno rastvaranje halkopirita u sumpornoj kiselini..

Eksperimentalne metode

Halkopiritna elektroda je napravljena od prirodnog minerala iz borskog nalazišta. Elektroda je hladno zaptivana sa materijalom na bazi metil-metakrilata. Radna površina halkopiritne elektrode je iznosila 0.68 cm². Priprema površine elektrode izvršena je mehaničkim poliranjem silikon karbidnim papirom i glinicom (Al₂O₃). Nakon toga elektroda je ispirana destilovanom vodom i sušena.

Serija rastvora leucina $1 \cdot 10^{-2}$ mol L⁻¹, $1 \cdot 10^{-3}$ mol L⁻¹; $1 \cdot 10^{-4}$ mol L⁻¹; $1 \cdot 10^{-5}$ mol L⁻¹; $1 \cdot 10^{-6}$ mol L⁻¹ je dobijena direktnim dodavanjem u rastvor $1 \cdot 10^{-2}$ mol L⁻¹ H₂SO₄.

Merjenja su urađena na aparaturi sastavljenoj od potencijostata, polarografskog anulatora koji je direktno vezan za kompjuter i AD kartice. Elektrodni sistem je sastavljen od tri elektrode: radne elektrode, referentne zasićene kalomelove elektrode (SCE) i pomoćne elektrode od platine.

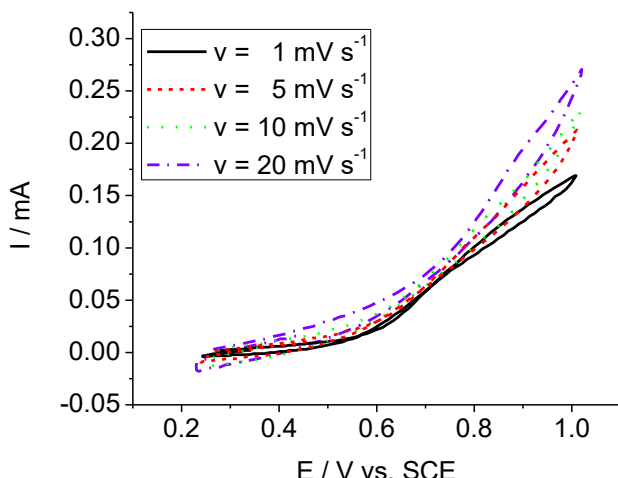
Određivan je potencijal otvorenog kola u trajanju od 15 min, a zatim su od potencijala otvorenog kola snimani ciklični voltamogrami u anodnom pravcu pri brzinama od 1 mVs⁻¹, 5 mVs⁻¹, 10 mVs⁻¹ i 20 mVs⁻¹.

Analiza rastvora

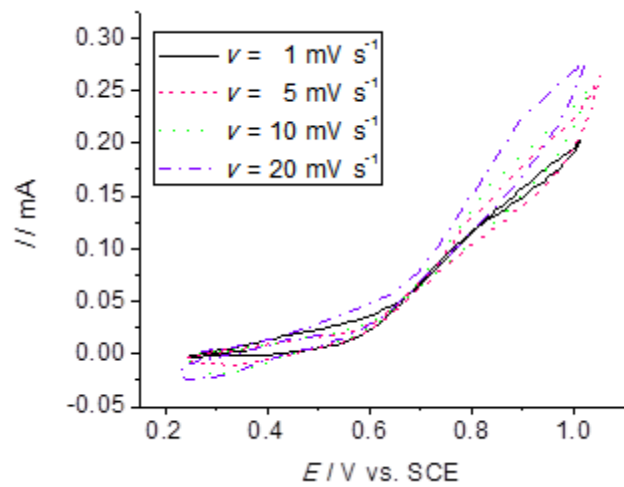
U rastvorima je nakon potencijala otvorenog kola i ciklične voltametrije izvršena analiza rastvorenih metala i sumpora na simultanom atomskom emisionom spektrometru sa induktivno kuplovanom plazmom (ICP AES), model Spectro ciros vision.

Rezultati i diskusija

Na slici 2 su prikazani ciklični voltamogrami za različite brzine skeniranja u rastvoru 10^{-2} mol L⁻¹ H₂SO₄ i 10^{-2} mol L⁻¹ Leu, a na slici 3 u rastvoru 10^{-2} mol L⁻¹ H₂SO₄ bez leucina. Rezultati analiza rastvora nakon ciklične voltametrije pri različitim promenama brzine snimanja su prikazani na slikama 4-6.

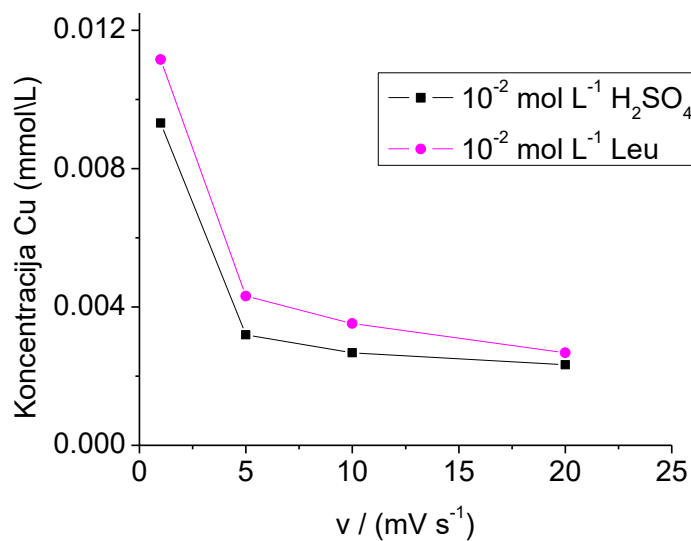


Slika 2. Ciklični voltamogrami za različite brzine snimanja u rastvoru 10^{-2} mol L⁻¹ H₂SO₄ + 10^{-2} mol L⁻¹ Leu



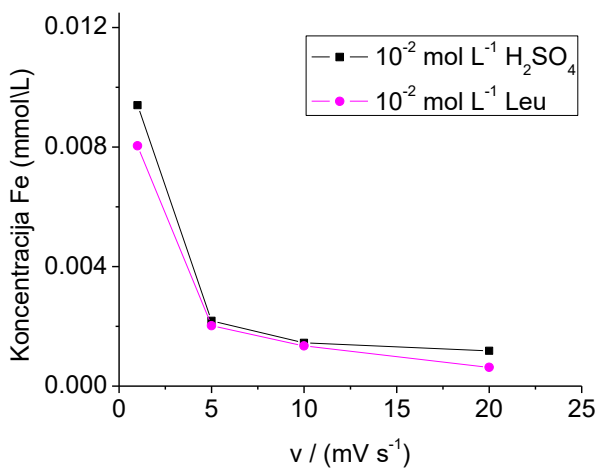
Slika 3. Ciklični voltamogrami za različite brzine snimanja u rastvoru 10^{-2} mol L⁻¹ H₂SO₄

Na slici 4 je prikazana koncentracija bakra u rastvorima nakon snimanja cikličnih voltamograma. Sa slike se vidi da je pri svim brzinama koncentracija bakra veća u rastvoru koji sadrži leucin nego u rastvoru sumporne kiseline bez leucina.



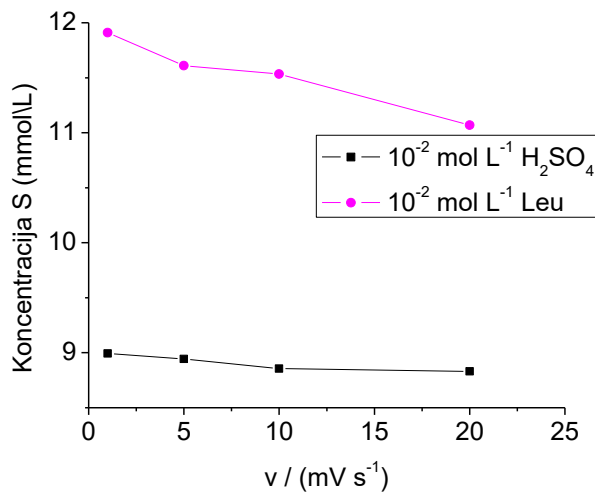
Slika 4. Koncentracija Cu u rastvorima sumporne kiseline sa i bez leucina, pri različitim brzinama snimanja.

Na slici 5 je prikazana koncentracija gvožđa u rastvorima nakon ciklične voltametrije. Kao što se vidi sa slike, koncentracija gvožđa je veća u sumpornoj kiselini bez leucina nego u rastvoru koji sadrži leucin. Upoređivanjem rezultata sa slikama 4 i 5 vidi se da su najveće koncentracije i bakra i gvožđa pri brzini od 1 mVs⁻¹ u oba rastvora.



Slika 5. Koncentracija Fe u rastvorima sumporne kiseline sa i bez leucina, pri različitim brzinama snimanja

Na slici 6 su prikazane koncentracije ukupnog sumpora nakon ciklične voltametrije. Sa slike se vidi da je koncentracija sumpora veća u rastvoru koji sadrži leucin nego u sumpornoj kiselini bez leucina. U rastvoru leucina izraženiji je pad koncentracije sumpora sa porastom brzine skeniranja, nego u rastvoru sumporne kiseline bez leucina.



Slika 6. Koncentracija S u rastvorima sumporne kiseline sa i bez leucina, pri različitim brzinama snimanja

U tabeli 1 je prikazan molski odnos Cu/Fe nakon ciklične voltametrije pri različitim brzinama u 10⁻² mol L⁻¹ H₂SO₄ i 10⁻² mol L⁻¹ Leu. Iz tabele se vidi da je najveći molski odnos bakra i gvožđa u rastvoru 10⁻² mol L⁻¹ Leu pri brzini od 20 mVs⁻¹.

Tabela 1. Molski odnos Cu/Fe u rastvorima leucina i sumporne kiseline bez leucina pri različitim brzinama snimanja

Brzina snimanja, mV s ⁻¹	Cu/ Feu 10 ⁻² mol L ⁻¹ H ₂ SO ₄	Cu/ Feu 10 ⁻² mol L ⁻¹ Leu
1	0.99097	1.3877
5	1.46229	2.13093
10	1.84442	2.62472
20	1.97067	4.26852

Dobijani eksperimentalni rezultati su u skladu sa rezultatima da leucin slabo inhibira rastvaranje gvožđa^{16,17}, dobro inhibira rastvaranje čelika¹⁴, a ubrzava rastvaranje bakra¹².

Singh i dr., 2008 su utvrdili da je rastvor 10^{-1} mol L⁻¹ leucina pasivni inhibitor čelika, a da do inhibicije dolazi usled fizičkih adsorpcionih procesa leucina na površini metala¹³. U skladu sa tim, moguće objašnjenje za smanjenu rastvorljivost gvožđa iz halkopirita u prisustvu 10^{-2} mol L⁻¹ rastvora leucina u odnosu na sumpornu kiselinu bez prisustva leucina je, da leucin i gvožđe iz halkopirita reaguju i grade nerastvorni kompleks.

Zaključak

Rezultati istraživanja pokazuju da prisustvo leucina utiče na povećano rastvaranje bakra. Ovo može biti značajno za hidrometalurško dobijanje bakra iz halkopirita. Takođe se može prepostaviti da je mutacija u rusticianinu koja dovodi do zamene metionina leucinom poželjna sa tehnološke strane u cilju povećanog dobijanja prinosa bakra. Međutim, s obzirom da leucin ulazi u sastav proteina onda bi prepostavku trebalo proveriti i sa samim mikroorganizmima koji sadrže mutirani rusticianin.

The effect of leucine on the anodic dissolution of chalcopyrite in sulfuric acid

In this paper, the effect of leucine on the anodic dissolution of chalcopyrite in sulfuric acid is investigated. The cyclic voltammograms in solution of 10^{-2} mol L⁻¹ H₂SO₄ and 10^{-2} mol L⁻¹ Leu at the scan rates of 1 mVs⁻¹, 5 mVs⁻¹, 10 mVs⁻¹ and 20 mVs⁻¹, were recorded. After that the analysis of the solutions were done. The results have shown that the presence of leucine increases the Cu dissolution and decreases the Fe dissolution from chalcopyrite with respect to corresponding dissolutions in the sulfuric acid without leucin. The most large Cu and Fe quantities are obtained at the scan rate of 1 mVs⁻¹.

Literatura

1. G. J. Olson, J. A. Brierley, C. L. Brierley, *Applied Microbiology and Biotechnology*, **63** (2003) 249–257.
2. M. E. Clark, J. D. Batty , C. B.van Buuren, D. W. Dew, M. A. Eamon, *Hydrometallurgy*, **83** (2006) 3-9.
3. N. Pradhan, K. C. Nathsarma, K. S. Rao, L. B. Sukla, B. K. Mishra, *Minerals Engineering* , **21** (5) (2008) 355–365.
4. H. R. Watling, *Hydrometallurgy*, **84** (2006) 81–108.
5. G. S. Hansford, T. Vargas, *Hydrometallurgy*, **59** (2001) 135–14.
6. F. Nunzi, M. Woudstra, D. Campese, J. Bonicel, D. Morin, M. Bruschi, *Biochim Biophys Acta*, **1162** (1-2) (1993) 28-34.
7. D. Rawlings, T. Kusano, *Microbiological reviews* , **58** (1) (1994) 39-55.
8. R. C. Blake II, K. Sasaki, N. Ohmura, *Hydrometallurgy*, **59** (2001) 357–372.
9. J. Zeng, M. Geng, Y. Liu, L. Xia, J. Liu, G. Qiu, *Biochimica et Biophysica Acta*, **1774** (2007) 519–525.
10. A. Sharma, Y. Kawarabayasi, T. Satyanarayana, *Extremophiles*, **16** (2012) 1–19.
11. L. D. Kanbi, S. Antonyuk, M. A. Hough, J. F. Hall, F. E. Dodd, S. Samar Hasnain, *Journal of Molecular Biology*, **320** (2002) 263–275.
12. I. Milošev, J .Pavlinac, M. Hodošček, A. Lesar, *Journal of the Serbian Chemal Society*, **78** (12) (2013) 2069–2086.
13. P. Singh, K. Bhrara, G. Singh, *Applied Surface Science*, **254** (2008) 5927–5935.
14. N. A. Abdel Ghany, A. E. El-Shenawy, W. A. M. Hussien, *Modern Applied Science*, **5** (4) (2011), 19- 29.
15. N. O. Eddy, F. E. Awe, C. E. Gimba, N. O. Ibisi, E. E. Ebenso, QSAR, *International Journal of Electrochemical Science*, **6** (2011) 931 – 957.
16. A. Aouniti, K. F. Khaled, B. Hammouti, *International Journal of Electrochemical Science*, **8** (2013) 5925 – 5943.
17. M. Zerfaoui, H. Oudda, B. Hammouti, S. Kertit, M. Benkaddour, *Progress in Organic Coatings*, **51** (2004) 134–138.

Fizička hemija / Physical Chemistry

Efekat isoljavanja i uticaj temperature na bifazne vodene sisteme na bazi dicijanamidnih jonskih tečnosti

Aleksandra Dimitrijević, Nebojša Zec*, Nikola Zdolšek, Sanja Dožić*, Slobodan Gadžurić*, Tatjana Trtić-Petrović

*Laboratorija za fiziku, Institut za nuklearne nauke „Vinča“, Mike Petrovića Alasa 12-14,
11001 Beograd, Srbija*

**Departman za hemiju, biohemiju i zaštitu životne sredine, Prirodno-matematički fakultet,
Univerzitet u Novom Sadu, Trg Dositeja Obradovića 3, 21000 Novi Sad*

Uvod

Pod jonskim tečnostima (JT) se podrazumevaju jonska jedinjenja koja su tečna na temperaturama ispod 100°C.¹ Jonske tečnosti se sastoje od velikih, asimetričnih organskih katjona (amonijum, fosfonijum, sulfonijum, imidazolijum, piridinijum, pirolidinijum itd.) i manjih organskih ili neorganskih anjona (bromid, hlorid, dicijanamid, metansulfonat, tetrafluoroborat itd.). Dimenzije i oblik samih jona, pre svega katjona, onemogućavaju njihovo „gusto“ pakovanje i obrazovanje jonske kristalne strukture, čime se objašnjava niska temperatura topljenja i tečno agregatno stanje ovih sistema na sobnoj temperaturi.^{2,3} Jonske tečnosti poseduju niz jedinstvenih svojstva kao što su zanemarljiv napon pare, hemijska i termalna stabilnost, širok elektrohemski prozor, visoku provodljivost, veliki topotni kapacitet, podesivu hemijsku strukturu i fizičke osobine i jaku sposobnost solvatacije.⁴ Jonske tečnosti su ekološki prihvatljiva i pogodna alternativa isparljivim i toksičnim organskim rastvaračima. Među brojnim zanimljivim svojstvima koje poseduju hidrofilne jonske tečnosti je i njihova sposobnost da grade dvofazne vodene sisteme u kombinaciji sa neorganskim ili organskim solima. Naime, dodatak neorganske soli u vodenim rastvorima jonske tečnosti uzrokuje razdvajanje tečnih faza i formiranje dvofaznog vodenog sistema.⁵ Bifazni vodenim sistemima mogu biti značajni pri recikliraju ili koncentrovanju hidrofilnih jonskih tečnosti iz vodenih rastvora, zatim u reakciji metateze pri sintezi novih jonskih tečnosti, a od naročitog su interesa u separacionoj hemiji. Izborom adekvatnih komponenata (jonske tečnosti i neorganske/organske soli) i jednostavnom manipulacijom sastava faza može se postići visoka selektivnost i željeni koeficijent raspodele za ekstrakciju velikog broja jedinjenja kao što su alkaloidi, lekovi, aminokiseline, proteini, hormoni, alkoholi, aromatična i fenolna jedinjenja itd.⁶ Ispitivanje faznih dijagrama dvofaznih vodenih sistema sa jonskim tečnostima predstavlja prvu fazu u optimizaciji uslova za ekstrakciju određenog jedinjenja.

Cilj ovog rada je da se odrede ravnotežni dijagrami dvofaznih vodenih sistema {JT + neorganska so + H₂O} za novosintetisane jonske tečnosti 1-etil-3-etilimidazolijum-dicijanamid [1-C₂3-C₂im][DCA] i 1-butil-3-etilimidazolijum-dicijanamid [1-C₄3-C₂im][DCA] i da se ispitaju uticaji jonske tečnosti, neorganske soli i temperature na mogućnost formiranja bifaznih vodenih sistema.

Eksperimentalni deo

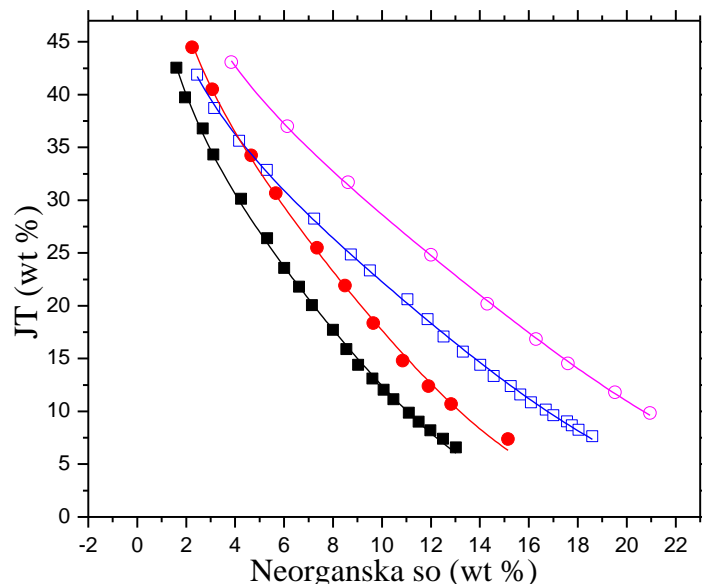
Ravnotežni dijagrami za bifazne vodene sisteme su određeni metodom titracije do tačke zamućenja (eng. cloud point method). Eksperimentalna procedura se sastoje od dva koraka: (1) u vodenim rastvorima jonske tečnosti poznate koncentracije se dodaje vodenim rastvorom soli do zamućenja odnosno do pojave bifaznog sistema; (2) zatim se dodaje voda dok se rastvor ne razbistri. Ovaj postupak se ponavlja dok se ne dobije dovoljan broj tačaka za formiranje krive.⁵ Određeni su ravnotežni dijagrami dvofaznih vodenih sistema za dve jonske tečnosti [1-C₂3-C₂im][DCA] i [1-C₄3-C₂im][DCA] u kombinaciji sa dve neorganske soli, K₃PO₄ i K₂CO₃, na tri temperature (295,15K; 308,15K i 328,15K). Jonske tečnosti su sintetisane i okarakterisane u Laboratoriji za analitičku hemiju Departmana za hemiju, biohemiju i zaštitu životne sredine Prirodno-matematičkog fakulteta u Novom Sadu.

Rezultati i diskusija

Na slici 1 su prikazani fazni dijagrami vodenih bifaznih sistema ispitivanih jonskih tečnosti ($[1\text{-C}_2\text{3-C}_2\text{IM}][\text{DCA}]$ i $[1\text{-C}_4\text{3-C}_2\text{IM}][\text{DCA}]$) u kombinaciji sa K_3PO_4 i K_2CO_3 . Binodalne krive su fitovane primenom empirijske jednačine koju su predložili Merchuk i saradnici⁷:

$$Y = A \exp(-BX^{0.5} - CX^3) \quad (1)$$

gde su Y i X maseni udeli jonske tečnosti i soli, a A , B i C su regresioni parametri koji su određeni metodom najmanjih kvadrata. Vrednosti određenih parametara su prikazane za sve ispitivane sisteme u Tabeli 1.⁸



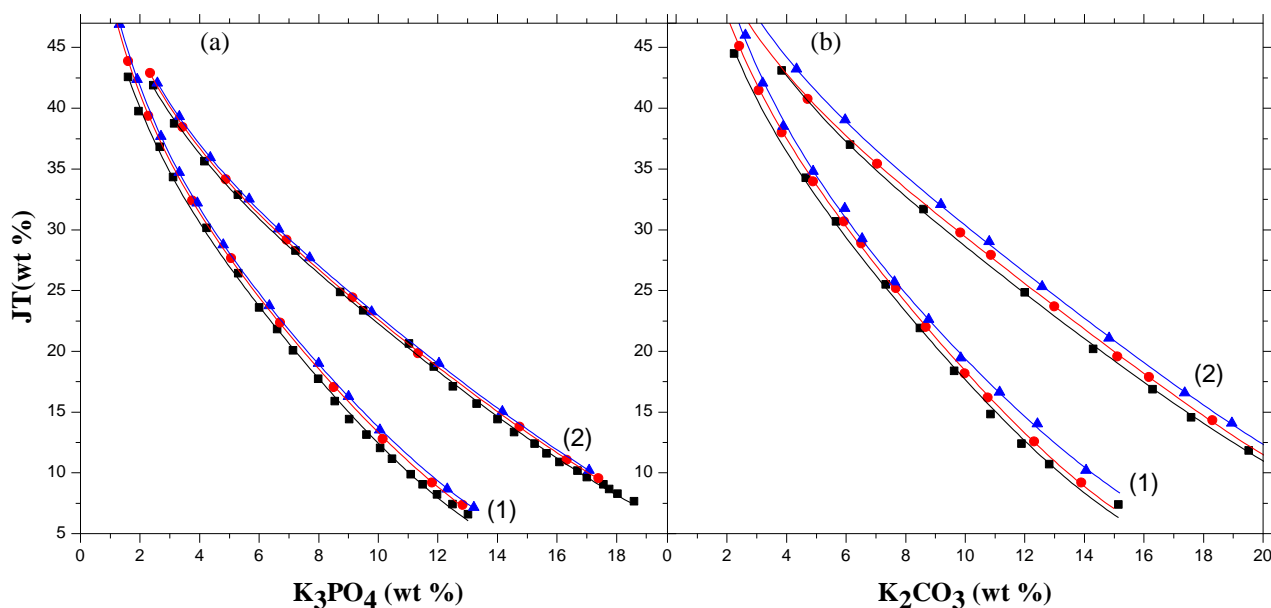
Slika 1. Fazni dijagram sistema $\{\text{JT} + \text{neorganska so} + \text{H}_2\text{O}\}$ na $T = 295,15\text{ K}$ i atmosferskom pritisku ($p = 0.1\text{ MPa}$):
 [■) $1\text{-C}_4\text{3-C}_2\text{IM}][\text{DCA}]/\text{K}_3\text{PO}_4$; (●) $[1\text{-C}_4\text{3-C}_2\text{IM}][\text{DCA}]/\text{K}_2\text{CO}_3$; (□) $[1\text{-C}_2\text{3-C}_2\text{IM}][\text{DCA}]/\text{K}_3\text{PO}_4$; (○) $[1\text{-C}_2\text{3-C}_2\text{IM}][\text{DCA}]/\text{K}_2\text{CO}_3$.

Tabela 1. Parametri Merchuk-ove jednačine (1)

JT+neorganska so+H ₂ O	T/K	A±σ	B±σ	C±σ	R
$1\text{-C}_2\text{3-C}_2\text{IM}][\text{DCA}]/\text{K}_3\text{PO}_4$	296.15	67.62 ± 0.77	-0.307 ± 0.005	$(1.388 \pm 0.032)10^{-4}$	0.9996
	308.15	69.34 ± 0.39	-0.314 ± 0.003	$(1.291 \pm 0.020)10^{-4}$	0.9999
	328.15	69.42 ± 0.29	-0.310 ± 0.002	$(1.278 \pm 0.016)10^{-4}$	0.9999
$1\text{-C}_4\text{3-C}_2\text{IM}][\text{DCA}]/\text{K}_3\text{PO}_4$	296.15	72.43 ± 1.27	-0.417 ± 0.010	$(4.439 \pm 0.179)10^{-4}$	0.9990
	308.15	75.50 ± 0.34	-0.426 ± 0.003	$(3.881 \pm 0.069)10^{-4}$	0.9999
	328.15	77.52 ± 0.24	-0.434 ± 0.002	$(3.547 \pm 0.048)10^{-4}$	0.9999
$1\text{-C}_2\text{3-C}_2\text{IM}][\text{DCA}]/\text{K}_2\text{CO}_3$	296.15	74.37 ± 1.38	-0.275 ± 0.008	$(8.568 \pm 0.309)10^{-5}$	0.9996
	308.15	71.53 ± 0.55	-0.253 ± 0.003	$(8.697 \pm 0.211)10^{-5}$	0.9998
	328.15	74.55 ± 0.24	-0.259 ± 0.003	$(8.028 \pm 0.236)10^{-5}$	0.9998
$1\text{-C}_4\text{3-C}_2\text{IM}][\text{DCA}]/\text{K}_2\text{CO}_3$	296.15	78.96 ± 3.06	-0.377 ± 0.019	$(3.049 \pm 0.243)10^{-4}$	0.9978
	308.15	81.72 ± 0.68	-0.379 ± 0.005	$(2.908 \pm 0.074)10^{-4}$	0.9998
	328.15	90.07 ± 0.99	-0.418 ± 0.006	$(2.146 \pm 0.109)10^{-4}$	0.9995

Na slici 1 se jasno uočava da je sposobnost isoljavanja fosfatnog anjona veća od karbonatnog za datu jonsku tečnost. Efekat isoljavanja (eng. salting-out) jonske tečnosti od strane neorganske soli je složen mehanizam. Uticaj anjona neorganske soli na solvataciju jonske tečnosti se može objasniti postojanjem dva tipa interakcija između njih. (1) Anjoni polarizuju molekule vode koji se jednim krajem vodoničnim vezama drže za molekul jonske tečnosti, čime se ta veza slabi pa je krajnji efekat lakša dehidratacija jonske tečnosti. Ovaj efekat je direktno proporcionalan entropiji hidratacije anjona ΔS_{hyd} tako da što je njena vrednost veća, so lakše isoljava jonsku tečnost i binodalna kriva je bliža koordinatnim osama. U

konkretnom slučaju $\Delta S_{\text{hyd}}(\text{K}_3\text{PO}_4) \sim 421 \text{ JK}^{-1}\text{mol}^{-1}$ je veće od $\Delta S_{\text{hyd}}(\text{K}_2\text{CO}_3) \sim 245 \text{ JK}^{-1}\text{mol}^{-1}$, što se slaže sa dobijenim rezultatima. (2) Povećanjem koncentracije neorganske soli dolazi do izražaja uticaj anjona na hidratacioni omotač oko hidrofobnog dela jonske tečnosti (bočnog alkil lanca) povećavajući površinski napon šupljine između bočne grupe i polarnog dela (imidazolijumovog prstena). Takođe na slici 1 se može uočiti uticaj dužine bočnog alkil lanca na imidazolijumovom prstenu na formiranje dvofaznih vodenih sistema. Sa povećanjem dužine bočnog lanca na N-1 poziciji imidazolijumovog prstena raste hidrofobnost jonske tečnosti odnosno smanjuje se afinitet prema vodi, a time se lakše nagrađuju dve faze. Na faznom dijagramu za sistem JT + neorganska so + voda se mogu očitati minimalni maseni udeli komponenata smeše koji su potrebni da bi se nagradile dve faze. Posle određivanja binodalnih krivih, poredili smo ravnotežne dijagrame sistema odnosno sposobnost jonskih tečnosti da nagrade bifazni sistem koja raste u nizu: $[\text{1-C}_2\text{3-C}_2\text{IM}][\text{DCA}]/\text{K}_2\text{CO}_3 < [\text{1-C}_2\text{3-C}_2\text{IM}][\text{DCA}]/\text{K}_3\text{PO}_4 < [\text{1-C}_4\text{3-C}_2\text{IM}][\text{DCA}]/\text{K}_2\text{CO}_3 < [\text{1-C}_4\text{3-C}_2\text{IM}][\text{DCA}]/\text{K}_3\text{PO}_4$. Sposobnost neorganskih soli da nagrade dvofazne vodene sisteme kada se dodaju vodenom rastvoru jonske tečnosti prati Hofmeister-ovu seriju.



Slika 2. Uticaj temperature na fazne dijagrame sistema $\{\text{JT} + \text{neorganska so} + \text{H}_2\text{O}\}$ sistem: (1a) $[\text{1-C}_4\text{3-C}_2\text{IM}]\text{DCA}$, (2a) $[\text{1-C}_2\text{3-C}_2\text{IM}]\text{DCA}$, (1b) $[\text{1-C}_4\text{3-C}_2\text{IM}]\text{DCA}$, (2b) $[\text{1-C}_2\text{3-C}_2\text{IM}]\text{DCA}$, ■ 295,15 K, ● 308,15 K, ▲ 328,15 K.

Na slici 2 prikazan je uticaj temperature na formiranje bifaznih vodenih sistema sa jonskim tečnostima. Binodalne krive su određene na tri temperature: 295,15K; 308,15K i 328,15K. Na slici 2 se vidi da je povećanjem temperature za određeni maseni udeo jonske tečnosti potrebno više soli da bi se nagradio dvofazni sistem, čime se smanjuje bifazna oblast faznog dijagrama. Ovaj efekta je posledica činjenice da su na višim temperaturama interakcije između jonske tečnosti i vode izraženije odnosno jonska tečnost biva jače solvatisana molekulima vode čime se povećava njena hidrofilnost i rastvorljivost.

Takođe, na slici 2 se jasno vidi da uticaj temperature zavisi i od vrste neorganske soli koja se upotrebljava. K_3PO_4 (slika 2(a)) je izrazito kosmotropna so, njena sposobnost isoljavanja je velika pa mala promena u rastvorljivosti jonske tečnosti pri povećanju temperature ne dovodi do značajnijeg pomeranja binodale. Sa druge strane karbonatni anjon ima manji, iako ne značajno manji, kosmotropni karakter od fosfatnog pa je uticaj temperature uočljiviji na faznom dijagramu prikazanom na slici 2(b). Takođe, poređenjem binodala vidi se da je efekat temperature značajniji za 1-butil-3-etilimidazolijum-dicijanamid u odnosu na 1-etyl-3-etilimidazolijum-dicijanamid za obe primenjene soli. Ovo je verovatno zbog toga što $[\text{1-C}_4\text{3-C}_2\text{IM}]\text{DCA}$ ima duži bočni alkil niz i hidrofobniji karakter koji se usled povećanja temperature smanjuje više nego kod $[\text{1-C}_2\text{3-C}_2\text{IM}]\text{DCA}$. Potrebna su dodatna istraživanja i preciznija merenja da bi se efekat temperature na bifazne vodene sisteme detaljnije objasnio.

Zaključak

Određeni su i okarakterisani fazni dijagrami (binodalne krive) za ispitivane bifazne vodene sisteme $\{\text{JT} + \text{neorganska so} + \text{H}_2\text{O}\}$ za dve novosintetisane jonske tečnosti: 1-etyl 3-etilimidazolijum-dicijanamid i 1-butil 3-etilimidazolijum-dicijanamid u kombinaciji sa neorganskim solima: K_3PO_4 i K_2CO_3 .

Eksperimentalni rezultati pokazuju da priroda jonske tečnosti kao i neorganske soli utiču u velikoj meri na formiranje bifaznih vodenih sistema. Povećanje bočnog niza na N-1 atomu imidazolijuma dovodi do lakšeg indukovanih bifaznih sistema tj. potrebna je manja količina neorganske soli da bi se nagradile dve faze. Takođe je pokazano da K_3PO_4 ima veću sposobnost za građenje bifaznih sistema od K_2CO_3 , što je posledica veće entropije hidratacije anjona $\Delta S_{hyd}(K_3PO_4) \sim 421 \text{ JK}^{-1}\text{mol}^{-1}$, a $\Delta S_{hyd}(K_2CO_3) \sim 245 \text{ JK}^{-1}\text{mol}^{-1}$. Uticaj temperature na građenje bifaznih sistema je uočljiviji kod jonske tečnosti sa dužim alkil nizom (1-butil 3-ethylimidazolijum-dicyanamid) i kod neorganskih soli sa manjom sposobnošću isoljavanja (K_2CO_3).

Zahvalnica: Ovaj rad je urađen u okviru projekata III 45006 i ON 172012 koji su finansirani od strane Ministarstva prosvete, nauke i tehnološkog razvoja Republike Srbije.

The salting-out effect and impact of temperature on phase diagrams of aqueous biphasic systems based on novel synthesized dicyanamide ionic liquids

In this work, novel phase diagrams for aqueous solutions of 1-ethyl-3-ethylimidazolium dicyanamide [$1-C_23-C_2im][DCA]$] and 1-butyl-3-ethylimidazolium dicyanamide [$1-C_43-C_2im][DCA]$] -based ionic liquids (ILs) combined with phosphate and carbonate based salts, K_3PO_4 and K_2CO_3 , are reported and discussed. Merchuk equation was applied in order to correlate the experimental binodal data. It was found that K_3PO_4 has better salting-out ability to induce aqueous biphasic system (ABS) than K_2CO_3 . The cation influence on the ability to form ABS is investigated for the IL with the same anion, dicyanamide $[DCA]^-$ and various alkyl chain lengths in the imidazolium N-1 position. It was found that ability to form ABS increases with the increase of the alkyl chain length on the imidazolium cation because of increasing ionic liquid hydrophobicity and poorer affinity for water. The effect of temperature and the alkyl chain length of ionic liquid on two phase formation were investigated. The experimental results show that biphasic region expands with reduction in temperature.

Reference:

1. N. J. Bridges, K. E. Gutowski, R. D. Rogers, *Green Chem.*, **9** (2007) 177
2. J. G. Huddleston, A. E. Visser, W. M. Reichert, H. D. Willauer, G. a. Broker, R. D. Rogers, *Green Chem.*, **3** (2001) 156
3. A. M. C. Ferreira, P. Esteves, I. Boal-Palheiros, A. B. Pereiro, L. P. N. Rebelo, M. G. Freire, *Green Chem.*, (2015) doi:10.1039/C5GC01610J
4. M. G. Freire, P. J. Carvalho, A. M. S. Silva, M. N. B. F. Lui, L. P. N. Rebelo, I. M. Marrucho, J. A. P. Coutinho, M. N. B. F. Santos, (2009) 202 doi:10.1021/jp8080035
5. K. E. Gutowski, G. A. Broker, H. D. Willauer, J. G. Huddleston, R. P. Swatloski, J. D. Holbrey, R. D. Rogers, *J. Am. Chem. Soc.*, **125** (2003) 6632
6. M. G. Freire, A. F. M. Cláudio, J. M. M. Araújo, J. a. P. Coutinho, I. M. Marrucho, J. N. C. Lopes, L. P. N. Rebelo, *Chem. Soc. Rev.*, **41** (2012) 4966
7. J. C. Merchuk, B. a Andrews, J. a Asenjo, *J. Chromatogr. B. Biomed. Sci. Appl.*, **711** (1998) 285
8. A. Chakraborty, K. Sen, *J. Chromatogr. A*, **1433** (2016) 41

Hemijsko inženjerstvo / Chemical Engineering

Phosphate removal from wastewater by electrocoagulation process using aluminium electrode

Borislav N. Malinović, Suzana Gotovac Atlagić, Tijana Malinović, Natalija Bjelajac, Aleksandra Milovanović

*Faculty of Technology, University of Banja Luka, 73 Stepe Stepanovića Street,
78000 Banja Luka, Bosnia and Herzegovina*

Introduction

Phosphorus is a natural nutrient, unavoidable in surface water which appears almost always as a phosphate ion¹. Phosphate ions could be in the form of the orthophosphates, condensed phosphates (pyro, meta and other polyphosphates) or organically bound phosphates. The origins of the phosphates are also diverse. Large quantities of phosphates can still be found in various detergents and cleaning products especially in less-developed countries which lack appropriate legislative on this problematic. Phosphates are also used for water treatment in water heaters in industries and heating plants. Especially extensive is the application of the phosphates in the agriculture as the fertilizer, where, if extensively used, they are carried toward surface water by rain, snow melting or other precipitations, as well as by the irrigation water. However, although precious nutrient highly valuable for the agriculture, phosphate released in extensive quantities into the surface waters, causes eutrophication².

Removal of the phosphate from the drinking waters and also from the wastewater started to draw the attention of the scientists and professionals from the 1960s³. Classical techniques for phosphate removal from this period are classified as: physical, chemical and biological. Physical methods remain quite expensive, and most of them, particularly electrodialysis or the reverse osmosis are very inefficient with phosphate removal only up to approximately up to 10%³. Chemical methods, par contrary, were more often and more widely used especially coagulation by aluminium sulphate or iron chloride. However, they also are expensive for maintenance due to problems with sludge managements and effluent neutralisation. In the third group of methods, the biological ones, efficiency is around 30 % which also demands additional treatments³. The adsorption methods as means of combined treatment with the biological ones were long considered, and they still are. Nevertheless, they also seem to be too complicated with necessity for following the number of factors influencing the process, thus there are continues efforts to find new removal techniques⁴.

This study consideres the electrocoagulation as the treatment for the phosphate removal from the synthetic wastewater. There are numerous studies on phosphate removal from wastewater with some of them dealing with the electrocoagulation itself. Authors like Behbehani *et al.*, Irdemez *et al.*, Attour *et al.* and others dealt with the application of the aluminium electrode in electrocoagulation⁵⁻⁹. For example, the efficiency of the aluminium and iron electrodes was compared in the batch reactor, in the presence of the NaCl as the supporting electrolyte, and the results have shown that phosphate removal efficiency was 100% for Al and 84,7 % for Fe (at pH=3, $\gamma_{(P-PO_4)}=100$ mg/L, $j=250$ A/dm²)⁵. In two separated studies, Irdemez *et al.* studied the pH (pH=3-9) and the current density ($j=0,25-1,0$ mA/cm²) influence on phosphate removal^{6,7}. Under optimal pH (pH=3), the efficiency was 86% without any supporting electrolyte with the duration of 20 min for the process⁶. With the current density increase the removal efficiency also increases. To obtain 80% efficiency at 25mg/L ($W_{sp}=0,305$ kWh/m³) 3 minutes was enough, for 50 mg/L ($W_{sp}=0,380$ kWh/m³) 5 minutes, while at 100 mg/L (0,610 kWh/m³) process demanded 12 min⁷. It is well known that the pollutant removal from the wastewater increases with increase of the solution conductivity¹⁰. According to the research done by Irdemez *et al.* , the highest efficiency in phosphate removal ($E_u=99,9\%$) is obtained with addition of the NaCl in concentrations of 4,5 mM ($\gamma_{(P-PO_4)}=50$ mg/L, $j=1$ mA/cm²) during 25 min of the treatment⁸. Results of the research by Attor *et al.* , indicate that with addition of the NaCl as the supporting electrolyte in concentrations of 25,5 mM, a complete phosphate removal is achieved (pH= 3, $\gamma_{(P-PO_4)} = 100$ mg/L, $j = 10$ mA/cm²)⁹.

Results and discussion

In present experimental research, a batch electrochemical reactor of 250 cm^3 capacity made from polypropylene with constant mixing was used, combined with two electrodes of the same area surface $P=37.3 \text{ cm}^2$, separated at $d=20 \text{ mm}$ distance. The electrode materials are of known composition and they satisfy the recommended standards: aluminium (Al 99.5/EN AW-1050 A; max. 0.25 % Si, max. 0.40 % Fe, max. 0.05% Cu, max. 0.05% Mn, max. 0.05 % Mg, max. 0.05% Ti, max. 0.07 % Zn, min. 99.50 % Al), stainless steel (EN 1.4301/AISI 304; max. 0.07 % C, 18.1 % Cr, 8.2 % Ni). As for the chemicals, a commercially available potassium dihydrogen phosphate (99.3 % KH_2PO_4 , Kemika, Croatia) and sodium chloride (99.5 % NaCl, Lachner, Czech Republic), were used. All the experiments were performed at the starting sample temperature of 20°C and pH=3 in accordance to the literature recommendations⁶⁻⁹. The electrodes were mechanically cleaned before each treatment, washed with detergent and the acetone for the grease and oil removal, while the surface stains removal was done by NaOH solution.

Synthetic wastewater was analysed before and after the treatment for the following parameters: phosphate contents (P-PO_4), total dissolved solids (TDS), pH-value, resistance (ρ), conductivity (κ). TDS, ρ , κ and pH value were determined by multimeter (Consort C861), phosphate concentration by spectrophotometry ($\lambda_{\text{max}}=410 \text{ nm}$) at Perkin Elmer, Lambda 25 in accordance with the standard method¹. To improve the efficiency of the electrocoagulation process, out of three available current regime, a pulsed current regime (PCR) was chosen. RS is defined by cathode current density, j_k , time of the cathode precipitation, t_k , density of the anode current, j_a , and the time of the anode dissolution, t_a . Reverse current period (step), T , represents a sum of the cathode precipitation, t_k and the time of the anode dissolution, t_a ¹¹.

Results for the phosphate removal by electrocoagulation are expressed by the mass concentration (mg/L) and the removal efficiency, E_u , in percent calculated by the formula (1). There the γ_i and γ_f are the initial and the final concentration of the phosphate in mg/L. Energy consumption for removal per unit of the contaminant is one of the most important technological parameters showing the efficiency of the electrochemical reactor, since it influences the total price of the treatment. It is expressed through the formula (2), where U is the tension, I - electric current, t - time, m - mass of the phosphates removed.

$$E_u = \frac{\gamma_i - \gamma_f}{\gamma_i} \cdot 100 / \% \quad (1); \quad W_{\text{sp}} = \frac{\int_0^{\theta} I E_r dt}{3600 \cdot 1000 m} / [\text{kWh/kg}_{\text{polutant}}] \quad (2).$$

Influence of the electrolysis duration, concentration of the supporting electrolyte, current density, initial phosphate concentration, energy consumption, cathode material and the pulsed current regime were studied. Figure 1 and 2 show the influence of the electrolysis duration (2,5, 5, 10, 30, 40 min) on wastewater phosphate concentration decrease ($\gamma_0=50 \text{ mg/L}$), or, it can also be said, on the removal efficiency without supporting electrolyte. A current density used was $j=1 \text{ mA/cm}^2$ which, in accordance to the literature, was cited as the optimal current density⁵. It can be clearly seen that with electrolysis duration prolongation, the phosphate concentration in wastewater decreases, or it can be said that removal efficiency is increasing, reaching the values of $E_u=98.9 \text{ \%}$, in 40 min of treatment.

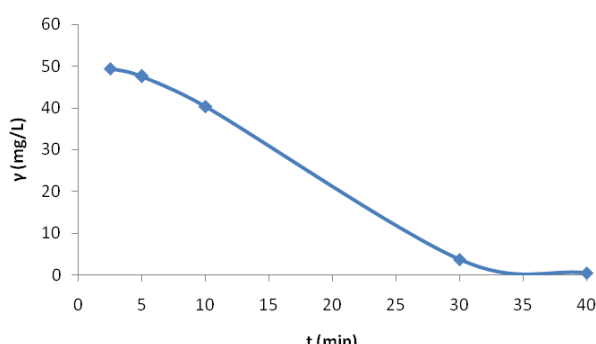


Figure 1. Phosphate concentration decrease in relation to the electrolysis duration ($j=1 \text{ mA/cm}^2$, $t=40 \text{ min.}$)

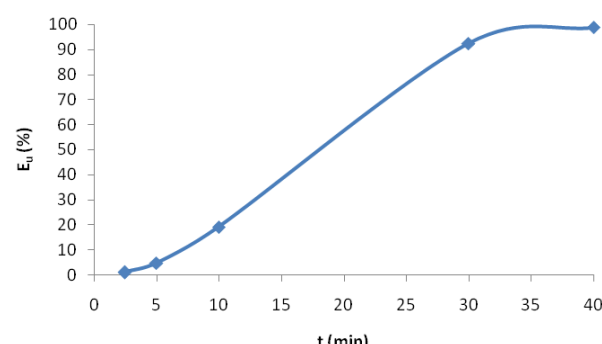


Figure 2. Phosphate removal efficiency in relation to the electrolysis duration ($j=1 \text{ mA/cm}^2$, $t=40 \text{ min.}$)

Influence of the NaCl as the supporting electrolyte on phosphate removal efficiency is shown at Figure 3. Efficiency is highest at $\gamma_{\text{NaCl}}=0,5 \text{ g/L}$ concentration, being $E_u=55,5\%$. Since there are no greater differences in removal efficiencies at concentrations of $\gamma_{\text{NaCl}}=0,25 \text{ g/L}$ ($E_u=52,1\%$) and $\gamma_{\text{NaCl}}=0,5 \text{ g/L}$, the rest of the research was performed under $\gamma_{\text{NaCl}}=0,25 \text{ g/L}$. Increase of the electrolysis duration ($t=20 \text{ min}$) achieves the removal efficiency of 93.6 % (Figure 4).

Figure 5. shows dependence of the phosphate removal efficiency on the current density ($0,25; 0,5; 1; 2 \text{ mA/cm}^2$) with $\gamma_0=50 \text{ mg/L}$, $\gamma_{\text{NaCl}}=0,25 \text{ g/L}$ and $t=10 \text{ min}$. Highest efficiency is reached under the current density of $j=2 \text{ mA/cm}^2$ and it has shown the value of $E_u=92,1\%$, while for the lower current densities, the removal efficiency did not differ significantly. Due to the small difference in efficiency achieved, but significantly higher energy consumption under higher current densities (for $j=0,25 \text{ mA/cm}^2$, energy consumption was $W_{sp}=4,73 \text{ kWh/m}^3$, and for $j=2 \text{ mA/cm}^2$ energy consumption was $W_{sp}=106,94 \text{ kWh/m}^3$). Therefore in further experiments the current density was set to $j = 0,25 \text{ mA/cm}^2$.

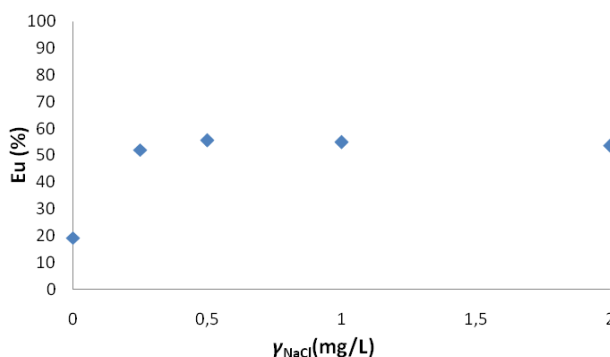


Figure 3. Relationship between phosphate removal efficiency and the NaCl concentration ($j=1 \text{ mA/cm}^2$, $t=10 \text{ min.}$)

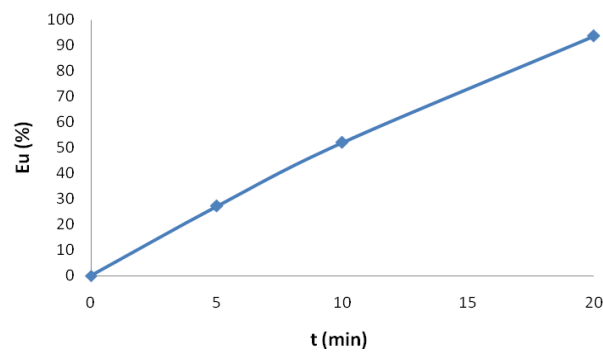


Figure 4. Relationship between the phosphate removal efficiency and the electrolysis duration ($j=1 \text{ mA/cm}^2$, $t=20 \text{ min}$, $\gamma_{\text{NaCl}}=0,25 \text{ g/L}$)

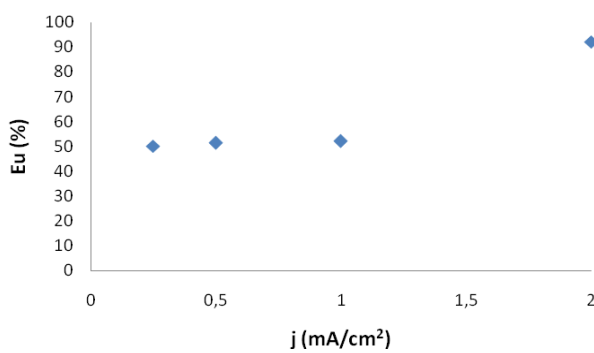


Figure 5. Efficiency of phosphate removal at varying current densities ($\gamma_0=50 \text{ mg/L}$, $\gamma_{\text{NaCl}}=0,25 \text{ g/L}$)

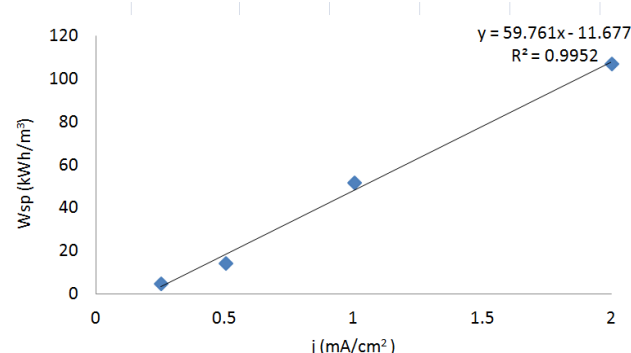


Figure 6. Relation between the energy consumption and the current density

Under the optimal experimental conditions ($j=0,25 \text{ mA/cm}^2$, $t=10 \text{ min}$, $\gamma_{\text{NaCl}}=0,25 \text{ g/L}$) the efficiency is increasing with the decrease of the initial phosphate concentration (25, 50 i 100 mg/L) in the wastewater, which is in accordance with previous findings⁷. Efficiency is highest at the phosphate concentration of 25 mg/L and goes up to $E_u=62,6\%$, while it is the lowest under phosphate concentration of 100 mg/L with value of $E_u=29,8\%$ (Figure 7). Removal efficiency and the lowering of the phosphate initial concentration show a linear relationship with $R^2=0,997$.

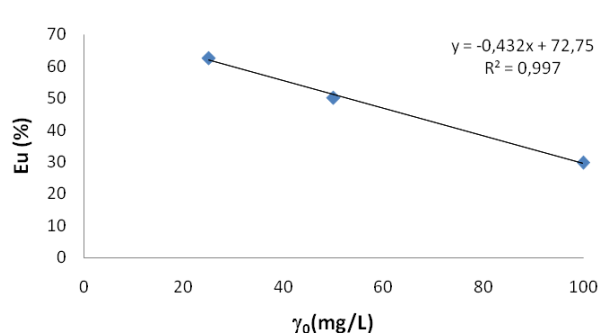


Figure 7. Relationship between efficiency and the phosphate initial concentration in wastewater

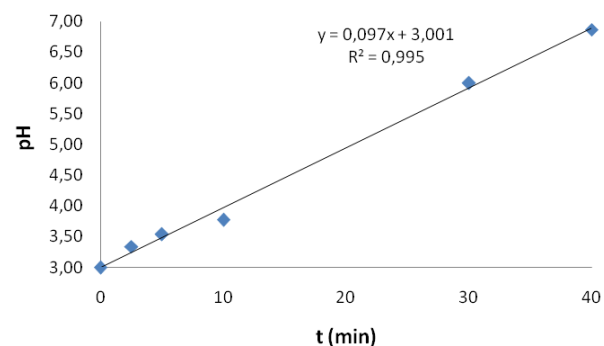


Figure 8. Dependence of the pH value on the electrolysis duration (t=40 min)

Figure 8 shows that during the electrolysis, the pH value is increasing. This trend is also linear with $R^2=0.995$. Influences of the stainless steel (SS) as the cathode material, and the PCR as the factors were also studied. Figure 9 shows the influence of the stainless steel as the cathode on phosphate removal efficiency, where it can be seen that the difference in removal efficiency is negligible and therefore, the aluminium cathodes can be successfully replaced by the SS cathodes efficient and easier for maintenance. Behbahani *et al.* suggest electrode replacement every 10 minutes in order to prevent their passivation⁵.

Figure 10 shows the negligible increase in efficiency of the phosphate removal after removal of the PCR. This behaviour is the sign that there is no threatening passivation or staining of the electrodes during electrolysis, and that PCR has no positive influence on the process itself.

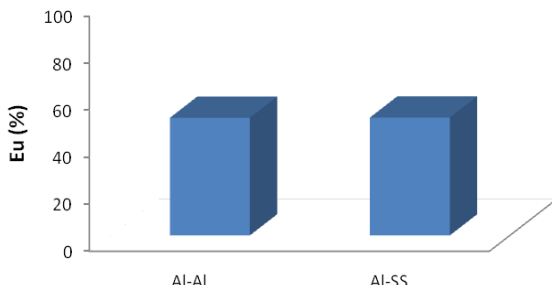


Figure 9. Phosphate removal efficiency with and without stainless steel electrode application

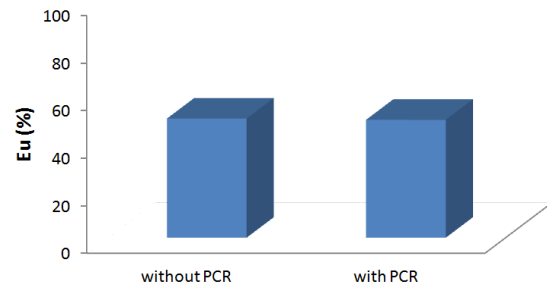


Figure 10. Phosphate removal efficiency with and without the PCR

Conclusion

The study has shown that the electrocoagulation is an efficient method for phosphate removal from wastewater. Efficiency of 98.9 % in phosphate removal was achieved in 40 minutes under pH=3, $j=1$ mA/cm² and $\gamma_0=50$ mg/L P-PO₄. With NaCl as a supporting electrolyte ($\gamma=0,25$ g/L), efficiency was 93.6 % in only 20 minutes of treatments. By applying lower current densities, somewhat lower efficiency was achieved, however, process was significantly more economical as far as the energy consumption is concerned ($j=0.25$ mA/cm², $E_u=50.1\%$, $W_{sp}=0.095$ kWh/kg_{P-PO₄}).

Acknowledgements: This work was supported in part by the Ministry of Science and Technology of the Republic of Srpska under Project 19/6-020/961-171/14.

Uklanjanje fosfata iz otpadne vode procesom elektrokoagulacije primjenom aluminijumske elektrode

U radu je vršeno ispitivanje efikasnosti aluminijumske (Al) elektrode pri elektrokoagulaciji otpadnih voda koje sadrže fosfate (P-PO₄). Istraživanja su sprovedena na sintetski pripremljenoj otpadnoj vodi u laboratorijskom elektrohemijском šaržnom reaktoru. Tokom istraživanja praćen je uticaj vremena trajanja elektrolize, gustine struje, različite koncentracije pomoćnog elektrolita i fosfata, primjene nerđajućeg čelika kao katode i uticaj

režima reversne struje. Rezultati su prikazani preko efikasnosti uklanjanja fosfata. Za 40 minuta tretmana postignuta je efikasnost uklanjanja od 98,9 %, pri $pH=3$, $j=1\text{ mA/cm}^2$ i $\gamma_0=50\text{ mg/L P-PO}_4$, a dodatkom NaCl kao pomoćnog elektrolita ($\gamma=0,25\text{ g/L}$), postiže se efikasnost uklanjanja 93,6% za 20 minuta tretmana.

Literature

1. APHA, EPA; Standard Methods for the Examination of Water and Wastewater, 1999.
2. R. M. Harrison, *Pollution: causes, effects and control*, Royal Society of Chemistry, Cambridge, UK, 2001
3. S. Vasudevan, G. Sozhan, S. Ravichandran, J. Jayaraj, J. Lakshmi & M. Sheela, *Industrial & Engineering Chemistry Research*, **47(6)** (2008) 2018
4. N. Boujelben, J. Bouzid, Z. Elouear, M. Feki, F. Jamoussi & A. Montiel, *Journal of Hazardous Materials*, **151(1)** (2008) 103
5. M. Behbahani, M. R. Alavi Moghaddam, M. Arami, *International Journal of Environmental Research*, **5(2)** (2011) 403
6. S. Irdemez, N. Demiricioglu, Y. S. Yildiz, *Journal of Hazardous Materials*, **B137** (2006) 1231
7. S. Irdemez, N. Demiricioglu, Y. S. Yildiz, Z. Bingul, *Separation and Purification Technology*, **52** (2006) 218
8. S. Irdemez, Y. S. Yildiz, V. Tosunoglu, *Separation and Purification Technology*, **52** (2006) 394
9. A. Attour, M. Touati, M. Tlili, M. Ben Amor, F. Lapicque, J.-P. Leclerc, *Separation and Purification Technology*, **123** (2014) 124
10. B. Malinović, M. Pavlović & N. Gorgi, *Zaštita materijala* , **55(4)**, (2014) 171
11. K. Popov, *Primena pulsnih režima u galvanskoj tehnici*, Institut za hemiju, tehnologiju i metalurgiju. Belgrade, Serbia, 1992

Experimental measurement of volumetric, transport, ultrasonic and refractive index properties of binary mixtures (ethyl oleate + *n*-hexadecane) at different temperatures and atmospheric pressure

Mohamed A. Aissa, Gorica R. Ivaniš, Ivona R. Radović, Mirjana Lj. Kijevčanin

Faculty of Technology and Metallurgy, University of Belgrade, Karnegijeva 4, 11120 Belgrade, Serbia

Abstract

Some of the most important properties in diesel engine design and operation are density and viscosity of a fuel under different conditions. Thanks to increasing awareness of global warming and environmental pollution, the interest in renewable energy sources and, particularly, non-toxic fuel supplements grows progressively. One of the best solutions for transport sector is the use of biodiesel and its mixtures with petro diesel which requires knowledge of the fundamental thermodynamic properties of their blends. Pure ethyl oleate, that is one of the main components of most of biodiesel fuels, and *n*-hexadecane, which serves as a reference for diesel fuels, were examined here, as well as their mixtures. Density, viscosity, sound velocity and refractive index data for the binary system (ethyl oleate + *n*-hexadecane) were measured in the whole concentration range and within a wide range of temperature (with temperature step 5 K) at atmospheric pressure. The measurements were performed on DMA 5000 densimeter, Stabinger SVM 3000 viscometer, DSA 5000 M density and sound velocity meter and RXA 156 refractometer, all produced by Anton Paar. Based on the corresponding experimental data, the isentropic bulk modulus was computed and presented.

Introduction

Transport sector has the largest share of oil consumption and is the major contributor of green house gases and of the global warming, via direct and indirect emissions of carbon dioxide (CO₂), nitrogen oxides (NOx), carbon monoxide (CO) and volatile organic compounds (VOCs) which affect the oxidation-reduction capacity of the atmosphere.¹⁻⁴ These issues have challenged researchers to seek for alternative fuels in order to mitigate the exhaust emissions globally, without significant modifications in diesel engines design. The idea of using vegetable oils instead of fossil diesel fuels has resurfaced as a way to reduce green house gases. However, direct use of pure vegetable oils face some technical problems, due to the values of their thermodynamic properties (i.e. density and viscosity), which make them inefficient for the most combustion engines.

Such investigations can be found in literature,¹ where focus has recently been on transesterification of vegetable oils into alkyl esters in order to achieve acceptable biodiesel properties and purity. One of the methods used to reduce higher values of density, viscosity and sound velocity of biodiesel is to blend them with diesel. However, property changes, associated with the differences in chemical structure between diesel and biodiesel fuel, might change engine performance and emission characteristics of diesel engine.^{5,6} The properties of the mixture are directly influenced by the temperature and pressure of engine operating condition as well as by the composition of biodiesel. The isentropic bulk modulus is, together with speed of sound, density and viscosity, one of the properties vastly affecting engine parameters like performance, efficiency and emissions.^{7,8} The presented study aims to report a new experimental data on volumetric (density), acoustic (sound velocity), transport (viscosity) and refractive index properties of pure components ethyl oleate and *n*-hexadecane, and their mixtures at wide temperature range and at atmospheric pressure. Based on the corresponding experimental data, isentropic bulk modulus is calculated.

Experimental

Materials. The chemicals used in this work were purchased from Sigma Aldrich with a mass purity > 99% and were used without further purification. Prior to use, all liquid were kept in dark bottles under dry nitrogen. The purity of components was ascertained by comparison of the experimental density, viscosity, sound velocity and refractive index values at four temperatures (303.15, 308.15, 313.15, and 318.15) K, with those reported in the literature. The measured density, viscosity and sound velocity values of pure ethyl oleate are in a good agreement with literature with a percentage maximum deviations 0.18 % for density,⁹ 7.3 % for viscosity⁹ and 0.17 % for sound velocity,¹⁰ while percentage

maximum deviations between the measured and literature values for *n*-hexadecane were 0.012 %,¹¹ 1.85 %¹¹ and 0.029 %,¹² respectively.

Apparatus and Procedure. Binary mixture was prepared using an electronic balance (Mettler toledo, model AG204) to an accuracy of $\pm 1 \cdot 10^{-4}$ g, over the entire composition range. Before analysis, the mixtures were thoroughly homogenized and degassed. The density, ρ , and dynamic viscosity, η , measurements were made using the Anton Paar DMA 5000 densimeter and Anton Paar Stabinger SVM 3000/G2 viscometer, respectively. A determination of sound velocity, u , was carried out with the Anton Paar DSA 5000 M, while refractive index, n_D , was measured using an automatic Anton Paar RXA 156 refractometer. The combined expanded uncertainties of the density, viscosity, refractive index and speed of sound measurements with a coverage factor of $k = 2$ (confidence level of 95 %) were estimated to be 0.08 kg m^{-3} , 0.003 mPa s , $5 \cdot 10^{-5}$ and 0.1 m s^{-1} , respectively.

The isentropic bulk modulus (β), can be calculated at each temperature level using equation (1):

$$\beta = \rho u^2 \quad (1)$$

where u is sound velocity and ρ stands for the density of a sample.

Results and discussion

The experimentally determined values for density in the temperature range 293.15–363.15 K, viscosity in the temperature range 293.15–373.15 K, sound velocity and refractive index at temperatures 293.15–343.15 K for pure ethyl oleate and *n*-hexadecane and their mixtures are presented in Fig. 1.

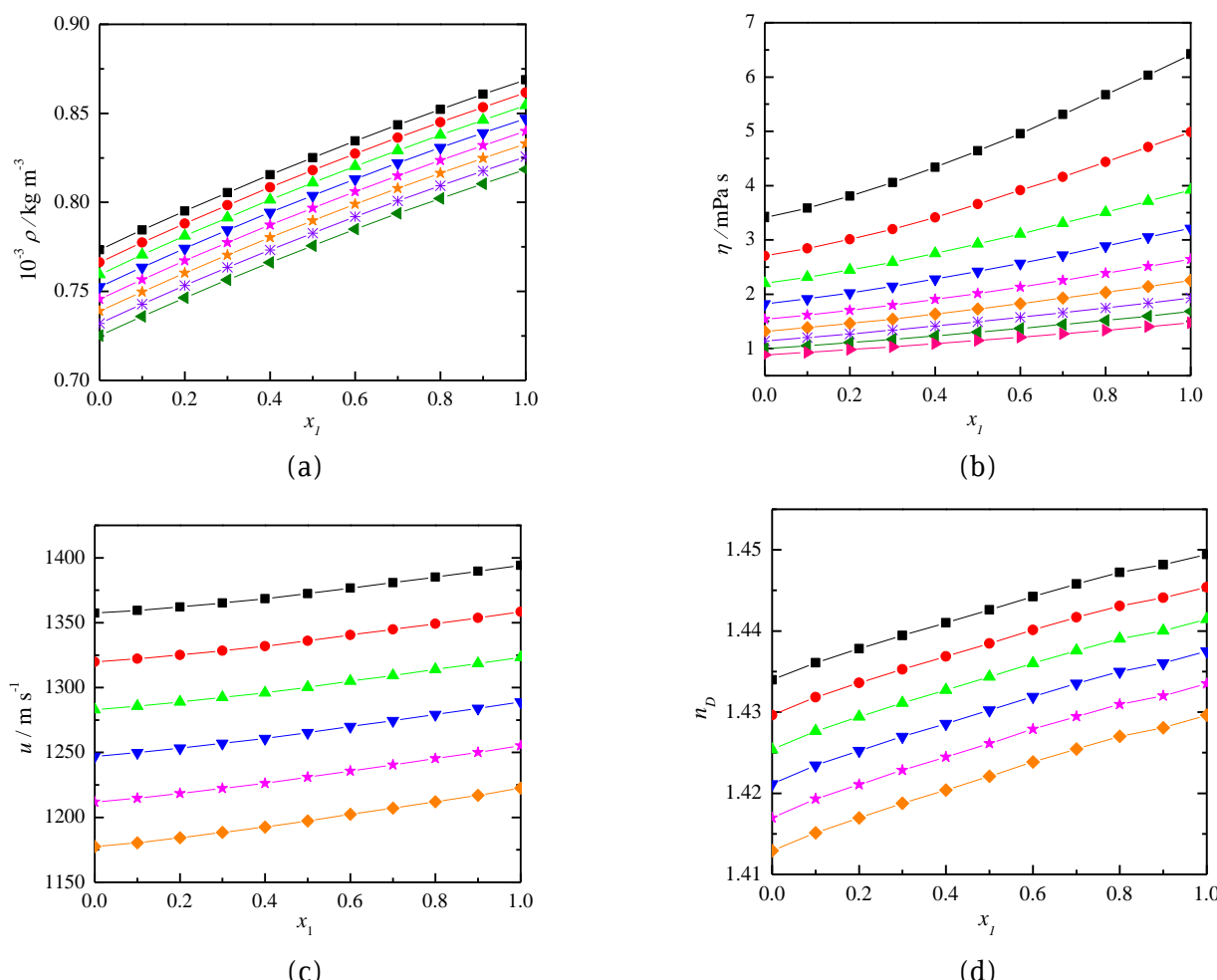


Figure 1. Experimental data of (a) density, (b) viscosity, (c) sound velocity and (d) refractive index for the binary system (ethyl oleate (1) + *n*-hexadecane) at atmospheric pressure and (■) 293.15 K, (●) 303.15 K, (▲) 313.15 K, (▼) 323.15 K, (★) 333.15 K, (◆) 343.15 K, (※) 353.15 K, (◀) 363.15 K and (▶) 373.15 K

As it can be seen, the values of density, viscosity, sound velocity and refractive index of the pure ethyl oleate are greater than of *n*-hexadecane. Also, all properties decrease with increase in temperature. Density is an important parameter in diesel engine performance since fuel injection equipment operates on a volume metering system. This will lead to a slightly greater mass of used biodiesel because of its higher density values. Viscosity, also a vital parameter, is a measure of resistance of fluid to flow, which is closely related to the operation of fuel injection system. The sound velocity is also an essential parameter. A higher speed of sound and the bulk modulus of biodiesel result in a quicker fuel pressure rise from the fuel pump towards the injectors leading to earlier injection timing which in turn produce higher NO_x emission. One of the methods to reduce higher values of density, viscosity and sound velocity of biodiesel is to blend it with diesel. The experimentally determined values for density, viscosity, sound velocity and refractive index for the system ethyl oleate + *n*-hexadecane over the entire composition range at different temperature are presented in Fig. 1. There is no experimental data in literature for the studied mixture. The increase of ethyl oleate concentration in the mixture promotes an increase of physical parameters.

It can be noticed that a continuous increase of sound velocity and density of mixture with decreasing of mole fraction of *n*-hexadecane was obtained, because these parameters are comparatively higher in ethyl oleate than in *n*-hexadecane. Viscosity of mixture also increases as the concentration of *n*-hexadecane decrease from 1 to 0, because ethyl oleate is more viscous than *n*-hexadecane at the same temperature. A refractive index of *n*-hexadecane is lower than ethyl oleate, consequently, an increase in ethyl oleate concentration increases the mixture's refractive index. The temperature dependence of physical parameters of binary mixture exhibits the usual behavior at all studied compositions. They decrease as the temperature increases. At each concentration, the viscosity decreases as the temperature increases making a mixture less viscous. A refractive index for both ethyl oleate and *n*-hexadecane decreases when the temperature increases. This happens due to higher temperature and smaller density, directly affecting the refractive index for the same temperature interval. It was noticed that for both, ethyl oleate and *n*-hexadecane, refractive index varies linearly and proportionally in the range of studied temperature, indicating that refractive index variation with temperature is practically the same.

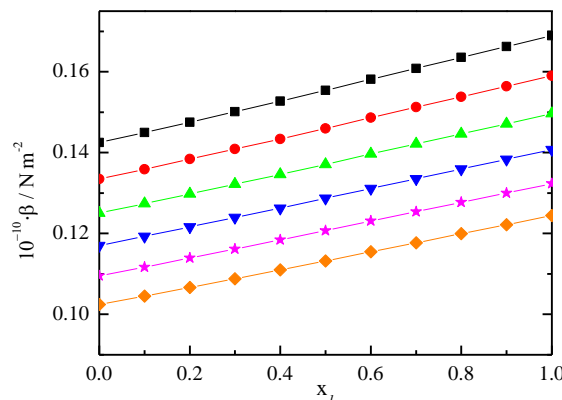


Figure 2. Isentropic bulk modulus for the binary system (ethyl oleate (1) + *n*-hexadecane) at atmospheric pressure and at (■) 293.15 K, (●) 303.15 K, (▲) 313.15 K, (▼) 323.15 K, (★) 333.15 K, (◆) 343.15 K, (※) 353.15 K, (◀) 363.15 K and (▶) 373.15 K

On the basis of the literature, the isentropic bulk modulus is related to the free space between molecules. Fig. 2 shows that ethyl oleate has higher bulk modulus and hence lower compressibility because it is an oxygenated fuel, which creates a permanent dipole moment in the molecule resulting in stronger bonding and increased molecular affinity compared to *n*-hexadecane. In other words, this will result in reducing of free space between molecules due to strong intermolecular forces. It is clearly seen from Fig. 2 that the concentration dependence of the bulk modulus of binary mixture exhibits the usual behavior at all studied temperatures. It increases as the concentration of ethyl oleate increases and the

slopes of the lines appear to be approximately the same. At each concentration, it decreases as the temperature increases.

Conclusion

Density, viscosity, sound velocity and refractive index of binary mixtures comprising ethyl oleate and *n*-hexadecane have been measured in the whole composition range at different temperatures and atmospheric pressure. The isentropic bulk modulus, which may relate to the engine performance, efficiency and emissions, was computed and presented. The results show that the increase of ethyl oleate concentration in the blends leads to an increase of the thermodynamic properties values at all studied temperatures. Density, viscosity, sound velocity, refractive index and isentropic bulk modulus values of the mixtures are between the values of the pure ethyl oleate and *n*-hexadecane, as expected. Viscosity dependence on ethyl oleate fraction in the blends is exponential, while for the rest of the studies properties it seems linear.

The authors gratefully acknowledge the financial support received from the Research Fund of Ministry of Education and Science (project No 172063), Serbia and the Faculty of Technology and Metallurgy, University of Belgrade.

Експериментално одређивање волуметријских, транспортних, ултразвучних својстава и индекса рефракције бинарних смеша (етил олеат + *n*-хексадекан) на различитим температурама и атмосферском притиску

Нека од најбитнијих својстава за дизајн и рад дизел мотора су тустина и вискозност шорива при различитим условима. Захваљујући распон свести о глобалном зајревању затрајењу животне средине, пројесиво распеће интересовање за обновљиве изворе енергије и, посебно, неоксичне додатке јоривима. Једно од најбољих решења у области трансформација јесте употреба биодизела и његових смеша са дизелом, што захтева познавање основних термодинамичких својстава њихових смеша.

Чист етил олеат, који је једна од основних компонената већине биодизел јорива, и *n*-хексадекан, који се користи као рејер за дизел јорива, су испитивани у овом раду, као и њихове смеше. Густина, вискозност, брзина простирања звука и индекс рефракције за бинарне системе (етил олеат + *n*-хексадекан) су мерење у чишћем ослеју концентрација и широком ослеју температуре (са кораком од 5 K) на атмосферском притиску. Мерења су вршена на тустиномеру DMA 5000, вискометру Stabinger SVM 3000, уређају за мерење тустине и брзине простирања звука у узорку DSA 5000 M и рефрактометру RXA 156, произвођача Anton Paar. На основу одговарајућих експерименталних података израчунат је и предстањен и изенетропски модул стапљивости.

References

1. A. K. Agarwal, *Prog. Energy. Combust.Sci.* **33** (2007) 233-271
2. D. Hernández, J. J. Fernández, F. Mondragón, D. Lopez, *Fuel* **92** (2012) 130-136
3. E. Uherek, T. Halenka, J. Borken-Kleefeld, Y. Balkanski, T. Berntsen, *Atmos. Environ.* **44** (2010) 4772-4816
4. J. Wade, C. Holman, M. Fergusson, *Energ. Policy* **22** (1994) 509-522
5. R. Altın, S. Çetinkaya, H. S.Yücesu, *Energ. Convers. Manage.* **42** (2001) 529-538
6. M. Lapuerta, O. Armas, J. R. Fernandez, *Prog. Energ. Combus.* **34** (2008) 198-223
7. J. Sun, A. C. Jerlad, J. J. Timothy, *Prog. Energ. Combus.* **36** (2010) 677-695
8. A. A. Rafaat, *Int. J. Environ. Sci. Te.* **6** (2009) 677-694
9. M. Pratas, S. Fritas, M. B.Oliveira, S. C. Monteiro, *J. Chem. Eng. Data.* **55** (2010) 3983-3990
10. S. V. D. Freitas, Â. Santos, M. J. M. Maria-Luísa, L. A. Follegatti- Romero, *Fuel*, **108** (2013) 840-845
11. S. Outcalt, A.Laesecke, T. J. Fortin, *J. Chem. Thermodyn.* **42** (2010) 700-706
12. X. Wang, X.Wang , H.Lang, *J. Chem. Thermodyn.* **97** (2016) 127-134.

Influence of resolution in digital characterization of sand particles size and shape

Zorana Arsenijević, Mihal Đuriš, Tatjana Kaluđerović Radoičić*

Institute for Chemistry, Technology and Metallurgy, University of Belgrade, Njegoseva 12, Belgrade, Serbia,

**Faculty of Technology and Metallurgy, University of Belgrade, Karnegijeva 4, Belgrade, Serbia*

Abstract

This paper investigated the influence of resolution and two image analysis softwares for image analysis (*SigmaScan Pro* and *ImageJ*) on parameters and shape factors commonly used in the characterization of particles. In our previous paper¹ characterization of polydisperse sand particles was investigated at two scanning resolutions, and arisen a need to examine in more detail the impact of different scanning resolutions on shape factors. The analyzed particles were the polydisperse fractions of quartz filtration sand with sieve diameters in the intervals of 0.85-1.030 mm, 1.406-1.600 mm and 2.00-2.83 mm. The scanned image of particles was used for analysis. In addition, the images of circles as reference were generated. The scanning resolutions used in this study were 75 to 4800 dpi, and grayscale thresholds were optimized for discrimination of particle background. The results indicate that the resolution (pixel size) and algorithms used in image analysis softwares have influences on obtained shape factors, and most significant effect was observed in the calculated particle perimeters.

Keywords: image analysis; resolution; shape analysis; pixel size; sand particles

Introduction

The particle shape is an important factor that determines the behavior of particulate systems in various fields of science and engineering²⁻⁶. The correct characterization is particularly important when polydisperse mixture of non-spherical particles are used, as in sand filters, which are used in installations for production of drinking water. Quartz filtration sand is a natural material composed of particles of different shapes and sizes. To adequately predict the behavior of fluidized beds of non-spherical particles with wide size distribution and most often non-uniform shape it is very important to determine the representative particle diameter and shape factor as well as their distributions⁷. The lack of models and correlations for prediction the mechanical and hydrodynamic behavior of irregularly shaped particles can be attributed to the variety and complexity of particle shapes⁸, the difficulty of defining shape parameters suitable for modeling, and the lack of classifying techniques to characterize particle shape⁹. Many of the physical and chemical properties of bulk solids and multiparticulate systems depend on particle shape and surface geometry. Shape factors are mathematical functions that require previous determination of particle size, such as length, diameter, perimeter, area or volume. They are categorized in 1D, 2D and 3D shape factors^{4,6,8,10-12}. The available literature shows that there is no agreement on the usage of shape parameters and is not clear which parameter is the best^{8,12,13}. Particle shape determination using computer assisted methods is of great help¹⁴ and the benefits are obvious: a large number of measurements can be taken in a short time, and they provide an economic, consistent and objective analytical method. Image analysis consisting of: image formation, image scanning, digitized particle boundary detection, digitized particle analysis by count, shape, size or other selected parameter, data processing and analyzing and data presentation. One of the most important parameters that should be taken into account is the resolution of the analyzed image because it affects parameters such as the perimeter¹⁵.

The aim of this paper was to determine the minimum resolution of particle digital image which would lead to the desired accuracy in size and shape characterization. 2D particle characterization was chosen due to the manageable and convenient methodology that can be used for image capturing and in order to avoid expensive equipment. Two image analysis softwares, *ImageJ* and *SigmaScan Pro* were used for image analysis.

Experimental

In this work three polydisperse fractions of quartz filtration sand were analyzed with sieve diameters $d_m = 0.85\text{-}1.030\text{ mm}$, $1.406\text{-}1.600\text{ mm}$ and $2.00\text{-}2.83\text{ mm}$. The basic particles characteristics are shown in

Table 1. Basic particles characteristics

Particles	$d_{s,n+1}$ / mm	$d_{s,n}$ / mm	d_m / mm	d_R	ρ_p kg/m ³
I	2.000	2.830	2.415	1.415	2638
II	1.406	1.600	1.503	1.138	2638
III	0.850	1.030	0.940	1.212	2638

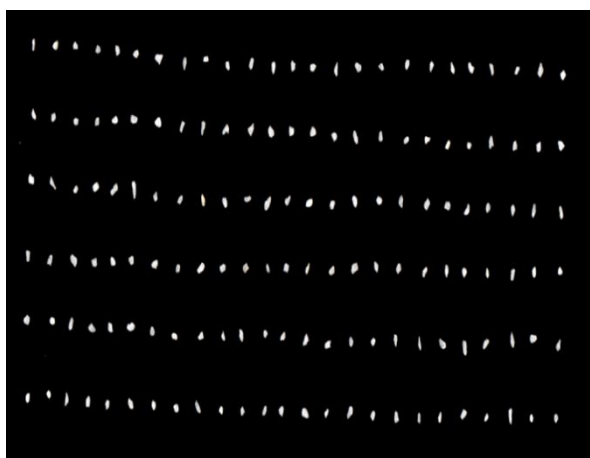
Fig. 1. Example of scanned image of irregular sand particles

Table 1, where d_R is ratio between two successive sieve sizes, $d_{s,n}$ and $d_{s,n+1}$, and d_m is the mean sieving diameter $[(d_{s,n} + d_{s,n+1})/2]$.

The images were captured by 2D scanner HP Scanjet 300 and were stored at a different resolutions in TIFF format for processing. Before scanning, the particles were carefully distributed on a contrasting background at the distance of 3-5 mm between them to avoid overlap and touching each other (Fig.1). The particle is assumed to lay over its most stable axis, e.g. longest and intermediate axis lie more or less parallel to the scanner glass while the shortest axis is perpendicular or random. The number of scanned particles fluctuated over 150 particles per scan, in order to reach a compromise between operating time and reliability of experimental results. The projected diameter, perimeter, circularity, etc., were determined using SigmaScan Pro and ImageJ softwares^{16,17}. It is necessary to enhance the contrast between particles and background and to convert the images to binary. On the basis of given color intensity the programs outline each particle and calibrate the distance between three reference points in the image, as the basis for software calculations of particle area, perimeter, etc. The scanning resolutions used in this paper were 75 to 4800 dpi, and grayscale thresholds were optimized for discrimination of particle background. Increasing the resolution, the scanning time also grew, for example, the scanning at 4800 dpi for one vertical line of sand particles (Fig.1) took about 50 min. The obtained scanned images were processed in SigmaScan Pro and ImageJ and image processing is relatively similar in both softwares. In addition, the images of circles of 1-3 mm were drawn in Corel Draw Suite 12 with an 8-bit grey scale as reference particles for the evaluation of the influence of different resolutions and image analysis softwares on size and shape factors.

Table 2. Shape descriptors defined in Image J and Sigma Scan Pro

	ImageJ	SigmaScan Pro
Projected area, A	Surface area of the projection of the object - sum of pixels areas in calibrated units (e.g., mm ² , µm ² , etc.)	Surface area of the projection of the object - sum of pixels areas in calibrated units (e.g., mm ² , µm ² , etc.)
Projected diameter, d_A	Not calculated	$\sqrt{\frac{4}{\pi}} A$
Perimeter, P	Based on differential method	Calculated on the basis of horizontal, vertical and diagonal contributions
Circularity, ϕ	$4\pi \frac{A}{P^2}$	$4\pi \frac{A}{P^2}$

The parameters used for particle characterization in this work are presented in Table 2. The area (A) and perimeter (P) estimations differ in ImageJ and SigmaScan Pro, since the number of pixels per particle is different. Also, the shape descriptors in two softwares are different. The missing shape descriptors were manually calculated by appropriate equations in order to compare results from two softwares. In this way, two image analysis programs complement each other.

Results and discussion

In this paper, large amount of data was processed since 3 different sand fractions were scanned in 7 different resolutions and the obtained images were processed in 2 softwares using 3 different values of threshold. Influence of threshold intensity and image resolution on different size and shape factors was analyzed. Digitalization process of the particle image itself can lead to errors¹⁵. Increasing the number of pixels that represent the particle, increases the quality of shape representation. In this paper, the limit to which this increase in number of pixels leads to the improved results of particle size and shape analysis was investigated.

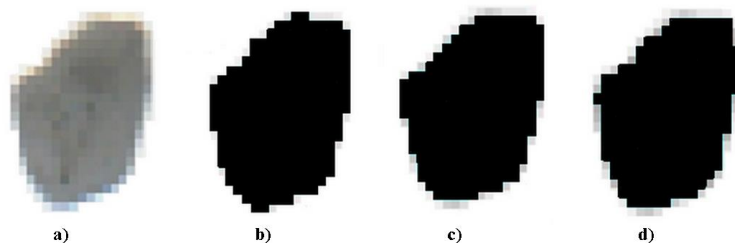


Fig. 2. Influence of threshold on particle boundaries, **a)** scanned particle, threshold ranges of: **b)** 40-230, **c)** 60-230, and **d)** 80-230

Threshold intensity. Threshold is the only parameter that must be manually set in the image processing softwares. Fig.2 shows how different threshold ranges influence the sand particle boundaries. By visual observation, it was concluded that the best results are achieved with threshold interval of 40-230 in the case of sand particles analysis, since the particle is better covered with black pixels. This indicates that the lower threshold limits of 60 and 80 gave poor results in distinguishing the particles from the background. It should be noted that the actual threshold value for each case of digital particles characterization must be based on visual observation of the scanned image and the experience of the investigator, and that there can be no general recommendation for the threshold intensity which should be used.

Influence of resolution on size and shape factors. Accuracy of digital representation of an object is, among other factors, determined by the image resolution. The pixel density will have a significant impact upon what the thresholded image looks like¹⁸. As a continuation of our previous investigation¹, it was needed to examine the impact of different scanning resolutions on shape factors in more detail. In this work, the scanning resolutions of 75, 150, 300, 600, 1200, 2400 and 4800 dpi were used and the corresponding pixel sizes were 338.7, 169.3, 84.7, 42.3, 21.2, 10.6 and 5.3 μm , respectively. The particle sizes were in the range of 0.85-1.030 mm, 1.406-1.600 mm and 2.00-2.83 mm.

Influence of resolution on particle projected area is shown in Fig.3-a for finest sand fraction. Values of projected area are considerably higher at low resolutions (< 600 dpi) compared to the values obtained at higher resolutions (> 600 dpi). This indicated that at low resolutions the pixel is too large to accurately represent the particle. At 75 dpi the pixel size is 338.7 μm compared to the particle of 0.85-1.03 mm, so each particle is represented by ~9 pixels, which is clearly not enough to accurately represent its shape. As the resolution increases, the number of pixels increases, leading to the more accurate result of the projected area. This indicates that at higher resolutions the overlap between the real particle cross-sectional area and the projected area is much better due to the small pixels size. According to the obtained results (Fig.3-a), the minimal resolution for accurate values of projected area can be 600 dpi for the particles of this range of size. These results confirm observations from our previous paper¹ that d_A at 600 and 1200 dpi did not differ significantly.

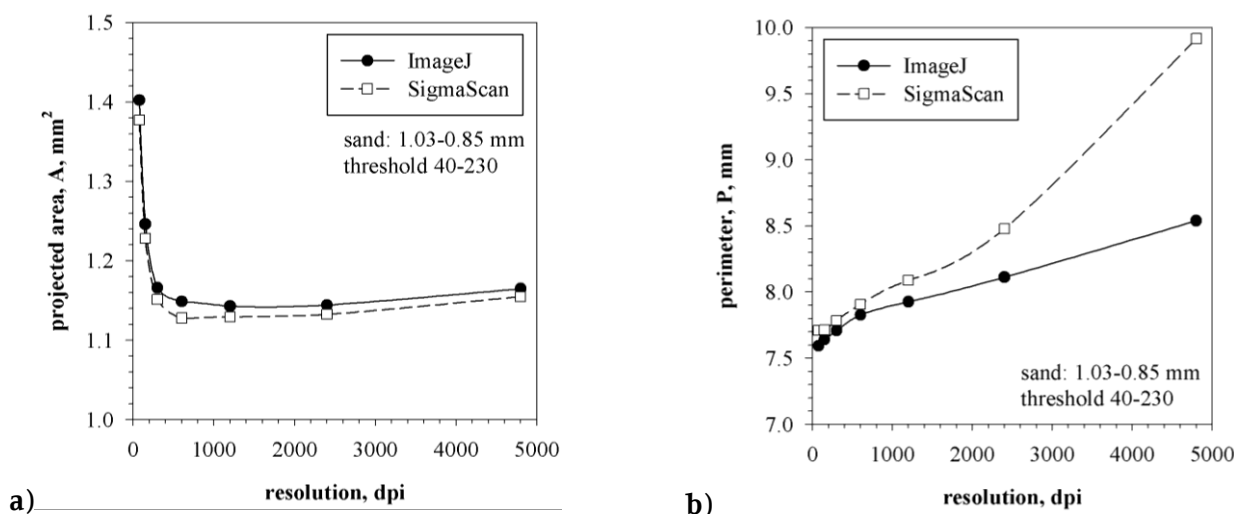


Fig. 3. Influence of resolution on a) particle projected area (A) and b) particle perimeter (P)

The particle perimeter is the most sensitive parameter to the scanning resolution change. The increase in resolution causes a large, continuous increase in particle perimeter (Fig. 3-b). For the largest sand fraction (2.00-2.83 mm) the increase in resolution from 75 to 4800 dpi leads to the increase of the particle perimeter up to 60% compared to the initial value. Since the circularity is calculated from the particle projected area, A , and the particle perimeter, P , (Table 2), it also shows significant dependence on resolution. The particle is represented by square pixels and the real border between the particles and the background is approximately a zigzag line. As the resolution increases, the number of pixels at the particle border increases also, making this effect more pronounced. Contrary, this effect is less pronounced for smaller resolutions, in which the image of the particle contains a smaller number of pixels at the border. Our results have shown that the variations in particle perimeter are less pronounced when ImageJ software was used in comparison to SigmaScan Pro, since different algorithm is used by the two softwares. As resolution is increased, the smaller and smaller surface unevenesses are recognized by scanning device, and particle perimeter increases. Scanning resolution of 600 dpi is recommended in this work as the optimal one based on projected area results in pixel size of 42.3 μm . It is our opinion that pixel size of 42.3 μm allows accurate determination of particle shape, not taking into account the surface roughness, which is adequate in most packed and fluidized bed applications. These results are in accordance with the literature data¹⁹. Different softwares calculate the image area and perimeter in different ways, yielding somewhat different results¹⁵. Podczeck *et al.*²⁰ suggested that an effective pixel size of at least 30 μm is required for accurate characterization of a particle of 1 mm diameter. Minimum pixel size will depend on both the resolution and the digitalization procedure used by the image analysis software.

Projected diameter has almost the same dependence on the change of resolution as the projected area. Projected diameter is changed to a maximum of 4%, with the change of resolution, indicating that the resolution does not significantly affect projected diameter, which is in accordance with our previous work¹.

Circularity represent degree at which the shape of a particle is similar to the shape of the circle, with highly elongated particles being described as having low circularity. This is one of the parameters that show the greatest sensitivity to the resolution change. Circularitv decreases with increase in number of pixels, i.e. with increase of resolution (Fig. 4). This result is expected according to the equation for circularity (Table 2), since the perimeter increases significantly with the resolution. Particularly low values of circularity are obtained in the SigmaScan Pro for high resolutions – as low as 0.36. The circularity for natural sand particles form the literature is in the range of 0.7 to 0.95²¹⁻²³. Values of circularity are below expected results at resolutions higher than 1200 dpi (Fig. 4). Obtained values of circularity also indicate that the resolution of 600 dpi gives the results of the circularity in the range of 0.73-0.80 which is expected for natural sand particles.

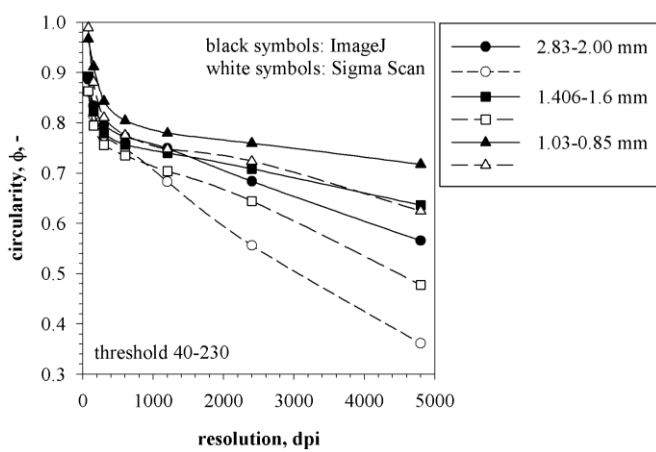


Fig. 4. Influence of resolution on particle circularity

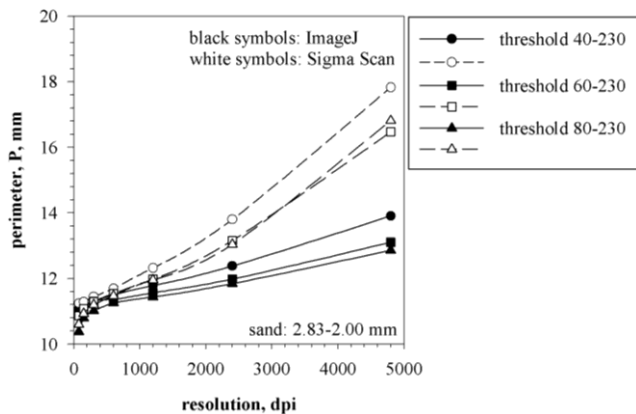


Fig. 5. Comparison of particle perimeters obtained in ImageJ and SigmaScan Pro at all threshold intensities and resolutions

Analysis of scanned images of circles as referent particles was performed to evaluate results for non-spherical sand particles from image analysis softwares and to assess their accuracy in particle characterization ("circle test"). This test was used to investigate the differences in the shape parameters obtained in two softwares as compared to the theoretical values for the circles. Circles, from 1.00 to 3.00 mm in diameter, drawn in CorelDraw Suite 12 was scanned at same resolutions as sand particles and the results were analyzed in ImageJ and SigmaScan Pro. Scanning resolutions had no significant influence on circle projected diameter, major and minor axis. Difference between theoretical and calculated values were between 0.82-4.64 % in ImageJ and 0.47-3.86 % in SigmaScan for projected diameter, 0.48-2.19 % in ImageJ and 2.18-7.30 % in SigmaScan for major axis and 1.97-5.32 % in ImageJ and 0.61-2.05 % in SigmaScan for minor axis. The resolution showed a significant effect on the circle perimeter and circularity. The circle perimeter increased with the increase in resolution, while the circularity decreased. Maximum discrepancy between theoretical and software calculated values of circularity was 12.3% for ImageJ and 14.7% for SigmaScan Pro at 1200 dpi. At the resolution of 300 dpi, the discrepancies were 7.9 % and 9.3% for ImageJ and SigmaScan Pro, respectively. Generally, better results were obtained for smaller circles, as was also reported by Kroner *et al.*¹⁵ and Brown¹⁸.

Size and shape parameters have the same trends with increasing resolution in both image analysis softwares. The most important difference is in particle perimeter, i.e. perimeter from SigmaScan Pro was always larger than respective value from ImageJ at all threshold intensities and resolutions (Fig. 5). Deviations of the shape parameters from the average values (for the same threshold and resolution) in ImageJ were lower. Image processing in SigmaScan Pro at higher resolutions requires much more time than in ImageJ.

Conclusions

2D image analysis represents an easy method for particle characterization, allowing characterization of a large number of particles in a relatively short time. Scanning resolution needs to be taken in consideration each time when image analysis is performed, because the effects of the resolution on the particle shape and size parameters could be considerable. Particle perimeter and circularity show the most significant dependence on resolution because the particle is represented by square pixels and the real border between particles and background is a zigzag line. This is more pronounced at higher resolutions, where the pixels are smaller. Different softwares use different algorithms by which the length of this zigzag line is approximated to calculate the particle border. The "circle test" also confirmed that the resolution had the largest effect on particle perimeter. The increase in resolution leads to the increase in error in predicting the perimeter and the circularity of the circles as compared to the theoretical values. Use of resolutions of 300-600 dpi for the determination of particle shape and size can be recommended for particles of ~1 mm and larger, because of reasonable results, less storage space and less time for image analysis. Generally, the use of resolution of 600 dpi is sufficient for reliable determination of shape parameters for particles of this size. Calculated values of all of size and shape parameters for particle characterization had the same trends with increasing resolution in both

image analysis softwares. The most important difference was in calculated values of particle perimeter, i.e. value in SigmaScan Pro was always larger than the respective value from ImageJ.

Acknowledgment: The financial support of the Serbian Ministry of Education and Science (Project ON172022) is gratefully acknowledged.

Утицај резолуције на дигиталну карактеризацију величине и облика честица песка

У овом раду је испитиван утицај резолуције и два софтвера за анализу слике, "SigmaScan Pro" и "ImageJ", на величину и фактуре облика који се обично користе у карактеризацији честица. У нашем претходном раду¹ карактеризација честица поступљене смеше песка је вршена на две резолуције и појавила се потреба да се испитана детаљније утицај скенирања при различитим резолуцијама на фактуре облика. Анализиране честице су различите фракције квадратног филтрационога песка пречника просејавања у интревалима од 0.85-1.030 mm, 1.406-1.600 mm и 2.00-2.83 mm. Поред тоа, анализиране су слике кругова ради поређења. Резолуција скенирања коришћена у овом раду је била од 75 до 4800 dpi и подесавањем "grayscale thresholds", тј. интензитета сивих тонова, на оптималну вредност одређена је траница честице у односу на позадину. Резултати указују да резолуција (величина пиксела) и алгоритми који се користе у софтверима за анализу слике имају утицаја на добијене фактуре облика, а најзначајнији утицај је зајажен при одређивању обима честица.

Literature

1. T. Kaluđerović Radočić, M. Đuriš, R. Garić-Grulović, Z. Arsenijević, Ž. Grbavčić, Powder Technol. 254 (2014) 63–71.
2. M. Taylor, Powder Technol. 124 (2002) 94–100.
3. L. Banta, K. Cheng, J. Zaniewski, Powder Technol. 132 (2003) 184–189.
4. C. Riley, W. Rose, G. Bluth, J. Geophys. Res. 108 (2003) 1–15.
5. G. Vallebuona, K. Arburo, A. Casali, Miner. Eng. 16 (2003) 323–329.
6. M. Taylor, E.J. Garboczi, S.T. Erdogan, D.W. Fowler, Powder Technol. 162 (2006) 1–15.
7. M. Đuriš, R. Garić-Grulović, Z. Arsenijević, D. Jaćimovski, Ž. Grbavčić, Powder Technol. 235 (2013) 173–179.
8. J.M. Rodriguez, T. Edeskär, S. Knutsson, Electronic Journal of Geotechnical Engineering (EJGE), 18/A (2013) 169–198.
9. C.L. Lin, J.D. Miller, Powder Technol. 154 (2005) 61 – 69.
10. G.H. Bagheri, C. Bonadonna, I. Manzella, P. Vonlanthen, Powder Technol. 270 (2015) 141–153.
11. D. Asahina, M. Taylor, Powder Technol. 213 (2011) 70–78.
12. S. Blott, K. Pye, Sedimentology 55 (2008) 31–63.
13. S. Almeida-Prieto, J. Blanco-Mendez, F.J. Otero-Espinar, J. Pharm. Sci. 93 (2004) 621–634.
14. J.M.R. Fernlund, Cement Concrete Res. 35 (2005) 1629– 1637.
15. S. Kröner, M.T. Doménech Carbó, Powder Technol. 245 (2013) 297–313.
16. T. Ferreira, W. Rasband, ImageJ User Guide, <http://imagej.nih.gov/ij/docs/guide>, 2012.
17. SigmaScan Software Pro 5.0, Jandel Scientific, USA, (1999).
18. L. Brown, Imaging Particle Analysis: Resolution and Sampling Considerations, Fluid Imaging Technologies. <http://fluidimaging.com/imaging-particle-analysis-white-papers.aspx>, 2009.
19. A.M. Bouwman, J.C. Bosma, P. Vonk, J.A. Wesselingh, H.F. Frijlink, Powder Technol. 146 (2004) 66–72.
20. F. Podczeck, S.R. Rahman, J.M. Newton, Int. J. Pharm. 192 (1999) 123–138.
21. J. Fonseca, C. O'Sullivan, M.R. Coop, P.D. Lee, Soils Found. 52(4) (2012) 712–722.
22. C. Lira, P. Pina, J. Coastal Res. SI 56 (2009) 1527-1531.
23. M.R. Cox, M. Budhu, Eng. Geol. 96 (2008) 1–16.

Friction factor for water flow through packed beds of spherical particles

Mihal Đuriš, Zorana Arsenijević, Nevenka Bošković-Vragolović*, Radmila Garić-Grulović,
Tatjana Kaluđerović Radoičić*

IChTM -Department for Catalysis and Chemical Engineering, University of Belgrade,
Njegoševa 12, Belgrade, Serbia

*Faculty of Technology and Metallurgy, University of Belgrade, Karnegijeva 4, Belgrade, Serbia

Abstract

The aim of this work was the experimental evaluation of different friction factor correlations for water flow through packed beds of spherical. The experiments were performed by measuring the pressure drop across the bed. Packed beds made of monosized glass spherical particles of seven different diameters were used. The range of bed voidages was 0.359 – 0.486, while the range of bed particle Reynolds numbers was from 0.3 to 286. The obtained results were compared using a number of available literature correlations. In order to improve the correlation results for spherical particles, a new simple equation was proposed in the form of Ergun's equation, with modified coefficients. The new correlation had mean absolute deviation between experimental and calculated values of pressure drop of 9.04 %.

Introduction

Packed beds of particles permit a widespread means of contact between fluid and solid phases and are used in many different industrial processes. Some examples of their application include filtration processes, ion-exchange, catalytic reactions, heat transfer, gas scrubbing, grain drying and the others. The shape and size of particles that make up the bed are chosen for the characteristics of the specific process. The particle size and shape always aim at high process effectiveness, so a wide range of particles are used. In some applications, like in down-flow granular filters, polydisperse natural materials are used as particulate phase. When natural materials are used, the shape of the particles is irregular and their size falls into some granulometric interval. Differently shaped particles pack with different degrees of bed voidage, which results in different pressure drop across the bed. The pressure drop through the packed bed is one of the most important parameters to be known for the adequate design of the process as well as for the estimation of the capital and operating costs and sizing the pumps or fans required to force the fluid through the bed.

The pressure gradient through packed beds has been studied extensively and a large number of correlations were proposed [1-12]. The most widely used equation for pressure drop calculation was proposed by Ergun [1]

$$-\frac{\Delta P}{H} = 150 \cdot \frac{(1-\varepsilon)^2}{\varepsilon^3} \frac{\mu}{d_p^2} U + 1.75 \cdot \frac{(1-\varepsilon)}{\varepsilon^3} \frac{\rho_f}{d_p} U^2 \quad (1)$$

The friction factor introduced by Ergun is:

$$f_p = \left(-\frac{\Delta P}{H} \right) \cdot \frac{d_p}{\rho_f U^2} \cdot \frac{\varepsilon^3}{1-\varepsilon} \quad (2)$$

According to Eqs. (1) and (2), Ergun's equation for friction factor is:

$$f_p = \frac{150}{\text{Re}_p} + 1.75, \quad \text{Re}_p = \frac{d_p \rho_f U}{\mu (1-\varepsilon)} \quad (3)$$

The other literature correlations for friction factor in packed beds of spherical are listed below:

Macdonald et al. [2]

$$f_p = \frac{180}{\text{Re}_p} + 1.80 \quad (4)$$

Gibilaro et al. [3]

$$f_p' = \left(\frac{18}{\text{Re}_p} + 0.33 \right) \frac{(1-\varepsilon)}{\varepsilon^{4.8}}, \quad f_p = f_p' \cdot \varepsilon^3 / (1-\varepsilon) \quad (5)$$

Montillet et al. [4]

$$f_p' = a \cdot \left(\frac{1-\varepsilon}{\varepsilon^3} \right) \cdot \left(\frac{D_c}{d_p} \right)^{0.2} \left(\frac{1000}{\text{Re}_p} + \frac{60}{\text{Re}_p^{0.5}} + 12 \right) \quad (6)$$

$a = 0.061 \ (e < 0.39), \ a = 0.050 \ ((e > .39); \text{ for } (D_c / d_p) > 50 \text{ term } (D_c / d_p)^{0.2} = 2.2$

Kuerten [5]

$$f_p' = \left(\frac{25 \cdot (1-\varepsilon)^2}{4\varepsilon^3} \right) \left(\frac{21}{\text{Re}_p} + \frac{6}{\text{Re}_p^{0.5}} + 0.28 \right) \quad (7)$$

Hicks [6]

$$f_p' = 6.8 \cdot \frac{(1-\varepsilon)^{1.2}}{\varepsilon^3} \text{Re}_p^{-0.2} \quad (8)$$

Tallmadge [7]

$$f_p' = \left(\frac{150}{\text{Re}_p} \frac{(1-\varepsilon)^2}{\varepsilon^3} \right) + \left(\frac{4.2 \cdot (1-\varepsilon)^{1.166}}{\varepsilon^3} \text{Re}_p^{-1/6} \right) \quad (9)$$

Lee and Ogawa [8]

$$f_p' = \frac{1}{2} \left(\frac{12.5 \cdot (1-\varepsilon)^2}{\varepsilon^3} \right) \cdot \left(\frac{29.32}{\text{Re}_p} + \frac{1.56}{\text{Re}_p^n} + 0.1 \right), \quad n = 0.352 + 0.1 \cdot \varepsilon + 0.275 \cdot \varepsilon^2 \quad (10)$$

Cheng [9]

$$f_p' = \frac{A \cdot M}{\text{Re}_p'} + B \cdot M \quad M = 1 + \frac{2}{3} \cdot \frac{1}{1-\varepsilon} \cdot \frac{d_p}{D_c}$$

$$A = \left[185 + 17 \cdot \frac{\varepsilon}{1-\varepsilon} \cdot \left(\frac{D_c}{D_c - d_p} \right)^2 \right] \cdot \frac{1}{M^2}, \quad B = \left[1.3 \cdot \left(\frac{1-\varepsilon}{\varepsilon} \right)^{1/3} + 0.03 \cdot \left(\frac{D_c}{D_c - d_p} \right)^2 \right] \cdot \frac{1}{M} \quad (11)$$

Eisfeld and Schnitzlein [10]

$$f_p' = \frac{154 \cdot M^2}{\text{Re}_p'} + \frac{M}{B}, \quad M = 1 + \frac{2}{3} \cdot \frac{1}{1-\varepsilon} \cdot \frac{d_p}{D_c} \quad (12)$$

Reichelt [11]

$$f_p' = \frac{165.3 \cdot A^2}{\text{Re}_p'} + 1.2 \cdot B, \quad B = \left[1.5 \cdot \left(\frac{d_p}{D_c} \right)^2 + 0.88 \right]^2 \quad (13)$$

Zhavoronkov et al. [12]

$$f_p' = \frac{165.3 \cdot A^2}{\text{Re}_p'} + 1.2 \cdot B, \quad A = B = 1 + \frac{1}{2 \cdot \left(D_c / d_p \right) \cdot (1-\varepsilon)} \quad (14)$$

Note that some authors used different forms for friction factor and Reynolds number with respect to Ergun's definitions of f_p .

The present study was conducted in order to investigate the optimal choice of friction factor correlation for calculating the pressure drop for water flow through packed beds of spherical particles. The

experimental evaluation of literature correlations was conducted by measuring the pressure drop across packed beds of different packing and for different water flow rates.

Experimental apparatus

The experiments were performed in water-particle system schematically shown in Fig. 1. The packed bed column (f) was used for pressure drop measurements. It was equipped with a distributor and the calming section (e) in order to ensure the uniform flow of water through the bed. The upwards water flow was induced using a pump (b) and the flow rate was measured using an electromagnetic flow meter (d). The packed bed bulk temperature was measured using the temperature indicator (TI). The pressure drop in packed beds of different particles was measured using piezometers (h). The experiments were performed with glass spherical particles. The fluid used was deaerated water at a nearly constant temperature of 20 °C. In each run, water temperature was recorded and water density and viscosity were calculated.

Seven kinds of mono-sized spherical glass particles were used. The experiments with glass spherical particles were conducted in two cylindrical columns: first column of the diameter of 40 mm was used for 0.840 – 3.020 mm particles and the second column of the diameter of 62 mm for 4.140 – 6.180 mm particles. The ratio of the column diameter to the particle diameter (geometric aspect ratio) in the experiments was between 10.0 and 47.6.

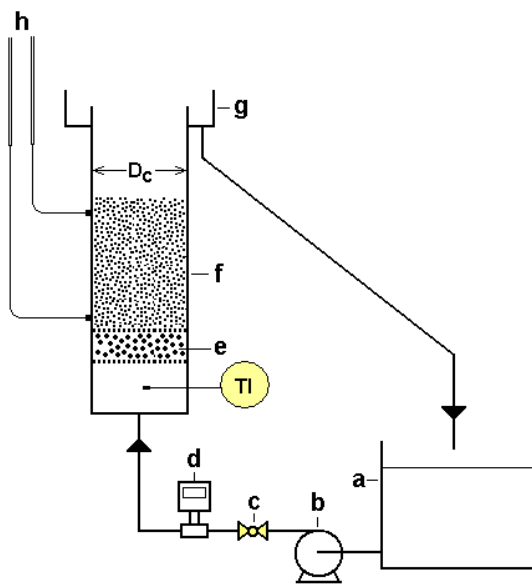


Fig. 1 Schematic diagram of the experimental system

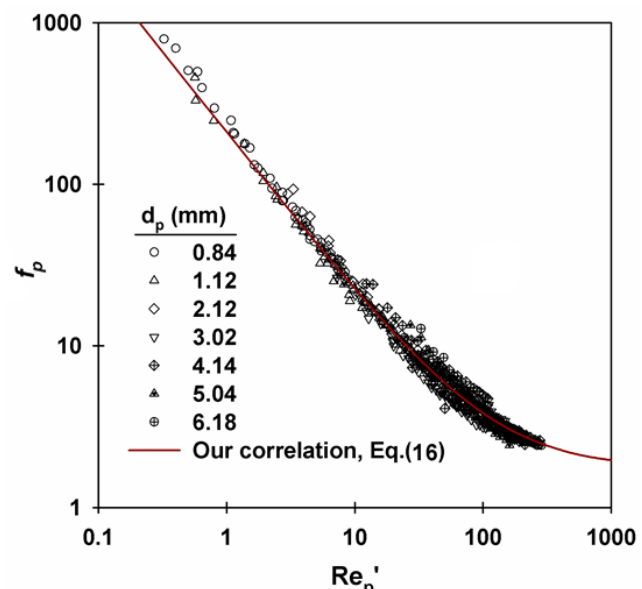


Fig. 2. f_p vs. Re'_p for spherical particles

Results and discussion

The results of the friction factor f_p vs. Re'_p obtained by the experimental measurements of pressure drop are shown in Figs. 2 for spherical. The comparison between the experimental results and the selected literature correlations is given in Table 2 and in Figs. 3.

The mean absolute deviation between the measured values of the pressure gradient and the values obtained from the literature correlations were calculated according to the following equation:

$$\sigma = \frac{1}{N} \sum_{i=1}^N \left| \frac{(\Delta P / H)_{calc} - (\Delta P / H)_{measured}}{(\Delta P / H)_{measured}} \right| \quad (15)$$

where N is the number of data points, $(\Delta P / H)_{calc}$ and $(\Delta P / H)_{measured}$ are the calculated and the measured pressure gradients.

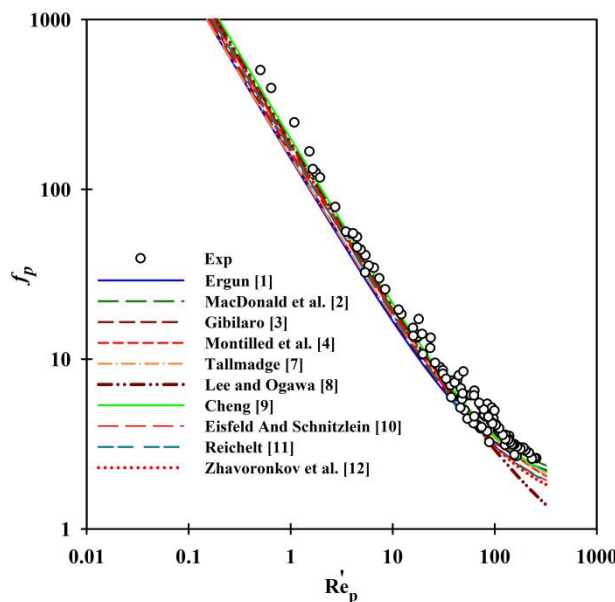


Fig. 3. Comparison of experimental data of f_p vs. Re'_p with chosen correlations for spherical particles

As can be seen from Table 2, the best fit of our experimental data for pressure drop in beds of spherical particles was obtained using Cheng [9] correlation, with mean absolute deviation of 10.89 %. The correlations of Macdonald *et al.* [2] and Montillet *et al.* [4] also gave very good results in fitting our experimental data with mean errors of 12.18 and 13.13 %, respectively. A number of other correlations tested gave results with mean absolute deviation in the range of 16-20 %. It should be noted that Hicks [6] correlation gave the mean error of 50.19 % for spherical particles. The reason for such a large error is that the range of Rep numbers in this paper was below 183, while the specified range of applicability of Hicks correlation is Rep>500.

Table 2. Comparison of experimental data for friction factor with different correlations from the literature.

Reference	$\sigma / \%$
Ergun [1]	19.82
Macdonald <i>et al.</i> [2]	12.18
Gibilaro <i>et al.</i> [3]	18.19
Montillet <i>et al.</i> [4]	13.13
Kuerten, ref. in [5]	29.36
Hicks [6]	50.19
Tallmadge [7]	16.04
Lee and Ogawa [8]	18.61
Cheng [9]	10.89
Eisfeld and Schnitzlein [10]	18.78
Reichelt [11]	20.02
Zhavoronkov <i>et al.</i> [12]	19.04
This paper (Eq.(25))	9.04

The correlations with mean absolute deviation between experimental and correlated pressure drop less than 20 % for beds of spherical particles are shown in Fig. 3. The correlations shown in Fig. 3 were calculated for $Dc/dp = 25$ and bed porosity of $\varepsilon = 0.40$ (the mean values in our experiments) in order to be able to show the correlations with direct dependence on ε as lines.

Compared to the data of our previous paper [13], in which air-spherical particles system was investigated, the results are in the similar range for Macdonald *et al.* [2] (~12%) and Cheng [9] (~11 and

12 %) correlations, which gave very good results at ambient temperature both for air-particles and water-particles systems. On the other hand, the correlations of Ergun [1], Tallmadge [7], Reichelt [11], Gibilaro *et al.* [3], Einstfeld and Schnitzlein [10] and Zhavoronkov *et al.* [12] performed better in air-particles system, while the correlation of Montillet *et al.* [4] performed better in water-particles systems. In order to improve the correlation results for spherical particles, a new simple equation is proposed in the form of Ergun's equation, with modified coefficient:

$$f_p = \frac{209}{\text{Re}_p} + 1.75 \quad (16)$$

The mean absolute deviation between the values calculated from Eq. (16) and the experimental data is 9.04%. The new correlation is shown in comparison to the experimental data in Fig. 2.

Conclusions

The present study was conducted in order to investigate the optimal choice of friction factor correlation for water flow through packed bed of particles. The best fit of experimental data for spherical particles was obtained using Cheng [9] correlation (mean absolute deviation of 10.89%). Ergun's equation was modified in order to improve the fit for spherical particles and a new correlation was proposed. The mean absolute deviation between the experimental data and the proposed correlation is 9.04%.

Most of the correlations that gave good results in correlating experimental data both for spherical and for non-spherical particles were in the form of Ergun's equation with modified coefficients, thus showing that the form of Ergun's equation with two added terms describing viscous and inertial effects is adequate for representing the friction factor in packed beds. However, the coefficients in the equation are very system-specific.

Koefficijent trenja pri strujanju vode kroz pakovani sloj sferičnih čestica

Cilj ovog rada je eksperimentalna procena različitih korelacionih modela za određivanje koeficijenta trenja f_p pri strujanju vode kroz pakovani sloj sferičnih čestica. Eksperimenti su izvedeni merenjem pada pritiska u pakovanom sloju. U eksperimentima su korišćeni 7 različitih pakovanih sloja sačinjenih od staklenih sferičnih čestica različitih prečnika. Opseg poroznosti sloja se kretao 0.359 – 0.486, dok je Rejnoldsov broj čestica bio u opsegu od 0.3 do 286. Dobijeni rezultati upoređeni su sa dostupnim literaturnim korelacijama. U cilju poboljšanja rezultata korelacija predložena je nova jednačina u formi Ergunove korelacije sa modifikovanim koeficijentima. Srednja apsolutna greška odstupanja između eksperimentalnih vrednosti pada pritiska u sloju i vrednosti dobijenih korišćenjem nove predložene jednačine je 9.04 %.

Literature

1. S.S. Ergun, Chem. Eng. Prog. 48 (1952) 89-94.
2. F. Macdonald , M. S. El-Sayed , K. Mow , F. A. L. Dullien, Ind. Eng. Chem. Fundam. 18 (1979) 199-208.
3. L. G. Gibilaro, R. Di Felice, S. P. Waldram, Chem. Eng. Sci. 40 (1985) 1817-1823.
4. A. Montillet, E. Akkari, J. Comiti, Chem. Eng. Process. 46 (2007) 329-333.
5. H. Watanabe, Inte. J. Eng. Fluid Mech. 2 (1989) 93-108.
6. R.E. Hicks, Ind. Eng. Chem. Fundam. 9 (1970) 500-502.
7. J.A. Tallmadge, AIChE J. 16 (1970) 1092-1093.
8. J. Lee, K. Ogawa, J. Chem. Eng. Jpn. 27 (1994) 691-693.
9. N.S. Cheng, Powder Technol. 210 (2011) 261-266.
10. B. Eisfeld, K. Schnitzlein, Chem. Eng. Sci. 56 (2001) 4321-4329.
11. W. Reichelt, Chem. Ing. Tech. 44 (1972) 1068-1071.
12. N.M. Zhavoronkov, M.E. Aerov, N.N. Umnik, J. Phys. Chem. 23 (1949) 342-361
13. R. Pešić, T. Kaluđerović Radojičić, N. Bošković-Vragolović, Z. Arsenijević, Ž. Grbavčić, Chem. Ind. Chem. Eng. Q., 2014, DOI:10.2298/CICEQ140618044P.

Pressure drop in packed beds of spherical particles at ambient and elevated air temperatures

Tatjana Kaluđerović Radočić, Radojica Pešić, Nevenka Bošković-Vragolović,
Zorana Arsenijević*, Mihal Đuriš*

Faculty of Technology and Metallurgy, University of Belgrade, Belgrade, Serbia,

**IChtM - Department for Catalysis and Chemical Engineering, University of Belgrade, Belgrade, Serbia*

Introduction

The packed beds of particles are widely used in process industry. The range of applications includes filtration, catalytic reactions, heat transfer, gas scrubbing, grain drying and many others. One of the most important parameters to be assessed is the pressure drop of the fluid flowing through the packed bed. Due to the complex nature of the fluid flow through the pores of the system was modeled by analogy with the tube fluid flow, taking that the channels through which the fluid flows are approximately of the diameter of the particles constituting the bed. Empirical constants were than added in order to adjust the obtained equations to the experimental results. Despite the great amount of studies dealing with the pressure drop across packed beds of particles¹⁻¹⁵, there are no investigations of the packed bed pressure drop at elevated temperatures.

The most widely used equation for pressure drop calculation was proposed by Ergun¹:

$$-\frac{\Delta P}{H} = 150 \cdot \frac{(1-\varepsilon)^2}{\varepsilon^3} \frac{\mu}{d_p^2} U + 1.75 \cdot \frac{(1-\varepsilon)}{\varepsilon^3} \frac{\rho_f}{d_p} U^2 \quad (1)$$

The friction factor based on Ergun's equation is defined as:

$$f_p = \left(-\frac{\Delta P}{H} \right) \cdot \frac{d_p}{\rho_f U^2} \cdot \frac{\varepsilon^3}{1-\varepsilon} \quad (2)$$

The applicability of Ergun equation was reviewed and the equation was modified by many authors: Macdonald *et al.*⁴, Gibilaro *et al.*⁵, Montillet *et al.*^{6,7}, Tallmire¹², Lee and Ogawa¹³, Allen *et al.*¹⁴, Nemec and Levec¹⁵.

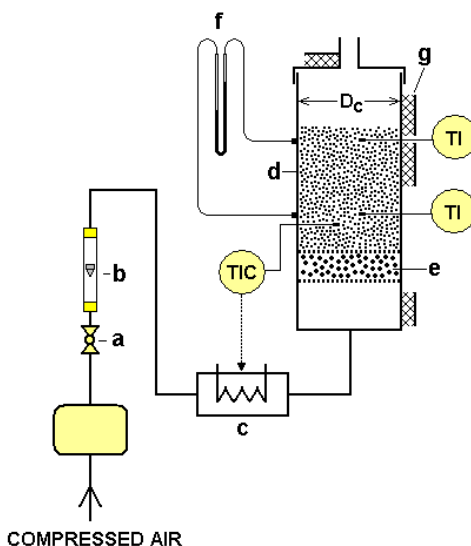


Fig. 1. Experimental system
(a-valve, b-rotameter, c-electric heater, d-column, e-distributor, f-manometer, g-thermal insulation)

The aim of this work was the experimental investigation of the influence of the temperature of the gas on the packed bed pressure drop and the applicability of the literature correlations at elevated

temperatures. To achieve this, experimental investigation of the particle friction factor, f_p for gas flow through packed beds of spherical glass particles at ambient and elevated temperatures was conducted. The experiments were performed by measuring the pressure drop across the packed bed, previously heated to desired temperature by the hot air flowing through it. The temperature range of the experiments was from 20°C to 350°C. The experimental results were compared to the available literature correlations.

Experimental

The experiments were conducted in plexiglas cylindrical column of the diameter of 119 mm and height of 300 mm. The thermally insulated column is schematically shown in Fig.1. The column was equipped with a distributor and the calming section in order to insure the uniform flow of air through the packed bed. The upwards air flow was induced using a compressor. The compressed air first flew through the rotameter and than through the electric air heater. The hot air was allowed to flow through the packed bed until the stable value of the bed bulk temperature was reached. The packed bed bulk temperature was regulated using temperature control system. The pressure drop through the packed bed was measured using water manometer. The height between the pressure taps was 200 mm. The measurements were performed for different particle diameters, air velocities and bed temperatures. Seven kinds of mono-sized spherical glass particles were used. A total of 24 runs were conducted and a total of 1274 data points were collected. Bed particle Reynolds number varied between 2.2 and 502.6. All of the air superficial velocities used in the experiments were below the minimum fluidization velocity for the respective particles. The velocities applied were in the range of 0.03-0.94 U_{mf} . The ratio of the column diameter to the particle diameter (geometric aspect ratio) in the experiments was between 12.6 and 108.1 which is in the range of the negligible wall effects. The particle characteristics and range of the experimental conditions are summarized in Table 2. The effects of glass dilatation were neglected in the calculations, as the volume change of glass is less than 1% for the temperature raise of 300°C.

Results and discussion

All of the results obtained in our experimental investigation are shown in Fig. 5 together with the correlations tested. The correlations that do not show direct dependence on ε , as well as the correlations in which the variations with ε are very small, are shown as lines, while the correlations with direct dependence on ε are shown as points, calculated for the same conditions as the experimental data. The results are shown for seven types of spherical particles of different diameters. For three particle diameters, the experiments were conducted both at ambient temperature of 20°C and at elevated temperatures between 100 and 350°C.

The comparison between the experimental results and the selected literature correlations was conducted using the mean absolute deviation. The mean absolute deviation of the measured values of pressure gradient and the values obtained from the literature correlations were calculated according to the following equation:

$$\sigma = \frac{1}{N} \sum_1^N \left| \frac{(\Delta P / H)_{calc} - (\Delta P / H)_{measured}}{(\Delta P / H)_{measured}} \right| \quad (3)$$

where N is the number of data points, $(\Delta P / H)_{calc}$ and $(\Delta P / H)_{measured}$ are the calculated and the measured pressure gradients. The mean absolute deviations were calculated for all of the experimental data and also, separately, for the data measured at ambient temperature ($T_g=20$ °C) and for the data measured at elevated temperatures ($T_g=100-350$ °C).

The overall best fit of all of our experimental data was obtained using the Ergun¹ correlation, with the mean absolute deviation of 10.90 %. The mean absolute deviation for the room temperature data was smaller (9.77 %) than for the data at elevated temperatures (12.38 %). Although Ergun's equation

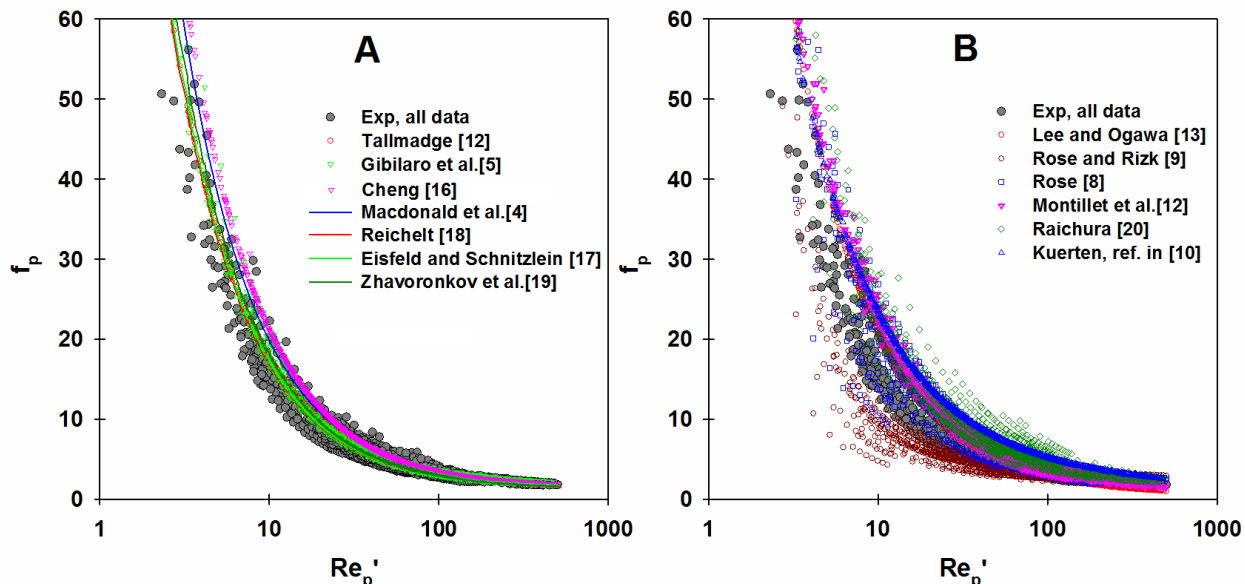


Fig. 5. Experimental and correlated data of f_p vs. Re_p' , all data points

performed best among the correlations tested, the correlations of Reichelt¹⁸ and Eisfeld and Schnitzlein⁵ gave better results for elevated temperature data only (10.83 and 11.59%, respectively). When all of the experimental data were tested, the correlations of Reichelt¹⁸ and Eisfeld and Schnitzlein¹⁷ had almost the same mean absolute deviation of 11.17 and 11.19%, respectively which is almost the same as the mean absolute error of Ergun's equation for all of the data points.

The correlations of Zhavoronkov *et al.*¹⁹, Tallmadge¹² and Gibilaro⁵ gave similar results in correlating our experimental data (with mean absolute deviations between 12.92 and 13.67 % for all of the experimental data tested). As the values of the Re_p numbers in our experimental system were in the range of 2.2-506, this similarity is in accordance with the observation of Gibilaro *et al.*⁵ that their correlation represents data in low Rep regime equally well as Ergun's equation. Also, as Tallmadge¹² modified only the turbulent term of the Ergun equation the results obtained using his equation in our range of Rep numbers are similar to the results obtained using Ergun's equation. It should be noted that the correlation of Tallmadge¹² actually gave better results than Ergun's equation for the room temperature data, while it performed much worse for the data at elevated temperature (the mean absolute deviations were 9.49 and 18.31 % for the room temperature data and for the elevated temperature data, respectively). The other correlations used gave much larger mean absolute deviations, in the interval of 14.47 to 56.95 % (Table 3).

For the majority of the correlations, the values of the mean absolute deviations calculated from the ambient temperature data are lower than the values calculated from the data obtained at elevated temperatures. The exceptions from this are the correlations of Reichelt¹⁸ and Rose and Risk⁹, which performed better at elevated temperatures. The values of the mean absolute deviations for elevated temperature data points in the cases of Tallmadge¹², Macdonald *et al.*⁴, Cheng¹⁶ and Rose⁸ equations are two or more two times larger than the ones calculated for 20°C data points.

Conclusions

The present study was conducted in order to investigate the particle friction factor for air flow through packed bed of spherical glass particles at ambient and elevated temperatures. The experiments were performed by measuring the pressure drop across the packed bed, heated to the desired temperature by the hot air. Also, the applicability of the available literature correlations was investigated.

The overall best fit of all of our experimental data was obtained using Ergun¹ correlation, with mean absolute deviations of 10.90 %. Ergun's equation gave better results in correlating the data at 20 °C

with mean absolute deviations of 9.77 % than the data at elevated temperatures, which was correlated with mean absolute deviation of 12.38 %. The Tallmadge¹² correlation gave the best results in correlating the room temperature data, with the mean absolute error of 9.49 %, which is just below the value of 9.77 % for Ergun's equation. At elevated temperatures, Reichelt¹⁸ and Eisfeld and Schnitzlein¹⁷ correlations gave better results than Ergun's equation. All of the correlations used, except Reichelt¹⁸ and Rose and Risk⁹ equation, gave better results when applied to ambient temperature data than to the data at elevated temperatures.

Based on the results obtained, Ergun's¹ equation could be proposed if one equation should be used for friction factor calculation both at ambient and at elevated temperatures. For elevated temperatures only, Reichelt¹⁸ correlation gives better results. The mentioned conclusions are valid in the lower range of Re_p numbers, i.e. for $Re_p < 500$.

Acknowledgment Financial support of the Serbian Ministry of Education and Science (Project ON172022) is gratefully acknowledged.

Pad pritiska u pakovanom sloju sferičnih čestica na sobnoj i povišenim temperaturama

Cilj ovog rada je bio eksperimentalno ispitivanje koeficijenta trenja fluid-čestice prilikom strujanja vazduha kroz pakovani sloj čestica, na sobnoj i povišenim temperaturama. Izvršeno je eksperimentalno merenje pada pritiska u pakovanim slojevima različitih temperatura zagrejanih korišćenjem vrelog vazduha. Kao materijal za pakovanje korišćene su sferične staklene kuglice 7 različitih prečnika. Temperaturni interval u kom su vršeni eksperimenti bio je od 20°C do 350°C, dok su poroznosti sloja iznosile od 0,3574 do 0,4303. Dobijeni rezultati korelirani su korišćenjem većeg broja literaturnih korelacija. Najbolje slaganje sa eksperimentalnim podacima pokazala je Ergunova jednačina¹, sa srednjim procentnim odstupanjem od 10,90%. Ergunova jednačina je dala bolje rezultate prilikom korelisanja podataka na sobnoj temperaturi (srednja procentna greška 9,77%), dok je korelisanje podataka na povišenim temperaturama izvršeno sa greškom od 12,38%. Većina testiranih literaturnih korelacija je dala bolje rezultate pri korelisanju podataka dobijenih na sobnoj temperaturi u odnosu na podatke dobijene na povišenim temperaturama. Na osnovu dobijenih rezultata, predlaže se korišćenje Ergunove jednačine za izračunavanje koeficijenta trenja fluid-čestice kako na sobnoj, tako i na povišenim temperaturama.

Literature

1. S.S. Ergun, *Chem. Eng. Prog.* **48** (1952) 89
2. M. Mayerhofer, J. Govaerts, N. Parmentier, H. Jeanmart, L. Helsen, *Powder Technol.* **205** (2011) 30.
3. A. Luckos, J.R. Bunt, *Fuel* **90** (2011) 917.
4. F. Macdonald , M. S. El-Sayed , K. Mow , F. A. L. Dullien, *Ind. Eng. Chem. Fundamen.* **18** (1979) 199.
5. L. G. Gibilaro, R. Di Felice, S. P. Waldrum, *Chem. Eng. Sci.* **40** (1985) 1817.
6. A. Montillet, *J. Fluids Eng.* **126** (2004) 139.
7. A. Montillet, E. Akkari, J. Comiti, *Chem. Eng. Process.* **46** (2007) 329.
8. H.E. Rose, *Proc. Inst. Mech. Eng.* **153** (1945) 154.
9. H.E. Rose, A.M.A. Rizk, *Proc. Inst. Mech. Eng.* **160** (1949) 493.
10. H. Watanabe, *Int. J. Eng. Fluid Mech.* **2** (1) (1989) 93.
11. R.E. Hicks, *Ind. Eng. Chem. Fund.* **9** (3) (1970) 500.
12. J.A. Tallmadge, *AIChE J.* **16** (6) (1970) 1092.
13. J. Lee, K. Ogawa, *J. Chem. Eng. Jpn.* **27** (5) (1994) 691.
14. K.G. Allen, T.W. von Backström, D.G. Kröger, *Powder Technol.* **246** (2013) 590.
15. D. Nemec, J. Levec, *Chem. Eng. Sci.* **60** (2005) 6947.
16. N.S. Cheng, *Powder Technol.* **210** (3) (2011) 261.
17. B Eisfeld, K Schnitzlein, *Chem. Eng. Sci.* **56** (14) (2001) 4321.
18. W.Reichelt, *Chemie Ingenieur Technik* **44**(8) (1972) 1068.
19. N.M. Zhavoronkov, M.E. Aerov, N.N. Umnik, *Journal of Physical Chemistry* **23** (1949) 342.
20. R.C. Raichura, *Exp. Heat Transfer* **12** (4) (1999) 309.
21. R. Di Felice, L.G. Gibilaro, *Chem. Eng. Sci.* **59** (14) (2004) 3037.

**Densities, viscosities and refractive indices of binary system
*N,N-dimethylaniline + 1-butyl-3-methylimidazolium triflate at 288.15 to 333.15 K
 and at atmospheric pressure***

Danijela Soldatović, Nikola Grozdanić*, Jelena Vuksanović*, Ivona Radović*, Mirjana Kijevčanin*

Public Company Nuclear Facilities of Serbia, 12-14 Mike Petrovića Alasa, Vinča, 11351 Belgrade, Serbia

**Faculty of Technology and Metallurgy, University of Belgrade, Karnegijeva 4, 11120 Belgrade, Serbia*

Abstract

In this study densities, viscosities and refractive indices of binary system N,N-dimethylaniline + 1-butyl-3-methylimidazolium triflate ([bmim][OTf]), were measured at atmospheric pressure and in temperature range T = 288.15 to 333.15 K. Excess molar volumes, deviations in refractive indices, viscosity deviations and excess molar Gibbs free energies of activation of viscous flow were calculated and the results were fitted to a Redlich-Kister polynomial equation. Considering the calculated thermodynamic properties, molecular interactions in the investigated binary system were analyzed and discussed.

Introduction

Ionic liquids¹ are ionic compounds (salts) that have normal melting points below 100°C. Their negligible vapor pressures in a wide temperature range² and diverse solvent power are two main characteristics that qualify them as promising alternatives to classical (toxic) solvents. Therefore, ionic liquids (ILs) found their application as separation/extraction solvents for diverse solutes: for amino acids separation and purification³, carbohydrate separation⁴, for extraction of proteins⁵, phenols⁶, or for removal of free fatty acids⁷.

Ionic liquids have specific structure represented by polar (ionic) and non-polar (aliphatic) domains, which is very important for the diverse solvent power. They also allow a variety of interactions in their mixtures, such as dispersion forces between aliphatic chains present in the mixtures of imidazolium ionic liquids with alcohols, strong ion-dipole interactions, hydrogen bonds, and specific interactions with aromatic compounds.

Following the aforementioned attractiveness and importance of ionic liquids and their mixtures, we have carried out the study that includes the detailed analysis of thermophysical properties for one ionic liquid in a binary mixture with aromatic compound. In this work, densities, refractive indices and viscosities have been measured for binary system containing N,N-dimethylaniline + 1-butyl-3-methylimidazolium triflate ([bmim][OTf]). All the measurements were carried out at temperatures between 288.15 and 333.15 K with a step of 5 K and at atmospheric pressure. From these experimental data, excess molar volumes, deviations in refractive index, deviations in viscosity and excess molar Gibbs free energies of activation of viscous flow were calculated and correlated by Redlich-Kister equation.

Experimental section

Chemicals. N,N-dimethylaniline was supplied by Merck with high mass purity of 99 %, while ionic liquid [bmim][OTf] was purchased from IOLITEC with the >99 % mass purity.

Measurements. The experimental measurements of density ρ , refractive index n_D and viscosity η were performed on Anton Paar devices; DMA 5000 digital vibrating U-tube densimeter, automatic Anton Paar RXA 156 refractometer and Stabinger SVM viscometer. Detailed description of all apparatus can be found in our previous work⁸.

All the mixtures were prepared gravimetrically using a Mettler AG 204 balance with a precision $1 \cdot 10^{-7}$ kg. The uncertainty of the mole fraction calculation was less than $\pm 1 \cdot 10^{-4}$. Density measurements and excess molar volume calculations were performed with the experimental uncertainty of $\pm 4 \cdot 10^{-2}$ kg·m⁻³ and $\pm 4 \cdot 10^{-6}$ m³·kmol⁻¹, respectively. The uncertainty of the refractive index data measurements is ± 0.00005 units. The relative uncertainty in dynamic viscosity measurements was estimated to be ± 0.4 %. The uncertainties for refractive index and viscosity deviations are ± 0.00009 units and ± 1 %, respectively.

Results and discussion

The experimental values of densities ρ refractive indices n_D and viscosities η for the system *N,N*-dimethylaniline + [bmim][OTf] were measured in a temperature range $T = (288.15 \text{ to } 333.15) \text{ K}$ and at atmospheric pressure.

The excess molar volumes V^E were calculated using the experimental densities ρ of binary mixtures and the pure components ρ from the equation:

$$V^E = \sum_{i=1}^N x_i M_i \left[\left(\frac{1}{\rho} \right) - \left(\frac{1}{\rho_i} \right) \right] \quad (1)$$

where N is the number of components, x_i is the mole fraction of component i in a mixture and M_i is the molecular weight of a component i .

The refractive index deviations Δn_D were obtained using the equation:

$$\Delta n_D = n_D - \sum_{i=1}^N x_i n_{Di} \quad (2)$$

where n_D and n_{Di} refer to the refractive index of a mixture and a pure component i , respectively.

The viscosity deviations $\Delta \eta$ were calculated from the viscosity of a pure component η_i and a mixture η , according to the equation:

$$\Delta \eta = \eta - \sum_{i=1}^N x_i \eta_i \quad (3)$$

Excess molar Gibbs free energies of activation of viscous flow, ΔG^{*E} , were calculated combining the obtained volumetric and viscosity data, following the equation:

$$\Delta G^{*E} = RT \left[\ln \left(\frac{\eta V}{\eta_1 V_1} \right) - x_1 \ln \left(\frac{\eta_1 V_1}{\eta_2 V_2} \right) \right] \quad (4)$$

In equation (4) η and V represent viscosity and molar volume of a solution, respectively; the subscripts 1 and 2 indicate pure components of a binary mixture.

Four properties calculated by equations (1)-(4) were correlated with Redlich-Kister (RK) polynomial equation⁹:

$$Y = x_i x_j \sum_{p=0}^k A_p (2x_i - 1)^p \quad (5)$$

In equation (5) Y represents V^E , Δn_D , $\Delta \eta$ or ΔG^{*E} ; A_p are the fitting parameters, and $k+1$ is the number of parameters, which was optimized using the F-test. The corresponding root-mean-square deviation, (rmsd) σ , is defined as follows:

$$\sigma = \left(\sum_{i=1}^m (Y_{\text{exp},i}^E - Y_{\text{cal},i}^E)^2 / m \right)^{1/2} \quad (6)$$

In equation (6) m is the number of experimental data points. RK polynomial fitting showed good agreement with experimental data.

All calculated properties: V^E , $\Delta \eta$, ΔG^{*E} and Δn_D for the investigated binary system *N,N*-dimethylaniline + [bmim][OTf] along with the values calculated from RK polynomial are presented in Figures 1 (a) and (b), 2 and 3, respectively.

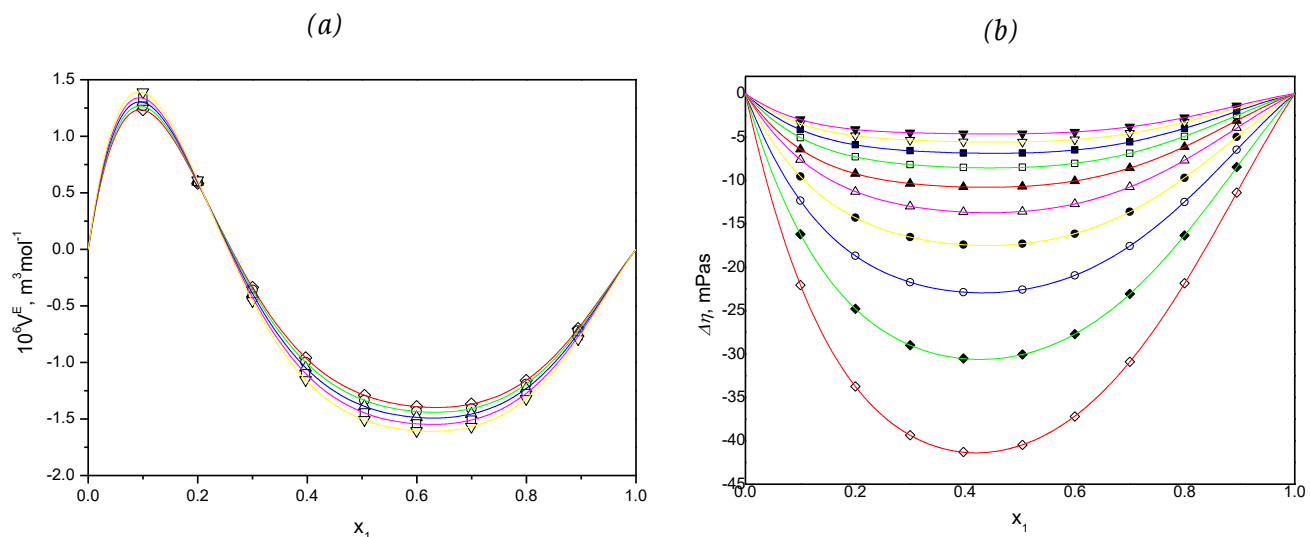


Figure 1. Experimental (symbols) and correlated (lines represent RK equation) data of (a) excess molar volume (V^E) and (b) viscosity deviation ($\Delta\eta$), as a function of mole fraction x_1 , for the binary system N,N -dimethylaniline (1) + $[bmim][OTf]$ (2) at following temperatures: (◊) 288.15 K, (◆) 293.15 K, (○) 298.15 K, (●) 303.15 K, (Δ) 308.15 K, (▲) 313.15 K, (□) 318.15 K, (■) 323.15 K, (▽) 328 K.15, (▼) 333.15 K and at atmospheric pressure.

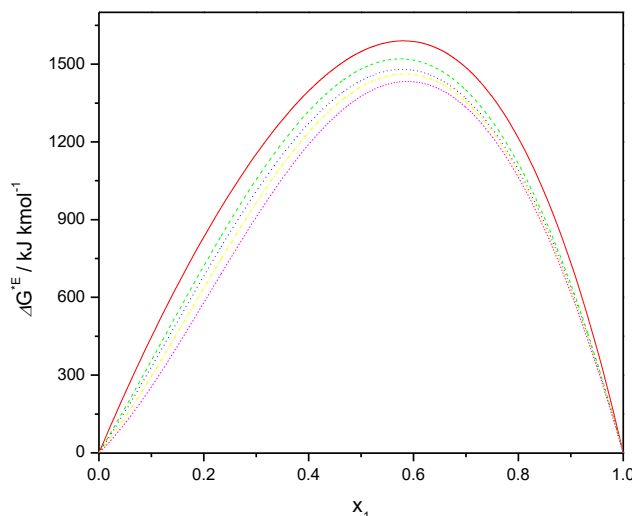


Figure 2. Correlated (RK equation) data of excess molar Gibbs free energy of activation of the viscous flow ΔG^E , as a function of mole fraction x_1 , for the binary system N,N -dimethylaniline (1) + $[bmim][OTf]$ (2) at following temperatures: (—) 288.15 K, (---) 298.15 K, (-·-) 308.15 K, (----) 318.15 K, (.....) 333.15 K and at atmospheric pressure.

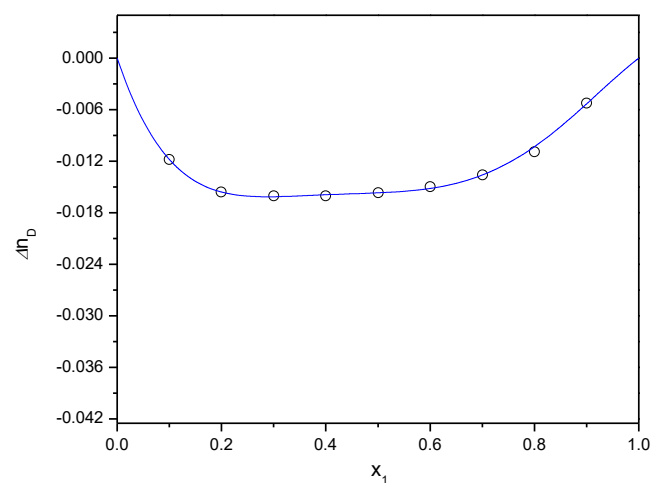


Figure 3. Experimental (symbols) and correlated (line represents RK equation) data of refractive index deviation (Δn_D) as a function of mole fraction x_1 for the binary system N,N -dimethylaniline (1) + $[bmim][OTf]$ (2) at 303.15 K and at atmospheric pressure.

The system *N,N*-dimethylaniline + [bmim][OTf] has an S-shaped V^E -curve which changes sign from positive to negative values as a mole fraction of *N,N*-dimethylaniline increases. The maximum and minimum of the curve are at $x_1=0.1$ and $x_1=0.6$, respectively (Figure 1(a)). Experimental viscosity deviations are plotted vs. x_1 along with the values calculated from the RK polynomial (Figure 1(b)). System exhibits negative $\Delta\eta$ values and absolute $\Delta\eta$ values decrease with increasing temperature from 288.15 K to 333.15 K. Figure 2 gives the RK curves representing the calculated values for the excess molar Gibbs free energies of activation of viscous flow ΔG^E for the same binary system. Due to visibility reasons, the curves are given for five selected isotherms. As the figure shows the ΔG^E values are positive over the entire concentration range. Refractive index deviations plotted vs. x_1 at 303.15 K are presented in Figure 3. The results are presented only at 303.15 K because of the negligible temperature influence on the refractive index deviation and overlapping of the curves.

N,N-dimethylaniline is a polar compound enabling dipole-dipole or ion-dipole interactions and hydrogen bonding. On the other hand, studied ionic liquid also shows proton accepting ability through its anion. Imidazolium based ionic liquids form specific cation and anion interactions with the aromatic arene ring which results in the formation of cage-like structures – liquid clathrates in solutions¹⁰. All aforementioned interactions lead to more efficient packing in the mixture compared to the pure liquids, and as a result negative V^E and Δn_D values appear in system *N,N*-dimethylaniline + [bmim][OTf] (Figures 1 (a) and 3, respectively).

However, the positive V^E values in IL rich phase (Figure 1 (a)) are the result of ion-pairing in ionic liquid - which prevailed over the attractive interactions between unlike molecules.

Negative $\Delta\eta$ values (Figure 1 (b)) are the result of the aforementioned ion aggregations in ionic liquids but do not reflect the overall existing interactions. Thus, if *N,N*-dimethylaniline is included in interstices of the ion aggregates there will be a fewer surfaces available for friction that may result in the reduction of viscosity¹¹. This can explain high values of viscosity deviations for the systems with *N,N*-dimethylaniline.

Excess molar Gibbs free energy of activation of viscous flow ΔG^E (Figure 2) is generally linked to the excess molar Gibbs free energy of mixing, but it's sign has the opposite physical significance to the nature of intermolecular interactions: positive values indicate the presence of strong, attractive interactions between unlike molecules while negative values show their absence and the domination of interactions between like molecules.

Conclusion

In this paper density, viscosity and refractive index data of binary mixture *N,N*-dimethylaniline + [bmim][OTf] are measured at atmospheric pressure and at temperatures ranging from 288.15 K to 333.15 K with a step of 5 K. Excess molar volumes, deviations of viscosity and refractive indices, as well as excess molar Gibbs free energies of activation of viscous flow were calculated from the experimental data and correlated by Redlich-Kister equation. These properties are discussed on the basis of the molecular interactions between like and unlike molecules existing in the studied mixtures. Generally highly negative excess molar volumes, deviations in refractive indices and viscosities, as well as positive excess molar Gibbs free energies indicate the domination of strong, attractive interactions between unlike molecules – Coulomb forces, hydrogen bonding and ion-dipole interactions.

The authors gratefully acknowledge the financial support received from the Research Fund of Ministry of Education, Science and Technological Development(project No 172063), Serbia and the Faculty of Technology and Metallurgy, University of Belgrade.

**Gustina, viskoznost i indeks refrakcije binarnog sistema
*N,N-dimetilanilin + 1-butil-3-methylimidazolium triflatna temperaturama
od 288.15 do 333.15 K i na atmosferskom pritisku***

U ovom radu merene su gustine, viskoznosti i indeksi refrakcije binarnog sistema N,N-dimetilanilin + 1-butil-3-methylimidazolium triflate ([bmim][OTf]) na atmosferskom pritisku i u temperaturnom opsegu T = 288.15 do 333.15 K. Na osnovu eksperimentalnih podataka vršeno je izračunavanje dopunske molarne zapremine, promene indeksa prelamanja, promene viskoznosti, promene dopunske molarne Gibsove energije. Rezultati su fitovani Redlich-Kister-ovim polinomom. Na osnovu izračunatih termodinamičkih veličina analizirane su i diskutovane molekulske interakcije u pomenutom binarnom sistemu.

Literature

1. D.R. MacFarlane, K.R. Seddon, *Aust. J. Chem.* 60 (2007) 3–5.
2. Y.U. Paulechka, G.J. Kabo, A. V. Blokhin, O.A. Vydriv, J.W. Magee, M. Frenkel, *J. Chem. Eng. Data.* 48 (2003) 457–462.
3. J. Wang, Y. Pei, Y. Zhao, Z. Hu, *Green Chem.* 7 (2005) 196–202.
4. A.P. Carneiro, O. Rodríguez, E.A. Macedo, *Fluid Phase Equilib.* 314 (2012) 22–28.
5. H. Yan, J. Wu, G. Dai, A. Zhong, H. Chen, J. Yang, et al., *J. Lumin.* 132 (2012) 622–628.
6. X. Ni, H. Xing, Q. Yang, J. Wang, B. Su, Z. Bao, et al., *Ind. Eng. Chem. Res.* 51 (2012) 6480–6488.
7. M.S. Manic, V. Najdanovic-Visak, M.N. da Ponte, Z.P. Visak, *AIChE J.* 57 (2011) 1344–1355.
8. J.M. Vuksanović, E.M. Živković, I.R. Radović, B.D. Djordjević, S.P. Šerbanović, M.L. Kijevčanin, *Fluid Phase Equilib.* 345 (2013) 28–44.
9. O. Redlich, A.T. Kister, *Ind. Eng. Chem.* 40 (1948) 345–348.
10. J.D. Holbrey, W.M. Reichert, M. Nieuwenhuyzen, O. Sheppard, C. Hardacre, R.D. Rogers, *Chem. Commun.* 9 (2003) 476–477.
11. M.A. Chowdhury, M.A. Majid, M.A. Saleh, *J. Chem. Thermodyn.* 33 (2001) 347–360.

Molecular interactions in the binary system diethyl succinate + 1-hexanol according to mixing deviation properties and FT-IR analysis

Divna M. Majstorović, Emila M. Živković, Jovan D. Jovanović, Slobodan P. Šerbanović,
Mirjana Lj. Kijevčanin

Faculty of Technology and Metallurgy, University of Belgrade, Karnegijeva 4, 11120 Belgrade, Serbia

Abstract

Density, viscosity and refractive index data for the binary system diethyl succinate + 1-hexanol have been measured in temperature range 288.15–323.15 K with temperature step 5K, and at atmospheric pressure. The measurements were performed on Anton Paar DMA 5000 digital vibrating tube densimeter, Anton Paar SVM 3000 digital viscometer and Anton Paar RXA 156 refractometer. Based on the corresponding experimental data, excess molar volumes (V^E), viscosity deviations ($\Delta\eta$) and refractive index deviations (Δn_D) were determined and fitted by the Redlich-Kister polynomial equation. Molar excess Gibbs free energies of activation of viscous flow (ΔG^{*E}) were additionally calculated from measured density and viscosity data. Excess and deviation functions, with FT-IR study, were further used in the analysis of molecular interactions present in the mixture.

Introduction

The thermophysical study of esters and alcohols is of increasing interest due to their wide usage in flavoring, cosmetic and pharmaceutical industry. The investigated substances are also important solvents in paint and plastic industries¹. Both substances, ester diethyl succinate and alcohol 1-hexanol, are formed naturally in small amounts during many fermentation processes and have been successfully extracted from wine samples².

Intermolecular interactions for thousands of mixtures used in the process industry are often not known so excess thermodynamic functions and mixing deviations (excess molar volumes, viscosity deviations, refractive index deviations) of binary or multicomponent liquid mixtures are essential for their understanding.

Fourier-transform infrared (FT-IR) spectroscopy studies of all the pure compounds and mixtures were also performed to obtain insight into major inter- and intramolecular interactions in the studied mixtures. It is a spectral technique that measures the association properties, hydrogen bonding capability and interactions of different molecules, analyzing band shifts, band width and the change of band shape.

Experimental Section

Chemicals. Diethyl succinate was supplied by Acros Organics with high mass purity of 99%, while 1-hexanol was purchased from Merck with the >99% mass purity.

Measurements. The experimental measurements were performed on Anton Paar devices; DMA 5000 digital vibrating tube densimeter, SVM 3000 digital viscometer and RXA 156 refractometer. More about the measuring procedure can be found in our previous papers^{3,4}.

The experimental uncertainty in the density, viscosity and refractive index measurements were about $\pm 8 \times 10^{-2} \text{ kg m}^{-3}$, $\pm 0.7\%$ and $\pm 9 \times 10^{-5}$, respectively, and the average uncertainty in excess molar volume, viscosity and refractive index deviation have been estimated at $\pm 5 \times 10^{-9} \text{ m}^3 \text{ mol}^{-1}$, better than $\pm 0.2\%$ and $\pm 6 \times 10^{-5}$, respectively.

The mixtures were prepared by measuring the masses of pure substances on a Mettler AG 204 balance with a precision $1 \times 10^{-7} \text{ kg}$. The uncertainty of the mole fraction calculation was less than $\pm 1 \times 10^{-4}$.

Spectra of pure components and binary mixtures were acquired directly using Attenuated Total-internal Reflection (ATR) accessory (with Zn-Se crystal) and FT-IR Spotlight 400 System (Perkin Elmer, Italy). The spectra were collected at 298.15 K, in the range 4000–650 cm⁻¹ with 4 cm⁻¹ resolution, and each spectrum was averaged across 16 scans in order to minimize noise in spectra.

Results and discussion

Density (ρ), viscosity (η) and refractive index (n_D) for the system diethyl succinate + 1-hexanol were measured at eight temperatures (T=288.15 - 323.15) K and at atmospheric pressure.

Excess molar volumes V^E were calculated from the density data by the equation:

$$V^E = \frac{x_1 M_1 + x_2 M_2}{\rho} - \left(\frac{x_1 M_1}{\rho_1} + \frac{x_2 M_2}{\rho_2} \right) \quad (1)$$

where x_1 and x_2 are mole fractions of pure components in the mixture; M_1 and M_2 their molecular masses, ρ , ρ_1 and ρ_2 measured densities of the mixture and the pure components 1 and 2, respectively.

The deviation functions were determined from the equation:

$$\Delta Y = Y - (x_1 Y_1 + x_2 Y_2) \quad (2)$$

in which ΔY refers to viscosity deviation $\Delta \eta$ or deviation in refractive index Δn_D ; Y denotes mixture property, viscosity η or refractive index n_D , while Y_1 and Y_2 are viscosities η_1 and η_2 , or refractive indices n_{D1} and n_{D2} , of the pure components.

The excess molar Gibbs energy of activation of the viscous flow ΔG^{*E} is also a property used for better analysis of molecular interactions in the mixtures, and a more adequate one than viscosity deviations $\Delta \eta$. This property were calculated using the equation⁵:

$$\Delta G^{*E} = RT[\ln(\eta V / \eta_2 V_2) - x_1 \ln(\eta_1 V_1 / \eta_2 V_2)] \quad (3)$$

in which V , V_1 and V_2 represent molar volume of the solution and molar volumes of pure components 1and 2, respectively.

The results of V^E , $\Delta \eta$, Δn_D and ΔG^{*E} for the investigated binary mixture were correlated with the Redlich-Kister (RK) equation⁶:

$$Y^E(\Delta Y) = x_1 x_2 \sum_{p=0}^k A_p (2x_1 - 1)^p \quad (4)$$

where $Y^E(\Delta Y)$ denotes $V^E / 10^{-6} \text{ m}^3 \text{ mol}^{-1}$, $\Delta \eta / \text{mPas}$, Δn_D or $\Delta G^{*E} / \text{J mol}^{-1}$; A_p , are the adjustable parameters of the related property, and $(k + 1)$ is the number of adjustable parameters, determined using the F-test.

The root-mean-square deviation (rmsd) of the correlation for the V^E , $\Delta \eta$, Δn_D and ΔG^{*E} is defined by the equation:

$$\sigma = \left(\sum_{i=1}^m (Y_{\text{exp},i}^E - Y_{\text{cal},i}^E)^2 / m \right)^{1/2} \quad (5)$$

where m is the number of experimental data points.

Data of excess molar volumes, viscosity deviations, refractive index deviations and excess molar Gibbs energy of activation of the viscous flow for the investigated binary system diethyl succinate + 1-hexanol along with the RK correlation results are presented in Figure 1(a), (b), (c) and (d), respectively.

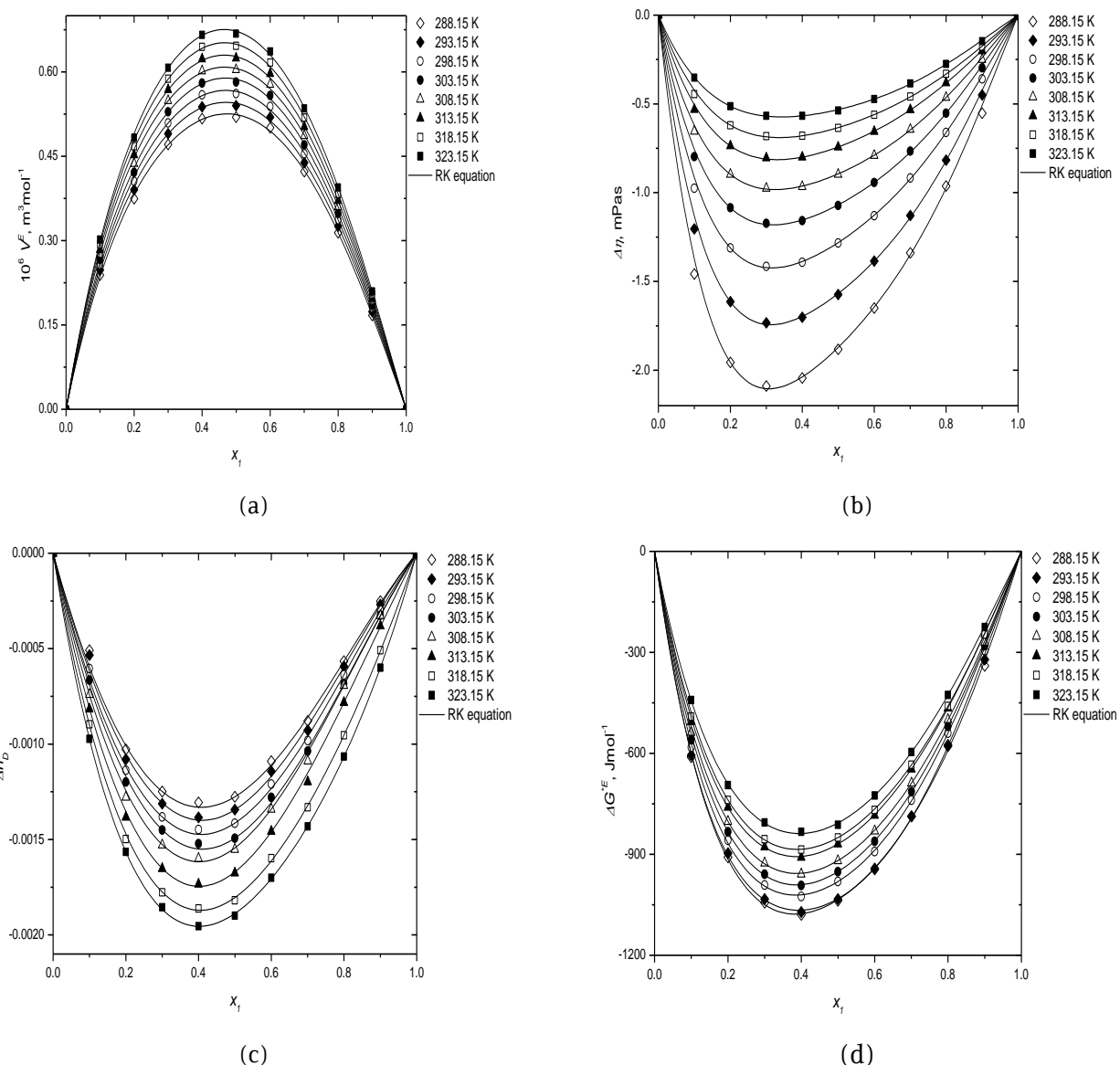


Figure 1. Experimental data of (a) excess molar volume (V^E), (b) viscosity deviations ($\Delta\eta$), (c) refractive index deviations (Δn_D) and (d) excess molar Gibbs energy of activation of the viscous flow ΔG^{*E} , for the binary system diethylsuccinate (1) + 1-hexanol (2) at 288.15 K-323.15 K and atmospheric pressure. Symbols refer to experimental data points. Solid lines present the results calculated by eq (4).

The excess molar volumes for investigated binary system are positive at all temperatures and for all mixture compositions as displayed on Figure 1(a). Curves are almost perfectly symmetrical, little shifted towards maximum of 0.45 molar fraction of diethyl succinate. For analyzed mixture V^E values are higher with temperature rise.

Viscosity deviations shown at Figure 1(b) are negative over the whole temperature and composition range with the maximum of deviations around 0.3 molar fraction of diethyl succinate. Absolute values of viscosity deviations $\Delta\eta$ are reduced with temperature rise.

In solution of diethyl succinate with 1-hexanol negative refractive index deviations are obtained at all temperatures through the whole composition range (Figure 1(c)). Absolute values of this deviation are very small, under 0.0020, and increase with temperature rise.

FT-IR spectra for the system diethyl succinate + 1-hexanol (Figure 2) is recorded at $x_1=0.5$, corresponding to the minimum of $V^E - x_1$ curve for this system.

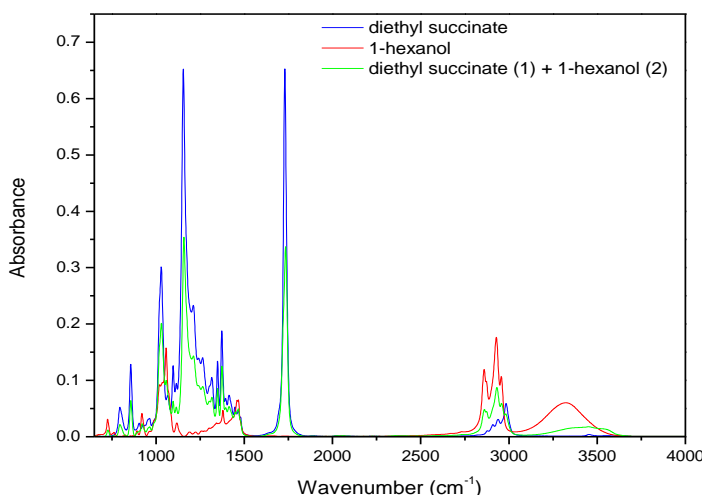


Figure 2. Infrared spectra of pure diethyl succinate, pure 1-hexanol, and the mixture diethyl succinate + 1-hexanol for molar fraction of diethyl succinate $x_1=0.5$.

The characteristic band for the OH stretching vibration of pure 1-hexanol is shifted from 3325 cm^{-1} for the pure substance to a higher wavenumber (3450 cm^{-1}) in the mixture.

Bands in the area 2800 cm^{-1} - 3000 cm^{-1} that result from the ν (C-H) stretching vibrations of alkyl groups from these solutions have not changed significantly the frequency value, shape and absorption maximum in the mixture.

The band at 1730 cm^{-1} , characteristic for the ν (C=O) stretching vibration of pure diethyl succinate, is slightly shifted towards higher frequencies in the mixture, but has smaller intensity of absorption maximum.

Inspection of the spectra reveals that bending frequencies of δ (OH) for pure 1-hexanol, deformation frequencies of δ_s (CH₃) and δ_s (CH₂), and stretching frequencies of ν_{as} [C-C(=O)-O] and ν_s (C-O) groups in diethyl succinate, remain unchanged in the solution.

The C-O asymmetrical stretching vibration band for pure 1-hexanol at 1057 cm^{-1} , in the mixture of diethyl succinate and 1-hexanol is weak, and absorption maximum has smaller value.

The obtained results of excess and deviation properties and FT-IR analysis allow insight into the molecular interactions existing in the mixture.

Positive values of excess molar volume values are usually a result of rupture or stretching of hydrogen bonds between self-associated molecules, or weakening of dipole-dipole interactions among molecules in the pure components⁷.

Also, the negative ΔG^{*E} values obtained within this work (Figure 1(d)) qualitatively concurs with the positive molar excess volumes. To a negative contribution to ΔG^{*E} and $\Delta\eta$ lead physical interaction, consisting mainly of dispersion forces or weak dipole-dipole interaction⁵.

Alcohol molecules are polar and self-associated through hydrogen bonding of their OH groups⁸. But from the shifting of OH stretching band can be concluded that intermolecular hydrogen bonds are formed between the alcohol and diethyl succinate (O--H-O)⁹, and it is a weak one because shifting from lower to higher frequencies indicates weakening of molecule interaction. This agrees with the fact that the disruption of alcohol multimers through breaking of hydrogen bonds makes a positive contribution to V^E .

Also, volume increase is a result of weakening of interactions between molecules of diethyl succinate. All the results suggest that attractive dispersion interactions in the pure ester and alcohol are stronger than in their mixture.

The authors gratefully acknowledge the financial support received from the Research Fund of Ministry of Education, Science and Technological Development (project No 172063), Serbia and the Faculty of Technology and Metallurgy, University of Belgrade.

Molekulske interakcije prisutne u binarnom sistemu dietil sukcinat + 1-heksanol prema izvedenim veličinama mešanja i FT-IR analizi

Eksperimentalno su određene gustine, viskoznosti i indeksi refrakcije binarnog sistema dietil sukcinat + 1-heksanol u temperaturnom intervalu 288.15–323.15 K sa korakom 5 K, i na atmosferskom pritisku. Eksperimentalna merenja su izvršena na digitalnom gustinomeru Anton Paar 5000, digitalnom viskozimetru Anton Paar SVM 3000 i refraktometru Anton Paar RXA 156. Na osnovu odgovarajućih eksperimentalnih podataka, izračunate su dopunske molarne zapremine (V^E), promene viskoznosti ($\Delta\eta$) i promene indeksa refrakcije (Δn_D), i korelisane Redlich-Kister polinomom. Dodatno je izračunata molarna dopunska Gibsova energija aktivacije viskoznog toka (ΔG^{*E}) iz izmerenih podataka za gustinu i viskoznost. Pomoći izvedenih veličina, kao i FT-IR merenja, urađena je analiza molekulskih interakcija prisutnih u smeši.

Literature

1. Y.-W. Sheu, C.-H. Tu, *J.Chem.Eng. Data*, **50** (2005) 1706.
2. M. Ortega-Heras, M.L. González-SanJosé, S. Beltrán, *Anal. Chim. Acta*, **458** (2002) 85.
3. A.Z. Tasic, D.K. Grozdanic, B.D. Djordjevic, S.P. Serbanovic, N. Radojkovic, *J. Chem. Eng. Data*, **40** (1995) 586.
4. E.M. Zivkovic, M.Lj. Kijevcanin, I.R. Radovic, S.P. Serbanovic, B.D. Djordjevic, *Fluid Phase Equilib.*, **299** (2010) 191.
5. V.K. Misra, I. Vibhu, R. Singh, M. Gupta, J.P. Shukla, *J. Mol. Liq.*, **135** (2007) 166.
6. O. Redlich, A.T. Kister, *Ind. Eng. Chem.*, **40** (1948) 345.
7. M.Lj. Kijevčanin, B.D. Djordjević, I.R. Radović, E.M. Živković, A.Z. Tasić, S.P. Šerbanović, *Molecular Interactions*, Prof. Aurelia Meghea (Ed.), InTech, Rijeka, 2012.
8. Y. Marcus, *Introduction to Liquid State Chemistry*, Wiley-Interscience, New York, 1977.
9. M. Hasan, A.P. Hiray, U.B. Kadam, D.F. Shirude, K.J. Kurhe, A.B. Sawant, *J. Solution Chem.*, **40** (2011) 415.

Meat processing industry wastewater – screening analysis

Maja M. Sremački, Jovana Lj. Simić*, Jelena R. Radonić, Maja M. Turk Sekulić,
Mirjana B. Vojinović Miloradov

Department of Environmental Engineering and Occupational Safety and Health, Faculty of Technical Sciences, University of Novi Sad, Trg Dositeja Obradovića 6, Serbia (majasremacki@uns.ac.rs, milenastosic@uns.ac.rs, jelenaradonic@uns.ac.rs, majaturk@uns.ac.rs, miloradov@uns.ac.rs)

**Department of Civil Engineering, Faculty of Technical Sciences, University of Novi Sad, Trg Dositeja Obradovića 6, Serbia (jovanasimic@uns.ac.rs)*

Abstract

Wastewater from meat processing industries is a complex mixture of different compounds with a high load of organic matter. The meat processing industry wastewater represents a serious threat to the river ecosystem, which has to be continuously monitored. The main problem with this type of wastewater in Serbia is lack of treatment and direct discharge into sewer and natural recipient. Very often, none of analysed samples meet the legal set of physicochemical and microbiological criteria. Since meat industry produces large amounts of wastewater, it would be of great significance if the treated wastewater could be reused for various agricultural activities. The newly recognised pollutant emerging substances (EmS) occur at very low concentration levels (ppb, ppt and lower) and are not included in the routine monitoring programs at EU level. The aim of this study was to perform a screening analysis of 8 wastewater samples taken from the discharges near meat processing industries and abattoir facilities, obtained in 3 different sampling campaigns, during the period from 2012 to 2014. During screening analysis, 1133 compounds were detected, and 314 identified with high certainty. The results of screening analysis for 3 samples will be presented in this paper. The three selected samples represent the wastewater before and after treatment.

Keywords: EmS, semi-quantitative screening analysis, concentration calculation and range, meat processing industry, wastewater

Introduction

Using a methodology that considers the entire chain of process activities, it is estimated that meat industry is responsible for 18 % of greenhouse gas emissions [1]. Slaughterhouse effluent discharge can cause deoxygenation of rivers and the contamination of groundwater [2]. Analysis of wastewater samples from meat processing industry in Novi Sad area was conducted by GCMS in SCAN mode, with the aim to identify emerging, priority, and hazardous priority organic pollutants. Organic compounds were extracted from wastewater samples via liquid-liquid extraction. Compounds identified during the analytical study, can be found on the NORMAN list of emerging substances as: industrial chemicals, personal care products PCPs, fragrances, wood preservatives and antifoaming agents and others [3]. A significant number of detected compounds have one or more hazardous characteristics – bioaccumulation, pseudoperistensy, nonmonotonic dose response with low and sublow concentration levels, irritability, toxicity, flammability, corrosively, ignitability, and/or reactivity [4].

Hundred and five substances were identified and their concentration levels were calculated using the known mass of the internal standard (method of internal standard). Samples MI3 and MI8 were taken from the same meat processing industry before and after wastewater treatment plant, and sample MI7 is a sample from a different meat processing industry after wastewater treatment process. The results of the screening analysis of 3 samples are presented in this paper.

During the secondary treatment, biodegradable organic matter is eliminated biologically, resulting in reduction of oxygen demand. The tertiary treatment involves chemical coagulation, flocculation, sedimentation, and filtration. In addition to disinfection, sterilization, advanced oxidation processes, and activated-carbon adsorption are frequently applied. [5-7]

Any of disposal ways for untreated wastewater, if it is not one suggested by legislation, can have diverse and negative effects on the environment and human health [8]. In meat processing, water is used primarily for carcass washing after hide removal from cattle, calves, and sheep, or hair removal from hogs and again after evisceration, for cleaning, and sanitizing of equipment and facilities, and

for cooling of mechanical equipment such as compressors and pumps. A large quantity of water is used for scalding of hogs for hair removal before evisceration[9].

One of the research goals was screening and identification of organic compounds and pollutants content in meat industry wastewater, with emphasis on hazardous and priority pollutants within the Water Frame Directive [10] and compounds that are on the NORMAN list of emerging substances[3]. Only peaks with higher reproducibility were taken into consideration .

Methods and materials

Semi-quantitative screening analysis was performed on Agilent 7890 gas chromatograph coupled to Agilent 5975 mass spectrometric detector. The system was equipped with a PTV injector system. Capillary GC analysis was performed on a 30 m x 250 mm I.D., 0.25 mm df DB-FFAP column. Helium was used as carrier gas. The SCAN mode of mass detector was used for all samples. Water samples of 1 L were placed into a 2 L glass separatory funnel and extracted with three 30 mL portions of dichloromethane for 30 minutes using automatic shaker. Benzophenon was used as an internal standard. Extracts were mixed and evaporated in Kuderna Danish apparatus to final volume maximum 2 mL [11].

LL-E coupled with Kuderna Danish was used, as it has been concluded from previous research that it is the optimal and the most suitable sample preparation techniques, giving the highest yield of targeted compounds [12]. The liquid liquid extraction (LLE) into dichloromethane favours the transport of hydrophobic organic compounds from water to an extraction solvent [13].

The identification of compounds was performed via NIST08 and Wiley7n MS libraries.

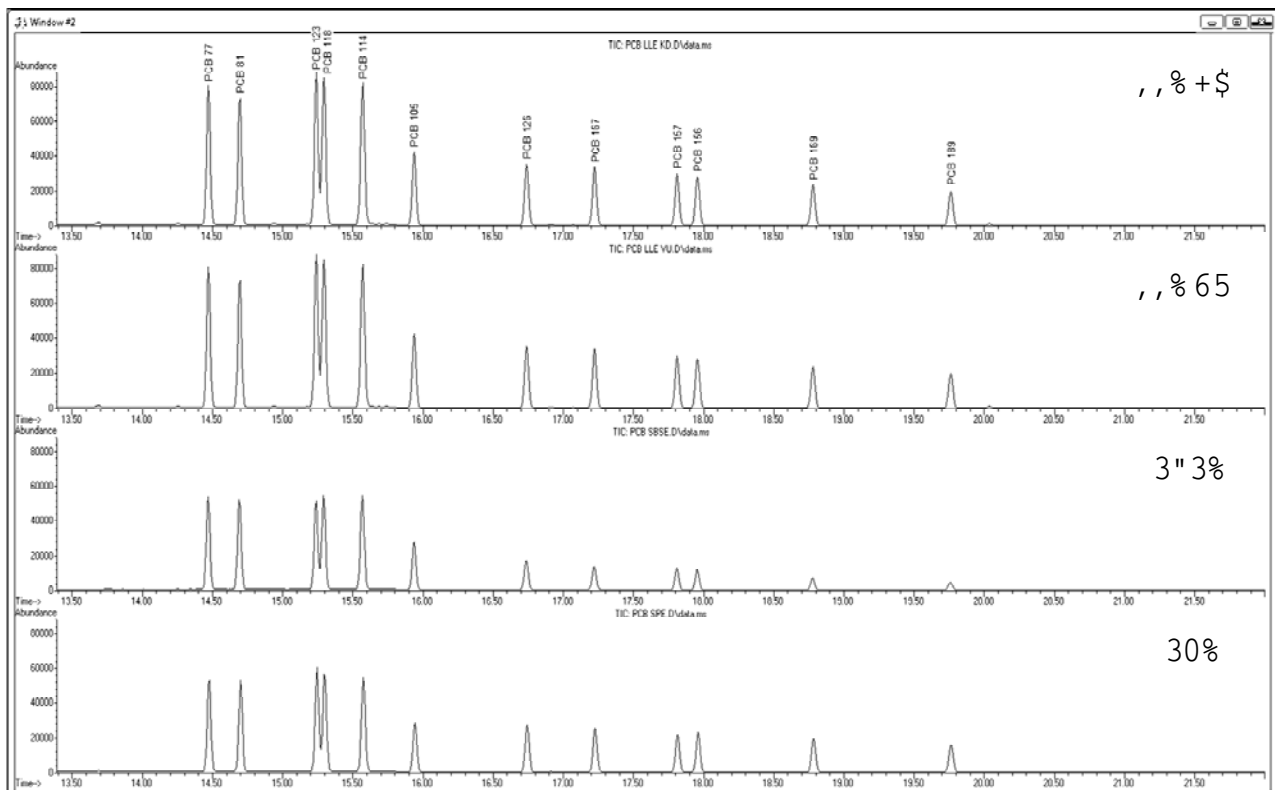


Figure 1. Yeald of selected target compounds in water samples prepared via different techniques

Concentration levels of identified substances have been calculated via equation 1, using the know values – mass of internal standard, peak area of internal standard and registered compound.

$$C_{\text{compound}} = \frac{A_{\text{compound}} \cdot m_{\text{internal standard}}}{A_{\text{internal standard}}} \quad (1)$$

where:

C_{compound} is concentration level of registered compound; A_{compound} is pick area of registered compound; $m_{\text{internal standard}}$ is a mass of internal standard; $A_{\text{internal standard}}$ is a pick area of internal standard

Results and discussion

During the analysis and analytical study of the three selected samples, 98 compounds were identified, and a significant number can be found on the NORMAN list of emerging substances as: industrial chemicals, PCPs, fragrances, wood preservatives and antifoaming agents (Table 1).

Allopregnane was used as a steroid marker hormone, since it was present in almost all 8 analysed samples in 3 different sampling campaigns, during the period from 2012 to 2014 (1-8). A significant number of detected compounds have one or several hazardous characteristics (NORMAN, 2015). Compounds detected in all 3 samples and their calculated concentrations are shown in Table 1 and Figure 1, respectively.

Table 1. Compounds detected in all 3 samples and concentration levels [g/L]

Compound	sample		
	MI3	MI7	MI8
Benzene, methyl-	0.007792573	0.000171579	0.00161107
2-Hexanone	1.82226·10 ⁻⁵	6.32139·10 ⁻⁵	5.56604·10 ⁻⁵
p-Xylene	1.26631·10 ⁻⁵	1.04996·10 ⁻⁵	1.69862·10 ⁻⁵
2-Pentanol, 4-methyl-;	0.001321589	1.64611·10 ⁻⁵	0.000126961
2-Buten-1-ol, 2-methyl-	1.79063·10 ⁻⁵	8.21696·10 ⁻⁶	8.25648·10 ⁻⁶
1-Hexanol, 2-ethyl-	0.000180006	4.74543·10 ⁻¹²	3.8724·10 ⁻⁵
Benzeneethanol	5.30404·10 ⁻⁵	1.12818·10 ⁻⁵	2.4941·10 ⁻⁵
Nonadecane	0.000182006	6.577·10 ⁻¹²	4.77624·10 ⁻⁶
Cyclododecane	3.29064·10 ⁻⁵	0.000102912	5.40227·10 ⁻⁵
Phenol	6.20749·10 ⁻⁵	1.61002·10 ⁻⁵	7.14741·10 ⁻⁵
Eicosane	0.000303707	4.57892·10 ⁻¹²	7.14709·10 ⁻⁶
Phenol, 1,4-methyl-	0.006696872	0.000304829	0.004600977
Heneicosane	0.000421992	1.17387·10 ⁻¹¹	1.76605·10 ⁻⁵
Phenol, 2,5-bis(1,1-dimethylethyl)-	8.06648·10 ⁻⁵	0.000327554	0.000163201
Diethyl Phthalate	4.74913·10 ⁻⁵	0.000676158	0.000268152
1H-Indole	0.001766277	0.000359304	0.001550599
Dodecanoic acid	0.000301484	2.34479·10 ⁻⁵	5.22563·10 ⁻⁵
1H-Indole, 3-methyl-	0.003840416	7.37487·10 ⁻⁵	0.001263892
Tetradecanoic acid	0.000775163	1.52155·10 ⁻⁵	0.000369388

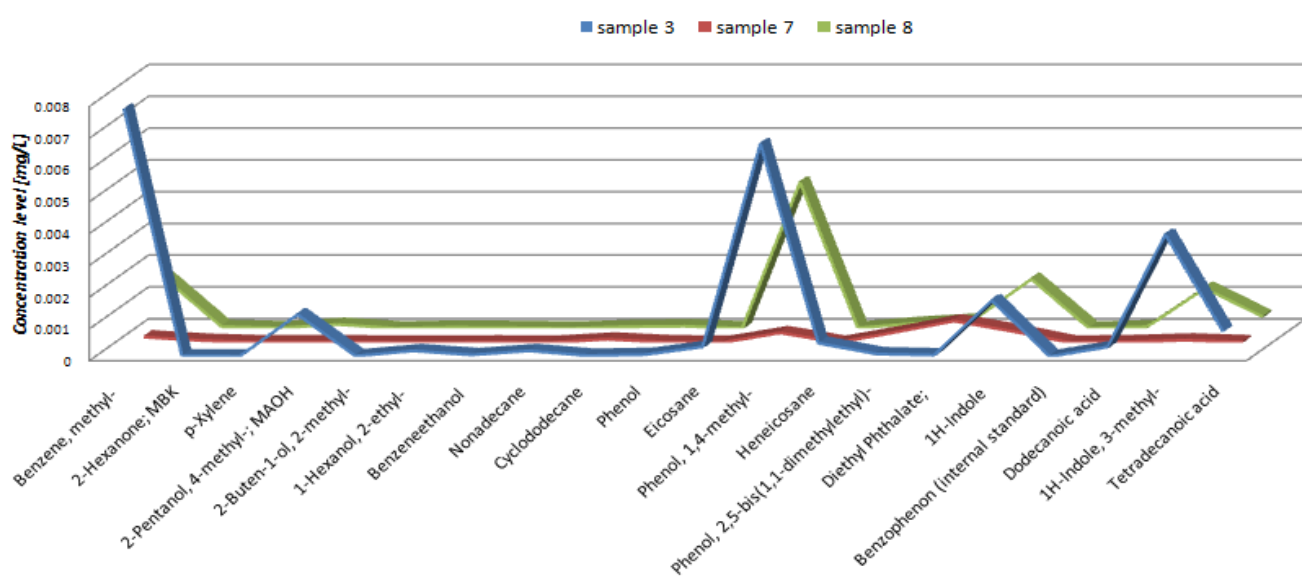


Figure 2. Detected compounds in all 3 samples

The substances detected and identified according to libraries, in all three samples during the screening analysis of wastewater could be suggested for target analyses.

The substances identified in each sample were taken into consideration only if the identification quality match (QM) was higher than 80% and if it has been identified in other analysed samples during this study, not shown in this paper.

Conclusion

The detected and identified chemicals during the research can be found on the NORMAN list of emerging substances, include industrial chemicals (p-xylene), PCPs (isocineole, 1,8-cineole, carvone), fragrances (dl-limonen), wood preservatives (p-cresole) and antifoaming agents (surfynol 104A). Presence of steroid hormones was detected and confirmed using the presence of allopregnane as a marker in almost all wastewater samples, which could confirm the existence of endocrine disruption substances and other xenobiotics in analyzed wastewater from the meat processing industry.

A significant number of detected compounds have one or more hazardous characteristics, such as bioaccumulation, pseudoperistensy, nonmonotonic dose response with low and sublow concentration levels, irritability, toxicity, flammability, corrosively, ignitability, and/or reactivity. Registered substances are high-risk substances which should not be present in natural water bodies – phenolic compounds, -2-Octenal, (E)-, (E,E)-2,4-Decadienal, 2-Methoxyphenol, Dioctyladipate, 2,6-Dimetilphenyl isocyanate, 2,6-dimethoksy-4-(2-propenyl)-, Etilallylftalat, 2-methoxy-4-(prop-1-en-1-yl)phenol, N-docosanol).

Acknowledgement: The research is supported by the Ministry of Education, Science and Technological Development (III46009 and Bilateral Project 680-00-140/2012-09/13) and NETREL Tempus Project.

Otpadna voda mesne industrije – skrining analiza

Otpadna voda mesne industrije je kompleksna mešavin jedinjenja sa visokim sadržajem organske materije. Otpadna voda mesne industrije predstavlja ozbiljnu pretnju za ekosistem, koji mora da se kontinuirano prati. Glavni problem ove vrste otpadnih voda u Srbiji je nedostatak njihovog tretmana i direktno ispuštanje u kanalizaciju ili prirodni recipijent. Vrlo često, analizirani uzoci ne ispunjavaju zakonski minimum fizičko-hemijski i mikrobioloških graničnih vrednosti. Pošto mesna industrija proizvodi velike količine otpadnih voda, bilo bi od velikog značaja ako se može ponovo koristiti u različite svrhe u poljoprivrednim aktivnostima. Emergentne supstance (EMS), koje se učestalo koriste u različitim antropogenim sferama (od industrije i privrede do proizvoda koji se koriste u domovima) se u prirodi nalaze u vrlo niskim koncentracijama (ppb, ppt i niže) i nisu uključene u rutinskim programima za monitoring ni nivou EU. Cilj istraživanja je da se izvrši skrining analiza 8 uzoraka otpadne vode mesa industrije i klanica, koji su dobijeni u 3 različite kampanje uzorkovanja, u periodu od 2012. do 2014. Tokom semi-kvantitativne skrining analize otkriveno je 1133 jedinjenja, a 314 jedinjenja je identifikovano sa visokom sigurnošću. Rezultati skrining analize za 3 uzoraka će biti prikazani u ovom radu. Tri odabrana uzorka predstavljaju uzorke pre i posle tretiranja otpadne vode.

References

1. FAO, Agriculture and Consumer Protection Department, "Livestock Impacts on the Environment" 2006
2. Masse D.I. and Masse L. "Characterization of wastewater from hog slaughterhouses in eastern Canada and evaluation of their in-plant wastewater treatment systems" Canadian Agricultural Engineering Journal Vol. 42 pp. 139–146, 2000
3. NORMAN, Network of reference laboratories, research centers and related organizations for monitoring of emerging environmental substances, list of emerging substances, <http://www.norman-network.net/?q=node/81>, 30.06.2015.
4. S.K. Rout, Wastewater treatment technologies, Int. J. Water Res. Environ. Sci. 2 (2013) 20–23.
5. Vojinović Miloradov M., Mihajlović I., Vyiurska O., Cacho F., Radonić J., Milić N., Spanik I. (2014) "Impact of Wastewater Discharges to Danube Surface Water Pollution by Emerging and Priority Pollutants in the Vicinity of Novi Sad, Serbia" Fresenius Environmental Bulletin, 23 (9), pp. 2137-2145

6. M.B. Pescod, Wastewater Treatment and use in Agriculture. FAO Irrigation and Drainage Paper No. 47, Food and Agriculture Organization of the United Nations, Rome, 1992.
7. Mittal G.S., (2006) Treatment of wastewater from abattoirs before land application - A review, Bioresour. Technol. 971119–1135.
8. Sremački, M., Simić, J., Radonić, J., Turk Sekulić, M., Sremački, D. (2013) Geospatial support for the monitoring of water pollution loads due to the meat industry facilities effluent discharge in the vicinity of Novi Sad, 6th Symposium EnviroChem 2013, ISBN 978-86-7132-052-8, pp. 250-251, Vršac
9. Technical Development Document for the Final Effluent Limitations Guidelines and Standards for the Meat and Poultry Products Point Source Category (40 CFR 432, 2004) EPA-821-R-04-011 The full document is available at: <http://www.epa.gov/ost/guide/mpp/>, accessed 05.09.2014.
10. Directive 2000/60/EC of the European Parliament and of the Council of 23 October 2000 establishing a framework for Community action in the field of water policy, 2000
11. Spanik, I., Sremački, M., Vyviurska, O., Radonić, J., Turk Sekulić, M., Vojinović-Miloradov, M. (2013) Characterization of environmental pollutants coming from meat industry in Vojvodina region, European Meeting on Environmental Chemistry "Environmental Chemistry" Association of Chemistry and the Environment, RSfMS; pp. 43-43, ISBN 978-5-89513-295-1, Moscow
12. Tempus NETREL Project, <http://www.netrel.uns.ac.rs/> 19.05.2016.
13. Milić N., Spanik I., Radonić J., Turk Sekulić M., Grujić N., Vyviurska O., Milanović M., Sremački M., Vojinović Miloradov M. "Screening of wastewater and Danube surface water in Novi Sad locality, Serbia" Fres. Environ. Bull. Vol. 23, no. 2, pp. 372-377, 2014

Study of pertechnetate adsorption from aqueous solution by surfactant-modified clinoptilolite

Dorđe Petrović, Sonja Milićević*, Ljiljana Matović, Anđelka Đukić, Vladan Milošević*,
Divna Đokić, Ksenija Kumrić

Vinča Institute of Nuclear Sciences, University of Belgrade, P.O. Box 522, 11001 Belgrade, Serbia,

**Institute for Technology of Nuclear and Other Mineral Raw Materials, Franchet d'Esperey 86, 11000
Belgrade, Serbia*

Introduction

The presence of the radionuclide ^{99}Tc in the environment comes from anthropogenic nuclear activities such as nuclear power plants, nuclear weapons testing facilities, reprocessing of spent nuclear fuel, nuclear accidents and medical application of $^{99\text{m}}\text{Tc}$. The predominant chemical form of the long-lived radionuclide ^{99}Tc ($t_{1/2} = 2.1 \times 10^5$ y) is the highly soluble and environmentally mobile pertechnetate anion (TcO_4^-), that easily penetrates the ecosystems.¹ The control of environment pollution by ^{99}Tc is therefore considered as a primary task. Many investigations are orientated toward the immobilization of ^{99}Tc , as well as its adsorption from contaminated groundwaters by using various adsorbent materials.

In recent years, many synthetic and natural materials have been evaluated for use in long-term immobilization of ^{99}Tc and its removal from contaminated groundwaters. Zeolites are hydrated aluminosilicates that possess a negatively charged surface, compensated by the presence of exchangeable cations, and therefore mainly cation exchange properties. Due to the high cation exchange capacity (CEC), these minerals are widely used for the removal of heavy metal ions from aqueous solutions.² However, numerous investigations have shown that chemical treatment and modification of the zeolite surface can provide them with an affinity for non-polar organic species, as well as inorganic anions.

Zeolite and its adsorption is limited to the external exchangeable cations. Therefore, more important than the CEC value is the external cation exchange capacity (ECEC), which has a theoretical value of 10% CEC. Surface modification of a zeolite by cationic surfactant involves both cation exchange and hydrophobic bonding: (i) at low loading levels, surfactant molecules are retained onto the surface of a zeolite by ion exchange with the formation of a monolayer and (ii) when the surfactant concentration in the solution exceeded ECEC, the hydrophobic tails of the surfactant molecules associate to form a bilayer on zeolite external surface with positive charges oriented toward the solution. Such modified zeolites provide sites where anions will be retained and cations repelled, while neutral species can partition into the hydrophobic core.³ By controlling the initial and final surfactant concentration a desired surfactant configuration on the zeolite surface can be achieved.

In this study, surface of the raw zeolite was modified by using cationic surfactant stearyl-dimethylbenzyl-ammonium chloride (SDBAC) in order to investigate the sorption of pertechnetate anions from aqueous solutions by batch adsorption technique. The aim of the study was to evaluate the effects of the surfactant loading, contact time and solution pH on the removal efficiency of pertechnetate by surfactant modified natural zeolite.

Experimental

Raw zeolite (clinoptilolite) from the Zlatokop deposit (Vranjska banja) in Serbia was used as the starting material for the surface modification by cationic surfactant SDBAC (Hoechst, Germany). After crushing and grinding, the sample was sieved to the fractions below 0.043 mm. CEC and ECEC, the most important parameters for the surface modification of the zeolite, were determined by the method of Ming and Dixon and by a modification of that method.^{4,5} The amount of released cations was measured by atomic absorption spectrophotometry (AAS) using the Analytic Jena Spekol 1300.

Organo-zeolite was prepared using the procedure previously reported in the literature⁶: the quantity (10 g) of thermally pretreated zeolite was added to 0.2 dm³ of surfactant solution having the concentration of the SDBAC up to and above the ECEC (10 - 350 meq kg⁻¹, i.e. 0.5 – 17.5 meq dm⁻³). The organo-samples were marked so that numbers next to the letter indicate the amount of the

added organic matter in meq kg⁻¹. The non-adsorbed surfactant in the supernatants was analyzed by the two-phase titration technique using dimidium bromide and disulfine blue as indicators.⁷ The amount of surfactant sorbed was determined as the difference between the initial and the equilibrium surfactant concentration.

Batch adsorption experiments were performed in closed glass vials containing 25 cm³ of working ^{99m}TcO₄⁻ solution and 0.04 g of adsorbent (either unmodified or SDBAC-modified clinoptilolite). ^{99m}Tc was eluted from a ⁹⁹Mo/^{99m}Tc generator (Vinča Institute of Nuclear Sciences, Belgrade, Serbia). The initial pH of the working solutions was adjusted to a definite value using HCl and NaOH solutions. Reaction mixture was shaken at a room temperature on a laboratory shaker in the course of desired time (1-240 min) at a stirring speed of 200 rpm. Thereafter, the liquid phases were separated from the solid phases by filtration through a 0.45 µm microporous membrane filter. The aliquot activity was determined with an automated 1282 Compugamma counter (LKB Wallac, Turku, Finland). The aliquot activity of all samples was measured at the same time, in order to avoid time correction in further calculations. All experiments were carried out in duplicate and the obtained data were used for analysis. The data were reported in terms of removal efficiency (*E*, %) of TcO₄⁻, Eq. (1):

$$E = \frac{(A_i - A_f)}{A_i} \times 100 \quad (1)$$

where *A_i* and *A_f* are the initial and the final activities of ^{99m}TcO₄⁻ in the liquid phase (counts per min), respectively.

Results and discussion

The CEC and ECEC values of the investigated clinoptilolite were found to be 1460 meq/kg and 130 meq/kg, respectively. The result of SDBAC loading onto clinoptilolite is presented in Fig. 1. In Fig. 1a, by matching the ECEC data with the results obtained by following the SDBAC concentration, adsorption can be observed. At the low loading level, up to the surfactant concentration equal to the ECEC, clinoptilolite adsorbed 100% of SDBAC. In Fig. 2b, the adsorption was linearly followed by the sum of exchanged cations, indicating that the surfactant was retained by ion exchange and formed a monolayer. When the initial concentration of surfactant exceeded the ECEC, the sum of exchangeable cations remained unchanged. The highest achieved adsorbed SDBAC amount was 193 meq kg⁻¹. This additional adsorption occurred because the hydrophobic tails of the surfactant molecules associated to form a bilayer.^{6,8}

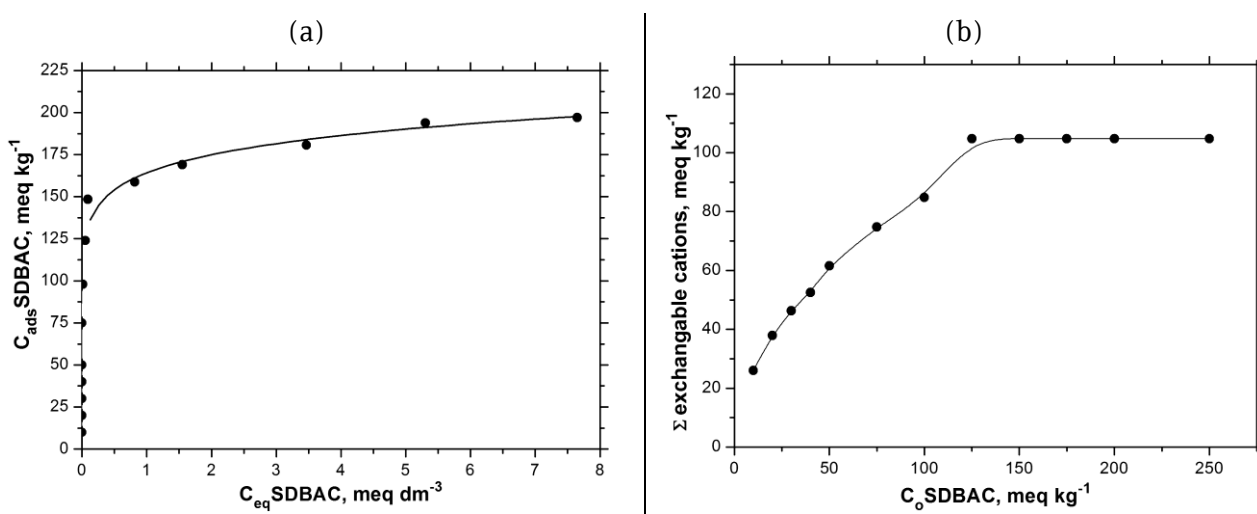


Fig. 1 (a) Adsorption equilibrium data modeled by the Langmuir isotherm, (b) Cations exchanged in the modification process (C_{eq} – equilibrium concentration of SDBAC, C_{ads} – adsorbed amount of SDBAC, C_0 – added amount of SDBAC).

Sorption of pertechnetate onto clinoptilolite, modified with different loading levels of SDBAC, was investigated. An attempt was made to find out a way in which the manner of clinoptilolite covering (modification conditions, i.e. the loading amount of SDBAC) influences its sorption ability to remove

pertechnetate from the aqueous solutions. In the first modified sample, when the surfactant concentration is close to the ECEC for clinoptilolite, the interaction between zeolite and surfactant molecules leads to the formation of monolayer due to the uptake of surfactant monomers by ion exchange on the zeolite surface. When the initial concentration of surfactant exceeded the ECEC, 130 meq kg⁻¹, additional adsorption of surfactant occurred because the hydrophobic tails of the surfactant molecules associated to form a bilayer.

Influence of adsorption contact time on TcO₄⁻ removal efficiency by either raw clinoptilolite (Z0) or SDBAC-modified clinoptilolite (Z100 and Z250) is summarized in Fig. 2. It is obvious that the equilibrium was established after 60 min for Z0 and Z100, while for the Z250 the equilibrium was reached faster, after only 15 min. Such a fast sorption of pertechnetate ions on the sample Z250 implies ion exchange mechanism of sorption on the surface of the bilayer. Further increase of the contact duration did not influence the sorption process.

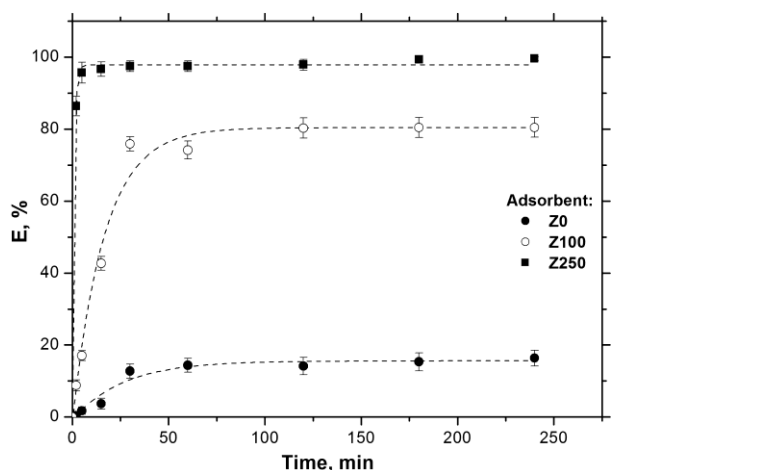


Fig. 2 Effect of contact time on the removal efficiency of TcO₄⁻ by the raw clinoptilolite (Z0) and organo-clinoptilolite (Z100 and Z250). Conditions: pH 5.5; stirring speed, 200 rpm; concentration of adsorbent, 1.6 g dm⁻³. Vertical error bars represent standard errors.

The results presented in Fig. 2 have also shown that the clinoptilolite Z0 is not efficient adsorbent for the removal of TcO₄⁻ ($E < 20\%$). The low affinity of Z0 for TcO₄⁻ results from negative charge of its crystal lattice, which provides sites for exchanging cations but not for anions. In contrast to the Z0, TcO₄⁻ sorption on the surfactant-modified clinoptilolite was significantly higher compared to that of the Z0. Removal efficiency of TcO₄⁻ from aqueous solutions by SDBAC-clinoptilolite Z100 and Z250 depends on the number of sorption sites available, which in turn depends on SDBAC surface coverage and ECEC. TcO₄⁻ sorption increases with increased SDBAC loading and at the surfactant loading above the ECEC of raw clinoptilolite (sample Z250) removal efficiency of TcO₄⁻ reached more than 98%. It can be attributed to the formation of bilayer coverage on the clinoptilolite external surface. The sample SDBAC-clinoptilolite Z250 was chosen for further experiments.

The effect of the solution pH on the removal efficiency of TcO₄⁻ by SDBAC-clinoptilolite Z250 is presented in Fig. 3. The obtained results have shown that in the pH range of 5.0-8.0 the removal efficiency of pertechnetate does not change significantly. At lower pH (< 4), as well as at higher pH (> 8), the efficiency drops sharply. The reason for lower removal of TcO₄⁻ at pH < 4 and pH > 8 can lie in the fact that, under the applied conditions, partial desorption of SDBAC from the bilayer occurred (up to 10% depending on the SDBAC loading), as previously shown by Lemić *et al.*⁶ Consequently, decrease of SDBAC concentration had an influence on the number of available sites for pertechnetate sorption, thus affecting the removal efficiency of TcO₄⁻. Also, the reason for lower removal of pertechnetate at pH > 8.0 can be explained by the presence of hydroxide ions in the solution and its competition with pertechnetate ions for the adsorption sites on the Z250. Similar results were reported for the removal of NO₃⁻ ions and As(V) from aqueous solutions using surfactant-modified zeolites as adsorbents.^{9,10} Based on the obtained results, pH at 5.0-8.0 was found as optimal for maximum removal of pertechnetate from aqueous solutions by the SDBAC-modified clinoptilolite.

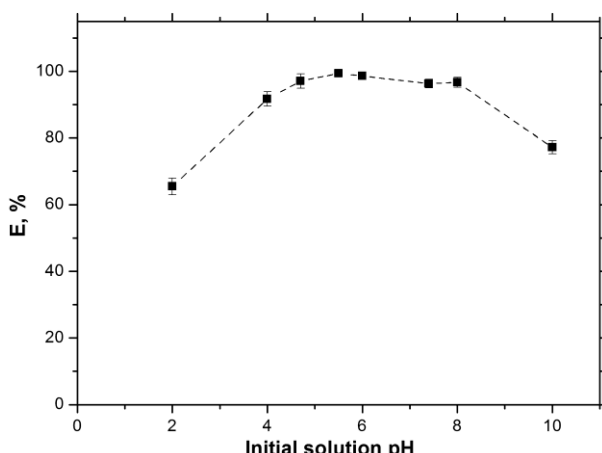


Fig. 3 Effect of pH on the removal efficiency of TcO_4^- by the organo-clinoptilolite Z250. Conditions: contact time, 60 min; stirring speed, 200 rpm; concentration of adsorbent, 1.6 g dm^{-3} . Vertical error bars represent standard errors.

Conclusion

Organic modification with the use of SDBAC leads to change of the surface properties of clinoptilolite and giving it the ability to adsorb anions. Removal of TcO_4^- from aqueous solutions depends on SDBAC loading level of clinoptilolite such that TcO_4^- sorption increases with increased SDBAC loading. The maximum pertechnetate removal ($> 98\%$) was achieved by using SDBAC-clinoptilolite with bilayer surfactant coverage in the pH range of 5.0-8.0. The adsorption process was very fast and the equilibrium was reached within 15 min. Such a fast process implied ion exchange mechanism of TcO_4^- adsorption on the surface of the bilayer. The obtained results suggest that SDBAC-modified clinoptilolite with organo-bilayer is effective sorbent for the removal of pertechnetate and has a potential to remove TcO_4^- from contaminated groundwaters.

Acknowledgement: We acknowledge the support to this work provided by the Ministry of Education, Science and Technological Development of Serbia through the projects III 45006, III 45012, III 45015 and TR 033007.

Proučavanje adsorpcije pertehnetata iz vodenog rastvora primenom površinski modifikovanog klinoptilolita

Prirodni zeolit klinoptilolit, modifikovan dugolančanim organskim stearildimetil benzil amonijum-hlorid (SDBAC) jonom, korišćen je kao adsorbens za uklanjanje pertehnetata (TcO_4^-) iz vodenih sistema. Ispitivanja su urađena u šaržnom sistemu, praćenjem uticaja različitih parametara (količina organskog katjona, vreme kontakta, pH vrednost polaznog rastvora) na efikasnost uklanjanja TcO_4^- iz vode. Rezultati su pokazali da je prirodni klinoptilolit neefikasan za uklanjanje TcO_4^- ($E < 20\%$). Klinoptilolit, modifikovan SDBAC katjom, pokazao je mnogo veću efikasnost za uklanjanje TcO_4^- u odnosu na prirodni, nemodifikovani klinoptilolit. Potvrđeno je da pokrivenost površine zeolita organskim katjonom ima važnu ulogu u poboljšanju efikasnosti uklanjanja TcO_4^- , zahvaljujući formiranju dvosloja SDBAC katjona. Klinoptilolit, na čijoj površini je formiran organski dvosloj, uspešno je primjenjen za uklanjanje TcO_4^- iz vode u opsegu pH vrednosti 5.0-8.0 ($E > 98\%$). Ravnoteža je uspostavljena nakon kontakta faza u trajanju od 15 minuta. Dobijeni rezultati pokazuju da klinoptilolit, modifikovan dvoslojem SDBAC katjona, ima potencijal da prečišćava otpadne vode od ekološkog zagađivača pertehnetata.

References

1. K. Shi, X. Hou, P. Roos, W. Wu, *Anal. Chim. Acta*, **709** (2012) 1.
2. E. Erdem, N. Karapinar, R. Donat, *J. Colloid Interface Sci.*, **280** (2004) 309.
3. B. de Gennaro, L. Catalanotti, S. R. Bowman, M. Mercurio, *J. Colloid Interface Sci.*, **430** (2014) 178.
4. Z. Li, R. S. Bowman, *Environ. Sci. Technol.*, **31** (1997) 2407.
5. D. W. Ming, J. B. Dixon, *Clays Clay Miner.*, **35** (1987) 463.
6. J. Lemić, S. Milošević, M. Vukašinović, A. Radosavljević-Mihajlović, D. Kovačević, *J. Serb. Chem. Soc.*, **71** (2006) 1161.

7. 7. S. O. Jansson, R. Modin, G. Schill, *Talanta*, **21** (1974) 905.
8. 8. J. Lemić, D. Kovačević, M. Tomašević-Čanović, D. Kovačević, T. Stanić, R. Pfend, *Water Res.*, **40** (2006) 1079.
9. 9. P. Chutia, S. Kato, T. Kojima, S. Satokawa, *J. Hazard. Mater.*, **162** (2009) 204.
10. 10. D. Bhardwaj, M. Sharma, P. Sharma, R. Tomar, *J. Hazard. Mater.*, **227-228** (2012) 292.

Hemija i tehnologija hrane / Chemistry and Technology of Food

Određivanje sastava masnih kiselina tokom fermentacije mleka kombuhom i konvencionalnim starter kulturama

Snežana Kravić, Spasenija Milanović, Dajana Hrnjez, Zvonimir Suturović, Ana Đurović,
Tanja Brezo, Zorica S. Stojanović

*Univerzitet u Novom Sadu, Tehnološki fakultet, Bulevar cara Lazara 1, 21000 Novi Sad
zorica.stojanovic@uns.ac.rs*

Uvod

Fermentisani mlečni proizvodi zauzimaju značajno mesto u svakodnevnoj ishrani usled visoke nutritivne vrednosti i pogodnih zdravstvenih efekata na humani organizam. Dobijaju se iz mleka, fermentacijom pomoću odabranih mikroorganizama (starter kultura). Pored tradicionalnih startera (*Streptococcus thermophilus* i *Lactobacillus delbrueckii spp. bulgaricus*) danas se sve više upotrebljavaju probiotske bakterije najčešće iz roda *Lactobacillus* i *Bifidobacterium*.¹ Savremena istraživanja ispituju mogućnost primene kombuhe – nekonvencionalnog startera za fermentaciju mleka u proizvodnji funkcionalne hrane.^{1,2-4} Primenjeni fermentativni procesi menjaju sastav mleka. Mlečno-kiselinska fermentacija utiče na stvaranje mlečne kiseline iz laktoze, masnih kiselina iz mlečne masti i aminokiselina iz proteina.^{5,6} Mlečna mast predstavlja veoma važnu komponentu fermentisanih mlečnih proizvoda. Mleko sadrži 3,5–5% mlečne masti, koja se sastoji od preko 400 različitih masnih kiselina, uglavnom u obliku triacilglicerola, što daje mlečnoj masti širok spektar funkcionalnih i nutritivnih karakteristika. Nutritivna vrednost, izgled, tekstura, senzorne karakteristike i stabilnost mleka i mlečnih proizvoda je u najvećoj meri u korelaciji sa sadržajem i sastavom mlečne masti.⁷

Mlečna mast obično sadrži visok procenat zasićenih i mononezasićenih masnih kiselina, a mali procenat polinezasićenih masnih kiselina.⁸ Klinička istraživanja su pokazala da različite masne kiseline imaju različit uticaj na ljudski organizam. Dok masne kiseline sa kratkim i srednjim lancem ne utiču na lipoproteine plazme, konzumiranje zasićenih masnih kiselina, posebno onih sa 12-16 ugljenikovih atoma, povećava ukupan nivo holesterola kao i LDL holesterola, a samim tim se povećava i rizik od kardiovaskularnih oboljenja.⁹ Stoga se u cilju prevencije koronarnih oboljenja preporučuje smanjenje unosa zasićenih masnih kiselina dugog lanca. Mononezasićene masne kiseline i određene polinezasićene masne kiseline imaju važnu ulogu u prevenciji i lečenju kardiovaskularnih bolesti, hipertenzije, dijabetesa, artritisa i drugih inflamatornih i autoimunih bolesti i tumora.¹⁰ Takođe je primećeno da polinezasićene masne kiseline dugog lanca kao što su α -linolenska kiselina i konjugovana linolna kiselina, ne samo što podstiču adheziju nekih laktobacila za mukozne površine u crevima, nego i ublažavaju simptome kod crevnih upala.^{11,12} Istraživanja su pokazala da su neki sojevi bakterija, kao rezultat rasta i metabolizma, sposobni da tokom fermentacije mleka promene profil masnih kiselina mleka i produkuju funkcionalne masne kiseline.¹³⁻¹⁵

U skladu sa navedenim, cilj ovog rada je bio određivanje sastava masnih kiselina tokom fermentacije mleka primenom nekonvencionalne starter kulture, kombuhe kultivisane na crnom čaju, i konvencionalnih starter kultura, jogurtne i probiotske.

Materijal i metode rada

Proizvodnja fermentisanih mlečnih napitaka

Fermentisani mlečni napici su proizvedeni od pasterizovanog (72 °C) i homogenizovanog mleka sa 2,8 % mlečne masti (AD „Mlekara“ Subotica, Subotica, Srbija) u Laboratoriji za mleko i mlečne proizvode na Tehnološkom fakultetu u Novom Sadu. Fermentacija mleka je izvedena primenom konvencionalnih starter kultura, jogurtne odnosno probiotske i nekonvencionalne starter kulture, inokulum kombuhe. Za proizvodnju tradicionalnog jogurta korišćena je starter kultura YF-L812 (termofilna starter kultura Yo-Flex®, *Streptococcus thermophilus* i *Lactobacillus delbrueckii* spp. *bulgaricus*), a za proizvodnju probiotskog jogurta kultura ABT-7-Probio-Tek® (LA-5® *L. acidophilus*, BB-12® *Bifidobacterium*, *S. thermophilus*, Chr.Hansen, Horsholm, Danska). Inokulum kombuhe dobijen je kultivacijom kombuhe na

crnom čaju (1,5 g/L) zaslađenom sa saharozom koncentracije 70 g/L. U čaj ohlađen na sobnu temperaturu dodato je 10 % (v/v) inokuluma iz prethodne fermentacije. Inkubacija je vršena na sobnoj temperaturi $25\pm1^{\circ}\text{C}$, 7 dana. Za inokulaciju mleka korišćeno je 10 % (v/v) ovako pripremljenog inokuluma kombuhe ($\text{pH}=3,21$). Jogurtna i probiotska kultura je dodata prema proizvođačkoj specifikaciji u količini 0,005 g/100 g. Proces fermentacije je izveden na 42°C do postizanja pH vrednosti 4,6. Potom su uzorci ohlađeni na 4°C , homogenizovani mešanjem i pakovani u odgovarajuću ambalažu. Tokom procesa fermentacije uzimani su uzorci za analizu pri sledećim pH vrednostima: 6,4 (samo kod kombuha fermentisanog mlečnog napitka); 6,0; 5,5; 5,0 i 4,6.

Priprema uzorka za analizu

Priprema uzorka u cilju određivanja sastava masnih kiselina gasnom hromatografijom u kombinaciji sa masenom spektrometrijom obuhvatala je ekstrakciju lipida i derivatizaciju masnih kiselina u metil estre. Ekstrakcija lipida je uz manje modifikacije izvedena u skladu sa dokumentovanom metodom.¹⁶ Mast je iz uzorka (20 cm^3) ekstrahovana dodatkom 40 cm^3 smeše rastvarača metanol:hloroform (1:1, v/v). Smeša je snažno mučkana jedan minut i nakon toga centrifugirana 10 minuta na 3000 o/min. Donja faza koja sadrži lipidnu frakciju je odvojena i uparena do suva strujom azota. Priprema metil estara je izvedena uz neznatne modifikacije prema dokumentovanoj metodi.¹⁷ Prethodno ekstrahovana mast iz uzorka je rastvorena u $2,4 \text{ cm}^3$ heksana. Dodato je $0,6 \text{ cm}^3$ rastvora kalijum-hidroksida u metanolu koncentracije 2 mol dm^{-3} . Epruveta je zavorena i intenzivno mučkana 20 sekundi, nakon čega je ostavljena jedan minut u vodenom kupatilu na 70°C . Nakon 20 sekundi mučkanja dodato je $1,2 \text{ cm}^3$ hlorovodonične kiseline (1 mol dm^{-3}). Nakon završetka fazne separacije, gornja faza koja sadrži metil estre masnih kiselina je dekantovana i korišćena za dalju analizu.

Gasno hromatografska – maseno spektrometrijska analiza

Za analizu metil estra masnih kiselina korišćen je gasni hromatograf 7890B sa maseno spektrometrijskim detektorom 5977A i autosemplerom 7693 (Agilent Technologies). Razdvajanje metil estara masnih kiselina izvedeno je primenom kapilarne kolone DB-23 ($60 \text{ m} \times 0,25 \text{ mm}; 0,25 \mu\text{m}$). Kao gas nosač korišćen je helijum sa konstantnim protokom od $1,2052 \text{ cm}^3/\text{min}$. Analize su izvedene primenom sledećeg temperaturnog programa: početna temperatura kolone od 50°C održavana je 1 minut, nakon čega je sledio porast temperature brzinom od $25^{\circ}\text{C}/\text{min}$ do temperature od 175°C , te potom brzinom od $4^{\circ}\text{C}/\text{min}$ do konačne temperature od 235°C , koja je održavana 5 minuta. Temperatura injektora iznosila je 250°C , zapremina uzorka $1,0 \mu\text{L}$, a odnos razdeljivanja 50:1. Maseni spektri su snimani SCAN tehnikom u intervalu m/z 50-400 a.m.u. Kvalitativno određivanje izvedeno je na osnovu masenih spektara i retencionih vremena, a kvantitativno u skladu sa AOAC (963.22) metodom¹⁸ pri čemu je za definisanje korekcionih faktora korišćen standardni rastvor smeše 37 metil estara masnih kiselina (37 component FAME Mix, 47885-U, Supelco).

Rezultati i diskusija

Sastav masnih kiselina u mleku i uzorcima jogurta, probiotskog jogurta i mlečnog napitka sa kombuhom tokom procesa fermentacije, uzimanim pri različitim vrednostima pH dat je u tabeli 1. Dominantne masne kiseline u svim fermentisanim mlečnim proizvodima bile su: palmitinska, oleinska, stearinska i miristinska (Tabela 1). Pokazalo se da je tokom fermentacije palmitinska kiselina dominantna zasićena masna kiselina sa prosečnim sadržajem od 31,73 % u jogurtu, 32,70 % u probiotskom jogurtu, i 33,28 % u kombuha fermentisanom mlečnom napitku. Palmitinska kiselina je najzastupljenija zasićena masna kiselina u mleku i najčešći je uzročnik povećanja nivoa holesterola u krvi dok oleinska kiselina ima pozitivan uticaj na ljudsko zdravlje. Oleinska kiselina je bila najzastupljenija nezasićena masna kiselina u svim fermentisanim mlečnim proizvodima sa prosečnim sadržajima od 27,30% (jogurt), 26,89% (probiotski jogurt) i 25,80 % (kombuha fermentisani mlečni napitak). Dobijeni rezultati su u skladu sa istraživanjem koje su sproveli Serafeimidou i sar.¹⁹ primenom jogurtne starter kulture na različitim vrstama mleka.

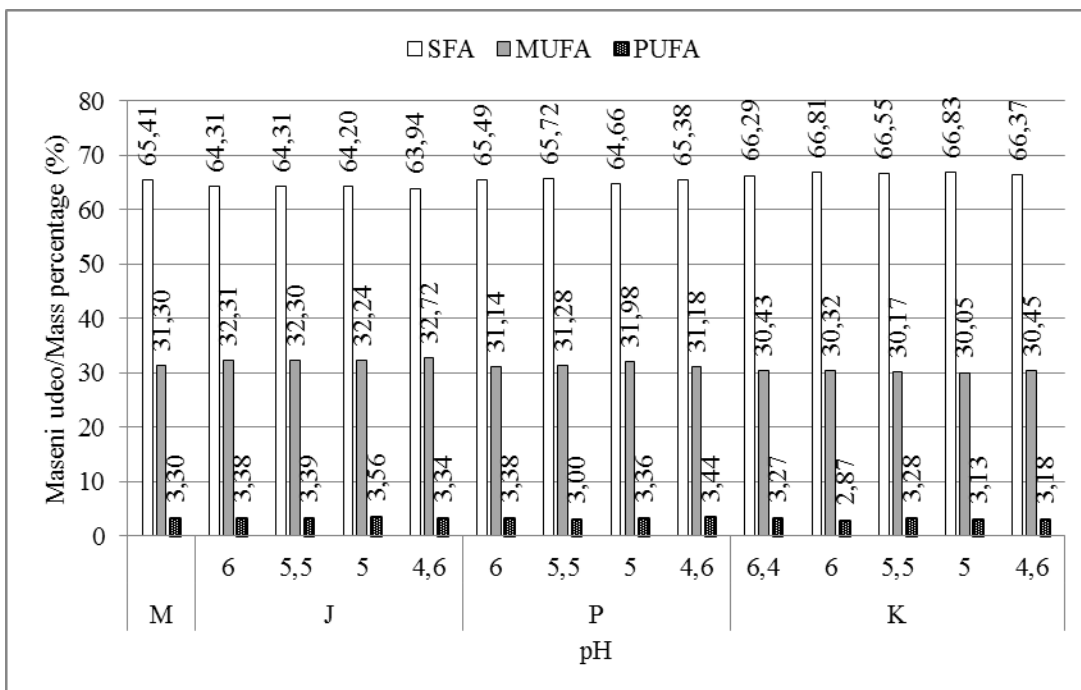
Tabela 1. Sastav masnih kiselina u mleku i uzorcima jogurta, probiotskog jogurta i mlečnog napitka sa kombuhom tokom fermentacije

Starter kultura	Jogurtna				Ptobiotska				Kombuha				Mleko	
pH	6.0	5.5	5.0	4.6	6.0	5.5	5.0	4.6	6.4	6.0	5.5	5.0	4.6	
Masna kiselina	Maseni udeo, %													
4:0	0.83	0.93	1.22	0.88	1.14	0.78	1.05	1.07	1.25	0.70	1.03	0.94	1.22	1.18
6:0	0.91	0.97	1.11	0.87	1.04	0.90	1.01	1.00	1.17	0.82	1.07	0.97	1.11	1.04
8:0	0.71	0.73	0.81	0.65	0.78	0.72	0.76	0.76	0.84	0.67	0.78	0.71	0.78	0.74
10:0	2.03	2.07	2.19	1.96	2.18	2.12	2.17	2.18	2.30	2.06	2.21	2.13	2.22	2.12
12:0	2.71	2.71	2.83	2.62	2.89	2.86	2.83	2.81	2.99	2.84	2.90	2.80	2.89	2.79
14:0	10.58	10.57	10.59	10.44	10.81	10.96	10.57	10.79	11.11	11.06	10.81	11.00	10.88	10.80
14:1	0.78	0.79	0.83	0.69	0.78	0.76	0.77	0.73	0.80	0.76	0.80	0.70	0.74	0.75
15:0 iso	0.18	0.18	0.18	0.15	0.18	0.17	0.18	0.16	0.18	0.18	0.19	0.17	0.18	0.17
15:0 aiso	0.39	0.40	0.40	0.34	0.39	0.39	0.38	0.36	0.40	0.40	0.41	0.37	0.39	0.36
15:0	1.13	1.13	1.16	1.07	1.13	1.13	1.10	1.08	1.14	1.17	1.16	1.05	1.14	1.12
16:0 iso	0.20	0.22	0.22	0.18	0.19	0.20	0.21	0.19	0.20	0.22	0.22	0.19	0.21	0.19
16:0	32.15	31.93	30.81	32.05	32.52	33.00	32.35	32.94	32.34	33.85	33.28	33.89	33.01	32.63
16:1	1.52	1.52	1.65	1.39	1.54	1.52	1.52	1.48	1.53	1.49	1.53	1.45	1.45	1.46
17:0 iso	0.26	0.20	0.26	0.26	0.21	0.34	0.26	0.28	0.26	0.23	0.28	0.26	0.22	0.23
17:0 aiso	0.38	0.37	0.40	0.32	0.38	0.38	0.37	0.35	0.37	0.39	0.38	0.34	0.37	0.35
17:0	0.64	0.63	0.67	0.55	0.65	0.60	0.61	0.58	0.61	0.62	0.64	0.60	0.60	0.59
17:1	0.22	0.21	0.23	0.16			0.20	0.17	0.20			0.16		
18:0	11.21	11.11	11.21	11.43	11.01	11.17	10.82	10.67	10.94	11.60	11.03	11.24	11.15	11.11
18:1t	2.54	2.55	2.63	2.40	2.17	2.15	2.20	2.05	2.16	2.24	2.26	2.07	2.13	2.44
18:1c	27.24	27.22	26.77	27.95	26.65	26.86	27.29	26.75	25.75	25.84	25.59	25.66	26.13	26.65
18:2c	3.00	3.05	3.17	2.99	3.03	3.00	3.00	3.03	2.92	2.87	2.94	2.81	2.86	2.94
18:3n3	0.37	0.35	0.39	0.35	0.34		0.36	0.41	0.35		0.33	0.32	0.32	0.36
20:0		0.16	0.15	0.16				0.19	0.17		0.16	0.17		

Udeo zasićenih (saturated fatty acids - SFA), mononezasićenih (monounsaturated fatty acids - MUFA) i polinezasićenih masnih kiselina (polyunsaturated fatty acids - PUFA) tokom fermentacije mleka tradicionalnom jogurtnom kulturom kretao se u intervalima od 63,94-64,31 %; 32,24-32,72 % i 3,34-3,56%, redom. Pri korišćenju probiotske kulture sadržaj SFA, MUFA i PUFA je iznosio 64,66-65,72 %; 31,14-31,98 % i 3,00-3,44 %, respektivno. Korišćenjem kombuhe kultivisane na crnom čaju za proizvodnju fermentisanih mlečnih napitaka procenat SFA, MUFA i PUFA kretao se u intervalima od 66,29-66,83%; 30,05-30,45 % i 2,87-3,28 %, redom (Slika 1). Ove vrednosti se nalaze u intervalima vrednosti koje su dobijene za mlečne napike proizvedene fermentacijom kravljeg mleka pomoću kombuhe kultivisane na čaju koprive i mente.^{5,20} Naime, sadržaj zasićenih masnih kiselina u tim uzorcima se kretao u opsegu 62,86-70,42 %, mononezasićenih 27,85-32,62 % i polinezasićenih 1,56-4,25 %.

Na slici 1 se može uočiti da se najpovoljniji masno-kiselinski sastav sa najnižim sadržajem zasićenih i najvišim sadržajem mononezasićenih i polinezasićenih masnih kiselina postiže primenom tradicionalne jogurtne kulture. Takođe, tokom procesa fermentacije, pad vrednosti pH je u slučaju jogurta praćen povoljnim blagim padom vrednosti SFA, i porastom MUFA, do maksimalnih vrednosti pri vrednosti pH od 4,6. Maksimalni sadržaj PUFA se postiže na pH 5,0. Kod probiotskog jogurta se pak najniži sadržaj SFA i najviši sadržaj MUFA postiže pri vrednosti pH 5,0, dok je udeo PUFA najveći pri 4,6. U slučaju primene nekonvencionalne starter kulture, kombuhe, najpovoljniji sadržaj SFA se postiže na samom početku fermentacije (pH 6,4), maksimalni sadržaj MUFA na kraju fermentacije (pH 4,6), a najviši

sadržaj PUFA pri pH 6,0. Udeo SFA u fermentisanim mlečnim proizvodima proizvedenim primenom konvencionalnih starter kultura (jogurtnom i probiotiskom) je manji, a MUFA i PUFA je jednak ili veći u poređenju sa uzorkom mleka iz kog su proizvedeni. Sa druge strane, u slučaju primene kombuhe, sadržaj SFA je porastao, dok su se sadržaji MUFA i PUFA smanjili u poređenju sa uzorkom mleka. Do sličnih rezultata su došli Vitas i sar.⁵ prilikom ispitivanja sastav masnih kiselina u fermentisanim mlečnim napicima dobijenim primenom kombuhe prethodno kultivisane na rtanjskom čaju, što ukazuje da vrsta čaja za inokulaciju ne utiče značajno na sastav masnih kiselina u kombuha fermentisanim mlečnim napicima.



Slika 1. Sadržaj zasićenih (SFA), mononezasićenih (MUFA) i polinezasićenih masnih kiselina (PUFA) u kontrolnom uzorku mleka (M) i uzorcima mlečnih napitaka tokom fermentacije jogurtnom (J), probiotiskom (P) i kombuha (K) starter kulturom

Zaključci

Tokom fermentacije mleka primenom nekonvencionalne starter kulture, kombuhe, i konvencionalnih starter kultura, jogurtne i probiotske nije došlo do značajnijih promena u pogledu sadržaja masnih kiselina. Tokom fermentacije u svim fermentisanim mlečnim napicima dominantna zasićena masna kiselina je bila palmitinska kiselina, dok je oleinska kiselina bila najzastupljenija nezasićena masna kiselina. Najpovoljniji sastav masnih kiselina, sa najnižim sadržajem zasićenih i najvišim sadržajem mononezasićenih i polinezasićenih masnih kiselina, dobijen je u napitcima fermentisanim primenom tradicionalne jogurtne kulture.

Zahvalnica: Istraživanja predstavljena u ovom radu finansirana su od strane Ministarstva prosvete i nauke Republike Srbije (projekat br. III 46009).

Determination of fatty acids during the fermentation of milk by kombucha and conventional starter cultures

Fermented milk products are very important component of the daily diet primarily because of their high nutritional value and beneficial health effects. The health aspect of fermented milk beverages depends on the fatty acid composition of milk fat, as one of the most important components of those products. In order to investigate the influence of starter cultures on the fatty acid composition of fermented milk products, in this work the fatty acid composition during the fermentation of milk using non-conventional starter culture, kombucha, and conventional starter cultures or probiotic yoghurt was monitored. For fermentation a milk

with 2.8% fat was used, at a temperature of 42 °C. Fatty acid analysis was performed using capillary gas chromatography in combination with a quadrupole mass spectrometry after previous extraction and derivatization steps. The dominant fatty acid in fermented dairy products were: palmitic, oleic, stearic and myristic acids in content of 32.62; 26.59; 11.12 and 10.78 %, respectively. The most favourable fatty acid composition, with the lowest content of saturated and the highest content of monounsaturated and polyunsaturated fatty acids, was derived from the fermented beverage using the traditional yoghurt cultures.

Literatura

1. A.Y. Tamime, R.K. Robinson, *Yoghurt. Science and Technology*, Woodhead Publishing Limited, Cambridge, England, 2004, p. 619
2. G. Beloso-Morales, H. Hernández-Sánchez, H. *Revista Latinoamericana de Microbiología* **45** (2003) 5
3. R. Malbaša, S. Milanović, E. Lončar, M. Đurić, M. Carić, M. Iličić, Lj. Kolarov, *Food Chem.* **112** (2009) 178
4. R. Malbaša, J. Vitas, E. Lončar, S. Kravić, *Acta Period. Technol.* **42** (2011) 81
5. J. Vitas, R. Malbaša, E. Lončar, S. Kravić, S. Milanović, *Prehrambena ind. – Mleko i mlečni proizvodi*, **22** (2011) 25
6. S. Milanović (1997): Jugoslovenski mlekarski simpozijum-Kvalitet mleka i fermentisanih proizvoda, Zlatibor, Srbija, p. 49
7. C. Cifelli, J. German, J. O'Donnell (2011). Nutrition and Health | Nutritional and Health-Promoting Properties of Dairy Products: Contribution of Dairy Foods to Nutrient Intake. Encyclopedia of Dairy Sciences (Second Edition). J. W. Fuquay. Academic Press, San Diego, USA, 2011, p. 1003
8. A.L. Lock, K.J. Shingfield, *Optimising milk composition. In: Dairying—Using Science to Meet Consumers' Needs*, E. Kebreab, J. Mills, D.E. Beever (eds.), Nottingham University Press, Loughborough, UK, 2004, p 107
9. K. He, Y. Xu, L. Van Horn, L. J. Am. Diet. Assoc. **107** (2007) 287
10. E.B. Feldman, *Am. J. Clin. Nutr.* **70** (1999) 953
11. P. Kankaanpää, S. Salminen, E. Isolauri, Y. Lee, *FEMS Microbiol. Lett.* **194** (2001) 149
12. U. Das, M. Fams, *Nutrition* **18** (2002) 786
13. H. Yadav, J. Shalini, P. Sinha, *Int. Dairy J.* **17** (2007) 1006
14. F. Ekinci, O. Okur, B. Ertekin, Z. Guzel-Seydim, *Eur. J. Lipid Sci. Technol.* **110** (2008) 216
15. K. Kanurić, Promene komponenata i strukture mleka tokom fermentacije dodatkom nekonvencionalnog startera, Doktorska disertacija, Tehnološki fakultet Novi Sad, 2014.
16. M. Havemose, M. Weisbjerg, W. Bredie, J. Neilsen, *Int. Dairy J.* **14** (2004) 563
17. S. Kravić, Određivanje trans masnih kiselina u prehrambenim proizvodima gasnom hromatografijom-masenom spektrometrijom, Doktorska disertacija, Univerzitet u Novom Sadu, Tehnološki fakultet, Novi Sad, 2010
18. AOAC, Official Method 963.22, Methyl Esters of Fatty Acids in Oils and Fats, Published by AOAC, Washington, 2000
19. A. Serafeimidou, S. Zlatanos, G. Kritikos, A. Tourianis, *J. Food Compos. Anal.* **31**(2013) 24
20. T. Brezo, S. Kravić, Z. Suturović, A. Karišik-Đurović, J. Vitas, R. Malbaša, S. Milanović, (2011). Influence of kombucha inoculum on the fatty acidcomposition of fermented milk products. *Prehrambena ind. – Mleko i mlečni proizvodi* **22** (2011) 21

Sadržaj sekundarnih metabolita i njihov uticaj na antioksidativnu aktivnost u različitim sortama jagoda

Zoran Kukrić, Iva Martić*, Ladislav Vasilišin, Goran Vučić

Univerzitet u Banjoj Luci, Tehnološki fakultet Banja Luka, Bosna i Hercegovina

**Univerzitet u Banjoj Luci, Prirodnomatematički fakultet Banja Luka, Bosna i Hercegovina*

Uvod

Jagoda (*Fragaria ananassa*) koja spada u familiju Rosaceae, je višegodišnja zeljasta, grmolika biljna vrsta koja radi svog jedinstvenog okusa i mirisa zauzima vodeće mjesto među ljetnim voćnim vrstama.¹ U posljednjih nekoliko godina proizvodnja jagoda bilježi vrlo značajan porast u svijetu, a bilježi određeni napredak i u Bosni i Hercegovini. Ova biljna vrsta ima širok spektar klimatskog prilagođavanja koji obuhvata mediteransku, umjerenu i suptropsku klimu.² Jagode su karakteristične po specifičnom ukusu i aromi, veoma su bogate bioaktivnim jedinjenjima koje doprinose zdravlju a takođe su veoma interesantne za farmaceutsku, prehrambenu i kozmetičku industriju. Takođe, veliki broj studija govori o uspostavljanju mehanizma za povećanje sinteze polifenolnih jedinjenja u jagodama prilikom njihovog gajenja. Njihov sadržaj varira među vrstama i sortama, ali na tu raznolikost mogu da utiču i drugi faktori kao što su uslovi rasta, faktori životne sredine i tehnike gajenja.³ Nekoliko studija je pokazalo da jagode generalno posjeduju visok nivo antioksidativne aktivnosti, koji je povezan sa sadržajem ukupnih fenola i antocijana u plodu.⁴⁻⁷ Primjera radi, u literaturi je poznato^{6,7} da sok jagoda pokazuje visok stepen antioksidativnog kapaciteta prema slobodnim radikalima, uključujući superoksid radikal, vodonik-peroksid, hidroksil radikal i singlet kiseonik, a također je potvrđeno da postotak inhibicije svake aktivne vrsta kiseonika varira između različitih sorti jagoda, što je sve bilo povezano sa sadržajem bioaktivnih jedinjenja u jagodama.⁵ Cilj ovog rada je bio ocjena i poređenje nekih biokemijskih i bioaktivnih sadržaja u divljim i kultiviranim plodovima jagode kao i procjena njihovog uticaja na antioksidativnu aktivnost jagoda.

Prikupljanje uzoraka

U radu su korišćene četiri sorte gajenih jagoda (*Fragaria ananassa*) (Albion, Senga Sengana, Elsanta i Cleary) i jedna divlja jagoda (*Fragaria vesca* L.) – u daljem tekstu označena kao "Šumska". Sorta Albion i Šumska jagoda prikupljene su u okolini Travnika (srednja Bosna i Hercegovina) a ostale sorte iz okoline Velike Kladuše (zapadna Bosna i Hercegovina). Voće je ubrano pri punoj zrelosti na početku sezone branja jagoda – krajem maja mjeseca 2015 godine. Masa od 500 g je uzeta slučajnim izborom za svaku sortu, i voće je analizirano odmah nakon uzimanja uzorka.

Priprema uzorka

Uzorak se usitni, odvaže 5 ± 0.001 g i kvantitativno prenese u erlenmajericu sa 20 mL 80 %-tnog v:v etanola. Nakon toga tikvica sa uzorkom je stavljena u ultrazvučnu kadu (50Hz) (dva puta po pet minuta), a zatim je spojena na povratno hladilo i ekstrakcija je trajala 10 minuta od trenutka ključanja. Nakon hlađenja na sobnu temperaturu filtrira se u tikvicu (50 mL) a preostali talog je zajedno sa filter papirom vraćen nazad u erlenmajericu uz dodatak 20 mL 80 %-tnog rastvora etanola i ekstrahovan još 10 minuta, ponovo filtriran u tikvicu u kojoj se nalazi prvi filtrat i dopunjeno 80 %-nim rastvorom etanola do oznake. Na ovaj način je dobijen matični rastvor koncentracije 0,1 g/mL koji se koristio za sva ostala određivanja. Za određivanje ukupnih i monomernih antocijana uzorci (20 g) su ekstrahovani sa 20 mL rastvora za ekstrakciju (85 mL 95 %-tnog rastvora etanola i 15 mL 1.5 M rastvora HCL) na temperaturi 0°C u trajanju od 24 sata. Nakon toga, smjesa je filtrirana preko filter papira, a dobijeni filtrat je korišćen za dalju analizu.

Određivanje sadržaja sekundarnih metabolita i antioksidativne aktivnosti

Ukupni fenoli su određeni modifikovanom metodom Folin-Ciocalteu.⁸ Za izradu baždarene krive korištena je galna kiselina ($y=0,003x - 0,0226$; $R^2=0,9975$ gdje je y- apsorpcija a x – koncentracija galne kiseline $\mu\text{g/mL}$). Rezultati su izraženi kao fenoli ekvivalentni galnoj kiselini, tj. $\mu\text{mol GAE/g}_{\text{FW}}$.

Određivanje ukupnih flavonoida vršeno je metodom po Ordon-u.⁹ Ukupni sadržaj flavonoida računati su kao flavonoidi ekvivalenti kvercetinu ($\mu\text{mol Q}_c / \text{g}_{\text{FW}}$) koristeći jednačinu baždarnog pravca ($y=0,0368x - 0,135$; $R^2=0,9996$), gdje je y-apsorpcija a x – koncentracija kvercetina $\mu\text{g/mL}$). Rezultati su izraženi kao μmol kvercetina (Q_c)/ g_{FW} . Određivanje ukupnih flavonola je vršeno metodom po Kumaran-u i Karunakaran-u.¹⁰ Za izradu baždarenih kriva je korišćen takođe kvercetin hidrat i dobijena je jednačina pravca ($y=0,0214x+0,004$; $R^2=0,9993$), gdje je y-apsorpcija a x– koncentracija kvercetina $\mu\text{g/mL}$). Rezultati su izraženi kao μmol kvercetina (Q_c)/ g_{FW} .

Sadržaj ukupnih i monomernih antocijana u uzorcima je određen spektrofotometrijski, modifikovanom "singl" pH i pH diferencijalnom metodom.⁶ Rezultati su izraženi kao $\text{mg cijanidin-3-glukozida}/100\text{g}_{\text{FW}}$. Izračunat je i indeks degradacije po obrascu $ID = \frac{c_{\text{ukupni antocijani}}}{c_{\text{monomerni antocijani}}}$. Efekat uzorka na DPPH radikal određen je metodom Liyana-Pathiranan i Shahidi¹¹ a za ABTS test korišćena je modifikovana metoda Re i saradnika.¹² Za izradu baždarenih pravaca je korišćen Trolox. Za DPPH test jednačina za baždarni pravac Trolox-a je iznosila

$$y = 7,0993x - 0,434 \quad R^2 = 0,9722 \text{ a za ABTS test } y = 15,94x + 10,527 \quad R^2 = 0,9984.$$

Rezultati su predstavljeni TEAC vrijednošću (Trolox ekvivalent antioksidativne aktivnosti), tj. kao μmol Trolox-a/ g_{FW} . Eksperimenti su rađeni u 3 paralelna ponavljanja, a rezultati su izraženi kao srednja vrijednost \pm standardna devijacija. Korišćena je analiza varianse (ANOVA) a najmanja značajna razlika (LSD) pri $p<0,05$ je izračunata korištenjem programa Origin Pro 8.0. Koeficijent korelacije je određen prema Pearson-u.

Rezultati i diskusija

U tabeli 1 predstavljeni su rezultati mjerena sadržaja sekundarnih metabolita i antioksidativna aktivnost sorti jagoda Albion, Šumska, Elsanta, Senga Sengana i Cleary.

Sadržaj fenola u uzorcima se kretao od 2,52 do 7,3 $\mu\text{mol GEA/g}_{\text{FW}}$ (442 – 1242 $\mu\text{g GEA/g}_{\text{FW}}$), s tim što je u sortama Elsanta, Senga Sengana i Cleary količina ukupnih fenola približna i statistički značajno niža nego u sortama Albion i Šumska .

Tabela 1. Sadržaj sekundarnih metabolita i antioksidativna aktivnost različitih sorti jagode

Određivani parametri	Sorta jagoda				
	Albion	Šumska	Elsanta	Senga Sengana	Cleary
Fenoli, $\mu\text{mol GEA/g}_{\text{FW}}$	$7,30^{*\text{a}} \pm 0,52$	$6,68^{\text{a}} \pm 0,51$	$2,99^{\text{b}} \pm 0,38$	$2,59^{\text{b}} \pm 0,24$	$2,52^{\text{b}} \pm 0,25$
Flavonoidi, $\mu\text{mol Q}_c/\text{g}_{\text{FW}}$	$0,75^{\text{a}} \pm 0,06$	$1,11^{\text{b}} \pm 0,06$	$0,58^{\text{c}} \pm 0,03$	$0,75^{\text{a}} \pm 0,01$	$0,62^{\text{c}} \pm 0,01$
Flavonoli, $\mu\text{mol Q}_c/\text{g}_{\text{FW}}$	$1,14^{\text{a}} \pm 0,16$	$1,24^{\text{a}} \pm 0,02$	$0,66^{\text{b}} \pm 0,10$	$0,67^{\text{b}} \pm 0,03$	$0,61^{\text{b}} \pm 0,14$
Antocijani ukupni, $\text{mg}/100\text{g}_{\text{FW}}$	$14,62^{\text{a}} \pm 1,03$	$15,25^{\text{a}} \pm 1,13$	$14,74^{\text{a}} \pm 0,91$	$23,88^{\text{b}} \pm 2,52$	$8,47^{\text{c}} \pm 0,67$
Antocijani monomerni, $\text{mg}/100\text{g}_{\text{FW}}$	$10,31^{\text{a}} \pm 0,78$	$10,39^{\text{a}} \pm 0,62$	$11,74^{\text{a}} \pm 0,98$	$19,14^{\text{b}} \pm 1,43$	$6,25^{\text{c}} \pm 0,72$
ID	$1,42^{\text{a}} \pm 0,01$	$1,47^{\text{a}} \pm 0,06$	$1,25^{\text{b}} \pm 0,03$	$1,24^{\text{b}} \pm 0,06$	$1,35^{\text{a,b}} \pm 0,05$
DPPH, $\mu\text{mol Trolox/g}_{\text{FW}}$	$44,96^{\text{a}} \pm 6,24$	$40,56^{\text{a}} \pm 2,72$	$15,46^{\text{b}} \pm 1,06$	$9,3^{\text{b}} \pm 1,02$	$9,68^{\text{b}} \pm 1,69$
ABTS, $\mu\text{mol Trolox/g}_{\text{FW}}$	$38,74^{\text{a}} \pm 8,37$	$46,46^{\text{a}} \pm 0,42$	$27,76^{\text{b}} \pm 0,16$	$19,49^{\text{b}} \pm 1,48$	$23,26^{\text{b}} \pm 3,14$

* srednje vrijednosti \pm standardna devijacija tri nezavisna mjerena; različita slova u superskriptu označavaju statistički značajnu razliku uz nivo pouzdanosti od 95%, Fw -svježa masa (fresh weight)

Ovi rezultati su bili u skladu sa literaturnim podacima za određivanje ukupnih fenola za različite sorte jagoda koji su se kretali od 96 mg/100 gFW do 133 mg/100 gFW.¹³ S druge strane, naši rezultati su bili nešto niži od rezultata nekih drugih istraživača^{14,15} koji govore o sadržaju ukupnih fenola različitih sorti koje rastu u različitim zemljama i čije se vrijednosti kreću od 96 do 223 mg GAE / 100 gFW.

Sadržaj flavonoida u uzorcima se kretao od 0,58 do 1,11 $\mu\text{mol Q}_c/\text{g}_{\text{FW}}$.(176 – 335 $\mu\text{g Q}_c/\text{g}_{\text{FW}}$). Sorte Albion i Senga Sengana su imale statistički niži sadržaj flavonoida od Šumske jagode a veći sadržaj od sorti Elsanta i Cleary. Ove vrijednosti su bile u skladu sa literaturnim podacima.^{14,16}

Određen je sadržaj flavonola i kretao se od 0,61 do 1,24 $\mu\text{mol Q}_c/\text{g}_{\text{FW}}$.(176 – 335 $\mu\text{g Q}_c/\text{g}_{\text{FW}}$) s tim što je količina flavonola, kao i kod fenola, u sortama Elsanta, Senga Sengana i Cleary približna i statistički značajno niža nego u sortama Albion i Šumska. Sadržaj flavonola je bio nešto malo niži od vrijednosti koje navodi Lal¹⁷ za različite sorte. Sadržaj ukupnih antocijana se kretao u rasponu od 8,47 do 23,88 mg/100g_{Fw}, dok je sadržaj monomernih antocijana u rasponu od 6,25 do 19,14 mg/100g_{Fw}. Najveći

sadržaj ukupnih antocijana i monomernih antocijana je imala sorta Senga Sengana a najmanji sorta Cleary. Sadržaj ukupnih i monomernih antocijana je bio unutar literaturnih vrijednosti.^{14,18-20} Na određene razlike u sadržaju ukupnih fenola, flavonoida, flavonola i antocijana zavisno od sorte, načina uzgoja, nivoa zrelosti kod berbe klimatskih uslova i geografskih lokacija ukazao je Milivojević.³

U tabeli 1 prikazana je i antioksidativna aktivnost različitih vrsta jagoda prema stabilnim DPPH i ABTS radikalima. Vrijednosti antioksidativne aktivnosti prema DPPH radikalu kretala se od 9,3 do 44,96 $\mu\text{molTrolox/g}_{\text{FW}}$ s tim što je najveću antioksidativnu aktivnost pokazala sorta Albion a najnižu vrijednost sorta Senga Sengana, pri čemu sorte Elsanta, Senga Sengana i Cleary imaju antioksidativna aktivnost približno jednaku i statistički značajno nižu nego sorte Albion i Šumska. Vrijednosti za antioksidativnu aktivnost su bile nešto veće ili jednake literaturnim i to: 3,53-4,42¹⁴; 6,11²¹; 9,7²²; 7,94-11,38²³; 10,1-12,83¹⁵ and 8,29-11,15²⁴ $\mu\text{molTrolox/kg}_{\text{FW}}$. Prema ABTS radikalu vrijednosti za antioksidativnu aktivnost su bile u rasponu od 19,49 do 46,46 $\mu\text{molTrolox/g}_{\text{FW}}$ pri čemu je najveću aktivnost pokazala Šumska jagoda a najnižu Senga Sengana. Takođe rezultati pokazuju da sorte Elsanta, Senga Sengana i Cleary imaju antioksidativna aktivnost prema ABTS stabilnom radikalu približno jednaku i statistički značajno nižu nego sorte Albion i Šumska.

Kao i kod DPPH radikala i vrijednosti za antioksidativnu aktivnosti prema stabilnom ABTS radikalu su bile nešto veće ili jednake literaturnim: 9,70²²; 12,0821²¹ and 26,92-30,06²⁴ $\mu\text{molTroloxa/kg}_{\text{FW}}$. Ove vrijednosti za antioksidativno djelovanje prema DPPH i ABTS radikalu su, kao što je navedeno, većinom u skladu ili su nešto veće od literaturnih vrijednosti. Međutim, čak i kada postoje dobri eksperimentalni dokazi, rezultate treba tumačiti s oprezom u odnosu na doprinos ljudskom zdravlju, jer polifenoli mogu imati ograničenu bioraspoloživost i znatno se međusobno razlikuju.

Takođe, najviše zastupljeni polifenoli nisu nužno oni koji imaju najbolji bioraspoloživi profil, jer ili imaju niže stvarno djelovanje ili se slabo apsorbuju iz crijeva ili se brzo otklanjaju iz organizma. Koeficijenti korelacije koji ukazuju na međusobne odnose sekundarnih metabolita u različitim vrstama jagoda i antioksidativnih testova (sadržaj ukupnih fenola, ukupnih flavonoida, ukupnih flavonola, ukupnih i monomernih antocijana, DPPH i ABTS vrijednosti) prikazani su u tabeli 2. Što se tiče aktivnosti na DPPH radikal, može se vidjeti da postoji vrlo visoka korelacija sa sadržajem sekundarnih metabolita u jagodama.

Tabela 2. Koeficijenti korelacije sadržaja sekundarnih metabolita i antioksidativnih testova u različitim vrstama jagoda

	Fenoli	Flavonoidi	Flavonoli	Antocijani ukupni	Antocijani monomerni	ID	DPPH	ABTS
Fenoli	1	0,659	0,975	-0,076	-0,23	0,849	0,998	0,933
Flavonoidi		1	0,808	0,209	0,06	0,711	0,654	0,759
Flavonoli			1	-0,003	-0,166	0,869	0,936	0,943
Antocijani ukupni				1	0,986	-0,42	-0,101	-0,204
Antocijani monomerni					1	-0,564	-0,25	-0,353
ID						1	0,844	0,881
DPPH							1	0,932
ABTS								1

Vrlo visoku vrijednost koreacionog koeficijenta, i neznatno različitu, pokazali su ukupni fenoli i flavanoli, $r=0,998$ i $r=0,936$, redom, dok su flavonoidi imali znatno niže vrijednosti $r=0,654$. Vrijednosti za ukupne i monomerne antocijane bile su malene i negativne, $-0,101$ i $-0,25$ redom. Međutim, nađena je visoka korelacija sa indeksom degradacije antocijana, odnosno sa vrijednošću ID i iznosila je $r=0,844$ p. Takođe, postoji vrlo visoka korelacija ovih jedinjenja na aktivnost prema stabilnom ABTS radikalu. Ponovo najveću korelaciju pokazuju flavonoli i ukupni fenoli $r=0,943$ i $r=0,933$, redom, pa flavonoidi $r=0,759$, dok ukupni i monomerni antocijani imaju male i negativne koeficijente korelacije i to $r=-0,101$ i $r=-0,25$ redom. Takođe i ovdje je nađena vrlo visoka korelacija između antioksidativne aktivnosti prema ABTS radikalu i indeksa degradacije antocijana i iznosila je $r=0,881$. Visoka pozitivna korelacija između ukupnih fenola i ukupnog antioksidativnog djelovanja (DPPH, ABTS) je u skladu sa literaturnim podacima.^{17,23}

Ovi rezultati upućuju na zaključak da je antioksidativna aktivnost više povezana s ukupnim sadržajem fenola i flavonola nego s ukupnim sadržajem flavonoida i antocijana. Ovi rezultati su u skladu s drugim istraživanjima.²⁵ Takođe, kada govorimo o antocijanima i njihovom uticaju na antioksidativnu aktivnost

rezultati ukazuju da moramo uzeti u obzir odnos ukupnih i monomernih antocijana odnosno indeks degradacije, a ne ukupne sadržaje ovih spojeva.

Nadalje visoka korelacija između DPPH i ABTS i ukupnog sadržaja fenola može se pripisati činjenici da oba ispitivanja oslanjaju na isti reakcijski mehanizam. Očito je da doprinos za ove antioksidativne aktivnosti ne možemo pripisati samo jednom biološki aktivnom jedinjenju, već je ova aktivnost najvjerojatnije, rezultat zajedničkog djelovanja prisutnih biološki aktivnih jedinjenja.

Zaključak

Naši rezultati pokazuju da postoji značajna razlika u sadržaju sekundarnih metabolita odnosno biološki aktivnih spojeva kao i u antioksidativnoj aktivnosti u različitim sortama jagoda. Takođe pronađene su visoke pozitivne korelacije između antioksidativne aktivnosti i sadržaja ukupnih fenola, flavonola i flavonoida. Praktična korist visokih pozitivnih korelacija može, eventualno, biti od pomoći u uzgoju za daljnje poboljšanje kultivara koji su deficitarni sa bioaktivnim spojevima.

The content of secondary metabolites and their impact on the antioxidant activity in different varieties of strawberries

*Contents of secondary metabolites in four different varieties of cultivated strawberries (*Fragaria ananassa*): Albion, Senga Sengana, Elsanta and Cleary, and in a wild strawberry (*Fragaria vesca L.*) were determined. At the same time the antioxidant activities according to the stable free radical DPPH and ABTS were determined. The results showed a statistically significant difference in the content of secondary metabolites and the antioxidant activity among different varieties of strawberries and that this activity was mostly influenced by the content of total phenols and total flavonols.*

Literatura:

1. C. Pelayo, S.E. Ebeler, A.A. Kader, *Postharvest Biol. Tec.* **27** (2003) 171
2. J.F. Hancock, J.L. Mass, C.H. Shanks, P.J. Breen, J.J. Luby, Strawberries (*Fragaria*), *Acta Hortic.* **290** (1991) 491.
3. J. Milivojević, V. Maksimović, M. Nikolić, J. Bogdanović, R. Maletić, D. Milatović, *J. Food Qual.* **34** (2011) 1
4. R. Azodanlou, C. Darbellay, J.L. Luisier, J.C. Villettaz, R. Amado, *J. Agric. Food Chem.* **51** (2003) 715
5. S. Tulipani, B. Mezzetti, F. Capocasa, S. Bompadre, J. Beekuilde, C.H. Ric de Vos, E. Capanoglu, A. Bovy, M. Battino, *J. Agric. Food Chem.* **56** (2008) 696
6. J. Sun, Y.F. Chu, X. Wu, R.H. Liu, *J. Agric. Food Chem.* **50** (2002) 7449
7. J.A. Vinson, X. Su, L. Zubik, P. Bose, *J. Agric. Food Chem.* **49** (2001) 5315
8. K. Wolfe, X. Wu, R.H. Liu, *J. Agric. Food Chem.* **51** (3) (2003) 609
9. A.A.L. Ordoñez, J.D. Gomez, M.A. Vattuone, M.I. Isla, *Food Chem.* **97** (3) (2006) 452
10. A. Kumaran, R.J. Karunakaran, *Food Sci. Technol.* **40** (2) (2007) 344
11. C.M. Liyana-Pathirana, F. Shahidi, *J. Agric. Food Chem.* **53** (7) (2005) 2433
12. R.N. Re, A. Pellegrini, A. Proteggente, M. Pannala, C. Yang, R. Evans, *Free Radical Bio. Med.* **26** (9-10) (1999) 1231
13. A.R. Torronen, K. Maatta, *Acta Hort.* **567** (2002) 797
14. S. Voća, N. Dobričević, N. Dragović-Uzelac, B. Duralija, J. Družić, Z. Cmelik, M.S. Babojelić, *Food Technol. Biotechnol.* **46** (3) (2008) 292
15. L.O. Pineli, C.L. Moretti, M.S. Dos Santos, A.B. Campos, A.V. Brasileiro, A.C. Cordova, M.D. Chiarello, *J. Food Comp. Anal.* **24** (2011) 11
16. J.Y. Lin, C.Y. Tang, *Food Chem.* **101** (2007) 140
17. S. Lal, A. Nazeer, R.S. Shyam, B.S. Desh, O.C. Sharma, R. Kumar, *Fruits*, **68** (5) (2013) 423
18. N. Dobričević, S. Voća, J. Š. Žlabur, A. Jakić, S. Pllestić, A. Galić, Kvalitete plodova jagoda sorti 'Alba', 'Albion', 'Asia', 'Clery' i 'Joly' 49th Croatian & 9th International Symposium on Agriculture Dubrovnik Croatia (2014) 662-666.
19. J. Oszmianski, A. Wojdylo, J. Kolniak, *Food Sci. Technol.* **42** (2009) 581
20. C. Pelayo-Zaldivar, S. Ebeler, A.A. Kader, *J. Food Quality*, **28** (2004) 78
21. L. Jakobek, M. Šeruga, I. Novak, M. Medvidović-Kosanović, *Deutsche Lebensmittel-Rundschau*, **103** Jahrgang, Heft 8 (2007).
22. A. Hartmann, C.D. Patz, W. Andlauer, H. Dietrich, M. Ludwig, *J. Agric. Food Chem.* **56** (2008) 9484
23. H. Yildiz, S. Ercisli, A. Hegedus, M. Akbulut, E.F. Topdas, J. Aliman, *J. Appl. Bot. Food Quality*, **87** (2014) 274
24. V. Dragović-Uzelac, B. Levaj, D. Bursać, S. Pedisić, I. Radojičić, A. Biško, *Agric. Conspec. Sci.* **72** (4) (2007).
25. G. Giovanelli, S. Buratti, *Food Chem.* **112** (2009) 903

Hemija i tehnologija makromolekula / Chemistry and Technology of Macromolecules

Comparative analysis of hydrolytic, enzymatic and degradation in compost of PCL/PEO diblock copolymers

Marijana M. Ponjavić, Marija S. Nikolić, Jasmina Nikodinović-Runić*, Sanja Jeremić*,
Sanja Stevanović**, Jasna Djonlagić

Faculty of Technology and Metallurgy, University of Belgrade, Karnegijeva 4, Belgrade, Serbia

*Institute of Molecular Genetics and Genetic Engineering, University of Belgrade,
Vojvode Stepe 444a, Belgrade, Serbia

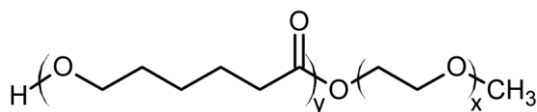
**Institute of Chemistry, Technology and Metallurgy, University of Belgrade, Njegoseva 12, Belgrade, Serbia

Introduction

In the last decades, biodegradable polymers have attracted significant attention due to their potential application in medicine, pharmacy as well as an environmentally friendly materials.¹ Biodegradable polymers can easily be degraded by microorganisms widely distributed in the nature which is the main driving force behind a recycling of biodegradable wastes.² Poly(ϵ -caprolactone) (PCL) is a biocompatible and biodegradable aliphatic polyester. The potential applications of PCL are considerably restrained by its high crystallinity and hydrophobicity. However, biodegradability of PCL can be tuned by copolymerization with hydrophilic poly(ethylene oxide) (PEO). Hydrolytic degradation of PCL is a bulk erosion process which proceeds quite slowly. Faster degradation of PCL can be achieved in the presence of lipase-type enzymes. The degradation of polymers in nature is attributed to a presence of wide range of microorganisms which secrete appropriate enzymes. In a present study, the hydrolytic and enzymatic degradation characteristics of PCL and PCL/PEO copolymers were investigated to get a better insight into the impact of structure on biodegradability. The enzymatic degradation experiments were performed using *Pseudomonas aeruginosa* PAO1 cell-free extracts containing lipases and other enzymes. Degradation ability of PCL/PEO block copolymers in model compost system, using augmentation with *P. aeruginosa* PAO1 cells, was also tested.

Results and discussion

PCL and diblock copolymers were synthesized by bulk ring-opening polymerization of ϵ -caprolactone in the presence of tin(II) octoate as a catalyst.³ Diblock (PCL/PEO) copolymers' structure with specified block lengths is shown in Scheme 1. The m-PEO block length incorporated as a lateral segment was fixed (M_n 1020 g/mol) while the lengths of PCL blocks were varied (in the range of 10000 to 40000 g/mol).



Diblock copolymers: x = 23, PCL/PEO-1 y = 184, PCL/PEO-2 y = 269, PCL/PEO-3 y = 381

Scheme 1. Structure of diblock copolymers with the specified degree of polymerization for each block.

Hydrolytic degradation

The hydrolytic degradation of aliphatic polyesters is a very complex process, which involves diffusion phenomena and chemical changes. Degradation process of PCL and diblock copolymers over 8 weeks was followed by weight loss changes and molecular weight changes, as well as by FTIR analysis (carbonyl index, CI and crystallinity index changes) (Table 1). Homopolymer PCL, is relatively stable against abiotic hydrolysis and even after 8 weeks of degradation, 0.5 wt% was lost. The diblock copolymers showed significant changes in weight after 7 weeks and as was expected, the most hydrophilic diblock copolymer sample (PCL/PEO-1) showed the highest weight loss (11 wt %). Smaller content of PEO segment in diblock copolymers (PCL/PEO-2 and PCL/PEO-3) caused lower degradation

ability (5 - 7 wt%) after 7 weeks, pointing out to the influence of short, hydrophylic PEO segment on hydrolysis patterns.

Changes in carbonyl index (CI) and crystallinity index after 7 and 8 weeks of degradation are presented in Table 1. The values of carbonyl index of diblock copolymers with higher weight loss increased while PCL and PCL/PEO-3 carbonyl indexes remained almost unchanged. Carbonyl index values for all samples ranged from 3.4 to 4.4, confirming hydrophobicity and small hydrolytic degradation extent of block copolymers. Crystallinity index of diblock copolymers increased after degradation providing additional proof of the influence of small PEO segment on degradation behaviour and their ability to crystallize during degradation period. Crystallinity index of non-degraded samples was quite similar for all samples ranged from 58 to 60 %.

Table 1. Weight loss, carbonyl index (CI) and crystallinity index after 7 and 8 weeks of hydrolytical degradation.

Sample	Water uptake 72 h, %	Weight loss, % 7 weeks	Weight loss, % 8 weeks	CI (7/8 weeks) ^{a,b}	Crystallinity index ^{b,c} , %
PCL	2.3	0.12±0.2	0.5±0.7	4.1 (3.9)	58/55 (58)
PCL/PEO-1	4.1	10.9±0.4	6.3±3.0	3.4 (4.0)	62/64 (60)
PCL/PEO-2	2.9	5.1±2.0	4.4±2.3	3.6 (4.1)	62/63 (57)
PCL/PEO-3	3.2	7.0±1.0	2.4±0.1	3.9 (3.9)	61/62 (58)

^a from the ratio of absorbance peaks at 1720 and 1398 cm⁻¹

^b in parenthesis the values of control sample are given

^c from the ratio of absorbance peaks at 1294 and 1167 cm⁻¹

Enzymatic degradation measurements

Enzymatic degradation experiments for diblock copolymers and PCL were carried out in PBS (pH 7.4, at 37 °C) over two weeks containing cell-free extract of *P. aeruginosa* PAO1 (1.8 to 2 mg of total protein/ml). Both PCL and diblock copolymers indicated significant weight loss caused by an enzyme action (Table 2). The small weight loss (~ 4 wt%) of PCL after two weeks is attributed to a poor biodegradation ability. According to the results, the percentage of weight loss was affected by the content of hydrophilic PEO block and length of PCL segments in copolymers. In addition, diblock copolymer with the highest content of PEO segment (PCL/PEO-1) showed remarkable weight loss (~12 wt%) due to a higher hydrophilicity but also the lowest molecular weight in the series. Weight loss of PCL/PEO-2 and PCL/PEO-3 (~6 wt%) confirmed the influence of molecular weight on degradation extent: with the increase of molecular weight of PCL block, the enzymatic degradation decreased.

Table 2. Analysis of enzymatically degraded block copolymers; weight loss, carbonyl index, CI, crystallinity index and AFM analysis (RMS, diameter).

Sample	Weight loss, %	CI ^{a,c}	Crystallinity index ^{b,c} , %	RMS, nm Glass side ^c	RMS, nm air side ^c	Diameter, µm
PCL	4.3	4.0 (3.9)	58 (58)	130 (100)	82 (70)	80
PCL/PEO-1	11.8	2.2 (4.0)	70 (60)	158 (120)	175 (166)	100
PCL/PEO-2	5.8	3.9 (4.1)	58 (57)	200 (113)	189 (160)	100-120
PCL/PEO-3	6.4	3.3 (3.9)	61 (58)	130 (85)	102 (60)	> 200

^a from the ratio of absorbance peaks at 1720 and 1398 cm⁻¹

^b from the ratio absorbance peaks at 1294 and 1167 cm⁻¹

^c in parenthesis the values of control sample are given

FTIR analysis of degraded samples

FTIR analysis was used for estimation of changes in crystallinity index and carbonyl index (CI) after enzymatic degradation of PCL and diblock copolymers. Representative FTIR spectra of non-degraded and degraded block copolymers are presented at Figure 1. Enzymatically degraded samples showed completely different intensity of characteristic bands used for the calculations of CI and crystallinity index (Table 2).

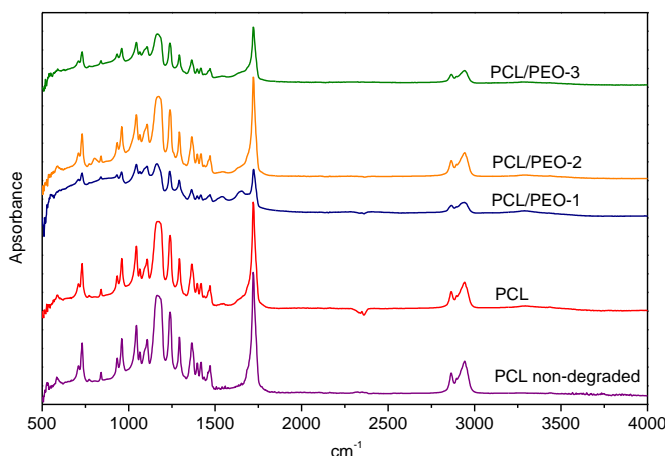


Figure 1. FTIR spectrum of PCL and diblock copolymer films after two weeks of enzymatic degradation.

Diblock copolymer with the highest weight loss, PCL/PEO-1 (11.8 wt%), indicated the most significant changes in carbonyl index (CI decreased from 4.0 to 2.2) while remarkable change in the crystallinity index (from 60 to 70 %) was also detected. This is in a line with some results showing that the degradation process starts preferentially from the amorphous parts of polymers while crystalline part is mostly remained. Although homopolymer PCL barely showed any changes in CI and crystallinity index, FTIR analysis confirmed that beside physical mass changes of copolymer samples, structural changes also happened.

GPC analysis of degraded samples

In order to detect changes in molecular weights, the number-average molecular weights (M_n) and polydispersity index, PI (M_w/M_n) were determined for samples before and after degradation (Figure 2). GPC analysis of PCL showed decrease in M_n of 13.1 % and M_w about 10.4 % while PI index values was almost unchanged (from 1.92 to 1.98). However, diblock copolymer sample PCL/PEO-2 showed a considerable decrease in molecular weight (M_n by 30.6% and M_w by 19.9%) and an significant increase in the polydispersity index from 1.70 to 1.96. The slightly higher decreases in M_n is connected with the increase of the fraction of lower molecular weight chains. The hydrolysis of polyesters could occur either as a random reaction or by end-initiated unzipping reaction. The presence of hydrophilic PEO segments increases the hydrophilicity of the polymer matrix, thus accelerating polyester hydrolysis in enzyme medium. Remarkable differences in PI values were detected for PCL/PEO-1 and PCL/PEO-2 samples which showed broader molecular weight distribution after degradation. However, sample PCL/PEO-3 indicated almost the same value of PI and the smallest change in molecular weights (~ 10 %).

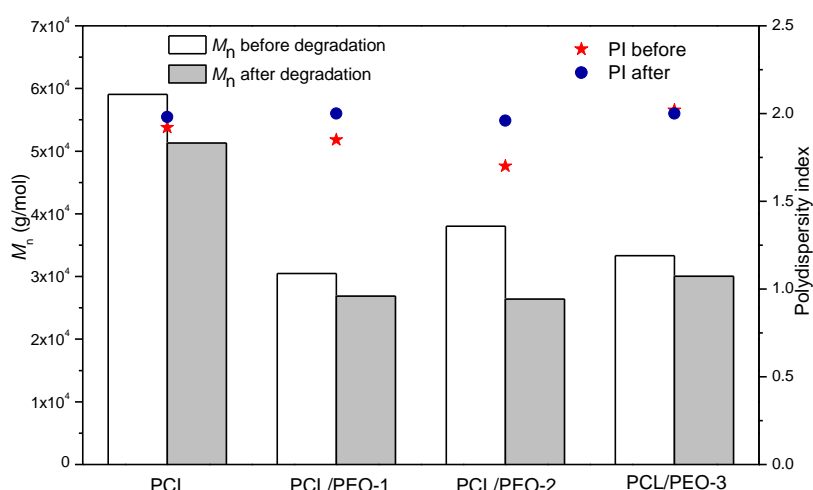


Figure 2. Changes in M_n and PI of PCL and PCL/PEO samples after enzymatic degradation.

AFM analysis of degraded films

Given that enzymatic degradation is performed via surface erosion mechanism, AFM is useful method for visualization of enzymatically degraded polymer samples. Surface erosion after enzymatic degradation was quantified by AFM analysis thought the assessment of changes in surface roughness (Table 2). Different surface morphology of PCL and diblock copolymers after degradation was detected (Figure 3).

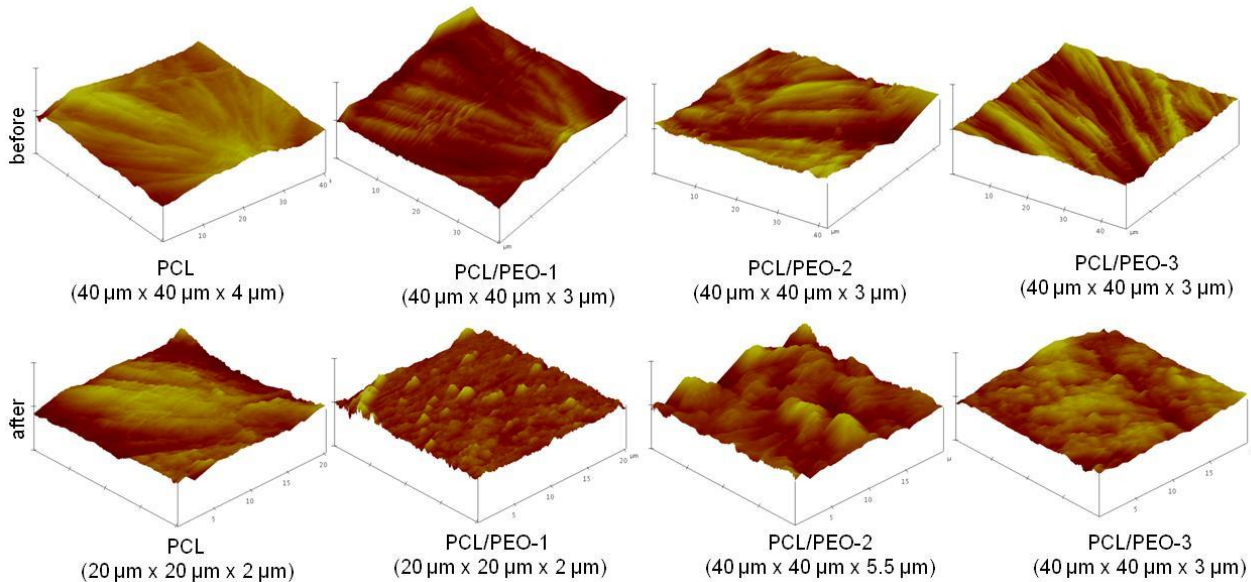


Figure 3. AFM micrographs of PCL, diblock copolymers before and after degradation.

Before degradation, perfect spherulites lamellar structure was clearly visible. The surface roughness of PCL and block copolymers was determined by the diameter of the spherulites; the larger spherulites, the smoother surface was observed. Sample PCL/PEO-3 (spherulite's diameter ~200 μm) possessed small RMS value before degradation (85 nm) compared to other diblock copolymers. According to the surface erosion mechanism of enzymatic degradation, changes in morphology and RMS values were in a line with a degradation extent of copolymer films. The lamellar structure of PCL and block copolymer films was destroyed and the intensity of morphological change was in agreement with degradation extent. Due to a higher degradation extent of diblock copolymers, surface erosion of those samples was more intensive, and higher RMS values after degradation were observed. For the PCL/PEO-1, which lost about 12 wt% of the weight, difference in RMS value before and after degradation was only about 30 nm in comparison to sample PCL/PEO-3 (weight loss 6.4 wt%) with RMS detected change of almost 60 nm. This could be explained by the spherulites' diameter of PCL/PEO-3 polymer which possessed smaller starting RMS value due to very large spherulites (200 μm). Because of the relatively small surface roughness of this diblock copolymer, compared to other samples, the enzymes presented in a cell-free extract could easily attack polymer surface.

Degradation in model compost system

Biodegradation of diblock copolymers and PCL was tested in model compost system containing a commercial mixture used for cultivation of white button mushroom and supplemented with culture of *P. aeruginosa* PAO1, at 37 °C. During four weeks of composting, diblock copolymer samples exhibit significantly higher surface degradation followed by roughing and polymer disintegration (Figure 4). Homopolymer PCL showed the smallest level of degradation indicating the best resistance to microorganisms. The highest disintegration was observed for PCL/PEO-1 sample due to higher content of hydrophilic PEO segment, but also to the smallest molecular weight. Higher molecular weight induced lower degradation, therefore copolymer PCL/PEO-3 were merely destroyed after four weeks in compost. For the samples highly degraded, some areas were more affected than others, resulting in an inhomogeneous mechanism of degradation. This might be explained by a possibly better contact of the compost in more degraded areas as well as by an inhomogeneous growth of the microorganisms on the polymer film surface.

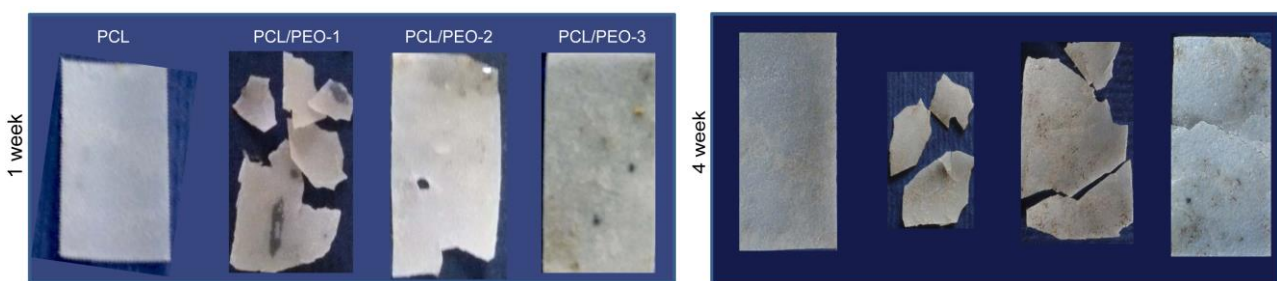


Figure 4. PCL and diblock copolymer samples photographed after 1 week and 4 weeks in compost.

Conclusions

Diblock PCL/PEO copolymers exhibited higher hydrolytic degradation in comparison to homopolymer PCL. Besides weight loss, FTIR analysis confirmed structural changes of samples manifested through carbonyl and crystallinity index changes. Enzymatic degradation of polymer samples in the presence *P. aeruginosa* PAO1 cell free extract indicated higher degradation compared to hydrolytic degradation. AFM analysis revealed the strong changes in surface morphology, and assessment of RMS values after enzymatic degradation confirmed surface erosion process. FTIR analysis of enzymatically degraded polymer films also indicated significant changes in carbonyl and crystallinity indexes while GPC analysis revealed higher decrease in molecular weight of diblock copolymers. Degradation tests in compost showed significant level of destruction of block copolymer films in comparison to PCL sample. Therefore, both PEO segment content and polymer molecular weight have significant impact on the biodegradation process. Finally, introduction of short PEO segment into PCL chains greatly affected bulk and surface erosion which is beneficial for biodegradation behaviour.

Poređenje hidrolitičke, enzimske i degradacije u kompostu PCL/PEO diblok kopolimera

U ovom radu je prikazana hidrolitička i enzimska degradacija poli(ϵ -kaprolaktona) (PCL) i serije diblok kopolimera (PCL/PEO) sa malim sadržajem hidrofilnog PEO segmenta. Ispitivan je uticaj uvođenja lateralnog PEO segmenta u PCL lanac na degradativna svojstva kopolimera. Hidrolitička degradacija je izvođena u fosfatnom puferu tokom 8 nedelja. FTIR analizom je utvrđena bolja degradativna sposobnost diblok kopolimera usled veće hidrofilnosti u poređenju sa PCL-om. Enzimska degradacija, testirana u "cell-free" ekstraktu *Pseudomonas aeruginosa* PAO1, tokom dve nedelje, je praćena na osnovu promena mase, hrapavosti površine polimernih filmova kao i FTIR analizom. Rezultati su potvrdili da svi uzorci podležu enzimskoj degradaciji, koja se odigrava po mehanizmu površinske erozije i uz smanjenje molarne mase. Diblok kopolimeri su pokazali značajno veći gubitak mase i smanjenje molarne mase u odnosu na PCL. AFM analiza je potvrdila intenzivnu površinsku eroziju i povećanje RMS vrednosti. Testirana je i biodegradacija polimernih filmova u kompostu na 37 °C gde je utvrđena izražena degradacija ispitivanih blok kopolimera.

Rad je finansiran od strane Ministarstva prosvete i nauke Republike Srbije: Projekat 172062 i 173048

References:

1. M. Vert, *Progress in Polymer Science*, **32** (2007) 755.
2. Y. Tokiwa, B. Calabia, C. Ugwu, S. Aiba, *International Journal of Molecular Sciences*, **10** (2009) 3722.
3. M. Ponjavic, M. S. Nikolic, S. Jevtic, J. Rogan, S. Stevanovic, J. Djordjevic, *Macromolecular Research* **24** (2016) 323.

Neorganska hemija / Inorganic Chemistry

Dinuklearni Pt(II) kompleksi kao efikasni katalitički reagensi za selektivnu hidrolizu peptida

Snežana Rajković

Institut za hemiju, Prirodno-matematički fakultet, Univerzitet u Kragujevcu, R. Domanovića 12, 34000 Kragujevac, Srbija, snezana@kg.ac.rs

Uvod

Poslednjih trideset godina intenzivno se izučavaju reakcije paladijum(II) i platina(II) kompleksa sa peptidima, koji u bočnom nizu sadrže aminokiseline L-metionin i L-histidin, jer ovi kompleksi predstavljaju veoma efikasne katalizatore hidrolize peptidne veze. Poznato je da nakon koordinovanja akva-derivata paladijum(II) i platina(II) kompleksa za heteroatom u bočnom nizu aminokiselina L-metionin i L-histidin, dolazi do hidrolize peptidne veze koja sadrži karboksilnu grupu koordinovane aminokiseline.^{1,2} U ovom radu prikazan je pregled rezultata postignutih u oblasti ispitivanja reakcija hidrolize peptidne veze u peptidima koji sadrže aminokiseline L-metionin i L-histidin u prisustvu dinuklearnih kompleksa platine(II).

Eksperimentalni deo

Kompleksi opšte formule $\{[Pt(L)Cl]_2(\mu-X)\}Cl_2$ (L je etilendiamin, en; (\pm) -1,2-propilendiamin, 1,2-pn; izobutilendiamin, ibn; *trans*- (\pm) -1,2-diaminocikloheksan, dach; 1,3-propilendiamin, 1,3-pd; 2,2-dimetil-1,3-propilendiamin, 2,2-diMe-1,3-pd; (\pm) -1,3-pentandiamin, 1,3-pnd i X je mostni diazinski ligand pirazin, pz ili piridazin, pydz) su dobijeni iz odgovarajućih mononuklearnih $[Pt(L)Cl_2]$ kompleksa po modifikovanom postupku koji je ranije opisan u literaturi.³⁻⁶ Strukture ovih kompleksa su prepostavljene na osnovu rezultata NMR (1H i ^{13}C) spektroskopije i elementarne mikroanalize, a u pojedinim slučajevima potvrđene su primenom rendgenske strukturne analize. Dinuklearni hlorido-platina(II) kompleksi prevedeni su u odgovarajuće akvakomplekse, $\{[Pt(L)(H_2O)]_2(\mu-X)\}^{4+}$. Reakcije $\{[Pt(L)(H_2O)]_2(\mu-X)\}^{4+}$ kompleksa sa *N*-acetilovanim peptidima koji u svojoj strukturi sadrže aminokiseline L-metionin i L-histidin (Ac-L-Met-Gly, Ac-L-His-Gly i Ac-L-Met-Gly-L-His-GlyNH₂) praćene su pomoću 1H NMR spektroskopije. Reakcije platina(II) kompleksa sa peptidima izvođene su u 1:1 i 2:1 molskim odnosima, na temperaturi od 37 °C, a pH vrednost reakcione smeše bila je u opsegu 2,0-2,5.

Rezultati i diskusija

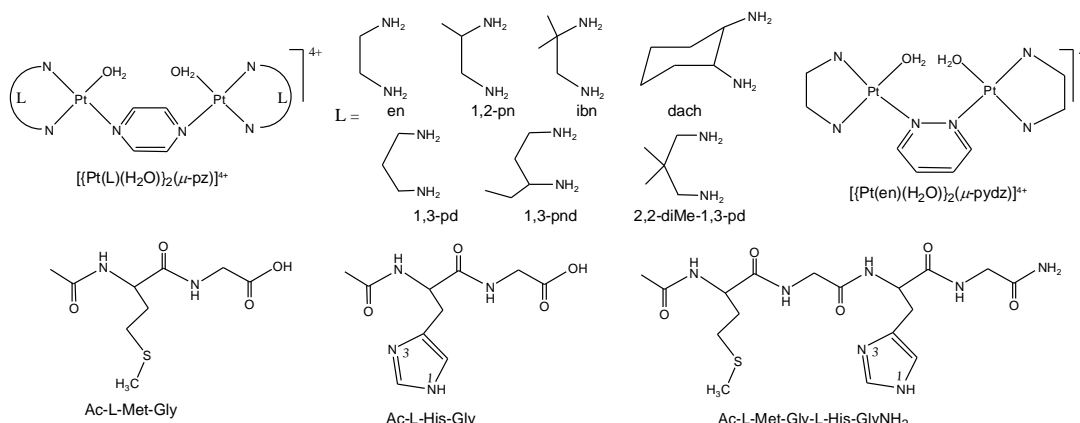
Ispitivanje reakcija hidrolize peptidne veze u Ac-L-Met-Gly i Ac-L-His-Gly dipeptidima pomoću različitih $\{[Pt(L)(H_2O)]_2(\mu-pz)\}^{4+}$ kompleksa

Primenom 1H NMR spektroskopije ispitana je uticaj bidentatno koordinovanog diaminskog liganada L u $\{[Pt(L)(H_2O)]_2(\mu-pz)\}^{4+}$ kompleksima (L je en, 1,2-pn, ibn, dach, 1,3-pd, 2,2-diMe-1,3-pd, 1,3-pnd) na brzinu hidrolize Met-Gly i His-Gly peptidnih veza u *N*-acetilovanom L-metionil-glicinu (Ac-L-Met-Gly) i *N*-acetilovanom L-histidil-glicinu (Ac-L-His-Gly) (Slika 1). Helatni diaminski ligandi L u $\{[Pt(L)(H_2O)]_2(\mu-pz)\}^{4+}$ kompleksima predstavljaju stabilni deo molekula i ostaju koordinovani za Pt(II) ion u toku reakcija sa dipeptidima.⁴⁻⁶

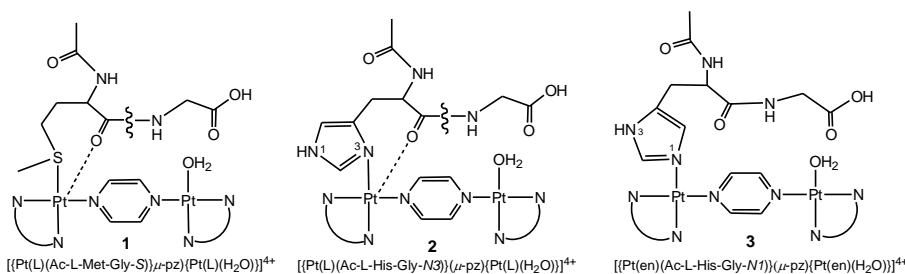
Ac-L-Met-Gly

U reakcijama $\{[Pt(L)(H_2O)]_2(\mu-pz)\}^{4+}$ kompleksa sa ekvimolarnom količinom Ac-L-Met-Gly dipeptida dolazi do monodentatne koordinacije dipeptida za Pt(II) kompleks preko atoma sumpora iz metioninskog ostataka, pri čemu se formira platina(II)-dipeptid kompleks koji je hidrolitički aktivan, $\{[Pt(L)(Ac-L-Met-Gly-S)}(\mu-pz)\{Pt(L)(H_2O)\}]^{4+}$, **1** (Slika 2). U svim ispitivanim reakcijama intermedijerni kompleks **1**, katalizuje hidrolizu peptidne veze koja sadrži karboksilnu grupu metionina. Reakcije hidrolize peptidne veze praćene su 24 sata, a vremenska zavisnost reakcija hidrolize Met-Gly peptidne veze u prisustvu platine(II) kompleksa, prikazana je na Slici 3a i 3b. Na osnovu podataka koji su prikazani na Slici 3a i 3b može se zaključiti da količina hidrolizovanog Ac-L-Met-Gly dipeptida zavisi

od veličine bidentatno koordinovanog diaminskog prstena u $[\{Pt(L)(H_2O)_2(\mu\text{-pz})\}]^{4+}$ kompleksu. Nađeno je da promenom petočlanog bidentatno koordinovanog diaminskog liganda u Pt(II) kompleksu brzina hidrolize opada sledećim redom: en > 1,2-pn > ibn > dach (Slika 3a).⁵ Međutim, u reakciji Ac-L-Met-Gly sa dinuklearnim $[\{Pt(L)(H_2O)_2(\mu\text{-pz})\}]^{4+}$ kompleksima, koji sadrže šestočlani helatni diaminski prsten (L je 1,3-pd, 2,2-diMe-1,3-pd, 1,3-pnd), količina hidrolizovanog Ac-L-Met-Gly dipeptida ne zavisi od veličine helatnog diaminskog prstena. Sterne modifikacije u šestočlanom diaminskom prstenu u $[\{Pt(L)(H_2O)_2(\mu\text{-pz})\}]^{4+}$ kompleksima nemaju značajan uticaj na brzinu hidrolize peptidne veze koja sadrži karboksilnu grupu metionina u Ac-L-Met-Gly dipeptidu.



Slika 1. Strukturne formule dinuklearnih platina(II) kompleksa i peptide

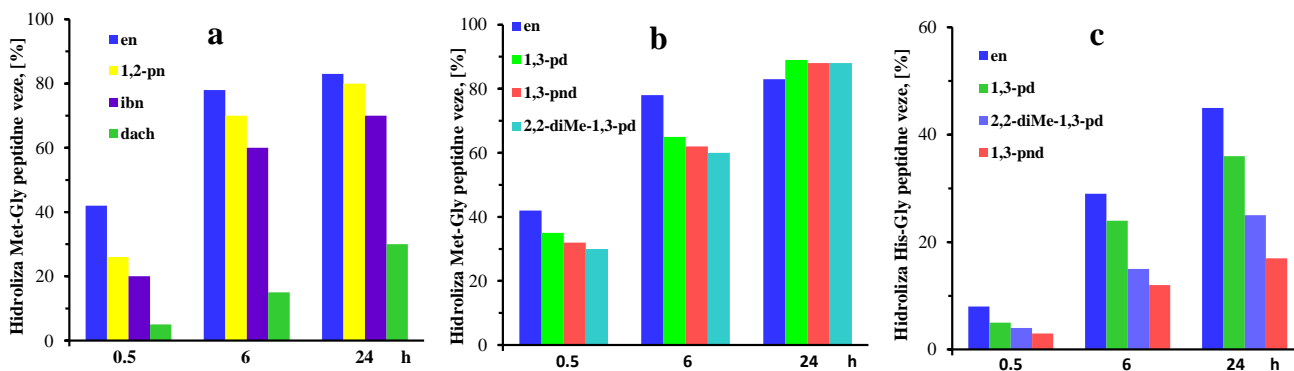


Slika 2. Strukturne formule intermedijernih platina(II) peptid kompleksa

Ac-L-His-Gly

Kada se dinuklearni $[\{Pt(en)(H_2O)\}_2(\mu\text{-pz})]^{4+}$ kompleksi i Ac-L-His-Gly pomešaju u 1:1 molskom odnosu primenom 1H NMR spektroskopije u rastvoru su identifikovani $[\{Pt(en)(Ac-L-His-Gly-N3)\}(\mu\text{-pz})\{Pt(en)(H_2O)\}]^{4+}$ **2** i $[\{Pt(en)(Ac-L-His-Gly-N1)\}(\mu\text{-pz})\{Pt(en)(H_2O)\}]^{4+}$ **3** kompleksi (Slika 2).⁶ Međutim, u reakciji $[\{Pt(L)(H_2O)_2(\mu\text{-pz})\}]^{4+}$ (L je 1,3-pd, 2,2-diMe-1,3-pd, 1,3-pnd) kompleksa, koji sadrže šestočlani diaminski helatni prsten, sa Ac-L-His-Gly u rastvoru je identifikovan samo jedan intermedijerni $[\{Pt(L)(Ac-L-His-Gly-N3)\}(\mu\text{-pz})\{Pt(L)(H_2O)\}]^{4+}$ kompleks **2**. Kompleksi **2** i **3** su okarakterisani na osnovu razlika u hemijskih pomeranjima za C2H i C5H protone imidazololova prstena iz histidina, Tabela 1. Na osnovu podataka 1H NMR spektroskopije nađeno je da je intermedijerni kompleks **2**, u kome je dipeptid koordinovan preko N3 atoma azota imidazololova prstena za Pt(II) ion, hidrolitički aktivan.⁶ Kompleks **2** katalizuje hidrolizu His-Gly peptidne veze u Ac-L-His-Gly dipeptidu. Vremenska zavisnost reakcije hidrolize His-Gly peptidne veze je prikazana na Slici 3c. Poređena je brzina hidrolize His-Gly peptidne veze u dipeptidu u prisustvu $[\{Pt(L)(H_2O)_2(\mu\text{-pz})\}]^{4+}$ kompleksa, koji sadrže šestočlani helatni diaminski prsten, u odnosu na $[\{Pt(en)(H_2O)\}_2(\mu\text{-pz})]^{4+}$ kompleks sa petočlanim diaminskim prstenom. Na osnovu podataka koji su prikazani na Slici 3c može se zaključiti da se količina hidrolizovanog Ac-L-His-Gly dipeptida smanjuje sa povećanjem sternog efekta dinuklearnog kompleksa platine(II) (en > 1,3-pd > 1,3-pnd > 2,2-diMe-1,3-pd). Razlika u katalitičkoj aktivnosti ispitivanih dinuklearnih $[\{Pt(L)(H_2O)_2(\mu\text{-pz})\}]^{4+}$ (L je 1,3-pd, 1,3-pnd 2,2-diMe-1,3-pd) i $[\{Pt(en)(H_2O)\}_2(\mu\text{-pz})]^{4+}$ kompleksa zavisi isključivo od brzine koordinovanja Ac-L-His-Gly dipeptide za odgovarajući Pt(II) kompleks. Ove reakcije su posmatrane kao reakcije drugog reda i na osnovu podataka koji su prikazani u Tabeli 2 može se zaključiti da vrednosti konstante brzine (k_2) opadaju sa

povećanjem sternog efekta diaminskog liganda u dinuklearnim kompleksima platine(II). Prema tome, modifikacijom dinuklearnog $\left[\{\text{Pt}(\text{L})(\text{H}_2\text{O})\}_2(\mu\text{-pz})\right]^{4+}$ kompleksa, odnosno uvođenjem sterno velikog diaminskog liganda L, može se uticati na brzinu formiranja hidrolitički aktivnog kompleksa **2** (Slika 2), a samim tim i inhibirati hidrolitičko raskidanje peptidne veze koja sadrži karboksilnu grupu histidina.



Slika 3. Vremenska zavisnost reakcije hidrolize Met-Gly (**a** i **b**) i His-Gly (**c**) peptidne veze u dipeptidima u reakciji sa $\left[\{\text{Pt}(\text{L})(\text{H}_2\text{O})\}_2(\mu\text{-pz})\right]^{4+}$ kompleksima^{4,5}

Ispitivanje reakcija hidrolize peptidne veze u peptidima koji sadrže aminokiseline L-metionin i L-histidin u prisustvu $\left[\{\text{Pt}(\text{en})(\text{H}_2\text{O})\}_2(\mu\text{-pz})\right]^{4+}$ i $\left[\{\text{Pt}(\text{en})(\text{H}_2\text{O})\}_2(\mu\text{-pydz})\right]^{4+}$ kompleksa

Dinuklearni $\left[\{\text{Pt}(\text{en})\text{Cl}\}_2(\mu\text{-X})\right]\text{Cl}_2$ kompleksi (X je pz ili pydz), čija je struktura potvrđena na osnovu rezultata rendgenske strukturne analize, prevedeni su u odgovarajuće akva analoge, $\left[\{\text{Pt}(\text{en})(\text{H}_2\text{O})\}_2(\mu\text{-pz})\right]^{4+}$ i $\left[\{\text{Pt}(\text{en})(\text{H}_2\text{O})\}_2(\mu\text{-pydz})\right]^{4+}$.^{4,6} Primenom ^1H NMR spektroskopije izučavane su reakcije ovih kompleksa sa Ac-L-His-Gly i Ac-L-Met-Gly-L-His-GlyNH₂ peptidima (Slika 1).

Ac-L-His-Gly

Kao što je prethodno navedeno, u reakciji $\left[\{\text{Pt}(\text{en})(\text{H}_2\text{O})\}_2(\mu\text{-pz})\right]^{4+}$ kompleksa sa Ac-L-His-Gly dipeptidom dolazi do formiranja dva intermedijerna Pt(II)-peptid kompleksa (kompleksi **2** i **3**; Slika 2 i Tabela 1). Međutim, u reakciji $\left[\{\text{Pt}(\text{en})(\text{H}_2\text{O})\}_2(\mu\text{-pydz})\right]^{4+}$ sa ovim dipeptidom ne dolazi do koordinovanja dipeptida za Pt(II) ion, ni za vreme od 48 sati. Kao posledica odsustva koordinacije atoma azota imidazolovog prstena dipeptida za Pt(II) ion, His-Gly peptidna veza ne hidrolizuje. Razlika u reaktivnosti $\left[\{\text{Pt}(\text{en})(\text{H}_2\text{O})\}_2(\mu\text{-pz})\right]^{4+}$ i $\left[\{\text{Pt}(\text{en})(\text{H}_2\text{O})\}_2(\mu\text{-pydz})\right]^{4+}$, kompleksa sa Ac-L-His-Gly može se pripisati prisustvu različitih mostnih liganda u ovim kompleksima.⁶

Tabela 1. ^1H NMR hemijska pomeranja (δ , ppm) za Pt(II)-peptid komplekse koji nastaju u reakcijama sa Ac-L-His-Gly i Ac-L-Met-Gly-L-His-GlyNH₂

peptid/Pt(II)-peptid kompleks	Imidazol (δ / ppm)		Ref.
	C2H	C5H	
Ac-L-His-Gly	8.61	7.33	6
$\left[\{\text{Pt}(\text{en})(\text{Ac-L-His-Gly-N3})\}(\mu\text{-pz})\{\text{Pt}(\text{en})(\text{H}_2\text{O})\}\right]^{4+}$ 2	8.09	7.10	6
$\left[\{\text{Pt}(\text{en})(\text{Ac-L-His-Gly-N1})\}(\mu\text{-pz})\{\text{Pt}(\text{en})(\text{H}_2\text{O})\}\right]^{4+}$ 3	7.96	6.95	6
$\left[\{\text{Pt}(1,3\text{-pd})(\text{Ac-L-His-Gly-N3})\}(\mu\text{-pz})\{\text{Pt}(1,3\text{-pd})(\text{H}_2\text{O})\}\right]^{4+}$ 2	8.08	7.06	
$[\text{Pd}(\text{en})(\text{H}_2\text{O})(\text{Ac-L-His-Gly-N3})]^{2+}$	8.03	7.11	7
$[\text{Pd}(\text{en})(\text{H}_2\text{O})(\text{Ac-L-His-Gly-N1})]^{2+}$	7.87	6.89	7
Ac-L-Met-Gly-L-His-GlyNH ₂	8.63	7.31	6
$\left[\{\text{Pt}(\text{en})(\text{Ac-L-Met-Gly-L-His-GlyNH}_2\text{-N3})\}(\mu\text{-pz})\{\text{Pt}(\text{en})(\text{H}_2\text{O})\}\right]^{4+}$ 2	8.07	7.09	6
$\left[\{\text{Pt}(\text{en})(\text{Ac-L-Met-Gly-L-His-GlyNH}_2\text{-N1})\}(\mu\text{-pz})\{\text{Pt}(\text{en})(\text{H}_2\text{O})\}\right]^{4+}$ 3	7.92	6.92	6
$\left[\{\text{Pt}(\text{dien})\}(\mu\text{-Ac-L-Met-Gly-L-His-GlyNH}_2\text{-S,N3})\{\text{Pt}(\text{en})(\text{H}_2\text{O})\}\right]^{4+}$	8.14	7.10	8
$\left[\{\text{Pt}(\text{dien})\}(\mu\text{-Ac-L-Met-Gly-L-His-GlyNH}_2\text{-S,N1})\{\text{Pt}(\text{en})(\text{H}_2\text{O})\}\right]^{4+}$	7.88	6.89	8

Tabela 2. Konstante brzine za reakcije formiranja hidrolitički aktivnog kompleksa 2

Kompleks	$k_2 / (10^3 k_2/M^{-1}s^{-1})$
$\left[\{\text{Pt}(\text{en})(\text{H}_2\text{O})\}_2(\mu\text{-pz})\right]^{4+}$	2.08 ± 0.06
$\left[\{\text{Pt}(1,3\text{-pd})(\text{H}_2\text{O})\}_2(\mu\text{-pz})\right]^{4+}$	1.58 ± 0.05
$\left[\{\text{Pt}(1,3\text{-pnd})(\text{H}_2\text{O})\}_2(\mu\text{-pz})\right]^{4+}$	1.09 ± 0.09
$\left[\{\text{Pt}(2,2\text{-diMe-1,3-pd})(\text{H}_2\text{O})\}_2(\mu\text{-pz})\right]^{4+}$	0.87 ± 0.01

Ac-L-Met-Gly-L-His-GlyNH₂

U reakcijama $\left[\{\text{Pt}(\text{en})(\text{H}_2\text{O})\}_2(\mu\text{-pz})\right]^{4+}$ i $\left[\{\text{Pt}(\text{en})(\text{H}_2\text{O})\}_2(\mu\text{-pydz})\right]^{4+}$ kompleksa sa ekvimolarnom količinom Ac-L-Met-Gly-L-His-GlyNH₂ dolazi do spontanog koordinovanja atoma sumpora metioninskog ostatka tetrapeptida za Pt(II) ion.⁶ Rezultati ¹H NMR spektroskopije su pokazali da u ovim reakcijama ne dolazi do koordinovanja atoma azota iz imidazolovog prstena histidina. Monodentatna koordinacija Ac-L-Met-Gly-L-His-GlyNH₂ za $\left[\{\text{Pt}(\text{en})(\text{H}_2\text{O})\}_2(\mu\text{-pz})\right]^{4+}$ i $\left[\{\text{Pt}(\text{en})(\text{H}_2\text{O})\}_2(\mu\text{-pydz})\right]^{4+}$ kompleksa dovodi do formiranja hidrolitički aktivnih, $\left[\{\text{Pt}(\text{en})(\text{Ac-L-Met--Gly-L-His-GlyNH}_2\text{-S})\}(\mu\text{-pz})\{\text{Pt}(\text{en})(\text{H}_2\text{O})\}\right]^{4+}$ i $\left[\{\text{Pt}(\text{en})(\text{Ac-L-Met-Gly-L-His-GlyNH}_2\text{-S})\}(\mu\text{-pydz})\{\text{Pt}(\text{en})(\text{H}_2\text{O})\}\right]^{4+}$ kompleksa. Ovi intermedijerni platina(II)-peptid kompleksi su strukturno analogni kompleksu 1 (Slika 2) i oni katalizuju hidrolizu Met-Gly peptidne veze u ispitivanom tetrapeptidu. Na osnovu podataka ¹H NMR spektroskopije nađeno je da nakon 48 sati hidrolizuje 80% Met-Gly peptidne veze u prisustvu $\left[\{\text{Pt}(\text{en})(\text{H}_2\text{O})\}_2(\mu\text{-pz})\right]^{4+}$ i samo 50% u prisustvu $\left[\{\text{Pt}(\text{en})(\text{H}_2\text{O})\}_2(\mu\text{-pydz})\right]^{4+}$ kompleksa. Reakcije Ac-L-Met-Gly-L-His-GlyNH₂ sa ovim dinuklearnim Pt(II) kompleksima izučavane su u višku kompleksa. U reakciji $\left[\{\text{Pt}(\text{en})(\text{H}_2\text{O})\}_2(\mu\text{-pz})\right]^{4+}$ sa ovim tetrapeptidom, pored $\left[\{\text{Pt}(\text{en})(\text{Ac-L-Met-Gly-L-His-GlyNH}_2\text{-S})\}(\mu\text{-pz})\{\text{Pt}(\text{en})(\text{H}_2\text{O})\}\right]^{4+}$ kompleksa, nastaju još dva Pt(II)-tetrapeptid kompleksa. Ova dva kompleksa predstavljaju izomere u kojima je tetrapeptid preko atoma azota (*N*1 odnosno *N*3) histidina koordinovan za Pt(II) ion i strukturni su analozi sa kompleksima 2 i 3 koji su prikazani na Slici 2. Nađeno je da, pored hidrolize Met-Gly peptidne veze, hidrolizuje i His-GlyNH₂ peptidna veza u čiju strukturu ulazi karboksilna grupa histidina. Hidroliza His-GlyNH₂ peptidne veze je posledica koordinovanja tetrapeptida preko *N*3 atoma azota za drugi Pt(II) ion dinuklearnog kompleksa. Nađeno je da nakon 48 sati hidrolizuje oko 80% Met-Gly i 28% His-GlyNH₂ peptidne veze. Međutim, u reakciji tetrapeptida sa $\left[\{\text{Pt}(\text{en})(\text{H}_2\text{O})\}_2(\mu\text{-pydz})\right]^{4+}$ kompleksom, u 1:2 molskom odnosu, hidrolizuje samo Met-Gly peptidna veza. U ovoj reakciji ne dolazi do hidrolize His-GlyNH₂ peptidne veze, jer se atom azota imidazolovog prstena (*N*1 odnosno *N*3) ne koordinuje se za Pt(II) ion. Dinuklearni Pt(II) kompleks, koji kao mostni ligand sadrži pz, je bolji katalizator hidrolize peptidne veze u odnosu na kompleks u kome je pydz mostni ligand. Ovo se objašnjava činjenicom da su dva Pt(II) jona u $\left[\{\text{Pt}(\text{en})(\text{H}_2\text{O})\}_2(\mu\text{-pydz})\right]^{4+}$ kompleksu na manjem rastojanju (3,2535(4) Å) od rastojanja dva Pt(II) jona u $\left[\{\text{Pt}(\text{en})(\text{H}_2\text{O})\}_2(\mu\text{-pz})\right]^{4+}$ kompleksu (6,7890(3) Å). Na osnovu ovoga možemo zaključiti da regioselektivna hidroliza peptidne veze, koja sadrži karboksilnu grupu aminokiseline metionina, u polipeptidima koji sadrže obe aminokiseline metionin i histidin može se postići upotrebom dinuklearnog Pt(II) kompleksa koji kao mostni ligand sadrži piridazin.⁶

Zaključak

U ovom radu dat je pregled do sada postignutih rezultata u oblasti ispitivanja reakcija hidrolize Met-Gly i His-Gly peptidnih veza u Ac-L-Met-Gly i Ac-L-His-Gly dipeptidima, kao i u Ac-L-Met-Gly-L-His-GlyNH₂ tetrapeptidu, u prisustvu različitih dinuklearnih kompleksa platine(II). Nađeno je da brzina hidrolize Met-Gly peptidne veze zavisi od sternog efekta bidentatno koordinovanog diaminskog liganda u $\left[\{\text{Pt}(\text{L})(\text{H}_2\text{O})\}_2(\mu\text{-X})\right]^{4+}$ kompleksu (L je en, 1,2-pn, ibn, dach). Sterne modifikacije u šestočlanom diaminskom prstenu (L je 1,3-pd, 1,3-pnd i 2,2-diMe-1,3-pd) nemaju značajan uticaj na brzinu hidrolize Met-Gly peptidne veze u peptidima. Promenom mostnog diazinskog liganda u $\left[\{\text{Pt}(\text{L})(\text{H}_2\text{O})\}_2(\mu\text{-X})\right]^{4+}$ kompleksu (X je py ili pydz) može se postići regioselektivna hidroliza samo Met-Gly peptidne veze u peptidima koji sadrže L-metionin i L-histidin.

Zahvalnica: Ovaj rad je finansijski podržan od strane Ministarstva prosvete, nauke i tehnološkog razvoja Republike Srbije (Projekat: 172036).

Dinuclear Pt(II) complexes as effective catalytic reagents for the selective hydrolysis of peptides

Recent years have witnessed an increasing interest in the study of the interactions of Pt(II) complexes with methionine- and histidine-containing peptides and proteins as effective catalyst for the hydrolytic cleavage of the above mentioned peptides. In general, it was shown that platinum(II) aqua complexes spontaneously bind to the heteroatom in the side chain of L-methionine or L-histidine and promote cleavage of the amide bond involving the carboxylic group of the anchoring amino acid. The present work provides overview of the results achieved in the studies of the hydrolytic reactions of the amide bond in L-methionine- and L-histidine containing peptides in the present of dinuclear $\{[Pt(L)(H_2O)]_2(\mu-X)\}^{4+}$ complexes (L is ethylenediamine, *en*; (\pm) -1,2-propylenediamine, *1,2-pn*; isobutylenediamine, *ibn*; *trans* (\pm) -1,2-diaminocyclohexane, *dach*; 1,3-propylenediamine, *1,3-pd*; 2,2-dimethyl-1,3-propylenediamine, *2,2-diMe-1,3-pd*; (\pm) -1,3-pantanediamine, *1,3-pnd* and X is bridging diazine ligand pyrazine, *pz* or pyridazine, *pydz*).¹ It was found that the amount of hydrolyzed peptide bound strongly depends from the steric bulk of bidentate coordinated diamine ligand L and pyrazine- or pyridazine-bridged ligand X in $\{[Pt(L)(H_2O)]_2(\mu-X)\}^{4+}$ complex.

Literatura

1. N.M. Milošević, N.M. Kostić, in: A. Sigel, H. Sigel (Eds.), *Metal Ions in Biological Systems, Palladium(II) and Platinum(II) Complexes as Synthetic Peptidases*, vol. XXXVIII, Marcel Dekker Inc., 2001, p. 145.
2. S. Rajković, M.D. Živković, M.I. Djuran, *Current Protein & Peptide Science*, **17** (2015) 95.
3. S. Komeda, G.V. Kalazda, M. Lutz, A.L. Spek, Y. Yamanaka, T. Sato, M. Chikuma, J. Reedijk, *J. Med. Chem.*, **46** (2003) 1210.
4. D.P. Ašanin, M.D. Živković, S. Rajković, B. Waržajtis, U. Rychlewska, M.I. Djuran, *Polyhedron*, **51** (2013) 255.
5. S. Rajković, D.P. Ašanin, M.D. Živković, M.I. Djuran, *Polyhedron*, **65** (2013) 42.
6. S. Rajković, U. Rychlewska, B. Waržajtis, D.P. Ašanin, M.D. Živković, M.I. Djuran, *Polyhedron*, **67** (2014) 27.
7. L. Zhu, N.M. Kostić, *Inorg. Chim. Acta*, **217** (1994) 21.
8. S. Rajković, M.D. Živković, C. Kállay, I. Sóvágó, M.I. Djuran, *Dalton Trans.*, (2009) 8370.

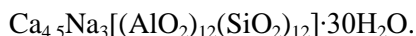
Adsorpcija bakarnih jona na modifikovanom i nemodifikovanom zeolitu 5A

Zora M. Levi, Jelena V. Penavin-Škundrić, Rada R. Petrović, Darko R. Bodroža

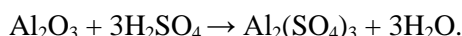
Tehnološki fakultet Banja Luka, Stepe Stepanovića 73

Uvod

Cilj rada je bio u pronalaženju najpogodnijeg oblika adsorbensa (zeolita 5A) za adsorpciju $\text{CuSO}_4 \cdot 5\text{H}_2\text{O}$. Upravo zbog toga, osim na izvornom uzorku zeolit 5A, adsorpcija je rađena u njegovoj baznoj i kiseloj modifikaciji. Na osnovu adsorpcionog kapaciteta ovih adsorbenasa, ispitana je promjena kiselosti njihove površine. Osnovni uzorak je bio zeolit 5A, formule: (1)



Radi se o sintetičkom uzorku, sa veoma pravilnom i definisanim kristalnom strukturom. Kako je procesom kiselinske i bazne aktivacije moguće značajno izmjeniti sorpcione karakteristike zeolita i učiniti ih boljim za određene adsorbate, ovaj rad je pokušaj da se u tome uspije. Kiselinska aktivacija je rađena sa vodenim rastvorom sulfatne kiseline, a bazna sa vodenim rastvorom natrijum karbonata. Baznom aktivacijom smo uspjeli poboljšati osobine zeolita 5A. Procesom kiselinske aktivacije očekivali smo, takođe, promjenu osobina zeolita. Naime, očekivanja su bila da će procesom kiselinske aktivacije biti uklonjen dio tetraedarski koordiniranog Al iz strukture zbog reakcije:



Na ovaj način bi se dobila veća aktivna površina, a samim tim i veće adsorpcione sposobnosti. (2)

Rezultati i diskusija

U radu je praćena adsorpcija bakar (II) sulfata pentahidrata ($\text{CuSO}_4 \cdot 5\text{H}_2\text{O}$) na izvornom uzorku zeolita 5A (proizvođač Organisch-Chemisch Institut der Univerzitaet Goettingen), te na njegovoj kiselinskoj i baznoj aktivnoj formi. Kiselinska aktivacija je vršena sa 20%-tним rastvorom H_2SO_4 . Bazna aktivacija je vršena sa rastvorom Na_2CO_3 , $c_1=0.094 \text{ mol/L}$ i $c_2=0.047 \text{ mol/L}$. Ove aktivacije zeolita 5A obavljene su u laboratorijskoj aparaturi. (3) Temperatura aktivacije je bila sobna, a vrijeme miješanja 6 časova. Odnos zeolita i rastvora je bio 1:5. rastvori su ostavljeni da odstojte preko noći, nakon čega su filtrirani i isprani. Nakon filtracije uzorci su sušeni na 105°C . Rastvor $\text{CuSO}_4 \cdot 5\text{H}_2\text{O}$ je bio masene koncentracije: 2 g/L - 10 g/L, a pripremljen je iz osnovnog rastvora (10g $\text{CuSO}_4 \cdot 5\text{H}_2\text{O}$ rastvorenog u destilovanoj vodi i razblaženog vodom do 1 L). Uzorci za adsorpciju su pripremljeni tako što je u 6 Erlenmayer tivkica odvagano po 1 g uzorka (izvornog i aktiviranih) i u svaki od njih dodano po 5 mL $\text{CuSO}_4 \cdot 5\text{H}_2\text{O}$, koncentracije $\gamma = 2\text{g/L}-10\text{g/L}$. Adsorpcija je rađena na 278 i 298 K u trajanju od 3 časa. Koncentracije uzorka prije i poslije adsorpcije su praćene spektrofotometrijski na spektrofotometru- PERKIN ELMER UV-VIS Spectrometer Lanbda 25; 830 nm.

Eksperimentalni podaci su prikazani u tabelama (1-7) i na slici (1).

Tabela 1. Adsorpcija $\text{CuSO}_4 \cdot 5\text{H}_2\text{O}$ na zeolitu 5A, $T=298 \text{ K}$, $t=3\text{h}$

$C_0 / \text{mol L}^{-1}$	$C_1 / \text{mol L}^{-1}$	$x \cdot 10^3 / \text{mol}$	$m_{\text{zeol}} / \text{g}$	$(x/m \cdot 10^3) / \text{mol}$	$\log(x/m)$	$\log(C_1 / \text{mol L}^{-1})$
0.0102	0.0033	0.345	1.0176	0.339	-0.4698	-2.4815
0.0176	0.0044	0.66	1.0027	0.6582	-0.1816	-2.3565
0.021	0.0046	0.82	1.1456	0.7158	-0.1452	-2.3372
0.024	0.0078	0.81	1.0629	0.7621	-0.118	-2.1079
0.0322	0.0155	0.835	1.0491	0.7959	-0.0991	-1.8097
0.0383	0.0172	1.055	1.0354	1.0189	0.0081	-1.7645

Tabela 2. Adsorpcija $\text{CuSO}_4 \cdot 5\text{H}_2\text{O}$ na izvornom zeolitu 5A, $T=278 \text{ K}$, $t=3\text{h}$

$C_0 / \text{mol L}^{-1}$	$C_1 / \text{mol L}^{-1}$	$x \cdot 10^3 / \text{mol}$	$m_{\text{zeol}} / \text{g}$	$(x/m \cdot 10^3) / \text{mol}$	$\log(x/m)$	$\log(C_1 / \text{mol L}^{-1})$
0.0102	0.003	0.36	1.0291	0.3498	-0.4562	-2.5229
0.0176	0.0038	0.69	1.0655	0.6476	-0.1887	-2.4202
0.021	0.0041	0.845	1.0081	0.8382	-0.0767	-2.3872
0.024	0.0047	0.965	1.0116	0.9539	-0.0205	-2.3279
0.0322	0.006	1.31	1.006	1.3022	0.1147	-2.2218
0.0383	0.0069	1.57	1.1777	1.3331	0.1249	-2.1612

Tabela 3. Adsorpcija $\text{CuSO}_4 \cdot 5\text{H}_2\text{O}$ na jače bazno aktiviranom 5A, $T= 298 \text{ K}$, $t= 3\text{h}$

$C_0 / \text{mol L}^{-1}$	$C_1 / \text{mol L}^{-1}$	$x \cdot 10^3 / \text{mol}$	$m_{\text{zeol}} / \text{g}$	$(x/m \cdot 10^3) / \text{mol}$	$\log(x/m)$	$\log(C_1 / \text{mol L}^{-1})$
0.0102	0.0034	0.34	1.0555	0.3221	-0.492	-2.4685
0.0176	0.0059	0.585	1.0237	0.5715	-0.243	-2.2291
0.021	0.0085	0.61	1.0248	0.5952	-0.2253	-2.0706
0.024	0.0114	0.63	1.0151	0.6206	-0.2072	-1.9431
0.0322	0.0145	0.885	1.0127	0.8739	-0.0585	-1.8386
0.0383	0.018	1.015	1.0128	1.0022	0.001	-1.7447

Tabela 4. Adsorpcija $\text{CuSO}_4 \cdot 5\text{H}_2\text{O}$ na jače bazno aktiviranom 5A, $T= 278 \text{ K}$, $t= 3\text{h}$

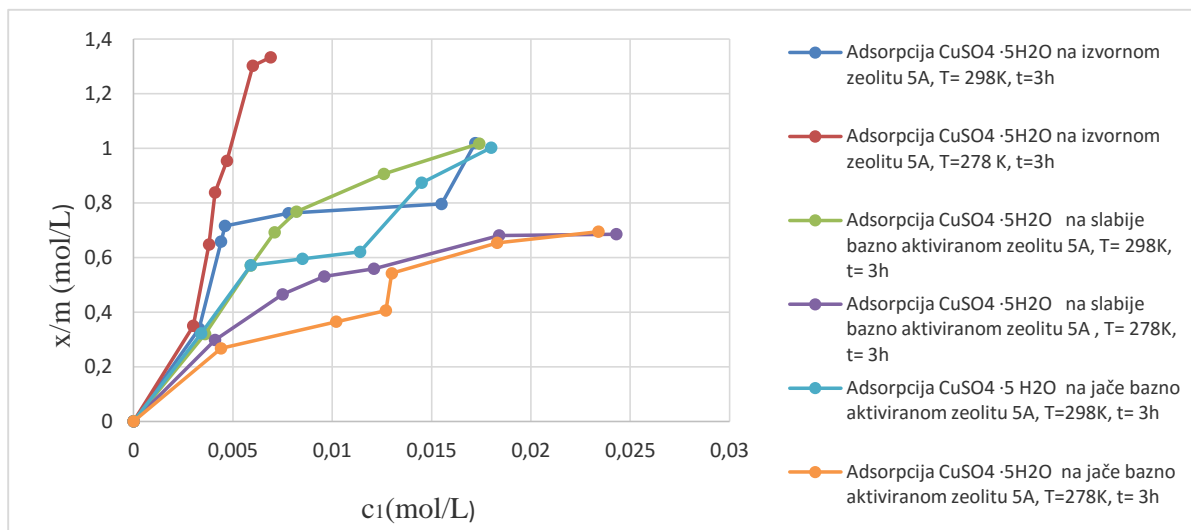
$C_0 / \text{mol L}^{-1}$	$C_1 / \text{mol L}^{-1}$	$x \cdot 10^3 / \text{mol}$	$m_{\text{zeol}} / \text{g}$	$(x/m \cdot 10^3) / \text{mol}$	$\log(x/m)$	$\log(C_1 / \text{mol L}^{-1})$
0.0102	0.0044	0.29	1.0857	0.2671	-0.5733	-2.3565
0.0176	0.0102	0.37	1.0137	0.365	-0.4377	-1.9914
0.021	0.0127	0.415	1.0226	0.4058	-0.3917	-1.8962
0.024	0.013	0.55	1.0149	0.5419	-0.2661	-1.8861
0.0322	0.0183	0.695	1.063	0.6538	-0.1846	-1.7375
0.0383	0.0234	0.745	1.0725	0.6946	-0.1583	-1.6308

Tabela 5. Adsorpcija $\text{CuSO}_4 \cdot 5\text{H}_2\text{O}$ na slabije bazno aktiviranom 5A, $T= 298 \text{ K}$, $t= 3\text{h}$

$C_0 / \text{mol L}^{-1}$	$C_1 / \text{mol L}^{-1}$	$x \cdot 10^3 / \text{mol}$	$m_{\text{zeol}} / \text{g}$	$(x/m \cdot 10^3) / \text{mol}$	$\log(x/m)$	$\log(C_1 / \text{mol L}^{-1})$
0.0102	0.0036	0.33	1.033	0.3195	-0.4955	-2.4437
0.0176	0.0059	0.585	1.0252	0.5706	-0.2437	-2.2291
0.021	0.0071	0.695	1.004	0.6922	-0.1598	-2.1487
0.024	0.0082	0.79	1.029	0.7677	-0.1148	-2.0862
0.0322	0.0126	0.98	1.0817	0.906	-0.0429	-1.8996
0.0383	0.0174	1.045	1.0275	1.017	0.0073	-1.7595

Tabela 6. Adsorpcija $\text{CuSO}_4 \cdot 5\text{H}_2\text{O}$ na slabije bazno aktiviranom 5A, $T= 278 \text{ K}$, $t= 3\text{h}$

$C_0 / \text{mol L}^{-1}$	$C_1 / \text{mol L}^{-1}$	$x \cdot 10^3 / \text{mol}$	$m_{\text{zeol}} / \text{g}$	$(x/m \cdot 10^3) / \text{mol}$	$\log(x/m)$	$\log(C_1 / \text{mol L}^{-1})$
0.0102	0.0041	0.305	1.024	0.2979	-0.5259	-2.3872
0.0176	0.0075	0.505	1.0862	0.4649	-0.3326	-2.1249
0.021	0.0096	0.57	1.0745	0.5305	-0.2753	-2.0177
0.024	0.0121	0.595	1.0646	0.5589	-0.2527	-1.9172
0.0322	0.0184	0.69	1.0133	0.6809	-0.1669	-1.7352
0.0383	0.0243	0.7	1.0211	0.6855	-0.164	-1.6144



Slika 1. Adsorpcija $\text{CuSO}_4 \cdot 5\text{H}_2\text{O}$ na izvornom 5A i njegovim bazno aktiviranim formama, $T=278\text{K}$ i 298K , $t=3\text{h}$

Tabela 7. Konstante n i k, ΔadsH Freundlichove adsorpcionie izoterme, visine platoa, broj ads. molekula, površina ads. molekula $\text{CuSO}_4 \cdot 5\text{H}_2\text{O}$ i pokrivenost površine zeolita 5A i njegovih bazno aktiviranih formi, $T=278\text{K}$ i 298K , $t=3\text{h}$

ZEOLIT	Tads.	n	$k \cdot 10^3$	$\Delta\text{adsH} / \text{J mol}^{-1}$	h platoa $x/m \cdot 10^3 / \text{mol}^{-1}$	$N \cdot 10^{-20}$	S ads mol / m^2	$\Theta / \% \text{ S/Sp}$
Neaktivirani 5A	278	0.640369	3.7222	-1480.0794	I=0.9 II=1.3	I=5.4198 II=7.8286	$S_1=0.5848$ $S_2=0.8447$	$\Theta_1=0.0012$, $\Theta_2=0.0017$
Neaktivirani 5A	298	0.803729	0.7158	1991.2972	I=0.76	I=4.5767	$S_1=0.4938$	$\Theta_1=0.0010$
Jače baz. akt. 5A	278	1.646091	0.0067	-3804.5958	I=0.38 II=0.67	I=2.2884 II=4.0347	$S_1=0.2469$ $S_2=0.4353$	$\Theta_1=0.0005$, $\Theta_2=0.0009$
Jače baz. akt. 5A	298	1.707359	0.0093	-4230.1041	I=0.60 II=0.9	I=3.6132 II=5.4198	$S_1=0.3899$ $S_2=0.5848$	$\Theta_1=0.0008$, $\Theta_2=0.0012$
Slabije baz. akt. 5A	278	2.137666	0.0043	-4940.7695	I=0.54 II=0.68	I=3.2519 II=4.0950	$S_1=0.3509$ $S_2=0.44185$	$\Theta_1=0.0007$, $\Theta_2=0.0009$
Slabije baz. akt. 5A	298	1.41223	0.0203	3498.9012	I=0.85	I=5.1187	$S_1=0.5523$	$\Theta_1=0.0011$

Na kraju smo izmjerili pH vrijednost neaktiviranog 5A, jače bazno aktiviranog 5A i slabije bazno aktiviranog 5A rastvorenog u destilovanoj vodi i u osnovnom rastvoru. Rezultate mjerjenja smo prikazali u tabeli 8.

Tabela 8. pH vrijednosti neaktiviranog 5A, jače bazno aktiviranog 5A i slabije bazno aktiviranog 5A rastvorenih u destilovanoj vodi i u osnovnom rastvoru

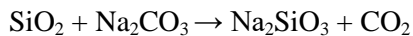
	Neaktivirani 5A	Slabije bazno aktivirani 5A	Jače bazno sktivirani 5A
Destilovana voda	pH=9.60 ($t=20.7^\circ\text{C}$)	pH 10.27 ($t=21^\circ\text{C}$)	pH 10.56 ($t=21^\circ\text{C}$)
Osnovni rastvor	pH=4.75 ($t=19.5^\circ\text{C}$)	pH 4.94 ($t=19.4^\circ\text{C}$)	pH 5.00 ($t=19.5^\circ\text{C}$)

Aktivni centri na zeolitnoj površini su Brönstedove i Lewisove kiseline i baze. Karakter, broj i lokacija kiselih aktivnih centara zavise od strukture zeolita, tipa prisutnog katjona, odnosa Si/Al, kao i uslova aktiviranja.

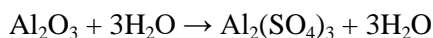
Kako je kod zeolita 5A odnos Si/Al= 1,0, aktivacijom smo pokušali uticati na njegovu kiselost.

Rezultati bazne aktivacije pkazuju da je oslobođena toplota adsorpcije najveća kod slabije baznog uzorka i ona je na 5°C $\Delta\text{adsH}= -4940,7695 \text{ Jmol}^{-1}$, dok je prema očekivanju na 25°C nešto manja i iznosi

$\Delta_{\text{ads}}H = -3498,9012 \text{ J mol}^{-1}$. Ovaj rezultat je bio u skladu sa našim očekivanjima, jer je navedeni rastvor CuSO₄·5H₂O slabo kiseo zbog hidrolize. Međutim ostali rezultati kao što su broj adsorbovanih molekula CuSO₄·5H₂O na površini zeolita, zaposjednutost površine (kojom se kvantitativno izražava adsorpcija) su najbolji na čistom, nemodifikovanom zeolitu 5A. Konstanta k, koja je pokazatelj interakcije adsorbats-adsorbens, takođe ima najvišu vrijednost za nemodifikovani uzorak. Zaključak je da se baznom aktivacijom izvornog uzorka sa Na₂CO₃ smanjivala količina Si zbog reakcije:



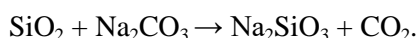
čime se donekle smanjivala i kiselost uzorka, ali ne dovoljno da bi aktivirani 5A dao bolje rezultate od neaktiviranog. Poznato je da suspenzija zeolita sa visokim sadržajem aluminijuma u skeletu reaguje alkalno i pokazuje pH 9 do 12 zbog parcijalne hidrolize. (4) U eksperimentalnom dijelu je izmjerena pH vrijednost neaktiviranog 5A i bazno aktiviranog zeolita 5A u vodenom rastvoru. Dobijeni rezultati su prikazani u tabeli 8 i kao što se vidi iz izmjerenih vrijednosti: neaktivirani 5A; pH= 9,60, slabije bazno aktivirani 5A; pH= 10,27, jače bazno aktivirani 5A; pH= 10,56 su očigledno imali uticaja na proces adsorpcije, koji je prethodno opisan. Promjena pH vrijednosti je neminovno dovodila do promjene ravnoteže prema L' Šateljeovom principu. Kao što je već pomenuto zeoliti su kristalne strukture, a kristalna rešetka je sastavljena od tetraedara SiO₄ i AlO₄ koji čine skelet kristala, između kojih se nalaze kanali i šupljine u kojima su vezani joni alkalnih i zemnoalkalnih metala. Joni metala se mogu lako izmjeniti sa drugim jonima u sredini u kojoj se nalaze. Silicijumski dio melekule je električki neutralan. Međutim aluminijski dio nosi negativan naboј, pa snažno vezuje jone sa pozitivnim nabojem u koje spada i jon vodonika. (5) Smatrali smo da je zbog toga moguće povećati njegovu unutrašnju površinu, tj. povećati prostor za adsorpciju Cu²⁺-jona. Takođe smo smatrali da će procesom kiselinske aktivacije biti djelimično uklonjen dio tetraedarski koordiniranog Al iz strukture zbog reakcije:



čime bi se takođe, dobila veća aktivna površina za adsorpciju Cu²⁺-jona. Međutim, adsorpcija na kiselinski aktiviranim uzorcima nije urađena. Najvjerovalnije je došlo do potpune ekstrakcije aluminijuma uz raspad rešetke i stvaranje želatinoznog SiO₂. Najvjerovalniji razlog je previsoka koncentracija H₂SO₄ sa kojom je rađena kiselinska aktivacija.

Zaključci

- Ispitivana je adsorpcija bakar (II) sulfata pentahidrata na zeolitu 5A, te njegovim modifikacijama. Adsorpcija je rađena na dvije temperature (278K i 298K) u trajanju od 3 časa.
- Rađena je bazna i kiselinska aktivacija uzorka 5A. Kiselinska aktivacija uzorka je rezultirala stvaranjem želatinoznog SiO₂, najvjerovalnije zbog previsoke koncentracije H₂SO₄. Na tim uzorcima nije praćena adsorpcija. Bazna aktivacija je rađena sa rastvorom Na₂CO₃, različitih koncentracija (c₁=0,094 molL⁻¹ i c₂=0,047molL⁻¹).
- Praćenjem adsorpcije, zaključeno je da je adsorpcija fizička i višeslojna. Ispitana je prema Freundlichovoj adsorpcionoj izotermi.
- Praćenjem adsorpcionih parametara, bazno aktiviranog 5A, zaključak je da uzorak bazno aktiviran (c(Na₂CO₃)=0,047 molL⁻¹) daje najbolje rezultate u pogledu toplove adsorpcije ($\Delta_{\text{ads}}H = 4940,7695 \text{ J mol}^{-1}$). Ostali adsorpcioni parametri, bazno aktiviranih uzoraka i izvornog 5A, kao što su broj adsorbovanih molekula CuSO₄·5H₂O na površini zeolita, zaposjednutost površine, vrijednost konstante k, idu u prilog nemodifikovanom zeolitu 5A. Zaključak je da se baznom aktivacijom zeolita sa Na₂CO₃ smanjivala i njegova kiselost, zbog reakcije:



Očigledno smanjenje kiselosti nije bilo dovoljno da aktivirani 5A da bolje rezultate od neaktiviranog zeolita 5A.

Adsorption of copper ions on modified and unmodified 5A zeolite

Ions of many metals, as well as of nonmetals, are often present in polluted natural waters. Copper ions are also some of those toxic metals, which may be found in water environment in three basic forms: suspended, colloidal and solution one. Since adsorption represents one of the procedures for purification of waste waters, this study is an attempt to find a more economical and, at the same time, better adsorbent for purification of water polluted with copper ions. The adsorbent used is synthetic 5A zeolite and its acid and base activated forms. The original sample 5A has been acid treated with 20% H_2SO_4 solution. Base activation is a more frequent manner of improving quality of zeolite, and in this study the original sample has been treated with 20% Na_2CO_3 solution. Examination of adsorption behavior of the original, acid and base activated 5A zeolite sample, in contact with Cu (II) sulfate pentahydrate, has been conducted in laboratory conditions. Adsorption of $CuSO_4 \cdot 5H_2O$ on original and modified 5A samples has been observed spectrophotometrically. By observing adsorption, it has been concluded that adsorption is physical and multilayer. It has been examined according to Freundlich adsorption isotherm.

Literatura

1. D. W. Breck, Zeolite Molecular Sieves, Wiley Inc., New York, USA, 1974
2. J. Penavin-Škundrić, S. Sladojević, Z. Levi, N. Čegar, B. Škundrić, D. Lazić, Protection "Ecological Truth", Proceedings of the 13th Scientific and Professional Conference on Natural Resources and Environmental Bor Lake, SCG, 2005, 99
3. M. Medenica, D. Malešev: „Eksperimentalna fizička hemija“, izd. Medenica M., Beograd, Srbija, 2002
4. D. Bodroža, „Hemija na površini nekih MFI, FAU i BEA zeolita“, magistarski rad, Tehnološki fakultet, Banja Luka 2015 godina.
5. G. T. Kerr, J. Phys. Chem. 72 (1968) 2594

Organska hemija / Organic Chemistry

Biološki aktivno vlakno sa ceftriaksonom

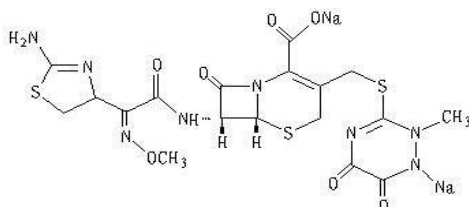
Pero S. Sailović, Branka B. Rodić Grabovac, Ljiljana N. Topalić-Trivunović

Univerzitet u Banjoj Luci, Tehnološki fakultet, Banja Luka, Republika Srpska, BiH

Uvod

Savremena nauka svakodnevno nudi nova rješenja za jednostavniju, sigurniju i kontrolisanu primjenu ljekovitih preparata^{1,2}. Posebnu oblast biološki aktivnih materijala predstavljaju materijali dobijeni vezivanjem ljekovitih preparata na polimerni matriks^{3,4}. Kao polimerni nosač sve češće se koristi celuloza kao netoksičan i ekološki prihvatljiv materijal. Vezivanjem različitih ljekovitih preparata na celulozu mogu se dobiti biološki aktivna vlakna sa lokalnom primjenom^{5,6}, koja omogućavaju otpuštanje optimalne koncentracije lijeka kontrolisanim brzinom, u dužem vremenskom periodu^{7,8}.

Kao polimerni matriks za vezivanje lijeka u ovom radu korištena je oksidovana celuloza (OC) dobijena modifikovanjem pamučnog zavoja procesom selektivne oksidacije. Za inkorporiranje na OC korišten je antibiotik ceftriakson (slika 1) koji djeluje baktericidno na veliki broj bakterija⁹.



Slika 1. Strukturalna formula ceftriaksona

Cilj ovog rada bio je dobijanje biološki aktivnog celuloznog materijala vezivanjem ceftriaksona na oksidovani celulozni zavoj. U radu je ispitana uticaj strukture antibiotika i funkcionalnih grupa oksidovane celuloze na količinu vezanog i otpuštenog lijeka i tip formiranih hemijskih veza. Takođe, ispitano je antimikrobno djelovanje dobijenog biološki aktivnog materijala *in vitro*.

Materijal i metode

Za dobijanje oksidovane celuloze korišten je kaliko zavoj (Saniteks Velika Kladuša, 100% pamuk). Proces oksidacije vršen je smjesom $\text{HNO}_3/\text{H}_3\text{PO}_4$ 2:1 i 1,43 % NaNO_2 na sobnoj temperaturi ($25 \pm 1^\circ\text{C}$) tokom 12, 24 i 48¹⁰. Sadržaj karboksilnih grupa oksidovanog celuloznog zavoja određen je kalcijum-acetatnom metodom¹¹.

Za inkorporiranje na OC korišten je antibiotik ceftriakson u obliku ceftriakson-dinatrijuma, triseskvihidrata (Galenika, $M=661,59 \text{ gmol}^{-1}$). Vezivanje antibiotika vršeno je u statičkim uslovima potapanjem 1 g oksidovanog zavoja u 200 ml vodenog rastvora lijeka koncentracije $c=3,4 \cdot 10^{-3} \text{ mol/L}$ na sobnoj temperaturi ($22 \pm 1^\circ\text{C}$) tokom 24 h. Spektrofotometrijsko mjerjenje količine lijeka u rastvoru vršeno je nakon 5, 15, 30 i 60 min. i 24 h.

Desorpcija vezanog ceftriaksona sa oksidovane celuloze vršena je u fiziološkom rastvoru (0,95% NaCl) u statičkim uslovima, na sobnoj temperaturi ($22 \pm 1^\circ\text{C}$), modul kupatila 1:100 u trajanju od 24 sata.

Količine vezanog i otpuštenog antibiotika sa oksidovanog celuloznog vlakna određene su spektrofotometrijski na UV-VIS spektrofotometru Perkin Elmer model Lambda 25, kod $\lambda_{\text{max}} 258 \text{ nm}$.

FTIR spektri OC i uzoraka OC sa vezanim ceftriaksonom, pripremljeni u obliku KBr pastila, snimljeni su na spektrofotometru FTIR-8300 Shimadzu-Niroshi, u području $4500-500 \text{ cm}^{-1}$.

Uzorci oksidovanog celuloznog zavoja (sa $1,464 \text{ mmol/g COOH}$) sa vezanim ceftriaksonom pripremljeni su za ispitivanje animikrobnog djelovanja tako da su isječeni na kvadratiće veličine $1 \times 1 \text{ cm}$ i tretirani UV lampom (30 minuta na 254 nm). Testiranje antimikrobnog djelovanja modifikovanog celuloznog zavoja s vezanim antibiotikom vršeno je *in vitro* određivanjem inhibitorne aktivnosti metodom difuzije

na agarnoj ploči¹². Antimikrobna aktivnost je ispitana u odnosu na kulture *Staphylococcus aureus*, *Bacillus subtilis* i *Escherichia coli*. Svi uzorci su testirani u 20 ponavljanja i rezultati su dati kao srednja vrijednost.

Rezultati i diskusija

Modifikovano celulozno vlakno dobijeno je selektivnom oksidacijom celulognog zavoja tokom 12, 24 i 48 sati. Dobijeno je oksidovana celuloza sa 0,555 mmol/g, 1,464 mmol/g i 2,276 mmol/g karboksilnih grupa, respektivno.

Na ovaj način uvedene su karboksilne grupe koje u kombinaciji sa hidroksilnim grupama celuloze predstavljaju dobru osnovu za vezivanje antibiotika ceftriaksona. Rezultati sorpcije antibiotika na OC su prikazani u tabeli 1.

Tabela 1. Količina vezanog ceftriaksona na OC (mmol/g), modul kupatila 1:200, temperatura 22±1°C

mmol COOH po g OC	Trajanje sorpcije, min				
	5	15	30	60	1440
0,555	0,0200	0,0428	0,0177	0,0297	0,0540
1,464	0,0400	0,0438	0,0277	0,0364	0,0768
2,276	0,0480	0,0442	0,0263	0,0436	0,1032

Iz tabele 1 se vidi značajno vezivanje lijeka u prvih 15 minuta procesa sorpcije, nakon kojeg se bilježi opadanje količine sorbovanog lijeka. Prilikom potapanja OC u vodenim rastvor antibioticima u prvih 15 minuta dolazi do kvašenja vlakana i kao rezultat upijanja bilježi se početno smanjenje koncentracije lijeka u rastvoru. Ovako labavo vezane molekule ceftriaksona se djelimično otpuštaju, što se nakon 30 minuta registruju kao smanjenje količine vezanog antibioticika na OC. Nakon tog vremena se uspostavljaju vodonične i jonske veze između molekula lijeka i OC i količina vezanog antibioticika postepeno povećava tokom 24 h.

Ceftriakson u svojoj strukturi sadrži tiazolni prsten sa amino grupom, i triazinski prsten čiji enolni tautomer ima OH grupu. Ceftriakson takođe sadrži karboksilnu grupu u obliku Na-soli kao i veći broj akceptora i donora elektrona. Kao rezultat prisustva pomenutih funkcionalnih grupa i struktura, ceftriakson može da gradi višestruke međumolekulske i hemijske veze sa oksidovanom celulozom.

Lijek ima sposobnost građenja velikog broja vodoničnih veza između atoma azota u tiazolskom i triazinskom prstenu i OH grupa oksidovane celuloze. Nespareni elektroni na atomima azota u heterocikličnim prstenovima ceftriaksona su lokalizovani i smješteni u sp^2 hibridnim orbitalama zbog čega mogu stvarati vodonične veze sa vodonikovim atomima OH grupa oksidovane celuloze.

Karboksilna grupa antibioticika može da stupi u interakciju sa karboksilnim grupama oksidovane celuloze stvaranjem vodoničnih veza, pri čemu nastaju dimeri.

Takođe, moguće je stvaranje jonske veze između primarnih amino grupa antibioticika i karboksilnih grupa oksidovane celuloze, koje su najjače od pomenutih veza. Mjerjenje pH vrijednosti tokom procesa sorpcije (tabela 2) pokazalo je da tokom vezivanja ceftriaksona na OC dolazi do opadanja pH vrijednosti rastvora antibioticika.

Tabela 2. Promjena pH tokom sorpcije ceftriaksona na OC temperatura 22±1°C

mmol COOH po g OC	Trajanje sorpcije, min				
	5	15	30	60	1440
0,555	4,11	3,95	3,82	3,72	3,43
1,464	4,08	3,90	3,73	3,64	3,36
2,276	4,03	3,80	3,67	3,57	3,23

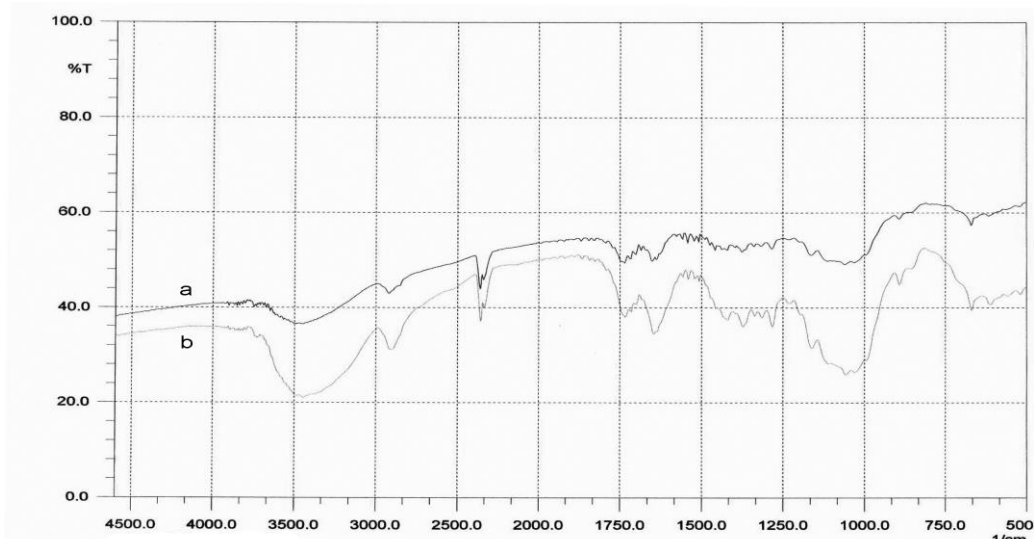
pH vrijednost rastvora ima višestruko djelovanje na količinu vezanog ceftriaksona na OC i tip vezivanja. Snižavanjem pH vrijednosti ispod 4, sa jedne strane, smanjuje se stepen disocijacije karboksilnih grupa

OC ($pK_a \approx 4$)¹⁴. S druge strane, izmjerene pH vrijednosti pogoduju disocijaciji karboksilne grupe antibiotika ($pK_a = 3$)¹² (jonizovane 60-80%). Takođe, pH vrijednosti tokom sorpcije omogućavaju ionizaciju amino grupe na tiazolnom prstenu ceftriaksona ($pK_a = 3,2$)¹² u katjonsku formu pogodnu za uspostavljanje jonske veze.

Pored toga, pH vrijednost utiče i na ionizaciju enolnih OH grupa ($pK_a=4,1$)¹² na triazinskom prstenu. Jonizovane enolne OH grupe mogu da grade vodonične veze sa OH i COOH grupama OC.

Uzimajući u obzir sve pomenute uticaje, može se zaključiti da se antibiotik na OC vezao najviše jonskim vezama, zbog dobre ionizacije NH_2 grupe lijeka. Istovremeno, pH vrijednosti tokom sorpcije pogodovalle su ionizaciji karboksilnih grupa antibiotika i OC, što znači da se dio lijeka vezao i vodoničnim vezama.

Na slici 2 prikazani su FTIR spektri oksidovane celuloze (a) i OC sa vezanim ceftriaksonom (b). Na FTIR spektru OC sa vezanim antibiotikom uočljivo je povećanje apsorpcijskog signala kod 3450 cm^{-1} . U području od 3000 do 3550 cm^{-1} široki apsorpcioni signal nastaje preklapanjem više traka, kao što su trake za vibracije istezanja O-H grupe alkohola i O-H karboksilne grupe kiselina. Povećanje intenziteta ovog signala upućuje na stvaranje vodoničnih veza i dimera. Apsorpcioni signal kod 1400 cm^{-1} u kombinaciji sa širokom apsorpcionom trakom kod 3450 cm^{-1} , ukazuje na formiranje dimera između karboksilnih grupa lijeka i OC. Uočljivo je da nema smanjenje apsorpcionog signala kod 1740 cm^{-1} koja odgovara vibracijama istezanja $>\text{C}=\text{O}$ grupe. Povećan je intenzitet signala kod 1630 cm^{-1} i 1420 cm^{-1} koje odgovaraju vibracijama istezanja karboksilatnog anjona čime se potvrđuje postojanje jonske interakcije karboksilne OC i amino-grupe ceftriaksona.



Slika 2. FTIR spektri OC (a) i OC sa vezanim ceftriaksonom (b)

Rezultati desorpcije (tabela 3) pokazuju da se antibiotik u fiziološkom rastvoru oslobađa postepeno. Nakon 24 h maksimalno se otpušta 6,99 % od ukupne količine vezanog ceftriaksona. Ovo se može tumačiti značajnim učešćem jonskih veza ceftriaksona sa OC kojima su pogodovalle disocijacija amino grupe antibiotika i karboksilnih grupa OC. Takođe, veliki broj vodoničnih veza, iako su slabije od jonskih, može imati sinergistički efekat čiji je rezultat jače vezivanja lijeka¹⁶.

Tabela 3. Količina otpuštenog ceftriaksona sa OC (mmol/g), modul kupatila 1:100, temperatura $22\pm1^\circ\text{C}$

mmol COOH po g OC	Trajanje desorpcije, h				
	1	2	3	4	24
0,555	0,0024	0,0026	0,0029	0,0033	0,0038
1,464	0,0024	0,0026	0,0031	0,0035	0,0042
2,276	0,0037	0,0040	0,0045	0,0051	0,0060

Antibakterijsko djelovanje testirano je na uzorku OC sa 1,464 mmol/g COOH koji je vezao 0,07680 mmol antibiotika po gramu vlakna. Rezultati mjerena inhibitorne aktivnosti uzoraka oksidovane celuloze sa vezanim ceftazidimom na rast *Staphylococcus aureus*, *Bacillus subtilis* i *Escherichie coli* su prikazani u tabeli 4.

Tabela 4. Zona inhibicije za OC sa vezanim ceftriaksonom nakon 24 i 48 časova

Rod bakterija	CFU ⁺ /mL	Zona inhibiranog rasta bakterija, mm	
		24 h	48 h
<i>E. coli</i>	10 ⁸	12,48	12,65
<i>S. aureus</i>	10 ⁸	12,60	12,70
<i>B. subtilis</i>	10 ⁸	4,93	4,99

CFU - Colony-forming unit

Obzirom da testirani antibiotik spada u treću generaciju cefalosporina, dobijeni rezultati su u saglasnosti sa povećanom aktivnošću ceftriaksona prema gramnegativnim bakterijama.

Zaključak

Sorpцијом ceftriaksona na OC moguće je dobiti biološki aktivan materijal sa antimikrobnim djelovanjem. Maksimalna količina ceftriaksona na OC nakon 24 sata sorpcije u vodenim rastvorima antibiotika iznosila je 0,1032 mmol/g OC. Uočeno je povećanje količine vezanog lijeka na OC sa porastom sadržaja karboksilnih grupa OC i sa vremenom sorpcije. Na osnovu FTIR spektara uzoraka ustanovljeno je da se ceftriakson vezao na OC jonskim i vodoničnim vezama. Obzirom da je vezivanje antibiotika vršeno u vodenim rastvorima koji nisu puferovani, pri zabilježenim pH vrijednostima dobijene su zadovoljavajuće količine sorbovanog i desorbovanog lijeka koje odgovaraju potencijalnoj namjeni zavoja.

Najbolje antimikrobno djelovanje u OC zavoj sa vezanim ceftriaksonom ispoljio je prema *Staphylococcus aureus*.

Biologically active fiber containing ceftriaxone

Properties of biologically active fiber depend on the type of carrier and the structure of the drug. In this paper oxidized cellulose (OC) with different carboxylic group content is obtained by selective oxidation and used for chemical bonding of antibiotic ceftriaxone.

*The bonding was performed in antibiotic water solution concentration of $c=3,4 \cdot 10^{-3}$ mol/L at room temperature (22 ± 1 °C), while desorption was performed in physiological solution. The amounts of bonded and released antibiotic were determined spectrophotometrically in UV range. Maximum amount of bound drug (0,1032 mmol/g) was obtained during the sorption on the oxidized bandage with 2,276 mmol/g COOH and the maximum amount of released drug was 0,0060 mmol/g. Antimicrobial activity of the samples with bonded ceftriaxone was tested in vitro against *Staphylococcus aureus*, *Bacillus subtilis* i *Escherichia coli* by agar diffusion test. The biggest zone of inhibition was obtained for *Staphylococcus aureus*.*

The paper studies the influence of ceftriaxone chemical structure, pH of solution in which sorption is performed and content of carboxyl group OC, on the amount of bonded drug. It was established that the drug bonding was achieved by ionic bonds and the hydrogen bonds of the drug functional groups with oxidised cellulose bandage.

Literatura:

1. M. Vuorio, J. A. Manzanares, L. Murtomaki, J. Hirvonen, T. Kankkunen, K. Kontturi, *J. Control. Release* **91** (2003) 439
2. A. Medović, P. Škundrić, M. Kostić, I. Pajkić-Lijaković, *J. Biomed. Mater. Res.* **79** (2006) 635
3. P. Škundrić, M. Kostić, A. Medović, J. Praskalo, *Glasnik hem. i teh. RS* **48** (2008) 93
4. B. Rodić-Grabovac, R. Đudić, *Glasnik hem. i teh. RS* **47** (2008) 55
5. B. Rodić Grabovac, R. Đudić, N. Ilišković, *Hem. Ind.* **61 (4)** (2007) 203

6. B. Rodić Grabovac, R. Đuđić, P. Sailović, *Contemp. Mater.* **V-2** (2014) 222
7. T. Saito, A. Isogai, *Carbohydr. Polym.* **61** (2005) 183
8. L. Zhu, V. Kumar, G. S. Bunker, *AAPS PharmSciTech* **5** (4) (2004)
9. H. M. Owens, A. K. Dash, Ceftriaxone Sodium: Comprehensive Profile, Profiles of drug substances, excipients, and related methodology, vol. 30, 1st edition, Academic Press, Omaha, USA, 2003, 21
10. V. Kumar, T. Yang, *Carbohydr. Polym.* **48** (2002) 403
11. USP (United States Pharmacopeia 23/National Formulary 18) (1995) *Oxidized cellulose* p. 318.
12. J. H. Ortez, Disc diffusion testing, Manual of Antimicrobial Susceptibility Testing, M.B. Coyle (Eds.), American Society of Microbiology, Washington, USA, 2005, p.39
13. T. Kankkunen, *Controlled transdermal drug delivery by iontophoresis and ion-exchange fiber*, Academic dissertation, Department of Pharmacy, University of Helsinki, (2002) 31.
14. Caterina Bissantz, Bernd Kuhn, Martin Stahl, *J. Med. Chem.* **53(14)** (2010) 5061

Index Autora / Author Index

A

- Aissa, MA..... 39
Arsenijević, Z..... 43, 49, 54

B

- Bjelajac, N..... 34
Bodroža, DR..... 97
Bošković Vragolović, N..... 49, 54
Brezo, T..... 78

D

- Dekanski, A..... 7, 20
Dimitrijević, A..... 30
Dimitrijević, M..... 26
Dožić, S..... 30
Drvenica, I..... 7, 20

Đ

- Đjonlagić, J..... 87
Đokić, D..... 73
Đukić, A..... 73
Đuriš, M..... 43, 49, 54
Đurović, A..... 78

G

- Gadžurić, S..... 30
Garić Grulović, R..... 49
Gotovac Atlagić, S..... 34
Grozdanić, N..... 58

H

- Hrnjez, D..... 78

I

- Ivaniš, GR..... 39

J

- Jeremić, S..... 87
Jovanović, JD..... 63

K

- Kaluđerović Radojić, T..... 43, 49, 54
Kijevečanin, MLj..... 39, 58, 63
Košević, M..... 20
Kovačević, R..... 26
Kravić, S..... 78
Kukrić, Z..... 83
Kumrić, K..... 73

L

- Levi, Z..... 97

M

- Majstorović, DM..... 63
Malinović, BN..... 34
Malinović, T..... 34
Maluckov, BS..... 26
Martić, I..... 83
Matović, Lj..... 73
Milanović, S..... 78
Milićević, S..... 73
Milošević, V..... 73
Milovanović, A..... 34
Mladenović, S..... 26
Momčilović, M..... 15
Mutić, J..... 15

N

- Nedić, O..... 7
Nikodinović Runić, J..... 87
Nikolić, B..... 20
Nikolić, MS..... 87

P

- Panić, V..... 20
Penavin Škundrić, JV..... 97
Pešić, R..... 54
Petrović, Đ..... 73
Petrović, RR..... 97
Ponjavić, MM..... 87

R

Radonić, JR.....	68
Radović, IR.....	39, 58
Rajković, S.....	92
Rodić Grabovac, BB.....	102

S

Sailović, PS.....	102
Savović, J.....	15
Simić, Jlj.....	68
Soldatović, D.....	58
Sremački, MM.....	68
Stevanović, S.....	87
Stojanović, ZS.....	78
Suturović, Z.....	78

S

Šekularac, G.....	20
Šerbanović, SP.....	63

T

Topalić Trivunović, LjN.....	102
Trtić Petrović, T.....	30
Turel, I.....	2
Turk Sekulić, MM.....	68

V

Vasilišin, L.....	83
Vojinović Miloradov, MB.....	68
Vučić, G.....	83
Vuksanović, J.....	58

Z

Zdolšek, N.....	30
Zec, N.....	30

Ž

Živković, EM.....	63
Živković, SM.....	15